BSCM

Biomedical Sciences and Clinical Medicine

Volume 65
Number 1
January-March
2026

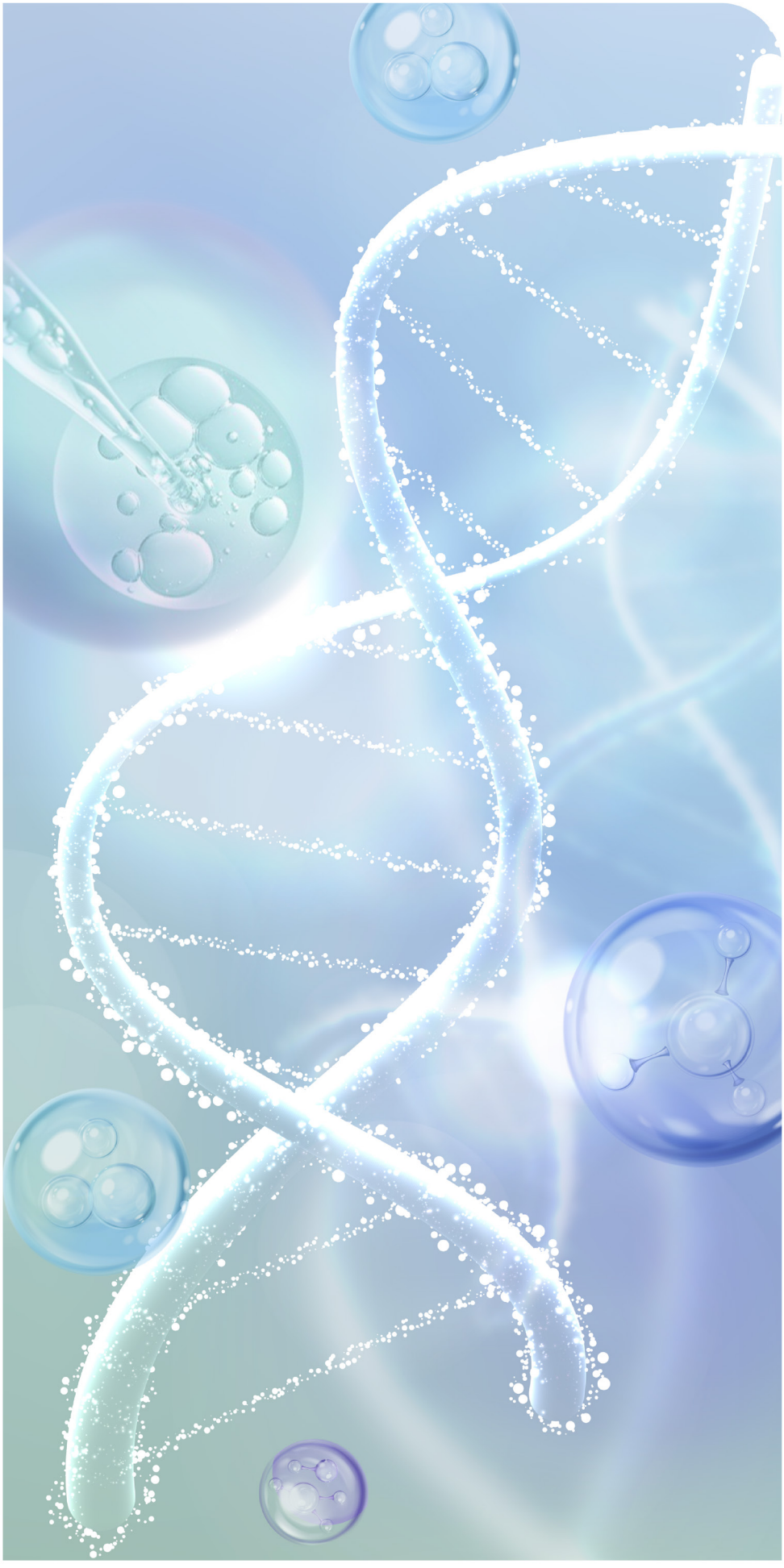

ISSN 2774-1079 (Online)

BSCM
Biomedical Sciences and Clinical Medicine

Volume 65 No.1 Jan.-Mar. 2026
https://he01.tci-thaijo.org/index.php/CMMJ-MedCMJ/index

CONTENTS

Original Articles

- Nanofibrous Scaffolds Functionalized with Serine for Dentin Mineralization: A Characterization Study — 1
  Aruna Krishnan, Sandhya Raghu and Jayalakshmi Somasundaram
- Prevalence of Vitamin D Deficiency in Diabetic Neuropathy Patients in the South Indian Population — 11
  Vadivel Mani, Madhavi Kandregula, Gayathri Venkatasan and Muninathan Natarajan
- Effects of Inflammatory Biomarkers (Fetuin-A and High Sensitivity C-reactive Protein) on Glycemic Control in Type 2 Diabetic Women — 23
  Ali Abdullateef Al-bayati, Shatha Alkhateeb and Walaa Jedda
- Development of Zinc Oxide Nanoparticle–Infused Carrageenan Membranes with Enhanced Structural and Antimicrobial Properties for Guided Tissue Regeneration — 32
  Priyangha PT, Ashritha M and Balaji Ganesh S
- Automated Immunohistochemistry as an Alternative to Conventional Immunohistochemistry for Analyzing the Expression of BCL2 and Ki-67 in Diffuse Large B-Cell Lymphoma Patients — 43
  Phuttirak Yimpak, Kanokkan Bumroongkit, Adisak Tantiworawit , Thanawat Rattanathammethee, Sirinda Aungsuchawan and Teerada Daroontum
- Comparative Study of Guava Leaf Bioactive Extracts Using Ultrasonication Assisted Extraction — 51
  Somya Khanna, Pragati Singh and Ekta Singh Chauhan
- Can the Indonesian Version of the Work-Related Quality of Life Scale-2 (WRQoLS-2) Be Used to Measure Quality of Work Life Among Hospital Personnel? — 58
  Aulia Rosinta, Naesinee Chaiear, Chatpong Ngamchokwathana and Nuri Purwito Adi
- Virgin Coconut Oil Inhibits Leukemic Cell Proliferation Via Apoptosis in K562 and MOLT-4 Cell Lines — 68
  Sawalee Saosathan, Supachai Yodkeere , Arunrat Warin, Natthachai Duangnin and Nittaya Peansub
- Sex-specific Differences in the Association between Insulin Resistance and Metabolic Syndrome and Ferritin in Korean Adults: A Nationwide Population-based Study — 81
  Mi Young Gi, Ju Ae Cha and Hyun Yoon
- Validity and Reliability of the Thai Version of the Barthel Index Self-Report (BI-SR-TH) for People with Spinal Cord Injury — 91
  Siam Tongprasert, Sirinna Mekkij, Pratchayapon Kammuang-lue and Tinakon Wongpakaran

BSCM
Biomedical Sciences and Clinical Medicine

Volume 65 No.1 Jan.-Mar. 2026
https://he01.tci-thaijo.org/index.php/CMMJ-MedCMJ/index

CONTENTS

Original Articles

- Uncovering the Molecular Landscape of Secreted Phosphoprotein 1 and Its Expression Network in Kidney Renal Papillary Cell Carcinoma 100

  Danang Prasetyaning Amukti, Ria Indah Pratami, Moch Saiful Bachri[2]and Daru Estiningsih

- Next-Generation Dental Bone Implants - Sustainable 3D Nanostructures Derived from Animal By-Products: A Preliminary Study 111

  Vajpayee Kritika and Rethinam Senthil

Review Articles

- *ANGPT2* as a Therapeutic Target in Endometriosis: Evolving Perspectives in Angiogenesis - ANGPT2, an Emerging Target in Endometriosis Therapy 119

  Sheeja MJ, Sumanth Kumar B, N Muninathan, K Ramesh Kumar, Joby P Jose, Jeena Jose, Sreekutty M, Jisha A M, Parvathy S, Jineesh V C, Sindhu K, Sreeja Sreenivasan and Dinesh Roy D

- MC4R: A Genetic Key to Metabolic and Cardiovascular Disorders 129

  Joby P Jose, Sumanth Kumar B, N Muninathan, K Ramesh Kumar, Vishnu M G, Sebastian J Pengiparambil, Sinha Mathew, Harisree P H, Roshma Retnakaran, Pinchulatha K, Thahira A, Swathi T and Dinesh Roy D

Short Communication

- Phenethylamine Does Not Accelerate Healing in *Staphylococcus aureus*-infected Wounds in Mice 140

  Hana Dian Mufida, Dewi Hidayati, Enny Zulaika and Arif Luqman

Biomedical Sciences and Clinical Medicine 2026;65(1):1-10.
doi: 10.12982/BSCM.2026.02
https://he01.tci-thaijo.org/index.php/CMMJ-MedCMJ/index

BSCM
Biomedical Sciences and Clinical Medicine

Original Article

Open Access

Nanofibrous Scaffolds Functionalized with Serine for Dentin Mineralization: A Characterization Study

Aruna Krishnan, Sandhya Raghu and Jayalakshmi Somasundaram

Department of Conservative Dentistry and Endodontics, Saveetha Dental College and Hospitals, Saveetha Institute of Medical and Technical Sciences, Saveetha University, Chennai, India

Correspondence:
Sandhya Raghu,
Department of Conservative Dentistry and Endodontics, Saveetha Dental College and Hospitals, Saveetha Institute of Medical and Technical Sciences, Saveetha University, 162, PH Road, Chennai 600077, Tamil Nadu, India.
E-mail: Sandhya.sdc@saveetha.com

Received: April 11, 2025;
Revised: July 24, 2025;
Accepted: July 31, 2025

ABSTRACT

OBJECTIVE Dentin repair and regeneration pose significant challenges in restorative dentistry due to its hierarchical structure and susceptibility to demineralization. Traditional approaches often fail to restore the natural architecture and functionality of dentin. The aim of this study was to develop and characterize a biomimetic polycaprolactone (PCL)/nanohydroxyapatite (nHA)/serine (Ser) scaffold to enhance dental mineralization and support tissue regeneration. The inclusion of serine, known for its ability to bind calcium and phosphate ions and guide hydroxyapatite crystal formation, could enhance nucleation and cell attachment, making the scaffold a promising biomaterial for dentin repair.

METHODS Nanofibrous scaffolds were fabricated using PCL, nHA, and Ser by the electrospinning method. The structural and functional properties of the scaffold were characterized through scanning electron microscopy (SEM), energy-dispersive x-ray spectroscopy (EDX), x-ray diffraction (XRD), and fourier transform infrared spectroscopy (FTIR). SEM and EDX were used to evaluate the morphology, porosity, and elemental composition. XRD analyzed the crystalline and amorphous phases, while FTIR analyzed chemical interactions among the components.

RESULTS SEM analysis revealed a uniform fibrous structure with interconnected porosity, mimicking the extracellular matrix. EDX confirmed the successful incorporation of calcium and phosphorus, indicating the presence of nHA. XRD analysis demonstrated a combination of crystalline and amorphous phases, highlighting the scaffold's structural stability and bioactivity. FTIR spectroscopy identified characteristic peaks corresponding to PCL, nHA, and Ser, validating their successful integration and interaction within the scaffold matrix.

CONCLUSIONS The nanofibrous scaffold exhibited structural and compositional properties, confirming the presence of PCL, nHA and Ser. The properties analyzed support its potential for biomineralization and tissue regeneration. The inclusion of Ser could enhance hydroxyapatite nucleation and cell attachment, making the scaffold a promising biomaterial for dentin repair. Further *in-vitro* and *in-vivo* studies are recommended to validate its clinical application.

KEYWORDS biomineralization, dentin regeneration, nanohydroxyapatite, polycaprolactone, serine, scaffolds, tissue engineering

INTRODUCTION

Dentin repair and regeneration remain persistent challenges in restorative dentistry due to its intricate hierarchical structure and susceptibility to demineralization. Conditions such as dental caries and erosion compromise the mechanical integrity of dentin, leaving it vulnerable to structural failure. While conventional restorative approaches such as dental fillings address these issues temporarily, they often fail to restore the natural functionality and microarchitecture of dentin. These limitations highlight the need for biomimetic strategies that replicate the biological processes underlying dentin formation and repair (1, 2). Dentin presents a greater challenge for remineralization than enamel due to its elevated organic composition (3). This challenge is largely attributed to the widely accepted notion that dentin remineralization does not proceed through spontaneous mineral precipitation or nucleation on its predominantly type I collagen organic matrix. Rather, it relies on the growth of existing crystals within the damaged regions (4, 5). Biomineralization, the biological process by which minerals are deposited onto organic scaffolds, governs dentin formation and repair. Central to this process is the interaction between collagen fibrils and non-collagenous proteins (NCPs). NCPs, such as dentin phosphoprotein (DPP), dentin matrix protein 1 (DMP1), and osteopontin, categorized as NCPs, actively regulate mineralization by drawing in calcium and phosphate ions and stabilizing amorphous calcium phosphate (ACP) precursors. These proteins guide the transformation of ACP into crystalline hydroxyapatite, forming an organized mineralized structure within the collagen matrix. Mutations or deficiencies in NCPs often result in impaired dentin mineralization, underscoring their critical role in this process (6, 7).

Amino acids, particularly serine (Ser), play a pivotal role in mimicking the functions of NCPs. Ser, a polar amino acid, facilitates hydroxyapatite nucleation by electrostatically binding calcium and phosphate ions, creating localized supersaturation conditions that are essential for mineral formation. Furthermore, Ser adsorbs onto mineral surfaces, influencing crystal morphology and growth patterns. These interactions are critical for achieving the structural and mechanical properties of natural dentin, making Ser an ideal candidate for incorporation into biomimetic scaffolds (6).

Electrospun nanofibrous scaffolds have emerged as promising biomaterials for replicating the extracellular matrix in dentin regeneration. These scaffolds provide high surface area, interconnected porosity, and mechanical flexibility, facilitating cell adhesion, proliferation, and biomineralization. Polycaprolactone (PCL), a biodegradable polymer, is widely used in scaffold fabrication due to its mechanical resilience and compatibility with bioactive agents. However, PCL exhibits hydrophobic properties. In contrast, materials like hydroxyapatite and calcium phosphate, known for their hydrophilicity, can be blended with PCL to produce electrospun composite fibers. HA, being both hydrophilic and osteoconductive, offers advantages over PCL alone. Incorporating nanohydroxyapatite (nHA) into PCL fibers can enhance their overall properties compared to using PCL fibers on their own (8). Hydroxyapatite is limited in its application for load-bearing purposes due to its poor biomechanical properties, including brittleness, low fatigue strength, and lack of flexibility (9). Consequently, increasing attention has been directed towards developing hydroxyapatite particles in various shapes and sizes and embedding them within biodegradable polymer frameworks (10). The integration of bioactive ceramics with degradable polymers to construct highly porous 3D scaffolds has proven to be an innovative method for creating composite systems tailored to bone tissue engineering (11). The incorporation of nHA further augments the biomineralization potential of these scaffolds. With its structural and compositional similarity to the inorganic phase of dentin, nHA enhances the bioactivity of scaffolds by releasing calcium and phosphate ions, promoting mineral deposition. Functionalization of PCL scaffolds with Ser enhances their capacity to emulate natural biomineralization processes, making them highly effective for regenerative dental applications (2, 12). The synergistic combination of PCL, nHA, and Ser provides a robust platform for creating scaffolds that mimic native dentin environments and support effective tissue repair (13).

This study investigates the development and characterization of a Ser-incorporated nanofibrous

scaffold designed to enhance dentin mineralization. This research aims to contribute to the growing field of biomimetic scaffolds for dental tissue engineering by offering insights into their potential applications for regenerative therapies. In our previous work, glutamic acid-loaded PCL nanofibrous scaffolds were shown to promote controlled calcium phosphate nucleation and dentin mineralization, suggesting that amino acid modification could enhance the regenerative potential of synthetic scaffolds (14). The aim of the study was to develop and characterize a biomimetic PCL/nHA/Ser scaffold which can potentially enhance dental mineralization and support tissue regeneration. The objectives were to evaluate the structural, compositional and elemental analysis using scanning electron microscopy (SEM), energy-dispersive X-ray spectroscopy (EDX), fourier transform infrared spectroscopy (FTIR), and x-ray diffraction (XRD).

METHODS

Materials

PCL (molecular weight: 80,000), nHA 200 nm were procured from Sigma-Aldrich (Bangalore, India) and Ser were obtained from Southern India Scientific Corporation (Chennai, India). Dimethylformamide (DMF), chloroform ($CHCl_3$) and 1% antibacterial-antifungal solutions, purchased from HiMedia Laboratories (Thane, India), were used as solvents for scaffold preparation. All the chemicals utilized in this study were of analytical grade and employed directly without undergoing any additional purification processes.

Scaffold fabrication

Ser was incorporated into the scaffold by dissolving 2 wt% Ser in water and adding it to the PCL/nHA solution, followed by stirring for an additional 12 hours to ensure uniformity. The concentration of 2 wt% Ser was selected based on previous studies that demonstrated effective ion binding and bioactivity at low amino acid loading, without compromising fiber integrity or electrospinning efficiency (15).

Electrospinning was carried out using a Holmarc Opto-Mechatronics electrospinning apparatus (Model: HO-NFES-040). The polymer solution was loaded into a syringe fitted with a metallic needle, and the process was optimized with the following parameters: a flow rate of 500 µL/h, an applied voltage of 10-15 kV, and a needle-to-collector distance of 7.5 cm. Aluminum foil was used to cover the collector plate, which was grounded to collect the nanofibers. The electrospinning process was conducted at room temperature for 3 hours. After the fibers were collected, the scaffolds were dried under vacuum in a desiccator overnight to remove residual solvents and ensure complete solvent evaporation. PCL and PCL/nHA scaffolds were fabricated as described above and were utilized as controls for this new investigation (16). The structural and compositional analysis of these scaffolds provided a comparative baseline to evaluate the performance of the newly developed PCL/nHA/Ser scaffold. These results establish the structural and compositional properties of the PCL and PCL/nHA scaffolds as reliable controls for assessing the enhanced functionality and biomineralization potential of the PCL/nHA/Ser scaffolds.

Characterization

SEM

The surface characteristics of the electrospun scaffolds were examined through SEM (JSM IT800, JEOL Ltd., Tokyo, Japan). The scaffolds were cut into small sections and attached to aluminum bases with a conductive carbon adhesive. To enhance the conductivity of the samples, a fine gold layer was deposited using a sputter coater. SEM analysis was performed at an accelerating voltage of 5-15 kV to visualize the fiber surface characteristic, morphology, surface texture, and distribution of nHA particles within the fibers. Images were captured at multiple magnifications, and ImageJ software was utilized for analyzing the samples.

EDX

The elemental composition of the scaffolds was investigated using the EDX detector attached to the SEM system. EDX was utilized to visualize the spatial distribution of these elements throughout the fiber network.

XRD

The crystalline phases and structural composition of the scaffolds were analyzed with XRD (Bruker diffractometer, Singapore). The scans covered 2θ angles from 10° to 80° with CuKα radiation (λ = 1.5406 Å). A scanning interval of 0.1° and a speed of 1 step per second were applied. Char-

acteristic peaks corresponding to nHA (at ~26° and ~32°) and PCL crystallinity (~21.5° and ~23.8°) were evaluated. The degree of crystallinity was calculated to assess the impact of Ser and nHA on the structural integrity of the scaffolds.

FTIR

FTIR analysis was carried out to identify the chemical interactions between PCL, nHA, and Ser within the scaffolds. The spectral data were obtained with a JASCO 4100 spectrometer, covering the range of 400 to 4,000 cm^{-1}, at a resolution of 4 cm^{-1} with 32 scans for each sample. Specific peaks corresponding to the functional groups of PCL (C = O stretching at ~1720 cm^{-1}), nHA (P-O stretching at ~1045 cm^{-1}), and Ser (O-H and N-H stretching at ~3200-3500 cm^{-1}) were analyzed to confirm their incorporation and interactions within the scaffold matrix.

This is a descriptive observational study hence statistics are not included.

RESULTS

SEM

The surface structure of the PCL/nHA/Ser scaffolds were analyzed using SEM to evaluate fiber formation, distribution, and the incorporation of nHA and Ser. The SEM micrographs revealed that the electrospun scaffolds exhibited a uniform fibrous structure with interconnected porosity, closely resembling the extracellular matrix as shown in Figure 1 A and B. The fibers displayed a smooth surface, with minimal bead formation, indicating optimized electrospinning parameters. The distribution of nHA was uniform throughout the scaffold, with no significant agglomeration observed, suggesting effective dispersion during the electrospinning process. Additionally, the scaffold fibers maintained structural integrity and flexibility, crucial for replicating the mechanical characteristics of natural tissue. The presence of Ser in the scaffold was indirectly confirmed through morphological changes in the fiber surface. The fibers showed slightly rougher textures compared to pure PCL fibers, which may be attributed to the functionalization of the polymer matrix with Ser and nHA. This enhanced surface roughness is expected to improve cell attachment and promote mineralization. Overall, the SEM analysis confirmed that the PCL/nHA/Ser scaffolds possess a highly porous and fibrous structure, with uniform incorporation of nHA and Ser. These characteristics make the scaffold suitable for supporting cell proliferation, nutrient diffusion, and biomineralization in tissue engineering applications.

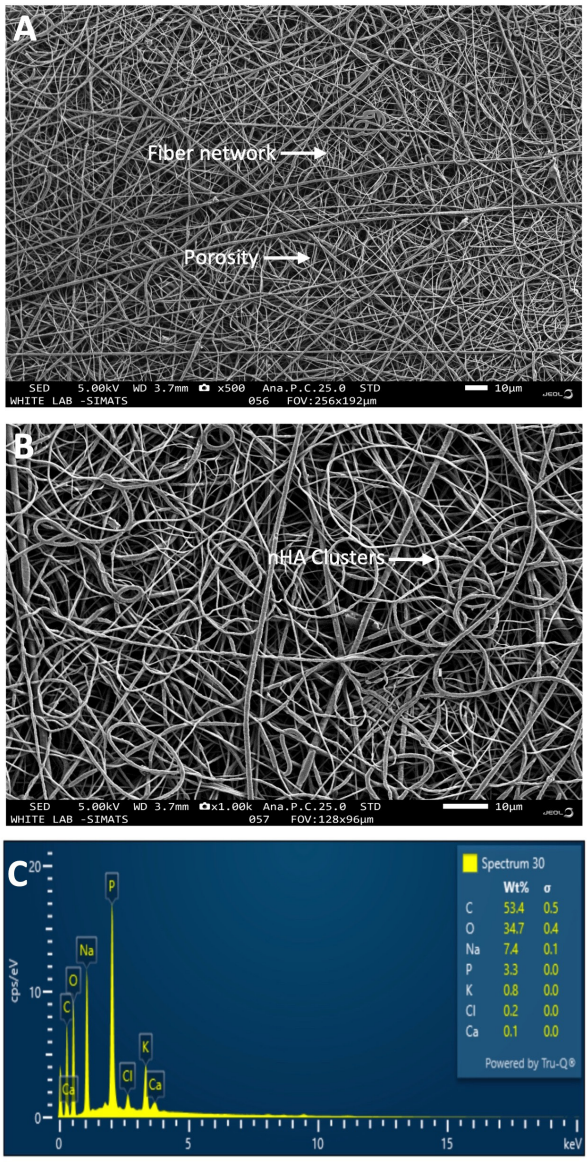

Figure 1. SEM images of electrospun nanofibrous scaffold (A and B) PCL/nHA/Ser at two different magnifications and their EDX spectrum (C)

EDX

The elements present in the PCL/nHA/Ser scaffold were examined through EDX to verify the effective integration of nHA into the fibers. The EDX spectra indicated the existence of characteristic elements, including carbon (C) and oxygen (O), which are attributed to the PCL polymer matrix, as shown in Figure 1C. Additionally, calcium (Ca) and phosphorus (P) were detected, confirming the incorporation of nHA within the

scaffold. The Ca/P ratio observed in the scaffold exhibited a deviation from the stoichiometric ratio of hydroxyapatite, which can be attributed to the dynamics of the electrospinning process (17). Sodium (Na) was also observed, indicating its presence as a component of the synthetic nHA. The elemental distribution suggests effective blending of nHA and Ser within the PCL matrix during the electrospinning process. These findings complement the SEM observations, confirming that the PCL/nHA/Ser scaffold is a composite system with well-distributed nHA and Ser, highlighting its potential as a biomimetic scaffold for tissue engineering applications.

XRD

The XRD examination of the PCL/nHA/Ser scaffold revealed a combination of crystalline and amorphous phases, which are key to its structural and functional properties. Distinct diffraction peaks at 21.43°, 23.63°, and 29.42° (2θ) were observed, corresponding to the crystallographic planes as shown in Figure 2. The sharp peaks at 21.43° and 23.63° are characteristic of the semi-crystalline nature of PCL. These peaks confirmed the retention of PCL's crystallinity during the fabrication process. Similarly, the peak at 29.42° (2θ) is attributed to nHA, indicating the effective integration of hydroxyapatite within the polymer matrix. In contrast to the crystalline peaks, the broader background signal observed in the XRD pattern is indicative of the amorphous regions within the scaffold. The amorphous phase is associated with the presence of Ser, which disrupts the regular packing of the crystalline lattice and contributes to the flexibility and bioactivity of the composite. The broader FWHM values of 0.359° and 0.392° at 21.43° and 23.63°, respectively, suggest the coexistence of both crystalline and amorphous domains. This combination of crystalline and amorphous phases provides the scaffold with a balance of mechanical strength and bioactive properties. The crystalline domains ensure structural integrity and stability, while the amorphous regions promote interactions with biological tissues, facilitating cell attachment and biomineralization. These results confirm the suitability of the PCL/nHA/Ser scaffold for applications in tissue engineering.

FTIR

The FTIR spectrum of the PCL/nHA/Ser scaffold was analyzed to confirm the successful incorporation of nHA and Ser into the polymer matrix. The spectrum displayed characteristic peaks corresponding to the functional groups of PCL, nHA, and Ser, demonstrating the composite nature of the scaffold, as seen in Figure 3. The PCL com-

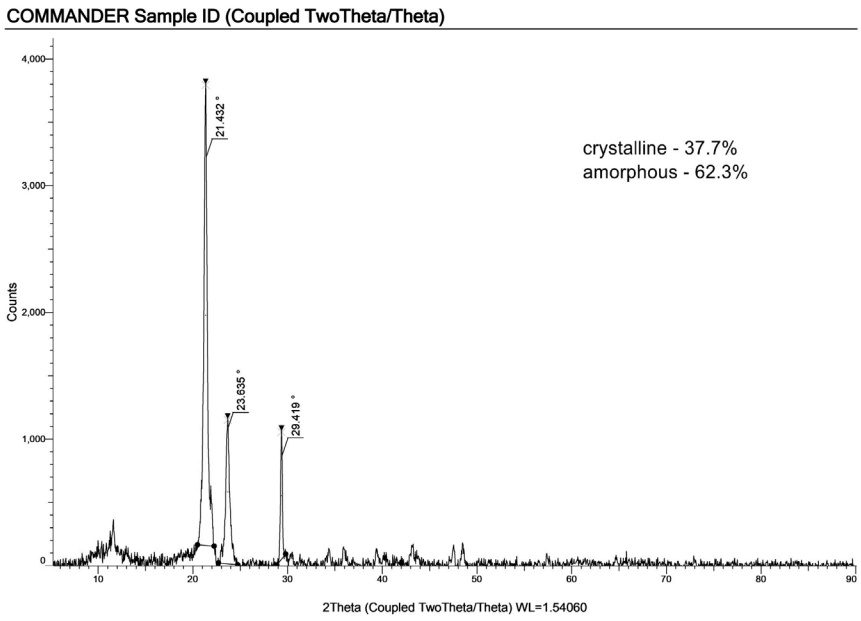

Figure 2. XRD spectrum of PCL/nHA/Ser scaffold

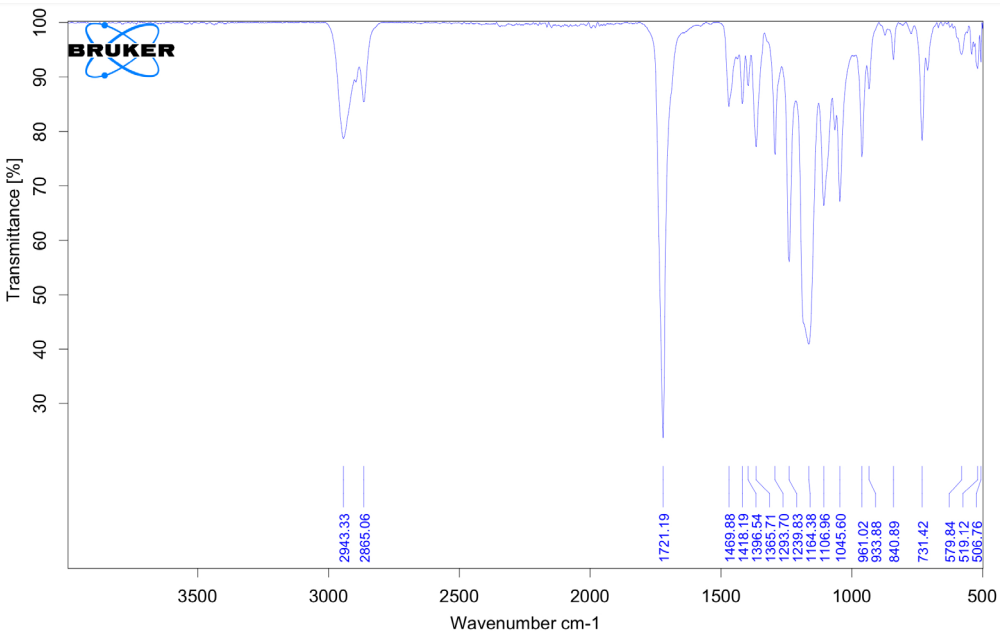

Figure 3. FTIR analysis of PCL/nHA/Ser scaffold

ponent showed prominent peaks at 1,721.19 cm^{-1}, attributed to the C = O stretching vibration, and at 2,943.33 cm^{-1} and 2,865.06 cm^{-1}, corresponding to CH_2 asymmetric and symmetric stretching, respectively. These peaks confirmed the presence of PCL as the base polymer in the scaffold.

The contribution of nHA was evident from the strong absorption band at 1,106.96 cm^{-1}, corresponding to the P-O stretching vibration, and the peaks at 579.84 cm^{-1} and 519.12 cm^{-1}, characteristic of phosphate bending vibrations. These features are consistent with the hydroxyapatite structure, validating its incorporation within the scaffold. Serine incorporation was confirmed by the presence of distinct peaks at 1,469.88 cm^{-1} and 1,365.71 cm^{-1}, corresponding to C-H bending and C-N stretching vibrations, respectively. Additionally, the sharp peak observed at approximately 933.88 cm^{-1} can be associated with the C-O stretching of the hydroxyl group in serine, while the region around 840.89 cm^{-1} corresponds to out-of-plane O-H bending, further supporting the presence of serine. Notably, the absence of a broad O-H/N-H band in the range of 3,200-3,500 cm^{-1} may be attributed to hydrogen bonding interactions or overlapping with polymer signals, yet the distinct peaks observed in the fingerprint region confirm the successful incorporation of serine.

The overlapping of characteristic peaks from PCL, nHA, and Ser within the FTIR spectrum indicates effective blending and molecular interactions between the scaffold components. The incorporation of serine is particularly significant, as its functional groups are expected to enhance scaffold bioactivity by promoting cell adhesion and mineralization processes. These findings confirm that the PCL/nHA/Ser scaffold integrates all components effectively, supporting its potential for application in tissue engineering.

DISCUSSION

The development and characterization of the PCL/nHA/Ser scaffold have demonstrated its potential as a biomimetic material for applications in tissue engineering. The results from SEM, EDX, XRD, and FTIR analyses provide compelling evidence of the scaffold's structural, compositional, and functional properties, highlighting its suitability for promoting mineralization and supporting cellular activity.

The SEM analysis revealed a uniform fibrous structure with interconnected porosity, closely mimicking the extracellular matrix of natural tissues. The smooth yet slightly roughened fiber surfaces, due to the incorporation of nHA and Ser, suggest enhanced bioactivity, which is critical for cell adhesion and proliferation. The homogeneous distribution of nHA within the fibers, observed through SEM and EDX mapping, ensures consistent mechanical properties and effective biomineralization across the scaffold.

The EDX analysis confirmed the presence of calcium and phosphorus, which are characteristic of nHA, indicating the successful integration. The calculated Ca/P ratio aligned with the theoretical values for hydroxyapatite, suggesting that the nHA maintains its structural integrity within the composite scaffold. This uniform elemental distribution further emphasizes the scaffold's ability to emulate the mineralized matrix of dentin and bone.

XRD analysis revealed the coexistence of crystalline and amorphous phases within the scaffold. The distinct peaks for PCL and nHA confirmed the retention of their structural identities, while the broadening of peaks suggested interactions with Ser, leading to partial disruption of crystalline order. The balance between crystalline and amorphous phases is particularly advantageous, as it provides mechanical stability while enhancing bioactivity. The crystalline regions contribute to the scaffold's strength, whereas the amorphous regions facilitate biological interactions and mineral deposition.

FTIR spectroscopy further validated the incorporation of PCL, nHA, and Ser into the scaffold. Characteristic peaks for PCL (C=O and CH_2 stretching), nHA (P-O and phosphate bending), and Ser (O-H and N-H stretching) were identified, confirming the composite nature of the scaffold. The overlapping peaks indicate interactions between these components, which could enhance the scaffold's ability to support biomineralization and promote tissue integration.

The incorporation of Ser into the PCL/nHA scaffold is particularly significant. Ser mimics the function of noncollagenous proteins (NCPs) in natural mineralization processes, enhancing hydroxyapatite nucleation and controlling crystal growth. This bioactive modification positions the scaffold as a superior alternative to conventional polymer-based materials, offering enhanced mineralization potential and cell compatibility.

The combination of PCL, a biodegradable polymer, with nHA and Ser addresses key limitations of individual materials. While PCL provides mechanical flexibility and a suitable platform for fiber formation, nHA improves osteoconductivity and mineral release, and Ser introduces bioactivity critical for tissue regeneration. This synergistic approach ensures that the scaffold not only mimics the structural and functional properties of the extracellular matrix but also facilitates cellular responses necessary for effective regeneration.

Negatively charged amino acids, including Ser through phosphorylation, play a crucial role in binding calcium and phosphate ions, facilitating nucleation and guiding the conversion of ACP into organized hydroxyapatite in Ser-incorporated scaffolds (18). The phosphorylation of Ser residues in proteins such as ameloblastin (AMBN) plays a critical role in enamel formation, acting as a post-translational modification necessary for proper mineralization and crystal organization (19). This underscores the potential of Ser in biomimetic scaffolds to mimic natural processes, stabilizing precursor minerals and guiding the deposition of hydroxyapatite.

Amino acid-functionalized scaffolds, such as those incorporating serine, have been shown to mimic NCPs and regulate nucleation, crystal growth, and signaling pathways crucial for dentin-pulp regeneration (20).

Electrospun scaffolds incorporating biofunctional molecules like amino acids offer promising results in dentin-pulp tissue engineering due to their controlled degradation, high porosity, and ability to promote mineralized tissue formation (21).

The incorporation of Ser into biomimetic systems for dentin and enamel remineralization demonstrates its critical role in stabilizing ACP and guiding its transformation into hydroxyapatite. As highlighted in previous studies, Ser's ability to form strong electrostatic interactions with calcium ions enhances the stability of ACP, mimicking natural biomineralization pathways such as those involving dentin sialophosphoprotein (DSPP) (22). When combined with carboxymethyl chitosan (CMC), Ser significantly prolongs the stability of ACP nanocomplexes, facilitating their sustained use in clinical applications. Additionally, Ser enhances the structural organization of remineralized layers, forming highly aligned, enamel-like crystals that resemble native tissue. These findings align with the current study, where Ser-incorporated PCL/nHA scaffolds promoted the deposition of orderly mineralized structures, demonstrating their potential as effective platforms for dentin repair.

The role of Ser-rich sequences in biomimetic remineralization is well-supported, as demon-

strated by the Aspartate-Ser-Ser (DSS) sequence in DPP. Peptides like 8DSS effectively bind to demineralized dentin collagen via electrostatic interactions, promoting hydroxyapatite nucleation and nano-crystal deposition on dentin surfaces and within tubules (23). This process significantly enhances the mechanical properties of demineralized dentin. The use of self-assembling peptides like P11-4, which promote enamel remineralization through a biomimetic approach (24), highlights the need for similar strategies in dentin. These peptides scaffold hydroxyapatite formation, a process potentially beneficial for the complex microstructure of dentin. This underscores the importance of researching biomimetic compounds tailored specifically to target dentin's unique properties.

Recent studies also highlight that phosphorylated amino acids such as phosphoserine can promote osteogenic differentiation and calcium deposition in nanohydroxyapatite-based scaffolds, underscoring the role of amino acid signaling in enhancing mineralization pathways (25).

Furthermore, biomimetic mineralized collagen-hydroxyapatite scaffolds engineered using synthetic analogues of noncollagenous proteins have shown enhanced intrafibrillar mineralization and osteogenic potential, supporting the rationale for amino acid-modified scaffolds in dental applications (26).

These findings highlight the potential of Ser to stabilize mineral precursors and direct organized crystal formation, aligning with the goals of this study to leverage Ser-incorporated scaffolds for biomimetic dentin remineralization.

Research highlighting the synergistic interaction between casein phosphopeptide-amorphous calcium phosphate (CPP-ACP) and fluoride for enamel remineralization (27) indicates a promising strategy that might be extended to dentin. Considering dentin's higher organic composition and increased porosity, it becomes essential to develop methods capable of penetrating deeply and reinforcing the collagen framework. Accordingly, exploring the capability of CPP-ACP to enhance the intradentinal deposition of calcium and phosphate ions warrants comprehensive evaluation.

Limitations and future directions

While the current study successfully demonstrates the scaffold's potential, additional investigations are warranted to fully validate its performance. Future studies should explore the scaffold's behavior in biological environments, such as *in-vitro* and *in-vivo* mineralization assays, to assess its long-term stability, biocompatibility, and degradation profile. Furthermore, understanding the influence of Ser concentration on the scaffold's mechanical and biological properties could provide valuable insights for optimizing its design.

Future investigations should also evaluate the scaffold's antimicrobial efficacy and mechanical stability under simulated oral conditions, including dynamic loading and exposure to salivary enzymes, to better replicate clinical performance.

CONCLUSIONS

The nanofibrous scaffold exhibited structural and compositional properties, confirming the presence of PCL, nHA and Ser. The properties analyzed support its potential for biomineralization and tissue regeneration. The inclusion of Ser could enhance hydroxyapatite nucleation and cell attachment, making the scaffold a promising biomaterial for dentin repair. Further *in-vitro* and *in-vivo* studies are recommended to validate its clinical application.

ACKNOWLEDGMENTS

We thank Saveetha Dental College and Hospital for providing with necessary infrastructure for developing the material and its testing.

FUNDING

This research received no specific grant from any funding agency in the public, commercial, or not-for-profit sectors.

CONFLICTS OF INTEREST

The authors have no conflicts of interest to declare that are relevant to the content of this article.

AUTHOR CONTRIBUTION

A.K.: conceptualization, methodology, software, writing & editing, data curation, writing - original draft preparation, visualization, investigation,

supervision, software, validation; S.R., J.S.: conceptualization, methodology, software, writing, review & editing, data curation, writing- original draft preparation, visualization, investigation, supervision, software, validation

DATA AVAILABILITY STATEMENT

The data that support the findings of this study are available from the corresponding author upon reasonable request.

INSTITUTIONAL REVIEW BOARD STATEMENT

Not applicable. This study did not involve human or animals.

INFORMED CONSENT STATEMENT

Not applicable. This study did not involve humans.

REFERENCES

1. He L, Hao Y, Zhen L, Liu H, Shao M, Xu X, et al. Biomineralization of dentin. J Struct Biol. 2019;207:115-22.
2. Liu C, Hao Z, Yang T, Wang F, Sun F, Teng W. Anti-Acid Biomimetic Dentine Remineralization Using Inorganic Silica Stabilized Nanoparticles Distributed Electronspun Nanofibrous Mats. Int J Nanomedicine. 2021;16:8251-64.
3. Chen Z, Cao S, Wang H, Li Y, Kishen A, Deng X, et al. Biomimetic remineralization of demineralized dentine using scaffold of CMC/ACP nanocomplexes in an in vitro tooth model of deep caries. PLoS One. 2015;10:e0116553. PubMed PMID: 25587986
4. Klont B, ten Cate JM. Susceptibility of the collagenous matrix from bovine incisor roots to proteolysis after in vitro lesion formation. Caries Res. 1991;25:46-50.
5. Sakoolnamarka R, Burrow MF, Kubo S, Tyas MJ. Morphological study of demineralized dentine after caries removal using two different methods. Aust Dent J. 2002;47:116-22.
6. Tavafoghi M, Cerruti M. The role of amino acids in hydroxyapatite mineralization. J R Soc Interface. 2016;13:20160462. PubMed PMID: 27707904
7. Orsini G, Ruggeri A, Mazzoni A, Nato F, Manzoli L, Putignano A, et al. A review of the nature, role, and function of dentin non-collagenous proteins. Part 1: proteoglycans and glycoproteins. Endodontic Topics. 2009;21:1-18.
8. Hassan MI, Sun T, Sultana N. Fabrication of nanohydroxyapatite/poly(caprolactone) composite microfibers using electrospinning technique for tissue engineering applications. J Nanomater. 2014;2014:1-7.
9. Nichols HL, Zhang N, Zhang J, Shi D, Bhaduri S, Wen X. Coating nanothickness degradable films on nanocrystalline hydroxyapatite particles to improve the bonding strength between nanohydroxyapatite and degradable polymer matrix. J Biomed Mater Res A. 2007;82:373-82.
10. Zhou H, Lee J. Nanoscale hydroxyapatite particles for bone tissue engineering. Acta Biomater. 2011;7:2769-81.
11. Raucci MG, D'Antò V, Guarino V, Sardella E, Zeppetelli S, Favia P, et al. Biomineralized porous composite scaffolds prepared by chemical synthesis for bone tissue regeneration. Acta Biomater. 2010;6:4090-9.
12. Maione S, Pérez-Madrigal MM, del Valle LJ, Díaz A, Franco L, Cativiela C, et al. Biodegradable nanofibrous scaffolds as smart delivery vehicles for amino acids. J Appl Polym Sci [Internet]. 2017;134. Available from: https://onlinelibrary.wiley.com/doi/10.1002/app.44883
13. Hassan MI, Sultana N. Characterization, drug loading and antibacterial activity of nanohydroxyapatite/polycaprolactone (nHA/PCL) electrospun membrane. 3 Biotech. 2017;7:249. PubMed PMID: 28714045
14. Krishnan A, Raghu S, Eswaramoorthy R, Perumal G. Biodegradable glutamic acid loaded polycaprolactone nanofibrous scaffold for controlled dentin mineralization. J Drug Deliv Sci Technol. 2025;104:106546.
15. Wang Z, Xu Z, Zhao W, Sahai N. A potential mechanism for amino acid-controlled crystal growth of hydroxyapatite. J Mater Chem B. 2015;3:9157-67.
16. Krishnan A, Raghu S, Arumugam P, Eswaramoorthy R. Assessment of Physicochemical Characterization and Mineralization of Nanofibrous Scaffold Incorporated With Aspartic Acid for Dental Mineralization: An In Vitro Study. Cureus. 2024;16:e61741. PubMed PMID: 38975499
17. Miranda M, Torrecillas R, Fernández A. Reactivity of Ca and P precursors to form hydroxyapatite and its influence on the properties of the obtained powders. Ceram Int. 2020;46:27860-5.
18. Moradian-Oldak J, George A. Biomineralization of Enamel and Dentin Mediated by Matrix Proteins. J Dent Res. 2021;100:1020-9.
19. Ma P, Yan W, Tian Y, He J, Brookes SJ, Wang X. The Importance of Serine Phosphorylation of Ameloblastin on Enamel Formation. J Dent Res. 2016;95:1408-14.
20. Sequeira DB, Diogo P, Gomes BPFA, Peça J, Santos JMM. Scaffolds for Dentin-Pulp Complex Regeneration. Medicina (Kaunas). 2023;60:7. PubMed PMID: 38276040
21. Noohi P, Abdekhodaie MJ, Nekoofar MH, Galler KM, Dummer PMH. Advances in scaffolds used for pulp-dentine complex tissue engineering: A narrative review. Int Endod J. 2022;55:1277-316.
22. Wang Y, Zhang S, Liu P, Li F, Chen X, Wang H, et al. L-serine combined with carboxymethyl chitosan guides amorphous calcium phosphate to remineralize enamel. J Mater Sci Mater Med. 2023;34:45. PubMed PMID: 37658964
23. Liang K, Xiao S, Shi W, Li J, Yang X, Gao Y, et al. 8DSS-promoted remineralization of demineralized dentin in vitro. J Mater Chem B. 2015;3:6763-72.
24. Gulzar RA, Ajitha P, Subbaiyan H. Self-Assembling Peptide P11-4 for Enamel Remineralization: A Biomi-

metic Approach. J Pharm Res Int. 2020;83-9.
25. Salgado CL, Teixeira BIB, Monteiro FJM. Biomimetic Composite Scaffold With Phosphoserine Signaling for Bone Tissue Engineering Application. Front Bioeng Biotechnol. 2019;7:206. PubMed PMID: 31552233
26. Yu L, Rowe DW, Perera IP, Zhang J, Suib SL, Xin X, et al. Intrafibrillar Mineralized Collagen-Hydroxyapatite-Based Scaffolds for Bone Regeneration. ACS Appl Mater Interfaces. 2020;12:18235-49.
27. Rajendran R, Antonys DP, Faizal N, Oommen S, Vijayasree G, Ashik PM. Comparative Evaluation of Remineralizing Potential of Topical Cream Containing Casein Phosphopeptide-Amorphous Calcium Phosphate and Casein Phosphopeptide-Amorphous Calcium Phosphate with Fluoride: An Study. J Pharm Bioallied Sci. 2024;16(Suppl_2):S1801-4.

Biomedical Sciences and Clinical Medicine 2026;65(1):11-22.
doi: 10.12982/BSCM.2026.15
https://he01.tci-thaijo.org/index.php/CMMJ-MedCMJ/index

BSCM
Biomedical Sciences and Clinical Medicine

Original Article

Open Access

Prevalence of Vitamin D Deficiency in Diabetic Neuropathy Patients in the South Indian Population

Vadivel Mani[1], Madhavi Kandregula[1], Gayathri Venkatasan[2] and Muninathan Natarajan[3]

[1]Department of Biochemistry, Konaseema Institute of Medical Sciences and Research Foundation, Amalapuram, East Godavari, Andhra Pradesh, India; [2]Department of Physiology, Sapthagiri Institute of Medical Sciences and Research Center, Bangaluru, Karnataka, India; [3]CRL Department, Meenakshi Medical College Hospital and Research Institute, Meenakshi Academy of Higher Education and Research, Kanchipuram, Tamil Nadu, India

Correspondence:
Vadivel Mani, PhD,
Department of Biochemistry,
Konaseema Institute of Medical Science and Research Foundation, Amalapuram, East Godavari -533201, Andhra Pradesh, India.
E-mail: velvdm.vel5@gmail.com

Received: May 24, 2025;
Revised: July 22, 2025;
Accepted: August 1, 2025

ABSTRACT

OBJECTIVE This research explores the prevalence of vitamin D deficiency among diabetic neuropathy patients in South India, highlighting the significant impact of this deficiency on health outcomes, particularly of the sensory-motor type.

METHODS A cross-sectional study at Koonaseema Institute of Medical Science and Research Foundation (KIMS&RF) found a significant association between vitamin D deficiency and diabetic neuropathy, with factors such as sociodemographic, risk factors, treatment duration, treatment modality, DPN score, hyperalgesia, and neuropathic pain.

RESULTS A study of 480 diabetic neuropathy patients found that 88.54% of them had a deficiency in vitamin D. Of those patients, 51.43% had insufficiency, while 37.11% had a more severe deficiency. The statistical analysis was conducted using Excel and the 16th edition of SPSS (Statistical Package for the Social Sciences). Literate individuals had lower vitamin D levels, while middle-class individuals were more likely. Obesity was linked to vitamin D insufficiency, with 65.60% of obese patients having insufficient vitamin D. Treatment modalities, sensory thresholds, and neuropathic pain symptoms were also associated with vitamin D deficiency.

CONCLUSIONS This study in South India found that 88.54% of individuals, particularly those with diabetic neuropathy, were deficient in vitamin D. This is lower than in Egypt, but higher than in the UAE and China. Factors affecting vitamin D levels affect both males and females, with a higher impact on males. Complications from diabetic neuropathy are linked to vitamin D insufficiency. Further research is needed to validate these findings.

KEYWORDS vitamin D, diabetic neuropathy, hyperalgesia, neuropathic pain

INTRODUCTION

Diabetic neuropathy (DPN) contributes significantly to the morbidity associated with diabetes mellitus as a chronic microvascular consequence (1). DPN causes significant morbidity, elevated mortality, and a reduced quality of life for those who have it (2). In addition to raising the chance of lower limb amputation, it also imposes additional financial strain on patients and their families since affected individuals must take more pain killers

and see a doctor more frequently, which makes it harder for them to work or carry out everyday tasks (3). Neuropathic pain, a crippling symptom of DPN, adds significantly to the burden of pain management worldwide.

Researchers anticipate an increase in DPN prevalence due to the ageing of the world's population and the growing number of diabetes mellitus patients (4). People with type 2 diabetes (T2DM) experience DPN more commonly than those with type 1 diabetes (T1DM) (5). Previous epidemiological research examined China's DPN prevalence and reported it to be 57.20%. According to estimates from 2020, between 18.80% and 61.90% of Indians have diabetic peripheral neuropathy (DPN), with the sensory-motor type being the most often reported among diabetics (6).

In addition to being essential for metabolic health, researchers have connected vitamin D to a number of physiological mechanisms that affect diabetic complications such as neuropathy. Because poor glycemic control exacerbates neuropathic symptoms, researchers found a substantial interaction between vitamin D levels and insulin sensitivity (7). The way that vitamin D affects insulin resistance and secretion emphasizes how vitamin D levels may impact the severity of DPN as well as diabetes management.

Researchers indicate that vitamin D deficiency widely prevails across the Indian subcontinent, with some groups reporting deficiency rates as high as 100.00% (8). For South Indian patients with diabetic neuropathy, who may experience exacerbated health problems due to their illness, this alarming statistic raises significant concerns. A systematic analysis emphasizes the critical need for public health interventions, reporting a pooled prevalence of 68.00% for vitamin D deficiency in South Asia, including India (9).

A comprehensive analysis has indicated that a significant percentage of Indians, ranging from 40.00% to 99.00%, may have a deficiency in vitamin D (10). Individuals with diabetes are particularly at risk due to their elevated dietary needs. This study underscores the importance of implementing food fortification programmes and conducting public awareness campaigns to mitigate the prevalence of vitamin D deficiency in individuals with diabetic neuropathy.

In addition to neuropathy, vitamin D insufficiency has been associated with other diabetes-related issues such as retinopathy, demonstrating its broader health impacts (11). This connection underscores the importance of comprehensive monitoring and intervention strategies for diabetic patients. Assy et al. suggests that vitamin D levels may influence not just neuropathy but the entire spectrum of diabetic complications.

Moreover, it is important to highlight the role of vitamin D in enhancing insulin sensitivity, underscoring its significance in effective diabetes management. Improving glycemic control is essential for minimizing the likelihood of complications, and increased insulin sensitivity can directly benefit people suffering from DPN (12). This research investigated the frequency of vitamin D deficiency among individuals with DPN in south India. It extends existing studies which emphasize the notable occurrence of this deficiency and its implications for health outcomes. Furthermore, the report identifies areas where information is lacking and provides recommendations for potential future research topics.

METHODS

Subjects

The study recruited 480 adult subjects aged 20-60 from the General Medicine OPD, Koonaseema Institute of Medical Science and Research Foundation, based on criteria such as diagnosis of T2DM mellitus, stable antidiabetic treatment, painful distal symmetrical and sensorimotor polyneuropathy, diabetic neuropathy, DPN characterized by a Neuropathy Disability Score (NDS) of 6 or higher, a reported Visual Analogue Scale (VAS) score of at least 4 for pain, and a Neuropathy Symptom Score (NSS) of 5 or above. Participants with T1DM, who were pregnant or lactating, and those with related endocrine disorders were excluded from the study. Other exclusion criteria included concurrent trials, inability to provide informed consent, malignancies, chronic liver disease, anemia, renal failure, obsessive- compulsive disorder, chronic inflammatory conditions, hypersensitivity to medication, and non-compliance with study medication.

Study design

A cross-sectional study was conducted in the Konaseema area of Andhra Pradesh. The study

focused on individuals with DPN who were receiving treatment at the General Medicine Outpatient Department of the Konaseema Institute of Medical Sciences and Research Foundation (KIMS&RF).

The study was conducted from September 2023 through August, 2024. The required approval from the Institutional Ethics Committee was obtained before starting the study (reference number IEC/PR/2023: 21/04.03.2023). After being evaluated for study eligibility, individuals found to meet the inclusion criteria a baseline measure of diabetic polyneuropathy was assessed using the NDS score, the NSS, and the VAS (visual analogue scale, to measure painful symptoms). According to the authors, Akter et al., a mean score of more than NDS ≥ 6, NSS ≥ 5, and VAS ≥ 4 indicates diabetic polyneuropathy (13). Vitamin D levels were categorised into three groups: vitamin D deficiency (< 15 ng/mL), vitamin D insufficiency (15-29 ng/mL), and vitamin D sufficiency (≥ 30 ng/mL) based on the national population represented in the NHANES 2001-2004 study (National Health and Nutrition Examination Survey) (14).

Ethics

The study protocol was approved by the Institution Committee of Ethics in Human Research, a division of the Konaseema Institute of Medical Sciences & Research Foundation, in accordance with Indian Council of Medical Research regulations (Ref. No. IEC/PR/2021:114). Each patient who wished to participate in the research signed a written informed permission form after being informed about the study.

Data collection

Upon obtaining written informed consent, sociodemographic information, the duration of diabetes, and the type of therapy received were collected. Common evaluation techniques, e.g., the VAS, NSS and NDS were utilised to assess DPN (15). The Toronto Clinical Neuropathy Scoring System was employed to quantify the severity of neuropathy, using the average DPN score (NSS+NDS+VAS) to categorise patients into mild, moderate, and severe groups (16). Blood samples were drawn from the antecubital vein and were then centrifuged at 4,000 rpm, with the resulting serum stored at -20°C for further examination. The COBAS 602 automated platform, which utilises Chemiluminescent Immunoassay (CMIA) technology, was employed to analyse 25-OH vitamin D levels. Patients with diabetic polyneuropathy were categorised into three groups based on their vitamin D levels: deficient (< 15 ng/mL), insufficient (20-30 ng/mL), and sufficient (> 30 ng/mL).

Quantitative sensory testing

Quantitative sensory testing (QST) was used to assess hyperalgesia, which is an increased sensitivity to pain (17). QST measures changes in sensitivity to different sensations like temperature, touch, and pressure. It helps evaluate the excitability of different pain pathways and provides insights into pain mechanisms. The CASE IV system is a QST that has been specifically designed to evaluate sensory thresholds and pain perception in individuals. This system utilises two different stimulators to measure the sensory thresholds for various stimuli, e.g., pressure, vibration, heat, and cold. The supplier of the CASE IV equipment was WR Medical Electronics Co., located in Maplewood, MN, USA. For temperature tests, the dorsal side of the hand was chosen, while the third finger was used for vibratory testing. (Supplement Table 1) The tests were conducted on the upper extremities of individuals with DPN and a control group without diabetic neuropathy, and the results were carefully recorded. After converting the raw QST findings to Z-transformation values, the criteria for hyperalgesia in the patients were established. It was observed that a difference of 1 SD was present between heat pain threshold (HPT) values of 0.5 and 5, while a difference of 2 SD was noted between the control group and the illness group.

Neuropathic pain screening

Ten "yes/no" questions about neuropathic pain make up the douleurneuropathique (DN)4 Questionnaire (18). The score is determined by adding up the "yes" responses, and ranges from "0" (no neuropathic pain) to "10" (the most severe neuropathic pain).

Statistical analysis

Continuous variables underwent normality testing using the Kolmogorov-Smirnov test to assess their distribution. Variables that exhibited a normal distribution are presented as mean ± standard deviation; others are reported as median

(interquartile range). Categorical variables are expressed using either percentages or proportions. Statistical Significance was set at $p < 0.05$, and appropriate tests of significance, such as the independent *t*-test and the chi-square test for categorical data, were employed. Data entry and analysis were facilitated using Excel and the 16th edition of SPSS (Statistical Package for the Social Sciences). Prevalence was determined based on the available data. Associations between vitamin D deficiency and various factors, including duration of diabetic treatment, treatment mode, DPN score, hyperalgesia, and neuropathic pain, were demonstrated using the 95% confidence interval (CI) and odds ratio (OR). The 'yes' response rate in the DN4 questionnaire was compared using McNemar's test.

RESULTS

A total of 424 individuals, 88.54% of the 480 DPN patients who took part in the study, had vitamin D deficiency, according to the national population as reported in the National Health and Nutrition Examination Survey (NHANES 2001-2004 study). Patients were categorised based on their vitamin D levels, with 180 patients (37.11%) having vitamin D deficiency (< 15 ng/mL) and 240 patients (51.43%) having vitamin D insufficiency (15-29 ng/mL). The mean age of those with vitamin D insufficiency was 38 years with a standard deviation of 12.4 years, and 59.40% of this group were men. Among the female participants, 108 (55.38%) were older compare to males and had vitamin D deficiency, with a statistically significant *p*-value of less than 0.00004.

Anthropometric, clinical characteristics and vitamin D level in the study population

An assessment of various characteristics in terms of their independence and correlation with vitamin D levels is pressented Table 1 presents. Several characteristics, such as education, employment position, socioeconomic level, marital status, and body mass index (BMI) status, exhibited statistically significant associations. The comparison of variables across deficient, insufficient, and sufficient categories is illustrated as row percentages. In the study group, it was

Table 1. Sociodemographic details of Diabetic Neuropathy participants with categorical representation of vitamin D levels

Variable	Total (n = 480)	Vitamin D deficiency (< 15 ng/mL) (n = 180)	Vitamin D insufficiency (15-29 ng/mL) (n = 244)	Vitamin D sufficiency (≥ 30 ng/mL) (n = 56)	*p*-value significant at $p < 0.05$
Age	37±11	44±8.34	48±12.4	28±4.55	
Male	285	95	158	32	Chi-square statistic =
Female	195	108	79	08	16.8596, $p < 0.00004^*$
Education					
Literate	320	108	180	32	Chi-square statistic =
Illiterate	160	30	50	80	95.4037, $p < 0.00001^*$
Employment status					
Employed	390	190	160	40	Fisher exact
Unemployed	90	30	50	10	$p < 0.0179^*$
Socioeconomic status					
Upper class	170	60	100	10	Chi-square statistic =
Middle class	220	80	120	20	80.3553, $p < 0.00001^*$
Lower class	90	20	30	40	
Marital status					
Married	396	190	150	56	Chi-square statistic =
Unmarried	84	28	24	32	26.6185, $p < 0.00001^*$
Hypertension	173	102	63	08	
BMI status					
Obese	320	82	210	28	Chi-square statistic =
Non-obese	205	106	88	11	33.7539, $p < 0.00001^*$

$^*p < 0.05$ were considered statistically significant

BMI, body mass index. In the table, results represent the arithmetic mean ± predictable error of diabetic neuropathy subjects.

observed that literate individuals (n = 320, 66.66%) were more likely to have lower vitamin D levels than non-literate individuals, especially those with insufficiency (n = 180, 56.30%); chi-square statistic = 95.4037; $p < 0.00001$. Examination of diabetic neuropathy found it to be relatively independent of socioeconomic position, with middle-class DPN individuals (n = 220) showing a higher likelihood of vitamin D deficiency (n = 120, 54.54%); chi-square statistic = 80.3553, $p < 0.00001$. Furthermore, it was observed that married individuals (n = 396) had a higher prevalence of vitamin D deficit (n = 190, 47.97%), while those with DPN tended to experience vitamin D insufficiency (chi-square statistic = 26.6185, $p < 0.00001$). A correlation was found between vitamin D status and BMI, with 65.60% of the 320 DPN individuals who were obese having vitamin D insufficiency. Additionally, 25.60% of the obese DPN patients were compared for vitamin D deficiency.

Correlation of vitamin D deficiency with different variables of diabetic neuropathy

The study looked at the relationship between a number of variables and the onset of vitamin D deficiency in diabetic neuropathy. With a non-adjusted odds ratio of 2.93 and a $p < 0.001$, suggesting high statistical significance, it was shown that vitamin D deficiency was significantly more common among patients (52.10%) who were taking long-term diabetes medication. Treatment modalities, including metformin and sulfonylurea at 49.00% (non-adjusted odds ratio 2.67, $p < 0.001$), moderate DPN score at 50.10% (non-adjusted odds ratio 2.83, $p < 0.001$), and DPN symptoms with hyperalgesia at 69.00% (non-adjusted odds ratio of 3.89, $p = 0.001$), were significantly associated with vitamin D deficiency as shown in Table 2. We studied the relationship between several factors and the onset of vitamin D insufficiency in diabetic neuropathy. It was discovered that of patients receiving long-term diabetic treatment, 52.10% had a significantly high chance of developing vitamin D deficiency, with a non-adjusted OR of 2.93, $p < 0.001$, which is highly significant. As shown in Table 2, along with vitamin D level, treatment modality with Metformin & sulfonylurea 49.00% (non-adjusted OR 2.67, $p < 0.001$), a moderate DPN score of 50.10% (non-adjusted OR 2.83, $p < 0.001$) and DPN symptoms with hyperalgesia 69.00% (non-adjusted OR of 3.89, $p = 0.001$) were also significantly associated with vitamin D deficiency.

Comparison of QST components in the diabetic neuropathy group and the controls without neuropathy

The levels of QST were compared between groups to assess sensory thresholds. In the tests of cold detection threshold (CDT), heat detection threshold (HDT), and vibration detection threshold (VDT), it was found that the group of DPN patients with vitamin D deficiency (n = 331) ex-

Table 2. Association between selected variables in diabetic neuropathy and vitamin D deficiency

Variable	n (%)	OR	95%CI	*p*-value
Duration of diabetic treatment				
0-5 years	150 (31.30)	1.35	1.02-1.82	0.015*
5-10 years	250 (52.10)	2.63	1.70-4.06	< 0.001*
11-20 years	80 (16.70)			
Treatment modality				
Metformin	80 (16.70)	1.40	1.08–1.79	0.010
Metformin with sulfonylurea	235 (49.00)	2.63	1.70-4.06	< 0.001*
Metformin with DPP-4 inhibitors	165 (34.30)	1.93	1.09-3.41	0.009*
DPN Score				
Mild (5-8)	105 (21.90)	1.43	0.95-2.67	0.052
Moderate (9-11)	244 (50.10)	2.93	1.62-4.11	< 0.001*
Severe (12-15)	141 (29.40)	3.05	1.76-4.28	< 0.001*
Hyperalgesia	331 (69.00)	2.89	1.82-4.17	< 0.001*
Neuropathic pain	149 (39.20)	2.03	1.63-3.89	< 0.005*

*$p < 0.05$ were considered statistically significant.
DPN, diabetic neuropath; CI, confidence interval; OR, odds ratio

Table 3. Comparison of quantitative sensory testing components in the diabetic neuropathy group and the group without neuropathy (control).

Variable	Control: diabetic without neuropathy (N = 56)	Diseases: diabetic neuropathy with vitamin D deficiency (N = 331)	*p*-value significant at $p < 0.05$
CDT	5.43±1.14	8.33±2.11	0.001
HDT	6.55±1.45	12±2.55	< 0.001
VDT	12.55±2.15	15.2±2.65	0.001
HPT 0.5	18.44±3.15	13.11±2.95	0.005
HPT 5.0	23.85±2.88	20.2±3.05	0.010
HPT 0.5–5.0	5.45±1.32	7.1±1.45	0.005

CDT, cold detection threshold; HDT, heat detection threshold; VDT, vibration detection threshold; HPT, heat pain threshold

Table 4. Comparison of Douleur Neuropathique (DN)4 questionnaire responses of adult patients with painful diabetic neuropathy.

Variable	Control: diabetic without neuropathy (N = 56)	Diseases: diabetic neuropathy with vitamin D deficiency (N = 331)
Burning	38 (67.90)	140 (94.0)*
Painful cold	39 (69.60)	146 (98.0)*
Electric shock tingling	26 (46.40)	139 (93.0)*
Pins and needles	33 (58.90)	140 (94.0)*
Tingling	41 (73.20)	146 (98.0)*
Numbness	45 980.40)	144 (96.6)*
Itching	36 (64.30)	145 (97.3)*
Hypoesthesia to touch	40 (71.40)	139 (93.0)*
Hypoesthesia to prick	44 (78.60)	136 (91.3)*
The pain is caused or increased by brushing	43 (76.80)	145 (97.3)*

*Statistically significant differences ($p < 0.05$; McNemar's test)
Data presented as n (%) of positive responses.

hibited higher sensory thresholds than the non-neuropathic controls in both their painful and nonpainful extremities ($p < 0.05$). Furthermore, it was observed that the DPN group's HPT 0.5 and HPT 0.5-5.0 values were lower than those of the healthy controls ($p < 0.05$). However, there was no statistically significant difference in HPT 5 readings between the groups ($p > 0.05$). For a detailed intergroup analysis, refer to Table 3.

Comparison of the (DN)4 questionnaire in the diabetic neuropathy group and the without neuropathy controls

Comparison of the (DN)4 questionnaire was performed between the groups. The group with DPN with vitamin D deficiency (n = 149 patients) had higher neuropathic pain symptoms than the non-neuropathic controls. Statistically significant reductions in neuropathic pain symptoms were noted by McNemar's test, p value less than 0.05 (Table 4).

DISCUSSION

Vitamin D is a fat-soluble vitamin that plays a crucial role in various physiological processes. Vitamin D deficiency potentially contributes to bone disorders like osteomalacia and osteoporosis, increasing fracture risk, and is associated with muscle weakness and falls. Furthermore, vitamin D deficiency is linked to autoimmune diseases, cardiovascular issues, and possibly certain cancers. Vitamin D deficiency can contribute to neuropathy through several interconnected mechanisms, including impaired nerve growth and repair, increased inflammation, increased oxidative stress and potential effects on blood

sugar control. Specifically, vitamin D, through its receptor (VDR), plays a role in nerve growth factor (NGF) production, which is crucial for nerve health. Furthermore, vitamin D deficiency can exacerbate inflammation, a process implicated in nerve damage, and may also affect glucose metabolism, a key factor in diabetic neuropathy. Supplementing with vitamin D has an impact on both extra skeletal and skeletal health. In addition to supporting bone health, vitamin D can also affect immunological, neuromuscular, and cell growth, while also helping to reduce inflammation. It's important to note that excessive supplementation of vitamin D can potentially lead to harmful effects such as renal damage and hypercalcemia.

This groundbreaking study is the first of its kind to be conducted in southern India with the primary objective of assessing the levels of serum vitamin D in individuals with diabetic neuropathy. In the study, 88.54% of the subjects were found to have decreased vitamin D: 51.43% had an insufficiency, while 37.11% had a deficiency. These findings indicate a remarkably high prevalence of vitamin D deficiency overall in the population studied. A cross-sectional study conducted in Egypt that included both urban and rural adult populations in Zagazig city, El-Sharkia, revealed significant findings. Two-thirds of the population had low vitamin D levels according to the study, and among those with painful diabetic neuropathy, 35.00% had low vitamin D levels, while 30.00% had painless diabetic neuropathy (19). Additionally, the study identified a notable negative correlation between vitamin D levels and neuropathy scores, suggesting that lower vitamin D levels were associated with higher neuropathy scores. In contrast, our study in southern India reported an even higher percentage of participants with serum vitamin D deficiency of 88.54%, surpassing the findings of the Egyptian study (20). Another cross-sectional study in China highlighted a high prevalence of vitamin D deficiency in distal symmetric subclinical DPN of 78.54%, as opposed to mononeuropathy and radiculopathy, diabetic neuropathy, and distal symmetric polyneuropathy (21). Furthermore, the study observed the highest prevalence of vitamin D deficiency among individuals with diabetic foot ulcers (97.44%), followed by those without foot ulcers (59.18%) (22).

A clinic-based cross-sectional survey conducted in two tertiary-level hospitals in Yogyakarta, Indonesia, revealed that 85.00% of patients were found to have vitamin D insufficiency. Moreover, the study reported that among individuals with painful diabetic neuropathy, the prevalence of vitamin D deficiency was 20.80% in men, 79.20% in women, and 98.11% in vitamin D insufficency group. The average age of the study participants was 57.83 ± 8.79 years (23). The investigators defined vitamin D deficiency as serum vitamin D levels below 30 ng/mL, and observed a high prevalence of low vitamin D levels. Using the same cut-off for vitamin D deficiency, a similar overall prevalence of 98.11% was found, with an 88.54% prevalence among diabetic individuals. Additionally, the study revealed a 79.20% prevalence of vitamin D deficiency among females with a mean age of 57.83 ± 8.79 years, whereas our study had a higher prevalence of vitamin D deficiency among males age 48 ± 12.4 years (24). In India, both men and women are susceptible to vitamin D deficiency, with a slight tendency for males to be more affected. This tendency is likely influenced by a combination of factors, such as dietary habits, lifestyle choices, and societal norms that impact sun exposure (25). Our study delved into the reasons behind the higher prevalence of vitamin D deficiency in males.

Research studies have extensively documented the frequency of vitamin D insufficiency in healthy individuals and in individuals with diabetes complications such as diabetic retinopathy and diabetic nephropathy in both Indian and Western populations (26). However, there is a lack of statistical documentation regarding the prevalence of vitamin D deficiency in the community of individuals with DPN in south India.

One study uncovered a high rate of vitamin D deficiency among employed individuals, with 39.60% found to be deficient, and 33.30% having insufficiency. These significant findings were obtained from a retrospective observational cross-sectional study conducted in south India which included both urban and rural adult populations in Nalanda District, Kerala, South India (27). The study indicated that 89.20% of employed individuals in the population had low levels of vitamin D. The figures were 27.60% for skilled workers, 28.10% for semiskilled workers, 7.90%

for unskilled workers, 9.20% for professionals, and 8.40% for semi-professionals. This trend is likely influenced by various factors, including dietary habits and employment choices impacting sun exposure, such as skilled and professional workers. The prevalence of indoor work among employees in South India is a significant aspect of the region's workforce, especially with the increased work-from-home practices post-pandemic, particularly in the IT sector (28). The study specifically investigated the reasons behind the greater incidence of vitamin D insufficiency among working people.

In South India, we conducted a comprehensive analysis of various socioeconomic variables among individuals with diabetic neuropathy. Out of the total population studied, 90 individuals (18.80%) were found to be living below or near the poverty level, while 220 individuals (45.70%) belonged to the middle class, and 170 individuals (35.50%) were classified as upper class. Comparing these findings with the national growth benchmark revealed that 31.00% of the population perceived themselves as middle class, aligning closely with national data. A National Institutes of Health (NIH) research study claims that higher socioeconomic classes and urban areas exhibit higher rates of risk factors for cardiovascular diseases (CVDs), including high cholesterol, diabetes, and hypertension (29). Furthermore, in India, it has been observed that families in the upper and middle classes are more inclined to use statins compared to those in lower socioeconomic levels (30). Our study corroborated this trend, revealing a greater incidence of vitamin D deficiency in middle-class households.

A study indicated that 31.30% of married people were insufficient in vitamin D, and 39.60% of them were deficient. Those results were obtained from a community-based cross-sectional study conducted in the West Bengali village of Singur, which revealed that 70.60% of the populace was deficient in vitamin D (31). The study highlighted that vitamin D deficiency is more prevalent among married individuals, particularly women, due to various factors including lifestyle, social roles, and biological differences. Reasons for this higher prevalence include consuming more calorie-dense foods and receiving less sun exposure as a result of domestic responsibilities. Furthermore, differences in fat distribution and hormonal fluctuations may contribute to lower vitamin D levels in women compared to men (32, 33).

According to one study, overall, 210 DPN individuals are obese, with 25.60% of obese individuals found to be deficient in vitamin D and 65.60% insufficient. These significant findings were gleaned from a case-control study conducted in the Endocrinology-Diabetology and Nutrition Department of a tertiary center in Oujda, Morocco. In that study, in the obese population 32.80% had vitamin D deficiency and 65.70% had vitamin D insufficiency (34). Individuals who are obese have a much higher likelihood of experiencing vitamin D insufficiency compared to those of normal body weight. A meta-analysis revealed that obese individuals have a 3.70 OR for vitamin D insufficiency, significantly higher than that of healthy study participants (35). This suggests that vitamin D deficiency is more prevalent among individuals who are obese. Studies have indicated that vitamin D insufficiency is widespread among obese individuals, with rates reaching as high as 78.30% of the population (36). The lower levels of vitamin D in obese individuals are associated with an increased risk of neuropathy.

Association between selected variables in diabetic neuropathy and vitamin D deficiency

Numerous pieces of evidence have established a clear link between vitamin D insufficiency and the consequences of diabetic neuropathy. The current study revealed that vitamin D deficiency is significantly more prevalent in DPN patients experiencing difficulties compared to diabetic patients without complications, with percentages of 88.54% and 11.46%, respectively. The current study also identified a robust correlation between vitamin D insufficiency and the severity of diabetic polyneuropathy, its symptoms, treatment techniques, and the duration of treatment. This study highlighted the high prevalence of vitamin D deficiency among diabetic patients with diabetic polyneuropathy who had been undergoing treatment for 5-10 years (52.10%) compared to those with below 5 years of treatment and above 10 years of treatment. The observed trend could potentially be attributed to the decreased metabolism of vitamin D in prolonged uncontrolled diabetes (37). Additionally, findings from previous

studies by Hassan et al. (2010) suggest that the duration of diabetes not only impacts glucose control but also influences other health outcomes, including vitamin D levels (38). This relationship underscores the importance of healthcare providers monitoring the vitamin D status as part of routine care for patients with prolonged diabetes.

The present study also highlighted the high prevalence of vitamin D deficiency among diabetic patients with diabetic polyneuropathy who had been undergoing treatment with metformin with sulfonylurea n = 235 (49.00%), in comparison to those with only metformin and treatment with metformin with DPP-4 inhibitors. Research has shown that combining metformin and sulfonylurea is effective in managing T2DM. It's important to be aware of potential adverse effects, such as vitamin deficiencies, when using these medications. In particular, the use of metformin may lead to reduced absorption of vitamin B12 (39). In long-term patients who continued to use sulfonylurea, studies have indicated that B12 levels were lower in 10 out of 17 observational studies of T2DM patients taking metformin, with reductions ranging from 28.00% to 48.00% (40). A deficiency in B12 can disrupt important metabolic functions, potentially impacting the body's ability to metabolise vitamin D and potentially worsening bone density-related health issues. Furthermore, a cross-sectional study revealed a correlation between communities at risk of vitamin D deficiency and the presence of anaemia due to B12 deficiency (41). Our study compared the frequency of vitamin D deficiency among diabetic patients receiving different treatments. We found a high frequency of vitamin D deficiency among diabetic patients with diabetic polyneuropathy who were treated with metformin and sulfonylurea. This was observed in 49.00% of the patients in the study group of 235 individuals. This discovery emphasises the influence of B12 deficiency on vitamin D levels in diabetic neuropathy.

The study also revealed a significant incidence of vitamin D deficiency among diabetes patients with a moderate polyneuropathy score (n = 244) at 50.10%, contrasting with individuals having mild and severe polyneuropathy scores. This retrospective, cross-sectional research involved Emirati patients, including those from the secondary care unit at University Hospital Sharjah, and produced noteworthy findings. The study indicates that 50.00% of the individuals had painful diabetic neuropathy, and approximately two-thirds of the population exhibited inadequate vitamin D levels (42). Furthermore, a cross-sectional study carried out in Indonesia established a correlation between vitamin D levels and the severity of neuropathy, with moderate neuropathy accounting for 35.80% and severe neuropathy for 43.30% of the cases of vitamin D deficiency (23).

In individuals with T2DM, there is a significant association between DPN and vitamin D deficiency. Studies show that a higher DPN score is linked to lower vitamin D levels, with some reports indicating a higher prevalence of DPN in those with vitamin D deficiency (43). Specifically, patients with painful DPN tend to have lower serum vitamin D2 levels. According to a meta-analysis, diabetic people who have low vitamin D levels are 1.22 times more likely to experience DPN than those with normal vitamin D levels (44).

Diabetic peripheral neuropathy is characterised by two main signs: hyperalgesia and neuropathic pain. These signs result from sensory and motor deficits caused by nerve injury in the extremities. The development and persistence of neuropathy are greatly impacted by hyperalgesia, which involves an increased sensitivity to pain (45).

This study revealed a significant frequency of vitamin D insufficiency among diabetic patients with diabetic polyneuropathy who experienced hyperalgesia, in contrast to individuals with neuropathic pain. The study conducted a case-control comparison of neuropathy with and without pain, and the results were found to be important. According to the findings, individuals with vitamin D deficiency exhibited a notably higher NDS compared to those with painful PDN (46). The study also observed that assessments of significantly high NDS scores, including the vibration perception test, cold sensation test, and warm sensation test, were abnormal in cases of vitamin D deficiency with painful diabetic neuropathy. Elevated NDS scores were found to indicate hyperalgesia in DPN patients, where the body becomes more sensitive to pain and pain signals are heightened. The prevalence of vitamin D insufficiency was associated with hyperalgesia, a condition linked to increased pain sensitivity in various illnesses like DPN and fibromyalgia, as reported in previous studies (47).

CONCLUSIONS

The study revealed a significant difference in serum vitamin D levels between diabetic patients with and without neuropathy. In southern India, a significant 88.54% of individuals were found to be deficient in vitamin D, especially those with diabetic neuropathy. Subnormal vitamin D levels were more common in DPN patients who were obese and had long-term uncontrolled diabetes. This suggests that the occurrence and prognosis of DPN are influenced by multiple factors, with vitamin D levels potentially playing a vital role. The link between vitamin D levels and DPN deserves careful consideration, and further interventional studies involving larger numbers of patients may provide additional evidence.

Limitations of the study

The small number of sites included in this study was one of its main shortcomings. To provide a more accurate representation of the South Indian population, a multicentre study would be appropriate. Furthermore, due to the study being conducted in a hospital setting, the findings may not be applicable to the general public. Additionally, the vitamin D levels of patients without neuropathy were not compared in this study. It is evident that clinical trials and further research are crucially needed.

ACKNOWLEDGMENTS

This work was supported by the Dean of Konaseema Institute of Medical Sciences & Research Foundation.

FUNDING

This research received no specific grant from any funding agency in the public, commercial, or not-for-profit sectors.

CONFLICTS OF INTEREST

The authors have no conflicts of interest to report.

AUTHOR CONTRIBUTION

V.M: conceptualization, methodology, investigation, formal analysis, and drafting the manuscript; M.K: investigation, Formal analysis, and writing-original draft, supervision, and project leadership; G.V: writing-original draft and investigation; M.N: visualization, and writing-review & editing. All authors have reviewed and endorsed the final manuscript.

DATA AVAILABILITY STATEMENT

The data that support the findings of this study are available from the corresponding author upon reasonable request.

INSTITUTIONAL REVIEW BOARD STATEMENT

The study was conducted following the Declaration of Helsinki and approved by the Institutional Review Board (or Ethics Committee) of the Faculty of Medicine, Konaseema Institute of Medical Sciences & Research Foundation, in accordance with Indian Council of Medical Research regulations (Ref No. IEC/PR/2021:114).

INFORMED CONSENT STATEMENT

Informed consent was obtained from all subjects involved in the study.

SUPPLEMENTARY MATERIALS

The following supporting information can be downloaded at: Supplementary file

REFERENCES

1. Lu Y, Wang W, Liu J, Xie M, Liu Q, Li S. Vascular complications of diabetes: A narrative review. Medicine (Baltimore). 2023;102(40):e35285. PubMed PMID: 37800828
2. Yang Y, Zhao B, Wang Y, Lan H, Liu X, Hu Y, Cao P. Diabetic neuropathy: cutting-edge research and future directions. Signal Transduct Target Ther. 2025;10(1):132. PubMed PMID: 40274830
3. Ziegler D, Tesfaye S, Spallone V, Gurieva I, Al Kaabi J, Mankovsky B, et al. Screening, diagnosis and management of diabetic sensorimotor polyneuropathy in clinical practice: International expert consensus recommendations. Diabetes Res Clin Pract. 2022; 186:109063. PubMed PMID: 34547367
4. Nabrdalik K, Kwiendacz H, Moos J, Moos Ł, Kulpa J, Brzoza Z, et al. Diabetic Peripheral Neuropathy is Associated with Diabetic Kidney Disease and Cardiovascular Disease: The Silesia Diabetes-Heart Project. Curr Probl Cardiol. 2023;48(8):101726. PubMed PMID: 36967071
5. Feldman EL, Callaghan BC, Pop-Busui R, Zochodne DW, Wright DE, Bennett DL, et al. Diabetic neuropathy. Nat Rev Dis Primers. 2019;5:42. PubMed PMID: 31197183
6. Mathiyalagen P, Kanagasabapathy S, Kadar Z, Rajagopal A, Vasudevan K. Prevalence and determinants of peripheral neuropathy among adult type II dia-

betes mellitus patients attending a non-communicable disease Clinic in Rural South India. Cureus. 2021;13:e15493. PubMed PMID: 34268025
7. Vasdeki D, Tsamos G, Dimakakos E, Patriarcheas V, Koufakis T, Kotsa K, et al. Vitamin D Supplementation: shedding light on the role of the sunshine vitamin in the prevention and management of type 2 diabetes and its complications. Nutrients. 2024;16(21):3651. PubMed PMID: 39519484
8. Ritu G. Vitamin D deficiency in India: prevalence, causalities and interventions. Nutrients. 2014;6:729-75.
9. Siddiqee MH, Bhattacharjee B, Siddiqi UR, Meshba hurRahman M. High prevalence of vitamin D deficiency among the South Asian adults: a systematic review and meta-analysis. BMC Public Health. 2021;21(1):1823. PubMed PMID: 34627207
10. Sanwalka N. Vitamin D Deficiency in Indians – Prevalence and the Way Ahead. J Clin Nutr Diet. 2016, 1.
11. Luo BA, Gao F, Qin LL. The association between vitamin D deficiency and diabetic retinopathy in type 2 diabetes: a meta-analysis of observational studies. Nutrients. 2017;9:307. PubMed PMID: 28335514
12. Argano C, Mirarchi L, Amodeo S, Orlando V, Torres A, Corrao S. The role of vitamin D and its molecular bases in insulin resistance, diabetes, metabolic syndrome, and cardiovascular disease: state of the art. Int J Mol Sci. 2023;24:15485. PubMed doi: 10.3390/ijms242015485
13. Akter S, Choubey M, Mohib MM, Arbee S, Sagor MAT, Mohiuddin MS. Stem cell therapy in diabetic polyneuropathy: recent advancements and future directions. Brain Sci. 2023;13:255. PubMed PMID: 36831798
14. Farag YMK, Guallar E, Zhao D, Kalyani RR, Blaha MJ, Feldman DI, et al. Vitamin D deficiency is independently associated with greater prevalence of erectile dysfunction: The National Health and Nutrition Examination Survey (NHANES) 2001-2004. Atherosclerosis. 2016;252:61-7.
15. Verriotis M, Peters J, Sorger C, Walker SM. Phenotyping peripheral neuropathic pain in male and female adolescents: pain descriptors, somatosensory profiles, conditioned pain modulation, and child-parent reported disability. Pain. 2021;162:1732-48.
16. Dalimunthe Dina, ArwinaSinambela, Duma Wenty Irene, Lubis Syahril Rahmat. Toronto clinical scoring system: A promising diagnostic tool in leprosy neuropathy. Dermatologica Sinica. 2022;40:231-4.
17. Arant KR, Katz JN, Neogi T. Quantitative sensory testing: identifying pain characteristics in patients with osteoarthritis. Osteoarthritis Cartilage. 2022;30:17-31.
18. Spallone V, Morganti R, D'Amato C, et al. Validation of DN4 as a screening tool for neuropathic pain in painful diabetic poly neuropathy. Diabet Med. 2012;29: 578-85.
19. Kumar J, Muntner P, Kaskel FJ, Hailpern SM, Melamed ML. Prevalence and associations of 25-hydroxyvitamin D deficiency in US children: NHANES 2001-2004. Pediatrics. 2009;124:e362-70.
20. Assy MH, Draz NA, Fathy SE, Hamed MG. Impact of vitamin D level in diabetic people with peripheral neuropathy. Egypt J Neurol Psychiatry Neurosurg. 2021;57:117-24.
21. Sun X, Yang X, Zhu X, Ma Y, Li X, Zhang Y, et al. Association of vitamin D deficiency and subclinical diabetic peripheral neuropathy in type 2 diabetes patients. Front Endocrinol (Lausanne). 2024;15:1354511. PubMed PMID: 38590822
22. Danny Darlington CJ, Suresh Kumar S, Jagdish S, Sridhar MG. Evaluation of Serum Vitamin D Levels in Diabetic Foot Infections: A Cross-Sectional Study in a Tertiary Care Center in South India. Iran J Med Sci. 2019;44:474-82.
23. PINZON R. T, A W PRADANA and ANGELA. The prevalence and determinant factors of low vitamin D levels in patients with painful diabetic neuropathy. Asian J Pharm Clin Res. 2021;14:116-20.
24. Shukla K, Sharma S, Gupta A, Raizada A, Vinayak K. Current scenario of prevalence of vitamin D deficiency in ostensibly healthy indian population: a hospital based retrospective study. Indian J Clin Biochem. 2016;31:452-7.
25. Senthil A, Anandh B, Jayachandran P, Thangavel G, Josephin D, Yamini R, et al. Perception and prevalence of work-related health hazards among health care workers in public health facilities in southern India. Int J Occup Environ Health. 2015;21:74-81.
26. Pradeepa R, Mohan V. Epidemiology of type 2 diabetes in India. Indian J Ophthalmol. 2021;69:2932-8.
27. Kodali NK, Bhat LD, Phillip NE, Koya SF. Prevalence and associated factors of cardiovascular diseases among men and women aged 45 years and above: Analysis of the longitudinal ageing study in India, 2017-2019. Indian Heart J. 2023;75:31-5.
28. Patanjali, S., & Bhatta, N. M. K. Work from Home During the Pandemic: The Impact of Organizational Factors on the Productivity of Employees in the IT Industry. Vision. 2022;29:326-38.
29. Samuel P, Antonisamy B, Raghupathy P, Richard J, Fall CH. Socio-economic status and cardiovascular risk factors in rural and urban areas of Vellore, Tamilnadu, South India. Int J Epidemiol. 2012;41:1315-27.
30. Schultz WM, Kelli HM, Lisko JC, Varghese T, Shen J, Sandesara P, Quyyumi AA, Taylor HA, Gulati M, Harold JG, Mieres JH, Ferdinand KC, Mensah GA, Sperling LS. Socioeconomic status and cardiovascular outcomes: challenges and interventions. Circulation. 2018;137:2166-78.
31. Pan T, Banerjee R, Dasgupta A, Paul B. Vitamin D status among women aged 40 years and above in a rural area of West Bengal: A community-based study. J Family Med Prim Care. 2018;7:1263-67.
32. Yan X, Zhang N, Cheng S, Wang Z, Qin Y. Gender differences in vitamin D status in China. Med Sci Monit. 2019;25:7094-9.
33. Elshafie DE, Al-Khashan HI, Mishriky AM. Comparison of vitamin D deficiency in Saudi married couples. Eur J Clin Nutr. 2012;66:742-5.
34. Derbel S, Zarraa L, Assarrar I, Bouichrat N, Rouf S, Latrech H. Assessment of vitamin D status in obese and non-obese patients: A case- control study. Diabetes Epidemiology and Management. 2025;17:100237.
35. Yao Y, Zhu L, He L, Duan Y, Liang W, A meta-analysis of the relationship between vitamin D deficiency and

obesity. Int J Clin Exp Med. 2015;8:14977-84.
36. Zakharova I, Klimov L, Kuryaninova V, Nikitina I, Malyavskaya S, et al. Vitamin D insufficiency in overweight and obese children and adolescents. Front Endocrinol (Lausanne). 2019;10:103. PubMed PMID: 30881343
37. Amrein K, Scherkl M, Hoffmann M, Neuwersch-Sommeregger S, Köstenberger M, Tmava Berisha A, et al. Vitamin D deficiency 2.0: an update on the current status worldwide. Eur J Clin Nutr. 2020;74:1498-513.
38. Hassan MM, Curley SA, Li D, Kaseb A, Davila M, Abdalla EK, et al. Association of diabetes duration and diabetes treatment with the risk of hepatocellular carcinoma. Cancer. 2010;116:1938-46.
39. Aseem S, Ruman S, Tabassum S, Tabasum S, Fatima S, Begum S, et al. Comparative study of hypovitaminosis B12 associated with metformin in combination with sulfonylurea or Dpp-4 Inhibitors. Indian J Pharmacy Practice. 2024;17:351-7.
40. Sim JJ, Lac PT, Liu IL, Meguerditchian SO, Kumar VA, Kujubu DA, et al. Vitamin D deficiency and anemia: a cross-sectional study. Ann Hematol. 2010;89:447-52.
41. Mathew AR, Di Matteo G, La Rosa P, Barbati SA, Mannina L, Moreno S, et al. Vitamin B12 deficiency and the nervous system: beyond metabolic decompensation-comparing biological models and gaining new insights into molecular and cellular mechanisms. Int J Mol Sci. 2024; 25:590. PubMed PMID: 38203763
42. Al Ali T, Ashfaq A, Saheb Sharif-Askari N, Abusnana S, Mussa BM. Investigating the association between Diabetic Neuropathy and vitamin D in Emirati patients with type 2 diabetes mellitus. Cells. 2023; 12:198. PubMed PMID: 36611991
43. Sijia Fei, Jingwen Fan, Jiaming Cao, Huan Chen, Xiaoxia Wang, Qi Pan. Vitamin D deficiency increases the risk of diabetic peripheral neuropathy in elderly type 2 diabetes mellitus patients by predominantly increasing large-fiber lesions. Diabetes Res Clin Pract. 2024;209:111585. PubMed PMID: 38364910
44. Qu GB, Wang LL, Tang X, Wu W, Sun YH. The association between vitamin D level and diabetic peripheral neuropathy in patients with type 2 diabetes mellitus: An update systematic review and meta-analysis. J Clin Transl Endocrinol. 2017;9:25-31.
45. Alam U, Petropoulos IN, Ponirakis G, et al. Vitamin D deficiency is associated with painful diabetic neuropathy. Diabetes Metab Res Rev. 2021;37:e3361. PubMed PMID: 32506740
46. Ou Y, Liang Z, Yang Y, Zhou YK. Association of diabetic peripheral neuropathy with vitamin D levels depends on vitamin d status. Med Sci Monit. 2021;27:e931244. PubMed PMID: 34711797
47. Shipton EE, Shipton EA. Vitamin D Deficiency and Pain: Clinical Evidence of Low Levels of Vitamin D and Supplementation in Chronic Pain States. Pain Ther. 2015;4:67-87.

Supplement Material

Application details for the QST measurement:

The testing was conducted in a space free from interruptions and distractions, with an air conditioner set at 22°C. With the use of an adjustable chair, the patients' positions were brought into harmony with the examination table. Test stimuli were provided to ensure that all patients understood the procedure, along with information regarding the testing's progression. In order to prevent the patients from seeing the level of the stimulus, the computer screen was turned away. The third finger was used for vibratory testing, while the dorsal side of the hand was selected for temperature testing. The patients' and healthy volunteers' upper extremities were examined, and the findings were noted.

Vibratory testing:

A component of the system, in the form of a lump of putty, was placed on the middle finger as the test site. The stimulator was positioned in the region between the fingernail and the distal interphalangeal joint. The system supplied putty and sponges to ensure the patients remained still during testing and to eliminate potential causes of external vibrations.

Thermal testing:

Before the test, the researchers made sure the participants' hands were dry and, if necessary, dried them with a towel. The 3x3 cm thermal stimulator was securely positioned on the dorsal side of the hand using velcro straps to ensure complete contact and participant comfort. Skin temperatures were measured using the QST system, and all stimuli were administered following the measurements and prior to each thermal test. The investigation employed the '4-2-1' method, one of the algorithms available for the Case IV system, to assess sensory thresholds. The researcher begins by testing and establishing the estimated threshold in this algorithm. Based on this predicted threshold, 20 stimuli are administered to the patient at each measurement. The strength of the subsequent stimulus is determined by the participants' answers; if they are unable to experience the stimulus, the subsequent stimulus is often more intense. The gadget randomly presents null stimuli among all these stimuli, and the accuracy of the participants' answers is examined because it is anticipated that they will respond negatively to them. The test is repeated for that component once three positive responses to the null stimuli are received.

A thermal stimulator was utilised to apply increasing thermal stimuli using a non-repeating ascending null stimuli algorithm to measure the heat pain threshold (HPT) stimulus. During the stimulation, participants rated their pain levels on a numerical scale ranging from 0 (indicating

no pain) to 10 (representing the worst conceivable pain). The test concluded when the discomfort reached a level corresponding to five on the numerical scale. Temperature values were recorded in comparison to the numerical scale, where the initial bothersome level corresponded to numerical scale 1 (HPT 0.5) and the pain level corresponded to 5 (HPT 5). Additionally, the difference between HPT 0.5 and HPT 5 (HPT 0.5–5) was calculated to demonstrate the fluctuation of pain scales with temperature.

Neuropathic pain screening:

Subjective Peripheral Neuropathy Screen Questionnaire (SPNSQ)

Neuropathic symptom
Do you ever have legs and/or feet that feel numb?
Do you ever have any burning pain in your legs and/or feet?
Are your feet too sensitive to touch?
Do you get muscle cramps in your legs and/or feet?
Do you ever have any prickling or tingling feelings in your legs or feet?
When you get into the tub or shower, are you unable to tell the hot water from the cold water with your feet?
Do you ever have any sharp, stabbing, shooting pain in your feet or legs?
Do you feel weak when you walk?
Are your symptoms worse at night?
Do your legs and/or feet hurt when you walk?
Are you unable to sense your feet when you walk?
Is the skin on your feet so dry that it cracks open?
Have you ever had electric shock-like pain in your feet or legs?

	Yes	No
Pain		
characteristic		
Burning Painful cold		
Electric shock Tingling		
Pins and needles		
Numbness		
Itching		
Hypoesthesia to touch		
Hypoesthesia to prick		
The pain is caused or increased by brushing		

Biomedical Sciences and Clinical Medicine 2026;65(1):23-31.
doi: 10.12982/BSCM.2026.01
https://he01.tci-thaijo.org/index.php/CMMJ-MedCMJ/index

BSCM
Biomedical Sciences and Clinical Medicine

Original Article

Open Access

Effects of Inflammatory Biomarkers (Fetuin-A and High Sensitivity C-reactive Protein) on Glycemic Control in Type 2 Diabetic Women

Ali Abdullateef Al-bayati, Shatha Alkhateeb and Walaa Jedda

Department of Chemistry and Biochemistry, College of Medicine, Mustansiriyah University, Iraq

Correspondence:
Ali Abdullateef Al-bayati, MD, PhD, Department of Chemistry and Biochemistry, College of Medicine, Mustansiriyah University, Baghdad, Iraq.
E-mail: alialbayati_biochem@uomustansiriyah.edu.iq

Received: July 14, 2024;
Revised: May 23, 2025;
Accepted: August 5, 2025

ABSTRACT

OBJECTIVE Inflammation plays an essential role in the development of insulin resistance and type 2 diabetes. The objective of this study was to evaluate the effects of inflammatory markers (hs-CRP and fetuin-A) on glycemic control in Iraqi women patients with type 2 diabetes, and to examine the correlation of these markers with indices of glycemic control.

METHODS This case-control study included 45 Iraqi type 2 diabetic female patients and 44 non-diabetic Iraqi female patients matched for age and sex as control subjects. For both patients and controls hs-CRP and fetuin-A were measured using ELISA, HbA1c by the turbidimetric immunoassay, FBG and lipid profile measures using the spectrophotometer method.

RESULTS High levels of both fetuin-A and hs-CRP were observed in diabetic patients compared to the healthy controls. hs-CRP was significantly higher in the diabetic group 3.1 ± 0.59 mg/dL than the control 1.22 ± 0.66 mg/dL and was statistically significantly correlated with the marker of glycemic control ($p < 0.001$). The serum level of fetuin-A in the diabetic group (768.7 ± 173.03 µg/mL) was also significantly higher than that of control (311.95 ± 94.13 µg/mL) ($p < 0.001$). A strong positive correlation was observed between fetuin-A concentrations with serum hs-CRP concentrations in the diabetic individuals but not in the controls.

CONCLUSIONS Diabetic Iraqi women have higher inflammatory markers (fetuin-A and hs-CRP) than non-diabetic women. A strong association was observed for these inflammatory biomarkers and glycemic control in diabetic subjects.

KEYWORDS inflammatory biomarkers, type 2 diabetes, fetuin-A, high sensitivity C-reactive protein

INTRODUCTION

Diabetes is a chronic disease that represents a major health problem and a great challenge to healthcare provision worldwide. Presently, there is great attention toward diabetes due to its growing prevalence. Because of this rapid rise, the disease was classified as “epidemic” by the Centres for Disease Control and Prevention in the USA in 2007. The type 2 diabetes mellitus population world-wide is predicted to rise to 629 million by 2045 (1). Among all types of diabetes, type 2 diabetes represents the most common form, accounting for 90–95% of all cases. The aetiology of the condition involves interaction between both genetic and environmental factors. According to Genome-Wide Association Studies

(GWAS), the risk of type 2 diabetes is related to more than 80 loci (2). During the last decade, epigenetic mechanisms have been proposed as being involved in disease development and progression. Environmental factors such as obesity and sedentary lifestyle are considered the most common factors increasing the risk of getting the disease. These factors also contribute substantially to the development of insulin resistance. Cumulative evidence has shown that inflammation plays a crucial role in the development of insulin resistance. Many inflammatory cytokines, such as TNFα, IL-32 and IL-6, have been shown to be associated with insulin resistance (3). Improved understanding of the exact mechanisms of developing diabetes, findings about other biomarkers and their interaction could potentially help improve disease management or even prevention. A dual effect of inflammation on type 2 diabetes has been observed: inflammation has been shown to cause insulin resistance, and in patients with overt diabetes, it also causes deterioration of glycemia as reflected by increasing levels of glycated haemoglobin- HbA1c (4).

High sensitivity C-reactive protein (hs-CRP) represents an important sensitive inflammatory marker of tissue damage and is used as an indicator which links inflammation with type 2 diabetes. Another emerging inflammatory biomarker of interest is fetuin-A, a Heremans Schmid alpha-2 glycoprotein (AHSG) that is secreted by liver cells (5).

In-vitro studies, fetuin-A has been shown to cause insulin resistance by inhibiting insulin receptor's tyrosine kinase, leading to impairment of insulin signalling in in muscle and fat cells (6).

Epidemiologically, in several prospective studies a link between a high level of fetuin-A and diabetes incidence has been reported (7, 8).

Our study aimed to evaluate the influence of inflammatory markers (hs-CRP and fetuin-A) on glycemic control in Iraqi women patients with type 2 diabetes, and to examine the correlation of these markers with indices of glycemic evaluation.

METHODS

Subjects

This case-control study included a total 90 female individuals aged 36-66 years of whom 45 were patients with type 2 diabetes recruited during routine visits to the specialized endocrine clinic of Dyala Teaching Hospital, Dyala, Iraq, between October 2020 and March 2021. An additional 45 age-matched healthy female subjects with no history of diabetes as confirmed by normal fasting plasma glucose and normal glycated hemoglobin levels were included as controls.

Exclusion criteria included women of other nationalities (non-Iraqis) and women with other endocrine abnormalities or inflammatory conditions such as chronic arthritis, chronic kidney disease and heart disease. The study was ethically approved according to national and/or international rules by the scientific committee of the Department of Chemistry and Biochemistry, College of Medicine, Mustansiriyah University. Verbal and signed consent of agreement were obtained from all participants.

Body mass index (BMI) of participants was calculated using the formula weight (kg)/square height (m^2).

For blood analysis, a fasting venous blood sample was obtained from all participants. HbA1c was measured using anti-coagulated whole blood (SD A1cCareTM System, Biosensor, Suwon-si, South Korea).

Spectrophotometric methods were used to examine serum samples including biochemical tests, fasting blood glucose (FBG), total cholesterols (TC), triglycerides (TG), low-density lipoprotein (LDL) and high-density lipoprotein (HDL) (Biolabo, Maizy, France).

Fetuin-A measurement was performed by enzyme-linked immune sorbent assay using ELISA kits from Abcam Company, Cambridge, UK (ab108855-fetuin A (AHSG) Human ELISA Kit and Human hs-CRP: ELISA Kit, Catalog No: MBS2506093-96T, MyBiosource, San Diego, San Diego, USA.

Data analysis

Data was analyzed using GraphPad Prism 8.0.2 (263). A mean ± standard deviation was used to describe the data. After testing data distribution using suitable tests, the significance of difference was tested using Student's t-test.

Correlation analysis was performed using Pearson's correlation for variables and the t-test was used for determining the statistical significance of the correlations. The correlation coefficient values (r) were either positive (having direct correlation), or negative (having inverse correla-

tion). Statistical significance was considered to be $p < 0.05$.

RESULTS

The demographic and clinical characteristics of subjects enrolled in the study are presented in Table 1. No age or BMI differences were observed between type 2 diabetes and healthy subjects. Both lipid profiles and glycemic indexes showed significant differences between groups ($p < 0.0001$).

The graph in Figure 1 is a representative of the comparison study of biomarkers between patients and controls. fetuin-A level was significantly higher in the diabetic group compared to the healthy control ($p < 0.0001$). The same observations were conducted regarding hs-CRP, total cholesterol, triglycerides and LDLc. The level of HDL was significantly lower in the diabetic group compared to the control $p < 0.0001$.

The correlation analysis of study parameters with fetuin-A in diabetic patients and control is presented in Figure 2. A positive correlation was observed between fetuin-A and both FBS and HbA1c in diabetics: r = 0. 723, $p < 0.0001$ and r = 0.811, respectively, $p < 0.0001$. No such correlation was observed in the controls. A positive correlation between fetuin-A and BMI was observed in both groups, but it was higher in the diabetics compared to control. A positive correlation was detected between Fetuin-A and age in the control group r = 0. 482, $p < 0.05$, but no such correlation was observed in the type 2 diabetic patients.

Figure 3 presents the correlation analysis of the study parameters with serum high sensitivity C-reactive protein in both diabetic patients and controls. A positive correlation was observed between hs-CRP and both FBS and HbA1c in the diabetics: r = 0. 826, $p < 0.0001$ and r = 0.781, $p < 0.0001$, respectively. No such correlation was observed in the controls. A positive correlation was observed in both groups between hs-CRP and BMI, but it was higher in the diabetics compared to the control. A positive correlation was detected between hs-CRP and age in both the control group and the type 2 diabetic patients.

Table 1. Anthropometric characteristics of the study subjects

	Type 2 diabetes patients No (45)	Healthy No (45)	*p*-value
Age (years)			
Mean±SD (range)	47.98±8.43 (29-68)	48.32±7.34 (36-66)	0.073^{ns}
BMI (kg/m^2)			
Mean±SD (range)	27.48±2.133 (22.61-32.14)	27.38±2.02 (22.11-30.93)	0.8185^{ns}
BMI (kg/m^2)			
Normal (18.5-24.9)	4 (8.9%)	8 (17.8%)	
Overweight (25-29.9)	37 (82.2%)	30 (66.6%)	
Obese (≥30)	4 (8.9%)	7 (15.6%)	
FBG (mg/dL)			
Mean±SD (range)	227±74.39 (111-365)	88.55±15.83 (65-125)	0.0001*
HbA1c %			
Mean±SD (range)	8.82±2.53 (4.25-13.56)	4.46±0.75 (3.1-6.84)	0.0001*
Total cholesterol (mg/dL)			
Mean±SD (range)	278.5±56.22 (166-422)	167.5±23.60 (122-237)	0.0001*
TGL (mg/dL)			
Mean±SD (range)	302.8±117.7 (141-631)	187±27.14 (129-260)	0.0001*
LDLc (mg/dL)			
Mean±SD (range)	188.2±62.67 (62.6-342.6)	98.16±24.21 (35-161)	0.0001*
HDLc (mg/dL)			
Mean±SD (range)	29.8±10.6 (17-54)	42.59±10.46 (30-67)	0.0001*

*Significant difference between two independent means using Students-t-test at 0.05 level; ^{ns}means no significant difference, * means there is significant difference

BMI, body mass index; FBS, fasting blood glucose; TGL, total triglycerides; LDLc, low density lipoprotein cholesterol; HDLc, high density lipoprotein cholesterol

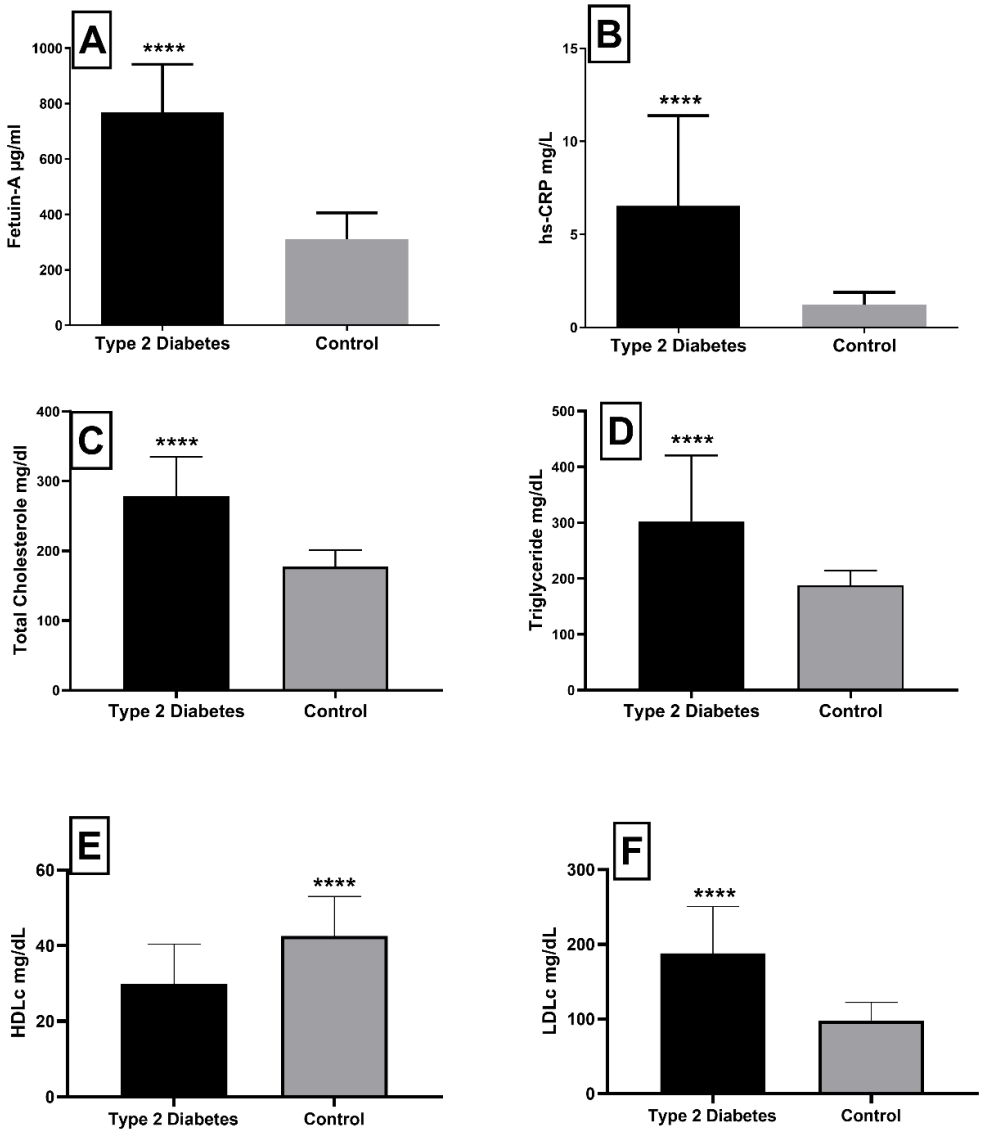

Figure 1. Graphs representative of the means measures for groups of the study (black bars - type 2 diabetes group; gray bars - healthy control group. A) represents the results of fetuin-A, B) represents serum hs-CRP, C) represents total cholesterol, D) represents triglycerides, E) for high density lipoprotein cholesterol and F) for low density lipoprotein cholesterol. Differences between means calculated by unpaired student t test; **** indicates p <0.0001

DISCUSSION

To our knowledge, this is the first study investigating the role fetuin-A and hs-CRP in glycemic control in Iraqi type 2 diabetes patients. The main results obtained from the current study are that statistically significantly higher levels of both fetuin-A and hs-CRP were observed in the diabetic group compared to the healthy controls. Furthermore, high significant positive correlations were observed between the level of glycemia and both fetuin-A and hs-CRP.

Glycemic control is the major target for management of type 2 diabetes. Advanced glycation end products (AGEs) like HbA1c represent the best reflection of the level of glycemic control. More than three decades ago, the American Diabetes Association recommended the use of HbA1c for routine monitoring of patients with diabetes (9). In addition, a significant reduction in HbA1c percentage has been shown to significantly reduce the onset and progression of diabetic associated complications (10, 11). Chronic inflammation is a direct cause and results in the complications associated with type 2 diabetes (12).

High HbA1c that results from chronic hyperglycemia can increase expression of pro inflammatory factors and initiate signals that lead to hepatic CRP production in diabetic and obese

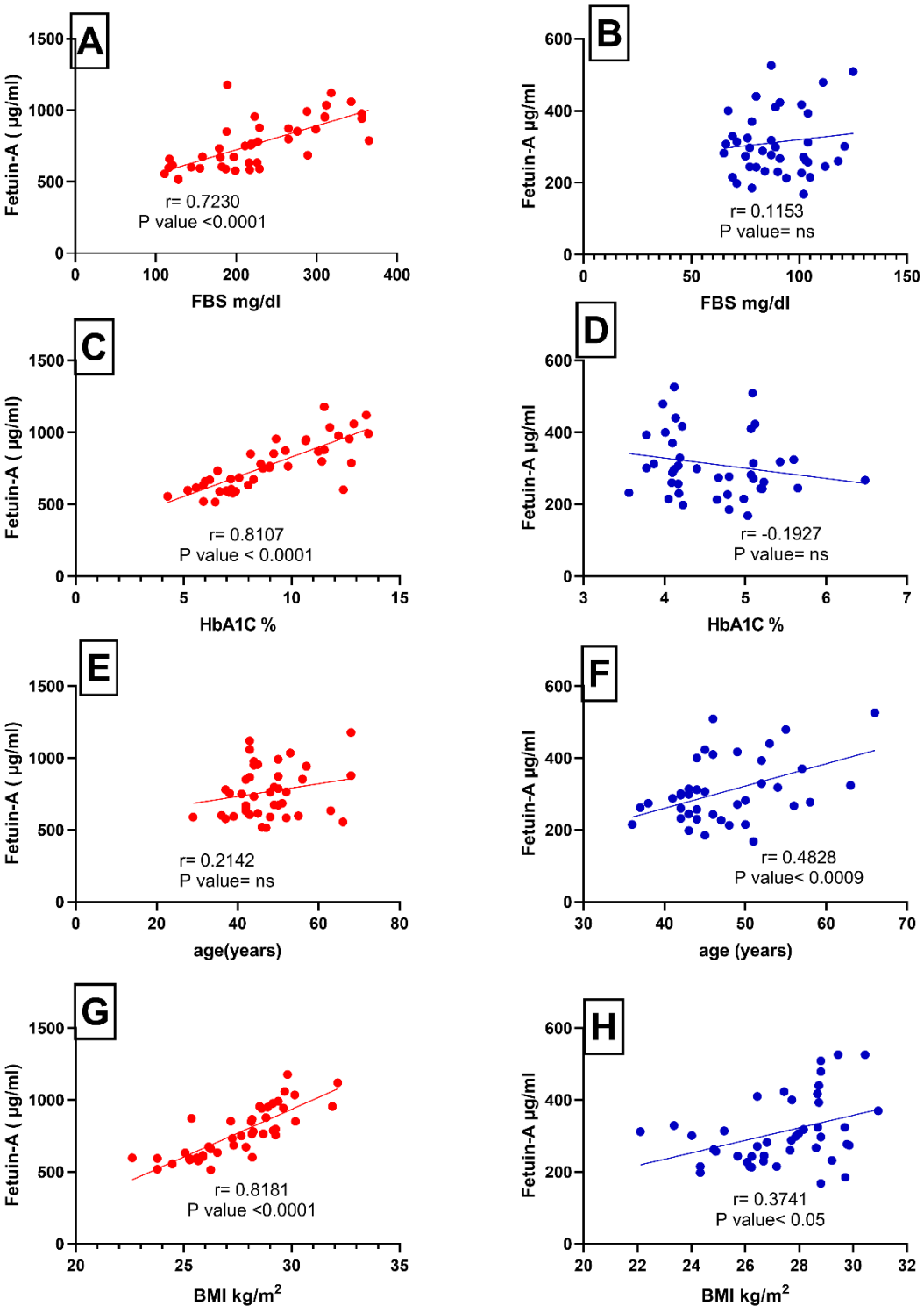

Figure 2. Graphs representative of correlation analysis of serum fetuin-a level with fasting blood sugar (FBS), glycated hemoglobin (HbA1c), age, and body mass index (BMI): left panel in red for the type 2 diabetes group and right panel in blue for the control group. A) and B) are correlation analyses of both type 2 diabetes and control groups for serum fetuin-a and FBS in mg/dL; C) and D) are correlation analyses for fetuin-a and HbA1c%; E) and F) are fetuin-a and age in years; G) and H) are fetuin-A and BMI in kg/m^2

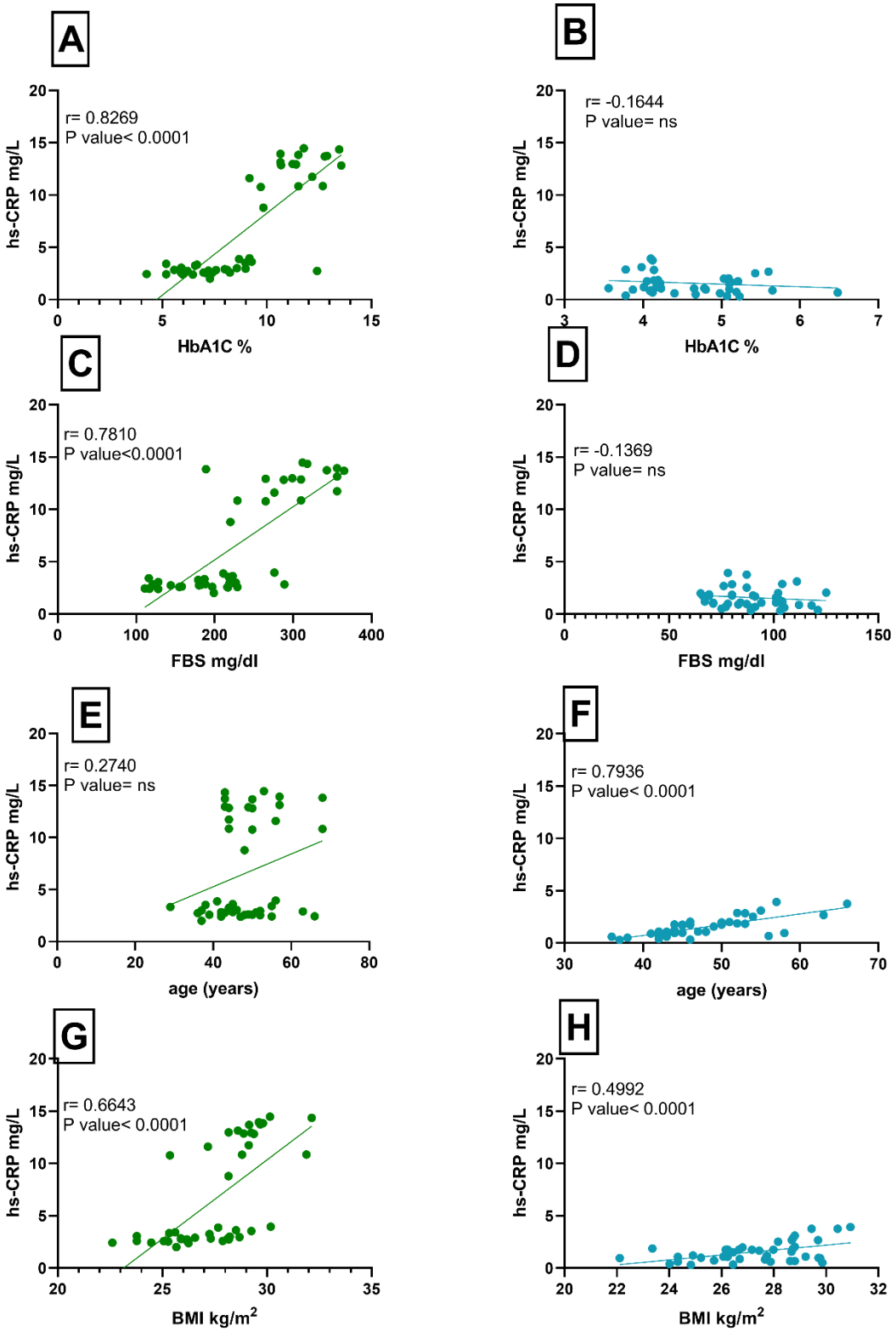

Figure 3. Graphs representative of correlation analyses of serum high sensitivity C-reactive protein (hs-CRP) level with fasting blood sugar (FBS), glycated haemoglobin (HbA1c), age, and body mass index (BMI) in the left panel in green for the type 2 diabetes group and in the right light blue for the control group. A) and B) are correlation analyses of both type 2 diabetes and control groups for serum hs-CRP and FBS in mg/dL; C) and D) are hs-CRP and HbA1c %; E) and F) are hs-CRP and age in years; G) and H) are hs-CRP and BMI in kg/m^2

subjects. Tan and Chow suggested that proinflammatory cytokine-like IL-6, tumor necrosis factor α and IL-1 are all primary signals that act on tissues through their downstream CRP (13).

In the current study, hs-CRP as a sensitive inflammatory marker was shown to be high in the diabetic group 3.1 ± 0.59 mg/dL compared to the control 1.22 ± 0.66 mg/dL and was significantly correlated $p < 0.001$ with the marker of chronic hyperglycemia, HbA1c, as well as with body mass index BMI as a contributor to insulin sensitivity.

Additionally, a large body of evidence has shown that an elevated concentration of inflammatory markers in patients with type 2 diabetes affects can affect insulin sensitivity and function. Examples of these inflammatory markers include C-reactive protein (CRP) (14), fibrinogen (15) and thrombin (16). The same observation was noted in our study that hs-CRP in type 2 diabetes was significantly higher than that observed in controls. The value of hs-CRP in the diabetic group put them at high risk for diabetic CVD complications.

Fetuin-A, a hepatic-produced glycoprotein (hepatokine), performs a variety of functions in humans, including skeletal, metabolic and anti-inflammatory functions (17). The focus of the current study is the association of fetuin-A with type 2 diabetes and glycemia. Previous studies have shown the existence of association of risk of type 2 diabetes with elevated fetuin-A levels (7, 18). The proposed mechanisms of this association include, firstly, that fetuin-A has been shown to inhibit insulin-stimulated insulin receptor tyrosine kinase which then alters the insulin signaling pathway and then leads to insulin resistance (19, 20). Secondly, genetic-based association studies described in many scientific papers show that the gene encoding fetuin-A represents type 2 diabetes susceptibility loci (21). In addition, fetuin-A has been shown to be associated with obesity and inflammation, the major risk factors for type 2 diabetes. Both experimental and clinical data have shown the role of fetuin-A in obesity (14).

In the current study, the serum level of fetuin-A in the diabetic group (768.7 ± 173.03 μg/mL) was significantly higher than that of the control (311.95 ± 94.13 μg/mL) ($p < 0.001$). These results are in concordance with results of a previous study by Song (22) as well as Lorant and Grujicic (23). Furthermore, in the current study a positive correlation was observed between fetuin-A and the level of glycemia represented by HbA1c and fasting glucose. These results are in agreement with a study by Yin (24) performed on newly diagnosed type 2 diabetes individuals and another study which included women with gestational diabetes mellitus (25).

The association of fetuin-A concentrations with serum hs-CRP concentrations is still controversial. On one hand, serum CRP concentrations have been found to be positively associated with metabolic syndrome and fetuin-A level, and these studies have also implicated fetuin-A in the pathogenesis of subclinical inflammation (26). On the other hand, studies such as that performed by Ombrellino (27) as well as Song (22) showed no correlation or even that the serum level of fetuin-A can modulate or downregulate the inflammatory response. In our study, a strong positive association was observed between fetuin-A concentrations with serum hs-CRP concentrations in diabetic individuals, but no such relation was found in the controls. These results provide additional evidence supporting previous studies which have observed that inflammation and fetuin-A are involved in the pathogenesis and progression of type 2 diabetes and its complications.

CONCLUSIONS

Fetuin-A levels are higher in type 2 diabetic Iraqi women patients compared to non-diabetic controls. The increased level of fetuin-A in diabetic groups is associated with glycemic control and with the level of systemic inflammation. The high level of inflammatory markers could have a role in diabetic complications and could be considered in modulating the modality of therapy in those patients.

Recommendations

Further study exploring the mechanisms that involve lower glycemic control with elevated fetuin-A levels and the effects of different treatment regimens on these inflammatory factors is needed.

ACKNOWLEDGMENTS

We would like to express our deep thanks to the teaching staff of the Department of Chemistry and Biochemistry, College of Medicine, Mustansiriyah University for their scientific support.

FUNDING

The work was totally funded by the authors themselves.

CONFLICTS OF INTEREST

We have no potential conflicts of interest relevant to this article.

AUTHOR CONTRIBUTION

The work performed by all the authors equally.

DATA AVAILABILITY STATEMENT

The data that support the findings of this study are available from the corresponding author upon reasonable request.

INSTITUTIONAL REVIEW BOARD STATEMENT

This study was conducted in accordance with the Declaration of Helsinki and approved by the Institutional Review Board (IRB) of [College of Medicine, Mustansiriyah University] (Approval No: 20234, Date: 22/10/2024)

INFORMED CONSENT STATEMENT

Written informed consent was obtained from all participants after explaining the study purpose, procedures, risks, and benefits.

REFERENCES

1. Forouhi NG, Wareham NJ. Epidemiology of diabetes. Medicine. 2019;47:22-7.
2. Cruz M, Valladares-Salgado A, Flores-Alfaro E, Romero JdJP. Genetic determinants of type 2 diabetes. the diabetes textbook. Cham, Switzerland: Springer; 2019. p. 117-25.
3. Fadaei R, Bagheri N, Heidarian E, Nouri A, Hesari Z, Moradi N, et al. Serum levels of IL-32 in patients with type 2 diabetes mellitus and its relationship with TNF-α and IL-6. Cytokine. 2020;125:154832. PubMed PMID: 31479874
4. Al-bayati AAH, AL-Khateeb SM, Ali EA. COVID-19 and preexisted diabetes, one insults the other narrative review". J Saudi J Biomed Res. 2021;6:137-47.
5. Trepanowski J, Mey J, Varady K. Fetuin-A: a novel link between obesity and related complications. Int J Obes (Lond). 2015;39:734-41.
6. Mathews ST, Srinivas PR, Leon MA, Grunberger G. Bovine fetuin is an inhibitor of insulin receptor tyrosine kinase. Life sciences. 1997;61:1583-92.
7. Sun Q, Cornelis MC, Manson JE, Hu FB. Plasma levels of fetuin-A and hepatic enzymes and risk of type 2 diabetes in women in the US. Diabetes. 2013;62:49-55.
8. Laughlin GA, Barrett-Connor E, Cummins KM, Daniels LB, Wassel CL, Ix JH. Sex-specific association of fetuin-A with type 2 diabetes in older community-dwelling adults: the Rancho Bernardo study. Diabetes Care. 2013;36:1994-2000..
9. ElSayed NA, Aleppo G, Aroda VR, Bannuru RR, Brown FM, Bruemmer D, et al. 7. Diabetes technology: standards of care in diabetes—2023. J Diabetes Care. 2023;46(Supplement_1):S111-S27.
10. Al-Bayati AAH, Al-Khateeb SMJ. The association between glycaemic level and lipid profile with Albuminuria in Iraqi type 2 diabetes patients-A cross sectional study. The Journal of the Pakistan Medical Association. 2021;71:S57-S62.
11. Shaheed HS, Ali SHJA-RJoMS. Association of carnosinase-1 gene polymorphism with serum carnosine and carnosinease-1 isoform levels in type 2 diabetics with cardiovascular diseases in Iraq. Al-Rafidain Journal of Medical Sciences. 2023;4:109-17.
12. Shaban A, Abbas SA-R, Abed BAJA-RJoMS. Estimation of Tenascin-C Levels in Iraqi patients with diabetic nephropathy. Al-Rafidain Journal of Medical Sciences. 2023;5(1S):S8-13.
13. Tan KC, Chow W-S, Tam S, Bucala R, Betteridge J. Association between acute-phase reactants and advanced glycation end products in type 2 diabetes. Diabetes Care. 2004;27:223-8.
14. Albayati AA, Rasool Hussein AA. Role of fetuin-a and HSCRP in CVD risk in hypothyroidism iraqi women. J Biochemical Cellular Archives. 2020;20(supplement_2): 3877-81.
15. Ganda OP, Arkin CF. Hyperfibrinogenemia: an important risk factor for vascular complications in diabetes. Diabetes Care. 1992;15:1245-50.
16. Al-bayati A, Lukka D, Brown AE, Walker M. Effects of thrombin on insulin signalling and glucose uptake in cultured human myotubes. J Diabetes Complications. 2016;30:1209-16.
17. Jirak P, Stechemesser L, Moré E, Franzen M, Topf A, Mirna M, et al. Clinical implications of fetuin-A. Adv Clin Chem. 2019;89:79-130.
18. Ix JH, Biggs ML, Mukamal KJ, Kizer JR, Zieman SJ, Siscovick DS, et al. Association of fetuin-a with incident diabetes mellitus in community-living older adults: the cardiovascular health study. Circulation. 2012;125:2316-22.
19. Mathews ST, Rakhade S, Zhou X, Parker GC, Coscina DV, Grunberger G. Fetuin-null mice are protected against obesity and insulin resistance associated with aging. Biochem Biophys Res Commun. 2006;350:437-43.
20. Mathews ST, Singh GP, Ranalletta M, Cintron VJ, Qiang X, Goustin AS, et al. Improved insulin sensitivity and resistance to weight gain in mice null for the Ahsg gene. Diabetes. 2002;51:2450-8.
21. Vionnet N, Dupont S, Gallina S, Francke S, Dotte S, De Matos F, et al. Genomewide search for type 2 diabetes–susceptibility genes in French Whites: evidence for a novel susceptibility locus for early-onset diabetes on chromosome 3q27-qter and independent rep-

lication of a type 2–diabetes locus on chromosome 1q21–q24. Am J Hum Genet. 2000;67:1470-80.
22. Song A, Xu M, Bi Y, Xu Y, Huang Y, Li M, Wang T, Wu Y, Liu Y, Li X, Chen Y, Wang W, Ning G. Serum fetuin-A associates with type 2 diabetes and insulin resistance in Chinese adults. PLoS One. 2011;6(4):e19228. Pub Med PMID: 21556362
23. Lorant DP, Grujicic M, Hoebaus C, Brix J-M, Hoellerl F, Schernthaner G, et al. Fetuin-A levels are increased in patients with type 2 diabetes and peripheral arterial disease. Diabetes Care. 2011;34:156-61.
24. Yin L, Cai W-J, Zhu L-Y, Li J, Su X-H, Wang X-L, et al. Association of plasma Fetuin-A and clinical characteristics in patients with new-onset type 2 diabetes mellitus. International journal of clinical and experimental medicine. 2015;8:991. PubMed PMID: 25785085
25. Iyidir OT, Degertekin CK, Yilmaz BA, Altinova AE, Toruner FB, Bozkurt N, et al. Serum levels of fetuin A are increased in women with gestational diabetes mellitus. Arch Gynecol Obstet. 2015;291:933-7.
26. Hennige AM, Staiger H, Wicke C, Machicao F, Fritsche A, Häring H-U, et al. Fetuin-A induces cytokine expression and suppresses adiponectin production. PloS one. 2008;3(3):e1765. PubMed PMID: 18335040
27. Ombrellino M, Wang H, Yang H, Zhang M, Vishnubhakat J, Frazier A, et al. Fetuin, a negative acute phase protein, attenuates TNF synthesis and the innate inflammatory response to carrageenan. Shock (Augusta, Ga). 2001;15:181-5.

Biomedical Sciences and Clinical Medicine 2026;65(1):32-42.
doi: 10.12982/BSCM.2026.03
https://he01.tci-thaijo.org/index.php/CMMJ-MedCMJ/index

BSCM
Biomedical Sciences and Clinical Medicine

Original Article

Open Access

Development of Zinc Oxide Nanoparticle–Infused Carrageenan Membranes with Enhanced Structural and Antimicrobial Properties for Guided Tissue Regeneration

Priyangha PT, Ashritha M and Balaji Ganesh S

Department of Periodontics, Saveetha Dental College and Hospitals, Saveetha Institute of Medical and Technical Sciences [SIMATS], Saveetha University, Chennai, India

Correspondence:
Priyangha PT, DMS, Department of Periodontics, Saveetha Dental College and Hospitals, Saveetha Institute of Medical and Technical Sciences [SIMATS], Saveetha University, Chennai, India.
E-mail: id-priyanghapt.sdc@saveetha.com

Received: April 24, 2024;
Revised: July 18, 2025;
Accepted: August 7, 2025

ABSTRACT

OBJECTIVE The fundamental aim of periodontal therapy is to promote the regeneration of tissues affected by the disease. In recent times, there has been a rising trend in using guided tissue regeneration (GTR) membranes. These membranes are increasingly relied upon to direct the growth of gingival tissue away from the root surface. Both resorbable and non-resorbable membranes presently in use serve as physical barriers, hindering the infiltration of connective and epithelial tissues into the defect area, thus fostering periodontal tissue regeneration. This study aims to develop a polymeric membrane reinforced with carrageenan and zinc oxide nanoparticles and assess its potential for periodontal regeneration.

METHODS 3g of dried Kappaphycus was mixed with 100 mL of distilled water in a container and autoclaved for 15 minutes at 121 degrees Celsius. After cooling, the mixture was blended thoroughly for carrageenan extraction. Then, 1.5 g of PEG 6000 was added as a plasticizer. Zinc oxide nanoparticles (ZnO) were added and homogenized into the carrageenan extract. The mixture was microwave-boiled for 2 minutes, poured onto a petri dish, and air-dried for 24 hours. Further drying at 50 degrees Celsius for 2 hours ensured complete moisture removal. Finally, the membrane was carefully peeled from the petri dish for testing and use. The membrane underwent SEM, tensile strength, Fourier transform infrared, and antimicrobial activity analysis.

RESULTS Scanning electron microscopy analysis revealed a densely packed and moderately rough surface in the ZnO-incorporated membrane, with a broader particle size distribution (1.28 ± 3.67 µm) compared to the smoother carrageenan-only membrane (1.15 ± 1.68 µm). Tensile testing showed improved mechanical strength in the ZnO composite (6.89 MPa) relative to the plain carrageenan membrane (5.39 MPa). FTIR spectra confirmed successful integration of ZnO nanoparticles through characteristic Zn–O peaks, along with preserved polysaccharide functional groups. Antimicrobial activity, evaluated via OD_{600} measurements over 4 hours, demonstrated time- and size-dependent bacterial inhibition against *S. mutans*, with the 4 cm^2 membrane showing superior performance, comparable or superior to chloramphenicol at later time points.

CONCLUSIONS The developed membrane reinforced with carrageenan and zinc oxide nanoparticles exhibited adequate tensile strength and sufficient antimicrobial properties, suggesting its suitability for utilization in periodontal therapy as an effective regenerative material.

KEYWORDS biomaterials, carrageenan, guided tissue regeneration, nanoparticles

INTRODUCTION

The human periodontium comprises several components, including the alveolar mucosa, gingiva, periodontal ligament, root covering cementum, and alveolar bone. Periodontitis, a prevalent pathological condition, results from persistent bacterial-induced inflammation of the gingival tissue, leading to progressive and irreversible damage to the periodontium (1). Left untreated, it can lead to soft tissue and hard tissue damage, ultimately tooth loss. Hence, there's a pressing need for restorative procedures to ensure complete and functional regeneration of periodontal tissues.

Guided tissue regeneration (GTR) techniques are employed for bone regeneration in periodontal cases. GTR aims to create a mechanical barrier around the affected periodontal area to facilitate new bone formation (2). The barrier membranes used in GTR must meet specific criteria, including mechanical obstruction, biocompatibility, biological functionality, resistance to exposure, natural degradation, and adequate porosity for new blood vessel formation (3). These membranes are classified into non-resorbable and resorbable types. While non-resorbable membranes like expanded polytetrafluoroethylene (e-PTFE) are common, they require removal post-healing. Resorbable membranes address this issue, but often lack sufficient mechanical properties for soft tissue recovery (4).

Growing apprehensions about the ecological consequences of synthetic materials and the exhaustion of fossil fuels utilized in their manufacturing processes are becoming more apparent. This highlights the significance of advancing eco-friendly materials, such as biomaterials sourced from natural reservoirs, including polysaccharides, proteins, and lipids. To address these challenges, our study focuses on developing a novel polymeric membrane reinforced with carrageenan and zinc oxide nanoparticles (ZnO).

Carrageenans (CG) are naturally occurring sulfated polysaccharides extracted from red algae. Under specific conditions, they form a helical structure similar to collagen (5).

CG demonstrate high solubility in water and are frequently employed as gelling agents within the food industry (5). Nonetheless, there is limited documentation regarding their utilization in membrane preparation. There are three main types of carrageenan, each with distinct properties (6). κ-CG, the most abundant type, forms strong gels in the presence of potassium salts, while λ-CG acts solely as a thickening agent (7). The primary limitations of these polymeric membranes include their inadequate mechanical characteristics and their propensity for high solubility in aqueous environments. Consequently, it is imperative to incorporate nanoparticles into the polymer matrix to enhance mechanical properties and mitigate solubility (8).

ZnO exhibit significant antimicrobial activity and can interact with bacterial surfaces, entering the cell and exhibiting distinct bactericidal mechanisms (9). They are effective against various microorganisms like *Escherichia coli*, *Pseudomonas aeruginosa*, *Klebsiella pneumonia*, *Pseudomonas vulgaris*, *Candida albicans*, and *Aspergillus niger* (10) and also possess anti-inflammatory properties (11).

Taking advantage of the individual benefits of these materials, our study aims to fabricate a CG and ZnO reinforced polymeric membrane and evaluate its potential for periodontal regeneration. Assessing various properties of this formulation can enhance its suitability for clinical use in periodontal therapy.

METHODS

3 grams of dried Kappaphycus (Natural Remedies Pvt. Ltd., Bangalore, India) were combined with 100 milliliters of distilled water in a container (Figure 1). This mixture was then transferred to an autoclave-safe container and autoclaved at 121 degrees Celsius for 15 minutes before being allowed to cool to room temperature. Once cooled, the mixture was thoroughly blended to aid in breaking down the Kappaphycus material for carrageenan extraction. After extraction, 1.5 grams of polyethylene glycol (PEG 6000) were added to the extract to act as a plasticizer, enhancing the flexibility and handling properties of the final membrane.

Subsequently, the required quantity of ZnO nanoparticles was introduced into the carrageenan extract mixture and thoroughly homogenized to achieve even dispersion (Figure 2). The mixture was subjected to microwave boiling in a container safe for microwave use for 2 minutes to effectively blend the components.

Figure 1. Kappaphycus seaweed in a borosilicate glass beaker

Figure 2. Carrageenan incorporated with zinc oxide nanoparticles

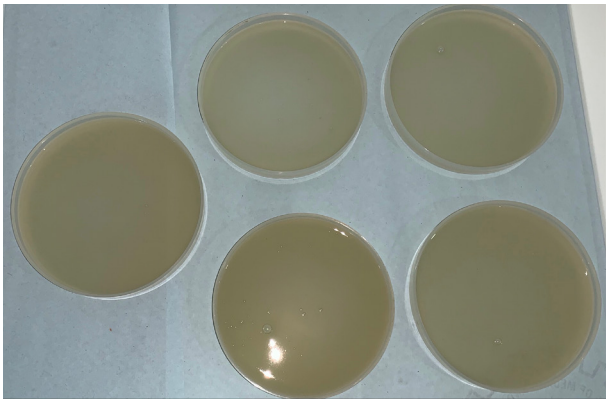

Figure 3. Film cast method of the carrageenan and zinc oxide nanoparticle membrane

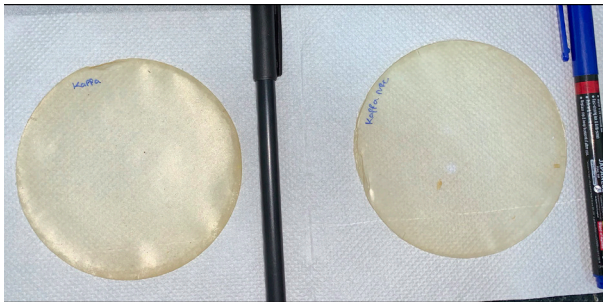

Figure 4. The dried carrageenan and zinc oxide nanoparticle membrane

Following this, the liquid mixture was poured onto a petri dish using the film casting technique and spread evenly to create a thin, uniform film (Figure 3).

Afterward, the film was left to air dry for 24 hours to remove excess moisture and solidify into a membrane. Following air drying, the membrane underwent additional drying at 50 degrees Celsius for 2 hours to ensure thorough moisture removal. Once dried, the membrane was delicately peeled off the surface of the petri dish, making it ready for testing and subsequent utilization (Figure 4).

Morphology of the membrane

For Scanning Electron Microscopy [SEM analysis], the samples were examined utilizing the FEI Quanta FEG 650 SEM [JSM IT-800, JEOL Ltd., Akishima, Tokyo, Japan]. Both the surface and cross-sections of the membrane were photographed at magnifications of 500X.

Tensile strength measurement

To assess tensile strength, the membrane was divided into smaller sections and affixed to the testing equipment with the cut ends. Tensile load, measured in MPa units, was incrementally applied to the membrane at a predefined rate until it fractured. Recorded data encompassed the tensile load observed at the moment of fracture. This examination was carried out utilizing a universal testing machine (Figure 5).

Fourier transform infrared (FTIR)

FTIR analysis was carried out using a BRUKER FTIR spectrometer. Attenuated total reflectance fourier transform infrared (ATR-FTIR) spectra were obtained from dry films to explore chemical interactions among carrageenan, ZnO, and other components involved in the manufacturing process.

Figure 5. Universal testing machine, Model- Instron Expert Electropulse 3000

Antimicrobial activity of carrageenan and zinc oxide nanoparticle membrane

The antimicrobial activity of the carrageenan and zinc oxide nanoparticle-based membrane was evaluated against *Streptococcus mutans* (*S. mutans*) using a broth turbidity assay. Membrane discs of four different surface areas (1 cm^2, 2 cm^2, 3 cm^2, and 4 cm^2) were aseptically introduced into individual test tubes containing 5 mL of Mueller-Hinton broth inoculated with a standardized suspension of *S. mutans*. Chloramphenicol at a concentration of 5 mg/mL served as the positive control. All samples were incubated at 37 °C, and bacterial growth was monitored by measuring optical density (OD) at 600 nm using a UV-Vis spectrophotometer at regular intervals of 1, 2, 3, and 4 hours. A reduction in OD values indicated bacterial growth inhibition by the test membrane. Each condition was tested in a single replicate due to material constraints.

Statistical analysis

Normality of the particle size data for the SEM analysis in each group was assessed using the Shapiro–Wilk test. Depending on the distribution, an independent samples t-test was applied to compare average particle sizes. Additionally, the F-test for equality of variances was used to evaluate differences in variance between groups.

RESULTS

The membranes were cut into 1 × 1 cm pieces and subjected to sterilization. Following sterilization, various evaluations were conducted, including SEM analysis, tensile strength measurement, FTIR analysis, and antimicrobial activity assay.

Scanning electron microscopy (SEM) analysis

SEM allows for direct observation of the surface of solid objects, providing detailed insights into the morphological structure of the membrane. In this study, SEM analysis was conducted at 300× magnification to evaluate the surface characteristics of the fabricated membranes. The membrane composed solely of carrageenan exhibited a relatively smooth and uniform morphology (Figure 6). In contrast, the membrane incorporating ZnO displayed a densely packed surface with moderate roughness, characterized by micro-scale protrusions and depressions, along with a relatively narrow pore size distribution (Figure 7).

Particle size analysis was performed on the SEM images using image analysis software calibrated to a 10 µm scale bar. For the pure carrageenan membrane, 88 particles were measured, revealing an average particle size of 1.15 ± 1.68 µm (mean ± SD), with a distribution range from 0.17 to 12.26 µm. The ZnO-incorporated membrane showed a more heterogeneous morphology; 36 particles were analyzed with an average size of 1.28 ± 3.67 µm and a distribution range from 0.17 to 22.65 µm. The higher standard deviation and broader size range in the ZnO-containing membrane suggest particle aggregation and structural modifications induced by the incorporation of ZnO into the carrageenan matrix.

Tensile strength

The tensile strength of the fabricated membranes was evaluated to qualitatively assess their mechanical integrity. The membrane incorporating ZnO into the carrageenan matrix exhibited a higher maximum tensile stress of approximately 6.89 MPa, in contrast to 5.39 MPa for the membrane composed of carrageenan alone. This increase indicates that the incorporation of ZnO nanoparticles contributed to enhanced structural reinforcement, likely due to improved intermolecular interactions and nanoparticle dispersion within the polymer matrix. However, owing to the preliminary scope of the study and limited availability of materials, tensile testing was performed on only a single membrane sample per formulation.

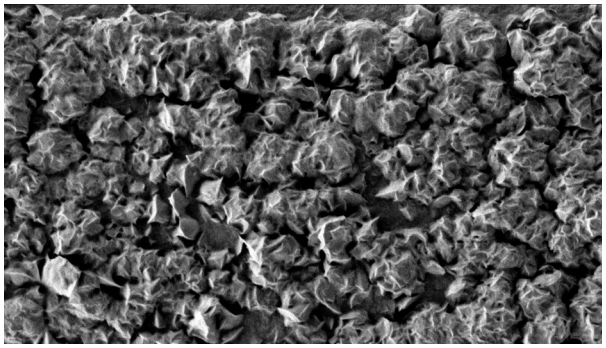

Figure 6. Scanning electron microscopy analysis of the carrageenan membrane

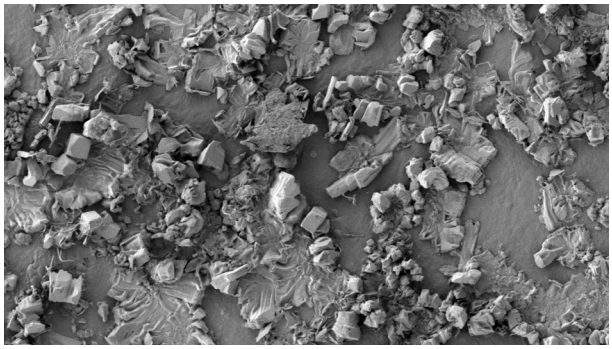

Figure 7. Scanning electron microscopy analysis of the carrageenan and zinc oxide nanoparticle membrane

FTIR analysis of carrageenan membrane

The FTIR spectrum of the pure carrageenan membrane (Figure 8) exhibited characteristic absorption bands corresponding to functional groups typically present in polysaccharides. A broad band at 3,393.12 cm^{-1} was attributed to O–H stretching vibrations, indicating the presence of hydroxyl groups involved in hydrogen bonding. A peak at 2,938.77 cm^{-1} was due to C–H stretching of aliphatic $-CH_2$ groups.

The absorption band at 1,611.03 cm^{-1} likely represented C = O stretching or O–H bending from absorbed moisture. Peaks observed at 1,456.06 cm^{-1} and 1,408.96 cm^{-1} were assigned to CH_2 bending vibrations and symmetric COO^- stretching, respectively, suggesting the presence of carboxylate groups. A strong peak at 1,238.56 cm^{-1} corresponded to S = O stretching vibrations, indicative of sulfate ester groups typical of sulfated polysaccharides like carrageenan.

Further, peaks in the region 1,147.35 to 1,021.24 cm^{-1} were attributed to C–O–C ether linkages and C–O stretching, representing glycosidic bonds in the polymer backbone. The fingerprint region below 930 cm^{-1}, including peaks at 928.31, 845.21, 772.24, and 578.29 cm^{-1}, corresponded to C–O–S stretching, sugar ring skeletal vibrations, and other out-of-plane bending modes. These findings confirmed the presence of key functional groups such as hydroxyl, carboxylate, sulfate, and ether linkages, consistent with the structural features of carrageenan.

FTIR analysis of carrageenan–ZnO nanocomposite membrane

The FTIR spectrum of the carrageenan membrane infused with ZnO (Figure 9) showed absorption bands characteristic of both the polysaccharide backbone and the incorporated inorganic phase. A broad peak at 3,353.32 cm^{-1} was attrib-

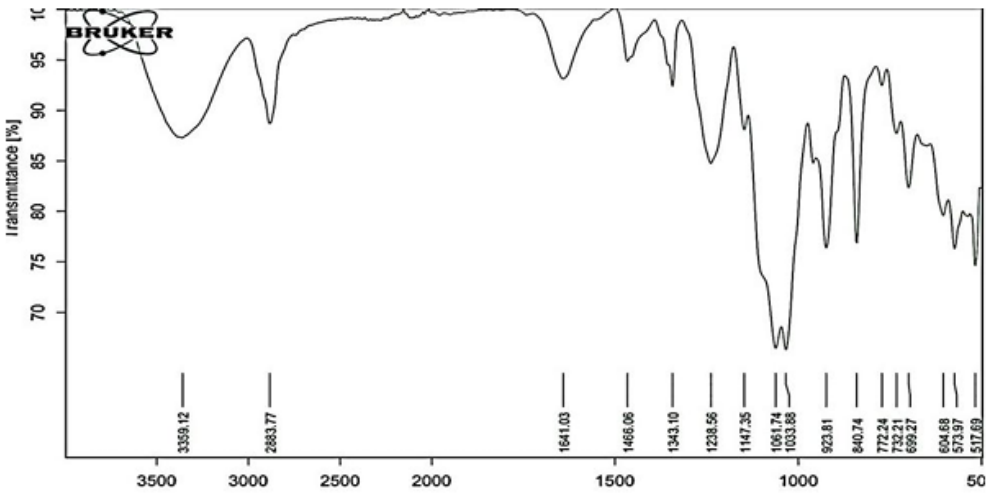

Figure 8. Fourier transform infrared spectra of carrageenan membrane

uted to O–H stretching vibrations, reflecting hydroxyl groups involved in hydrogen bonding within the carrageenan matrix. A peak observed at 2,885.91 cm^{-1} was assigned to C–H stretching from methylene groups.

The band at 1,644.39 cm^{-1} was likely due to C=O stretching or O–H bending from residual water content or carboxylate groups. Peaks at 1,458.30 cm^{-1} and 1,406.93 cm^{-1} corresponded to CH_2 bending and COO^- symmetric stretching, respectively, indicative of aliphatic hydrocarbon chains and carboxylate functionalities. A strong band at 1,236.42 cm^{-1} was assigned to S = O stretching, confirming the presence of sulfate ester groups within the sulfated polysaccharide.

The spectral region between 1,090.42 and 1,006.02 cm^{-1} exhibited strong bands corresponding to C–O–C and C–O stretching vibrations, associated with glycosidic linkages in the carrageenan polymer. Additional sharp peaks at 857.27 cm^{-1}, 701.82 cm^{-1}, and neighboring lower wavenumbers were attributed to Zn–O bond stretching vibrations, providing spectral evidence for the successful incorporation of ZnO into the membrane. These Zn–O peaks were distinct from the typical polysaccharide signals and indicated interaction between the ZnO nanoparticles and functional groups (such as hydroxyl or sulfate) in the carrageenan matrix. Collectively, the presence of characteristic hydroxyl, carboxylate, sulfate, ether, and metal-oxygen (Zn–O) vibrational modes confirmed the formation of a hybrid organic–inorganic membrane and supported the successful integration of ZnO within the carrageenan network.

Antimicrobial activity

The antimicrobial efficacy of the carrageenan–zinc oxide nanoparticle membrane was evaluated over time by measuring the OD at 600 nm. A general decline in OD values indicated effective bacterial inhibition (Figure 10).

At 1 hour, all membrane sizes showed moderate antimicrobial activity, with OD values decreasing progressively from the 1 cm^2 to 4 cm^2 membranes, suggesting a dose-dependent effect. The 4 cm^2 membrane exhibited the lowest OD (~0.14), while the 1 cm^2 membrane showed higher turbidity (~0.26), indicating lesser inhibition. Chloramphenicol, the positive control, had an OD of ~0.30.

At 2 hours, the 1 cm^2 membrane showed the highest OD (~0.36), indicating poor inhibition, while the 4 cm^2 membrane maintained a lower OD (~0.18), comparable to chloramphenicol (~0.22), demonstrating effective bacterial suppression with a larger membrane size.

At 3 hours, all membranes showed a notable decrease in OD values (~0.14–0.18), approaching the efficacy of chloramphenicol (~0.18), indicating time-dependent enhancement of antimicrobial activity.

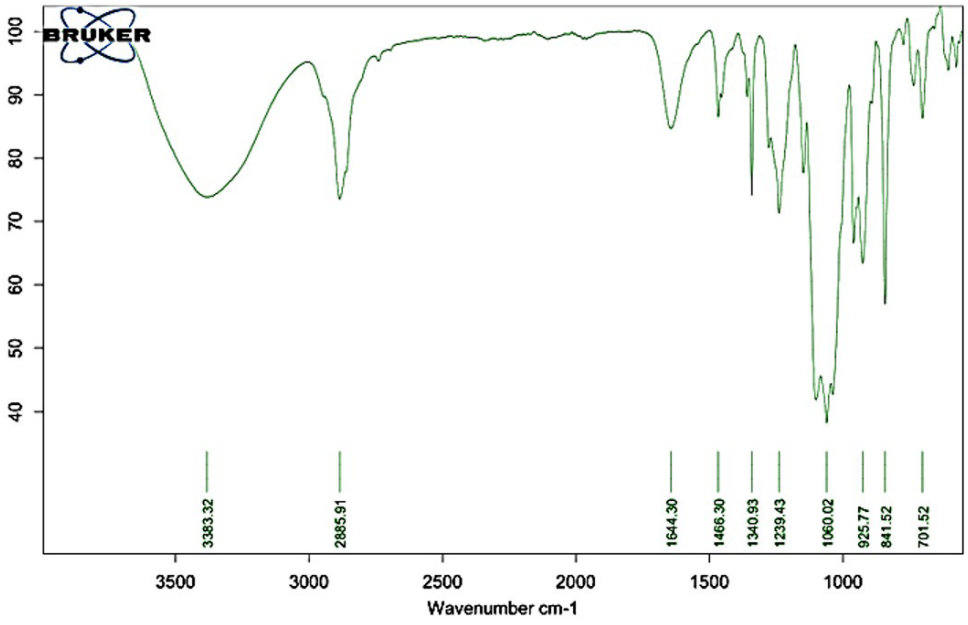

Figure 9. Fourier transform infrared spectra of carrageenan and zinc oxide nanoparticle membrane

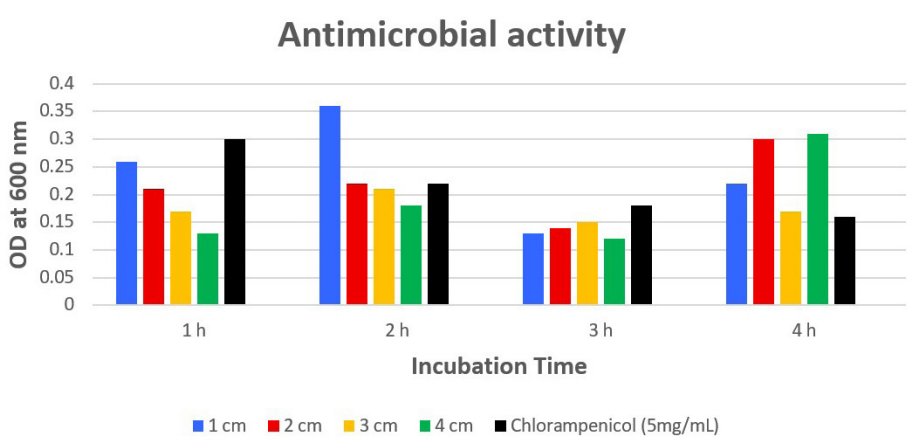

Figure 10. Antimicrobial activity of carrageenan and zinc oxide nanoparticle membrane, with the X-axis representing the incubation time, and the Y-axis representing the optical density

By 4 hours, the 2 cm² and 4 cm² membranes demonstrated the highest bacterial inhibition (OD ~0.30 and ~0.31, respectively), surpassing the chloramphenicol control (OD ~0.16), whereas the 3 cm² membrane showed lower OD (~0.18), indicating better performance.

DISCUSSION

Periodontitis is a chronic inflammatory disease of the supporting structures of the teeth, primarily caused by bacterial biofilm accumulation (12). It leads to progressive destruction of the periodontal ligament and alveolar bone, often resulting in tooth mobility and eventual tooth loss if left untreated. One of the hallmark manifestations of advanced periodontitis is the formation of intrabony defects, vertical bone loss patterns confined within the bone walls (13). These defects present a significant clinical challenge due to their complex anatomy and limited self-regenerative capacity. Effective management of intrabody defects is crucial for restoring periodontal health and function, often requiring regenerative strategies such as bone grafts, barrier membranes, or bioactive materials to promote tissue regeneration and bone fill.

GTR utilizes membranes as mechanical barriers to create a secluded space around periodontal defects, preventing the rapid migration of epithelial and connective tissue cells into the wound area. This selective repopulation encourages the regeneration of the periodontal ligament, cementum, and alveolar bone (14). Although current GTR membranes have demonstrated potential in supporting partial periodontal regeneration, full and predictable regeneration remains elusive. Many available membranes are often associated with biocompatibility concerns, risk of immunogenicity, and high costs.

To overcome these limitations, there is a growing focus on developing naturally derived, biocompatible membranes that can provide both mechanical support and biological activity. In this context, carrageenan, a natural marine-derived polysaccharide, offers an attractive alternative due to its biodegradability, hydrophilicity, and gel-forming properties (15). When combined with zinc oxide nanoparticles (ZnO NPs)—known for their antimicrobial, anti-inflammatory, and osteoinductive properties the resulting composite membrane holds promise for enhancing the regenerative microenvironment. Such carrageen-Zno NP-infused membranes not only act as physical barriers but may also actively promote tissue healing and prevent microbial contamination, making them highly suitable candidates for next-generation GTR applications.

Several studies have highlighted the individual advantages of carrageenan and ZnO. This study combines these materials to develop a polymeric membrane, leveraging their synergistic effects. CG, chosen for its biocompatibility and hydrophilic nature, is conducive to cell proliferation and migration, essential in regenerative membrane applications like wound healing or tissue engineering mechanisms, and has anti-viral activity (16). ZnO with antimicrobial properties (17) complement carrageenan's characteristics, offering a promising combination for periodontal regeneration.

A study investigating bi- and tri-layer nanofibrous membranes formulated with sulfated polysaccharide carrageenan for periodontal regeneration reported favorable outcomes. The membranes maintained structural stability and demonstrated a sustained release of Ca^{2} ions for at least three weeks, indicative of their potential to support osteoblast proliferation and enhance bone regeneration in periodontal applications. (18).

Another study explored an antibiotic-loaded cellulose nanofiber and κ-carrageenan hydrogel which showed strong antibacterial effects against key periodontal pathogens, significantly increasing MDA levels and reducing biofilm formation and bacterial activity, indicating promising potential for periodontitis treatment (19).

A separate study focused on the fabrication and characterization of a stimuli-responsive scaffold/bio-membrane using a novel carrageenan biopolymer for biomedical applications. The bio-membrane exhibited a high strength of 89.21 MPa, surpassing that of commercial membranes. Moreover, its smooth surface favored cell adhesion and proliferation (20).

One study evaluated the preparation of a carrageenan- and fucoidan-silica nanoparticle–based membrane for guided bone regeneration in dental implant sites, demonstrating its potential to promote osteoconduction. Another study investigated the applications of seaweed biopolymers, highlighting their effectiveness in scaffolds, due to their favourable biocompatibility and bioactive properties (21, 22).

ZnO nanoparticles were incorporated into the carrageenan-based membrane to enhance both its antimicrobial efficacy and mechanical performance. ZnO nanoparticles contribute to bacterial inhibition through multiple mechanisms, including the generation of reactive oxygen species (ROS), disruption of bacterial cell membranes, and the release of Zn^{2}_{2} ions, which are known to interfere with microbial metabolism and replication (23). Simultaneously, the nanoscale size and uniform distribution of ZnO within the carrageenan matrix contribute to improved tensile strength and elasticity of the membrane, as reflected by the measured tensile strength of approximately 6.89 MPa.

Several previous studies have highlighted the potential of combining carrageenan with reinforcing agents like ZnO to develop composite biomaterials with enhanced properties. Based on these insights, the present study aimed to develop a polymeric membrane that harnesses the synergistic benefits of carrageenan's biocompatibility and ZnO's multifunctionality. The resulting membrane demonstrates strong potential for application in GTR, offering both antimicrobial protection and mechanical stability essential for periodontal healing.

In one study, an overview of recent progress in dental applications of ZnO was provided. It stated that ZnO nanoparticles have osteoconductive ability, antibacterial activity, and flexibility suitable for periodontal tissue regeneration (24).

In another investigation, the antimicrobial efficacy of zinc against periodontal pathogens was examined, revealing its ability to hinder the vital functions, growth, and reproduction of various microorganisms and disrupting the integrity of bacterial cell walls (25).

Another study focused on the favorable properties of ZnO nanoparticles in promoting tissue integration of biomaterials. It was concluded that ZnO nanoparticles possess antibacterial properties and can enhance the cellular metabolic activity of fibroblasts and endothelial cells relevant for wound healing (26).

A study investigated the use of green nanomaterials such as zinc oxide and chitosan for their antimicrobial activity against oral pathogens, demonstrating significant inhibitory effects (27). Another study evaluated the antibiofilm efficacy of surface-modified gutta-percha incorporated with ZnO, revealing enhanced resistance to microbial colonization and improved potential for endodontic applications (28).

In our study, the polymeric membrane formulated with carrageenan and ZnO underwent *in-vitro* characterization. SEM analysis revealed that the pure carrageenan membrane had a smooth, uniform surface, ideal for controlled degradation. Incorporation of ZnO nanoparticles introduced micro-scale roughness, enhancing cell adhesion and regenerative interaction. The well-distributed surface features and moderate porosity are beneficial for periodontal applications. Particle size analysis confirmed successful ZnO integration with favorable morphological variation. These characteristics collectively

improve the membrane's functional potential in GTR.

These findings align with previous research, which investigated carrageenan-based antimicrobial bionanocomposite films incorporated with ZnO nanoparticles stabilized by melanin, revealing irregularly placed rod-shaped particles with protrusions and depressions (29).

The carrageenan–ZnO membrane showed a tensile strength of ~6.89 MPa, supporting its role in maintaining structural integrity during tissue regeneration. This mechanical property helps preserve space for tissue growth and prevents membrane collapse. Comparable findings were reported in a study showing 5.50 ± 2.62 MPa for κ-carrageenan/ZnO composites, aligning with the present results (30).

In FTIR analysis, the FTIR spectra confirmed the successful incorporation of ZnO into the carrageenan matrix. Characteristic peaks for hydroxyl, carboxylate, sulfate, and ether groups were present in both membranes, validating the structural integrity of carrageenan. In the ZnO-infused membrane, additional peaks corresponding to Zn–O stretching were observed, indicating effective interaction between the nanoparticles and functional groups in the polymer. These spectral features demonstrate the formation of a stable hybrid organic–inorganic membrane, suitable for biomedical applications.

Regarding antimicrobial activity, the results were comparable to those obtained from the control group treated with chloramphenicol alone. Chloramphenicol, a broad-spectrum antibiotic commonly used to treat bacterial infections, served as the standard antimicrobial agent in the study. There was a close resemblance between the antimicrobial effects observed in the tested group and the control group, indicating that the evaluated membrane demonstrated antimicrobial activity comparable to that of chloramphenicol. These results align with a study where zinc oxide nanoparticle and carrageenan-based composite films exhibited high antibacterial properties, particularly against *Escherichia coli* and *Listeria monocytogenes* species (31).

Thus, the formulated membrane, composed of naturally derived ingredients such as ZnO and carrageenan, presents a biocompatible and eco-friendly solution tailored for periodontal applications. This study is among the first to evaluate the synergistic potential of zinc oxide and carrageenan within a single membrane, highlighting the growing relevance of nanotechnology in oral care. Based on the findings, the developed polymeric membrane holds significant promise for regenerative periodontal therapy. Future comparative studies with existing membranes are warranted to further validate their clinical efficacy and real-world applicability.

Limitations

Study limitations include the use of a single sample per membrane type for tensile testing, limiting statistical strength. Additionally, MIC values for carrageenan-ZnO and chloramphenicol were not determined, restricting quantitative antimicrobial comparisons. Although OD data showed time- and dose-dependent inhibition, future studies will address these gaps and include *in-vivo* validation for clinical relevance.

CONCLUSIONS

The membrane developed using carrageenan reinforced with ZnO demonstrated promising characteristics for periodontal regeneration. SEM analysis confirmed a denser, moderately rough surface morphology, favorable for cell attachment. Mechanical testing showed improved tensile strength in the ZnO-reinforced membrane compared to carrageenan alone, indicating enhanced structural integrity. FTIR analysis validated the successful integration of ZnO nanoparticles within the carrageenan matrix through distinct Zn–O vibrational peaks. Moreover, antimicrobial assays revealed that the membrane exhibited time-dependent inhibition of *S. mutans*, with activity comparable to chloramphenicol by 4 hours of incubation. These findings support the membrane's potential as a multifunctional material for GTR in periodontal therapy.

Areas of future research

Future research can focus on enhancing the membrane by incorporating additional antimicrobial agents for synergistic effects, as well as bioactive molecules like growth factors or peptides to boost cell proliferation and tissue regeneration. These strategies could pave the way for more targeted and effective periodontal therapies.

ACKNOWLEDGEMENTS

The authors of this study express their sincere gratitude to the management and the Department of Periodontics at Saveetha Dental College and Hospitals, Chennai, for their invaluable guidance and support in facilitating the successful completion of this research.

FUNDING

This research received no specific grant from any funding agency in the public, commercial, or not-for-profit sectors

CONFLICTS OF INTEREST

The authors have no conflicts of interest to report.

AUTHOR'S CONTRIBUTION

P.T.: data curation, data curation, investigation, project administration, supervision, visualization, writing- original draft, writing- review & editing; A.M.: investigation, formal analysis, methodology, visualization, writing- original draft, writing- review & editing; B.G.S.: formal analysis, methodology, supervision, writing- original draft.

DATA AVAILABILITY STATEMENT

All the necessary data has been provided in the manuscript.

INSTITUTIONAL REVIEW BOARD STATEMENT

The institutional scientific research board [SRB/SDC/UG-2094/23/PERIO/152] was obtained before the start of the study.

INFORMED CONSENT STATEMENT

Not applicable.This study does not involve human participants or human tissue.

REFERENCES

1. Ayari H. The use of periodontal membranes in the field of periodontology: spotlight on collagen membranes. J Appl Biomed. 2022;20:154-162.
2. Kim K, Su Y, Kucine AJ, Cheng K, Zhu D. Guided Bone Regeneration Using Barrier Membrane in Dental Applications. ACS Biomater Sci Eng. 2023;9:5457-78.
3. Dimitriou R, Mataliotakis GI, Calori GM, Giannoudis PV. The role of barrier membranes for guided bone regeneration and restoration of large bone defects: current experimental and clinical evidence. BMC Med. 2012;10:81. PubMed PMID: 22834465
4. Usui M, Onizuka S, Sato T, Kokabu S, Ariyoshi W, Nakashima K. Mechanism of alveolar bone destruction in periodontitis - Periodontal bacteria and inflammation. Jpn Dent Sci Rev. 2021;57:201-8.
5. Dong Y, Wei Z, Xue C. Recent advances in carrageenan-based delivery systems for bioactive ingredients: A review. Trends in Food Science & Technology. 2021; 112:348-61.
6. Aga M, Dar A, Nayik G, Panesar P, Allai F, Khan S, et al. Recent insights into carrageenan-based bio-nanocomposite polymers in food applications: A review. Int J Biol Macromol. 2021;192:197-209.
7. Tarman K, Sadi U, Santoso J, Hardjito L. Carrageenan and its enzymatic extraction. Encyclopedia of Marine Biotechnology. 2020;1:147-59.
8. Madruga L, Sabino R, Santos E, Popat K, Balaban R, Kipper M. Carboxymethyl-kappa-carrageenan: A study of biocompatibility, antioxidant and antibacterial activities. Int J Biol Macromol. 2020;152:483-491.
9. Gudkov S, Burmistrov D, Serov D, Rebezov M, Se menova A, Lisitsyn A. A mini review of antibacterial properties of ZnO nanoparticles. Frontiers in Physics. 2021;9:641481.
10. Gharpure S, Ankamwar B. Synthesis and antimicrobial properties of zinc oxide nanoparticles. J Nanosci Nanotechnol. 2020;20:5977-96.
11. Lopez-Miranda JL, Molina GA, González-Reyna MA, España-Sánchez BL, Esparza R, Silva R, Estévez M. Antibacterial and Anti-Inflammatory Properties of ZnO Nanoparticles Synthesized by a Green Method Using Sargassum Extracts. Int J Mol Sci. 2023;24:1474. PubMed PMID: 36674991.
12. Kwon T, Lamster IB, Levin L. Current Concepts in the Management of Periodontitis. Int Dent J. 2021;71:462-76.
13. Ayari H. The use of periodontal membranes in the field of periodontology: spotlight on collagen membranes. J Appl Biomed. 2022;20:154-62.
14. Garcia J, Dodge A, Luepke P, Wang HL, Kapila Y, Lin GH. Effect of membrane exposure on guided bone regeneration: A systematic review and meta-analysis. Clin Oral Implants Res. 2018;29:328-38.
15. de Jesus Raposo MF, de Morais AM, de Morais RM. Marine polysaccharides from algae with potential biomedical applications. Mar Drugs. 2015;13:2967-3028.
16. Álvarez-Viñas M, Souto S, Flórez-Fernández N, Torres MD, Bandín I, Domínguez H. Antiviral Activity of Carrageenans and Processing Implications. Mar Drugs. 2021;19:437. PubMed PMID: 34436276
17. Agarwal H, Shanmugam V. A review on anti-inflammatory activity of green synthesized zinc oxide nanoparticle: Mechanism-based approach. Bioorg Chem. 2020;94:103423. PubMed PMID: 31776035.
18. Kikionis S, Iliou K, Karra AG, Polychronis G, Choinopoulos I, Iatrou H, et al. Development of Bi- and Tri-Layer Nanofibrous Membranes Based on the Sulfated Polysaccharide Carrageenan for Periodontal Tissue Regeneration. Mar Drugs. 2023;21:565. PubMed PMID: 37999389.

19. Johnson A, Kong F, Miao S, Lin HV, Thomas S, Huang YC, et al. Therapeutic effects of antibiotics loaded cellulose nanofiber and κ-carrageenan oligosaccharide composite hydrogels for periodontitis treatment. Sci Rep. 2020;10:18037. PubMed PMID: 33093521
20. Sudhakar M, Bargavi P. Fabrication and characterization of stimuli responsive scaffold/bio-membrane using novel carrageenan biopolymer for biomedical applications. Bioresour Technol Rep. 2023;21:101344
21. Akshayaa L, Ganesh B. Preparation of a Carrageenan and Fucoidan Silica Nanoparticle-Based Membrane for Guided Bone Regeneration in Dental Implant Sites. J Long Term Eff Med Implants. 2025;35:25-32.
22. Sudhakar MP, Nallasamy VD, Dharani G, Buschmann AH. Applications of seaweed biopolymers and its composites in dental applications. J Appl Biol Biotechnol. 2024;12:62-8.
23. Moradpoor H, Safaei M, Mozaffari HR, Sharifi R, Imani MM, Golshah A, et al. An overview of recent progress in dental applications of zinc oxide nanoparticles. RSC Adv. 2021;11:21189-206.
24. Griauzdyte V, Jagelaviciene E. Antimicrobial Activity of Zinc against Periodontal Pathogens: A Systematic Review of In Vitro Studies. Medicina (Kaunas). 2023 Nov 28;59(12):2088. PubMed PMID: 38138191
25. Raghupathi K, Koodali R, Manna A. Size-dependent bacterial growth inhibition and mechanism of antibacterial activity of zinc oxide nanoparticles. Langmuir. 2011;27:4020-8.
26. Wiesmann N, Mendler S, Buhr CR, Ritz U, Kämmerer PW, Brieger J. Zinc Oxide Nanoparticles Exhibit Favorable Properties to Promote Tissue Integration of Biomaterials. Biomedicines. 2021;9:1462. PubMed PMID: 34680579
27. Rajeshkumar AS, Pavithra BD, Tharani CM, Sulochana DG, Jayasree EA. Green nanomaterials, zinc oxide, and chitosan for antimicrobial activity against oral pathogens. RSC Publishing. 2024;62:74-129.
28. Manobharathi G, Raghu S, Ragavendran C. Antibiofilm efficacy of surface modified gutta percha with zinc oxide nanoparticle. International Journal of Oral Health 2024;4:1-3.
29. Roy S, Rhim J. Carrageenan-based antimicrobial bionanocomposite films incorporated with ZnO nanoparticles stabilized by melanin. Food Hydrocolloids. 2019;90:500-7.
30. Saputri AE, Praseptiangga D, Rochima E, Panatarani C, Joni I. Mechanical and solubility properties of bio-nanocomposite film of semi-refined kappa carrageenan/ZnO nanoparticles. AIP Conference Proceedings. 2018;1927:1629-52.
31. Shin G, Kim H, Park S, Park M, Kim C, Her J. Effect of zinc oxide nanoparticle types on the structural, mechanical and antibacterial properties of carrageenan-based composite films. Food Science and Preservation. 2024;31:126-37.

Biomedical Sciences and Clinical Medicine 2026;65(1):43-50.
doi: 10.12982/BSCM.2026.07
https://he01.tci-thaijo.org/index.php/CMMJ-MedCMJ/index

BSCM
Biomedical Sciences and Clinical Medicine

Original Article

Open Access

Automated Immunohistochemistry as an Alternative to Conventional Immunohistochemistry for Analyzing the Expression of BCL2 and Ki-67 in Diffuse Large B-Cell Lymphoma Patients

Phuttirak Yimpak[1], Kanokkan Bumroongkit[1], Adisak Tantiworawit[2], Thanawat Rattanathammethee[2], Sirinda Aungsuchawan[1] and Teerada Daroontum[3]

[1]Department of Anatomy, Faculty of Medicine, Chiang Mai University, Chiang Mai, Thailand; [2]Department of Internal Medicine, Faculty of Medicine, Chiang Mai University, Chiang Mai, Thailand; [3]Department of of Pathology, Faculty of Medicine, Chiang Mai University, Chiang Mai, Thailand

Correspondence:
Teerada Daroontum, MD, Department of Pathology, Faculty of Medicine, Chiang Mai University, 110 Intawaroros Road, Si Phum, Muang, Chiang Mai 50200, Thailand .
E-mail: Teerada.k@cmu.ac.th

Received: December 24, 2024;
Revised: July 22, 2025;
Accepted: August 7, 2025

ABSTRACT

OBJECTIVE Diffuse large B-cell lymphoma (DLBCL) is the most common subtype of non-Hodgkin lymphoma. Immunohistochemistry (IHC) is widely used to assess prognostic markers such as BCL2 and Ki-67. Conventional IHC relies on manual staining and visual estimation by pathologists, while automated IHC incorporates computer-based image analysis. This study aimed to evaluate the level of agreement between these two IHC workflows in assessing BCL2 and Ki-67 expression in DLBCL patients.

METHODS Formalin-fixed, paraffin-embedded tissue samples from nodal and extranodal sites of 42 and 60 DLBCL cases were analyzed for BCL2 and Ki-67, respectively. Conventional IHC involved manual staining and evaluation by a pathologist in 10.00% increments. Automated IHC used the Ventana BenchMark ULTRA system with digital image analysis. Expression levels of the two systems were compared using paired t-tests, intraclass correlation coefficients (ICC), Pearson's correlation, and Bland–Altman plots.

RESULTS For BCL2, no significant difference was found between the two methods (mean difference = 5.79%, $p = 0.103$), with moderate to good agreement (ICC = 0.739) and strong correlation (r = 0.772). For Ki-67, pathologist-based assessment yielded significantly higher values (mean difference = 13.91%, $p < 0.001$), with moderate agreement (ICC = 0.569) and strong correlation (r = 0.688). Bland–Altman analysis confirmed acceptable limits of agreement, although a slight underestimation in the automated Ki-67 results was observed.

CONCLUSIONS Automated IHC showed moderate to good agreement with conventional IHC, particularly for BCL2. Despite some differences in Ki-67 quantification, both methods demonstrated consistent trends. Automated IHC offers reproducibility and scalability, making it a promising complementary tool in pathology.

KEYWORDS conventional immunohistochemistry, automated immunohistochemistry, BCL2 expression, Ki-67 expression, diffuse large B-cell lymphoma

INTRODUCTION

Diffuse large B-cell lymphoma (DLBCL) is the most common subtype of non-Hodgkin lymphoma (NHL), accounting for approximately 30.00-40.00% of all NHL cases worldwide (1, 2). DLBCL is an aggressive form of B-cell malignancy that often requires immediate treatment due to its rapid progression (3). Understanding the molecular landscape of DLBCL is critical for the selection of appropriate treatment strategies, particularly as it pertains to the expression of key biomarkers such as B-cell lymphoma 2 (BCL2) and the proliferation marker Ki-67.

BCL2 is an anti-apoptotic protein that prevents programmed cell death (4), making it a crucial marker for the evaluation of chemoresistance and prognosis in DLBCL patients. Increased expression of BCL2 is frequently associated with adverse clinical outcomes (5, 6), as it can promote tumor survival despite aggressive therapies. In parallel, Ki-67 is a nuclear protein expressed during cell division (7, 8) and serves as a proliferation indicator in various malignancies, including DLBCL. A higher Ki-67 index correlates with increased tumor cell proliferation and, in some cases, with poor overall survival, making it an important diagnostic and prognostic marker (9, 10). Concurrent overexpression of BCL2 and Ki-67 suggests that lymphoma cells exhibit both enhanced survival and increased proliferative activity. This biological profile reflects a more aggressive disease behavior and is commonly associated with poor clinical outcomes and resistance to standard therapies (11). A recent study among upper northern Thai DLBCL patients found that a ≥ 50.00% cut-off was the most effective threshold for distinguishing the expression of Ki-67 and the prediction of three-year overall survival (12).

Immunohistochemistry (IHC) is a widely used technique in pathology for the detection of specific protein expressions, such as BCL2 and Ki-67, within tissue samples. Conventional IHC involves manual processes for tissue section staining, antibody incubation, and subsequent evaluation by a pathologist. While conventional IHC remains the gold standard, its reliance on manual steps can lead to variability in staining intensity, antibody performance, and human interpretation, potentially impacting diagnostic accuracy. In recent years, automated IHC has emerged as a viable alternative to conventional IHC, offering improved standardization and reproducibility through the automation of staining procedures. Automated IHC employs programmable systems that minimize human error, allowing for consistent antibody staining, reduced variability between tests, and more objective results due to the use of integrated digital analysis software. Automation in IHC holds great potential for improving diagnostic workflows, especially in high-throughput laboratories where time and efficiency are critical. This study aimed to evaluate the agreement between conventional pathologist-based IHC and automated computer-based IHC methods for assessing the expression levels of BCL2 and Ki-67.

METHODS

Sample collection

A retrospective study was performed on formalin-fixed paraffin-embedded tumor tissue specimens obtained from both nodal and extranodal sites of patients with de novo DLBCL who were diagnosed and treated at Maharaj Nakorn Chiang Mai Hospital in Chiang Mai, Thailand, between January 2018 and December 2019. Forty-two samples were included for BCL2 analysis and sixty for Ki-67 analysis. As the study was retrospective, it was conducted with a waiver of written consent following ethical approval from the Ethics and Research Committee of the Faculty of Medicine, Chiang Mai University (Certificate No. 248/2021, Study Code ANA-2563-07765).

Conventional immunohistochemistry study

All the tissue samples were analyzed and evaluated by experienced pathologists. Thin sections, each 3-μm thick, were cut from the paraffin block for conventional IHC assessment. The sections were placed on silane-coated slides and dried in a hot air oven at 60°C for 40 minutes. The sections were then dewaxed, rehydrated, and subjected to antigen retrieval by boiling in citrate buffer pH 6.0 for 20 minutes in a microwave oven at high power, maintaining a temperature of approximately 95–100°C. They were then washed with phosphate-buffered saline (PBS) for three 5-minute cycles. Endogenous peroxidase was blocked by immersing the slides in hydrogen peroxide on a shaker for 30 minutes at room temperature. To block non-specific binding sites, the slides were

treated with 5% normal goat serum (NGS) and 1% bovine serum albumin (BSA) in 0.1 M PBS for 1.5 hours. Next, the slides were incubated with primary antibodies (mouse anti-human BCL2, clone 124, and mouse anti-human Ki-67, clone MIB-1, both from Dako, Carpinteria, CA, USA, RTU) on a shaker for 1 hour, followed by overnight incubation at 4°C. The following day, the slides were shaken for 1 hour at room temperature, then washed with PBS for three 10-minute cycles. They were then incubated with a biotinylated secondary antibody and Streptavidin-HRP (horseradish peroxidase) for 1.5 hours at room temperature, followed by three 10-minute PBS washes. The signal was detected using 3,3'-diaminobenzidine (DAB), and the reaction was stopped with tap and distilled water. Mayer's hematoxylin was used for counterstaining, followed by alcohol dehydration and clearing with xylene. Coverslips were mounted on the slides, and a pathologist evaluated the slides by grading the percentage of positive tumor cells in 10.00% increments from 0.00-100.00% at 40X magnification.

Automated immunohistochemistry study

For the automated IHC assessment, sections of 3-µm thick, formalin-fixed, paraffin-embedded tissue were cut and placed on Superfrost Plus slides. These slides were heated for one hour at 60°C in a dry oven to enhance tissue adhesion and soften the paraffin. IHC was performed using a Ventana BenchMark ULTRA autostainer (Roche Diagnostics, Tucson, AZ, USA), following standard protocol. The tissue sections underwent deparaffinization, rehydration, and antigen retrieval with Ventana's CC1 solution (pH 8.0). Primary antibodies were applied, including mouse anti-human BCL2 (clone 124, Dako, Carpinteria, CA, USA, RTU) and mouse anti-human Ki-67 (clone MIB-1, Dako, Carpinteria, CA, USA, 1:200 dilution). BCL2 and Ki-67 were incubated for 32 minutes. Detection was carried out using the Ultraview universal DAB kit, followed by hematoxylin counterstaining and bluing. The slides were cleaned using tap water, dehydrated in ethanol and xylene, and mounted for microscopy. BCL2 and Ki-67 slides were scanned at 40X magnification using the Aperio Digital Pathology Slide Scanner (Leica Biosystem, Buffalo Grove, IL, USA). The digital slides were reviewed with Aperio ImageScope Ver.12.4.6.5003 (Leica Biosystem, Buffalo Grove, IL, USA). Regions of interest were selected manually within the full section of each case at 10X magnification, and ten equal-sized fields were selected for analysis at 40X magnification. Image analysis was carried out using Membrane Algorithm v.9 for BCL2 expression and Nuclear Algorithm v.9 for Ki-67 expression.

Statistical analysis

Mean expression percentages of BCL2 and Ki-67 were compared between conventional and automated IHC using paired t-tests. Pearson correlation coefficients and intraclass correlation coefficients (ICC, two-way mixed-effects model, absolute agreement) were used to assess the strength and consistency of agreement. Bland–Altman plots were constructed to visualize agreement and identify any systematic bias between methods. Statistical significance was defined as a $p < 0.05$. All statistical analyses were conducted using IBM SPSS Statistics version 23 (IBM Corp., Armonk, NY, USA) and GraphPad Prism 9 (GraphPad Software, LLC, San Diego, CA, USA).

RESULTS

The BCL2 expression showed membranous staining, while Ki-67 expression demonstrated nuclear staining. These staining patterns were clearly visualized in both the conventional and automated IHC techniques, as illustrated in Figure 1.

The pathologist-scored BCL2 percentages ranged from 0.00 to 90.00%, with a mean (± standard deviation, SD) of 42.38% ± 35.39% and a median interquartile range (IQR) of 40.00% (0.00-80.00%). Ki-67 percentages ranged from 10.00 to 90.00%, with a mean ± SD of 55.67% ± 20.45% and a median IQR of 60.00% (40.00-70.00%). The computer analysis showed BCL2 percentages ranging from 0.02% to 79.85%, with a mean ± SD of 36.59% ± 27.32% and a median IQR of 41.36% (6.04-61.66%). Ki-67 percentages ranged from 2.79% to 88.70%, with a mean ± SD of 41.76% ± 22.68% and a median IQR of 41.45% (24.27-60.99%). When comparing the mean percentages between the two methods (Figure 2), the results indicated no significant difference in the percentage of BCL2 protein expression between the pathologist and computer-based analyses (mean difference = 5.79; 95%CI: -1.22 to 12.79; p =

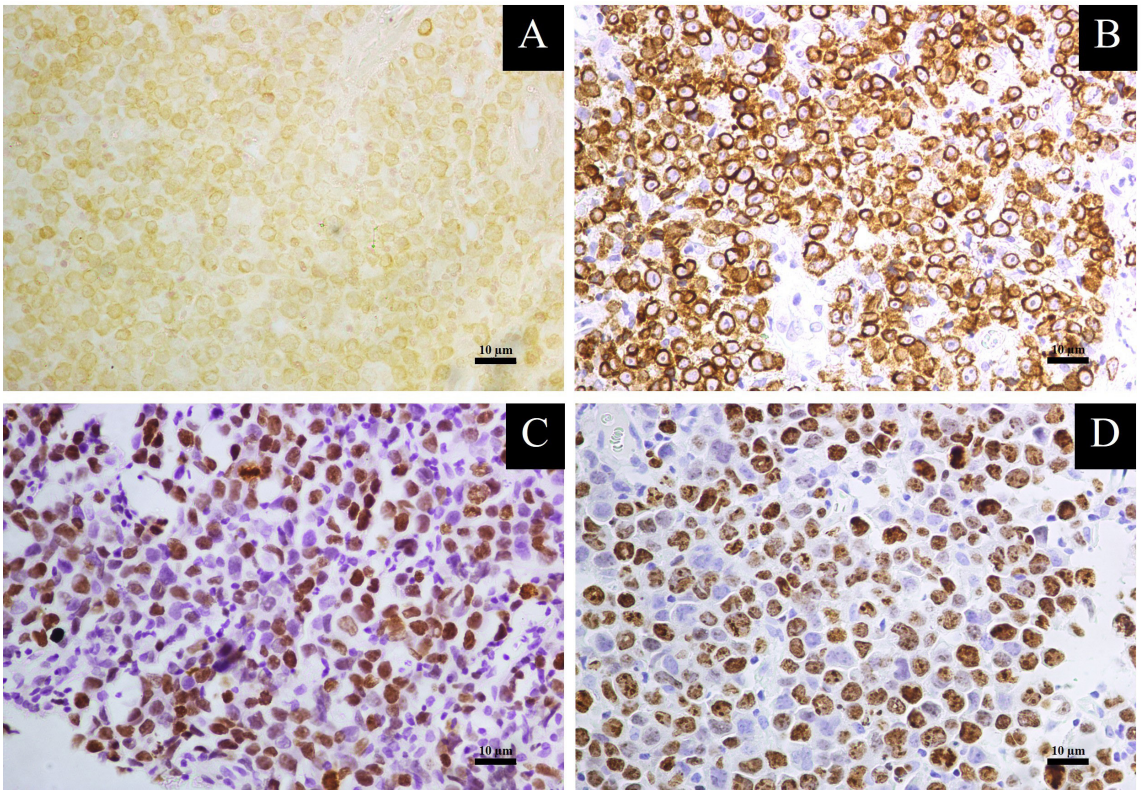

Figure 1. Representative immunohistochemical analysis of BCL2 and Ki-67 expression in DLBCL, captured at 40X magnification. (A) BCL2 membranous staining using conventional IHC technique, (B) BCL2 membranous staining using Automate IHC technique, (C) Ki-67 nuclear staining using conventional IHC technique, (D) Ki-67 nuclear staining using Automate IHC technique

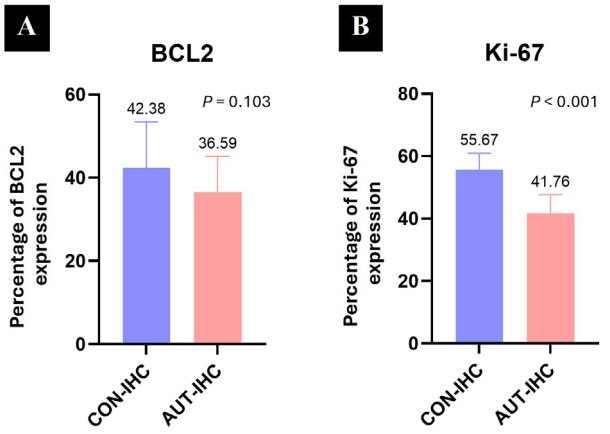

Figure 2. Comparison of the percentage expression of BCL2 (A) and the percentage expression of Ki-67 (B) analyzed using conventional IHC and automated IHC techniques. CON-IHC, conventional immunohistochemistry technique; AUT-IHC, automated immunohistochemistry technique

0.103). However, the analysis by the pathologist revealed a significantly higher percentage of the expression of the Ki-67 protein compared to computer-based analysis (mean difference = 13.91; 95%CI: 9.48 to 18.34; $p < 0.001$).

The agreement between the two methods was further evaluated using the ICC and Bland-Altman analysis. For BCL2, the ICC was 0.739 (95%CI: 0.564–0.851, $p < 0.001$), indicating moderate to good agreement between the conventional and automated assessments. For Ki-67, the ICC was 0.569 (95%CI: 0.137–0.779, $p < 0.001$), indicating moderate agreement.

The Bland-Altman plots (Figure 3) demonstrated a mean difference (bias) of 5.79% for BCL2, with limits of agreement (LoA) ranging from −38.29% to 49.87%. For Ki-67, the mean difference was 13.91%, with LoA ranging from −19.72% to 47.54%.

Additionally, a strong Pearson correlation was observed between the percentages of protein expression analyzed by the pathologist using conventional IHC and those from the computer-based automated IHC method for both BCL2 (r = 0.772, $p < 0.001$) and Ki-67 (r = 0.688, $p < 0.001$). The correlation data are illustrated in Figure 4.

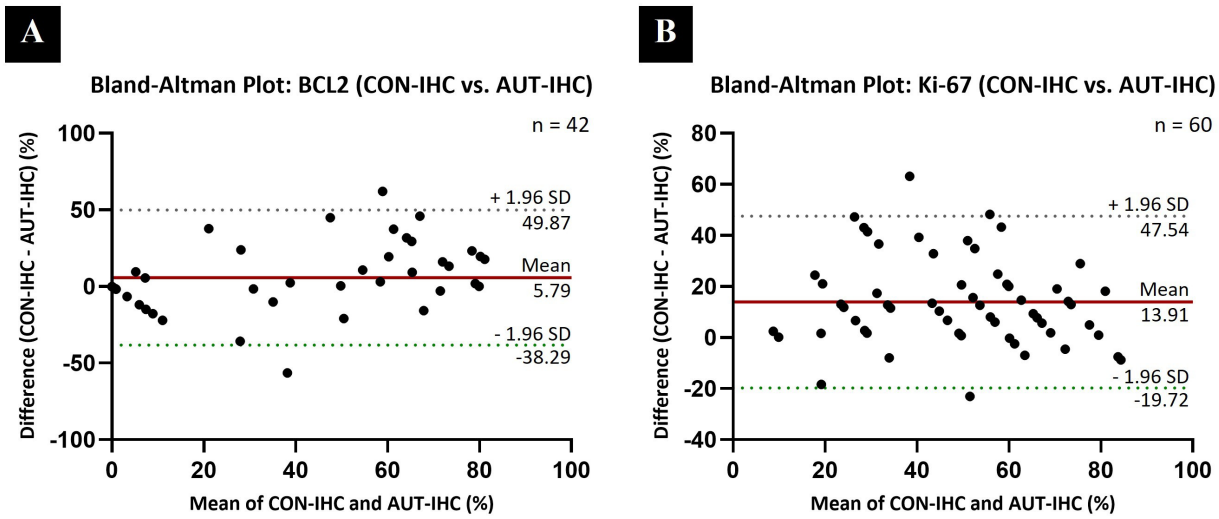

Figure 3. Bland-Altman plots showing the agreement between conventional IHC (CON-IHC) and automated IHC (AUT-IHC) for BCL2 (A) and Ki-67 (B). The solid line represents the mean difference (bias), while the dashed lines indicate the upper and lower limits of agreement (mean ± 1.96 SD).

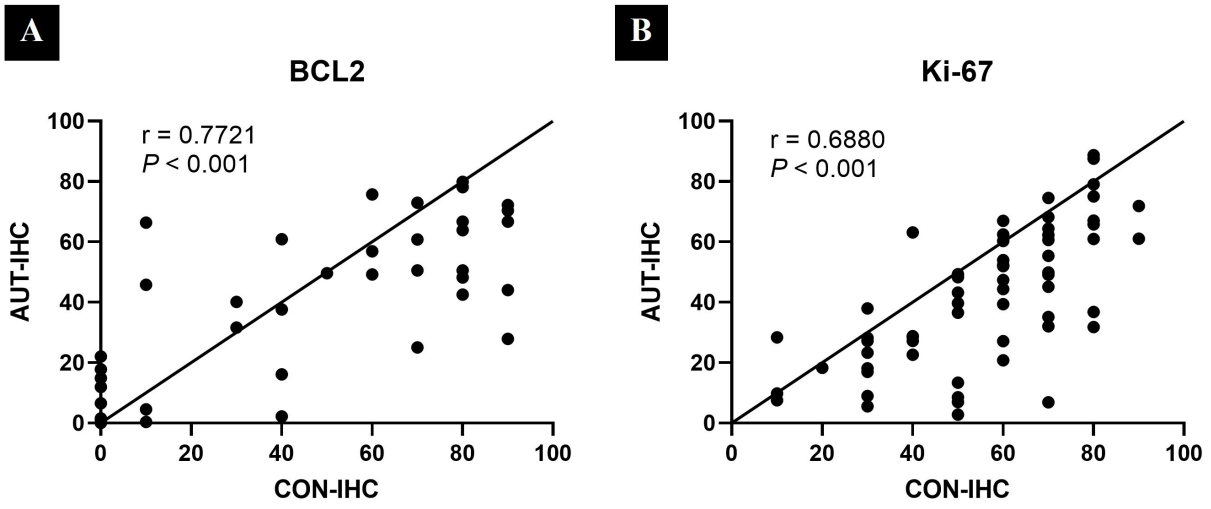

Figure. 4 Scatter plots showing the correlation between conventional IHC (CON-IHC) and automated IHC (AUT-IHC) for the expression of BCL2 (A) and of Ki-67 (B). Each dot represents an individual sample. A strong positive correlation was observed for both markers, indicating consistency between manual and automated evaluation methods.

DISCUSSION

Immunohistochemical staining methods have become essential tools in the daily practice of anatomic pathology worldwide. These techniques allow for the identification and localization of specific proteins within tissue sections, enabling and facilitating disease diagnosis, prognosis, and therapeutic decision-making. Traditionally, pathologists have manually evaluated IHC slides, but advancements in digital pathology have led to the development of automated analysis systems. These systems offer the potential for increased efficiency, consistency, and objectivity. However, questions remain about the accuracy and reliability of computer-based methods in comparison to human evaluation. In this study, we evaluated the agreement between conventional pathologist-based IHC assessment and automated computer-based IHC analysis of BCL2 and Ki-67 expression in patients with DLBCL.

The comparable results observed with the two methods for BCL2 suggest that both manual and automated analyses provide similarly reliable quantification of this marker. However, the results of the analysis revealed a notable difference in the measurement of expression of Ki-67, where pathologist-based assessment yielded a significantly higher percentage expression compared to the computer-based approach.

These results can be attributed to several key factors related to interpretative differences between human and automated evaluation. First, pathologists often focus on areas with the highest proliferative activity and estimate Ki-67 positivity in increments of 10.00%, relying on approximate visual categorization. In contrast, computer-based analysis typically assesses a broader region of the tissue, including both high and low proliferative zones, produces more continuous and specific percentages (e.g., reporting 12.00% rather than rounding to the nearest 10.00%), providing finer numerical detail that does not rely on set increments (13). Second, this discrepancy may also be influenced by biological variability in Ki-67 staining intensity, which fluctuates depending on the cell cycle phase (7, 14-16). Pathologists may recognize and incorporate such variability during evaluation and are generally more flexible in interpreting faint or borderline staining. In contrast, automated systems may treat such variations as below-threshold signals and exclude them from the final count. Additionally, pathologists typically exclude non-viable tissue and non-tumor elements such as endothelial cell nuclei or inflammatory cells from the analysis. In contrast, automated systems may not always effectively differentiate or exclude these areas, which can dilute the calculated Ki-67 index.

To assess agreement, we employed both ICC and Bland–Altman analysis. The ICC indicated moderate to good agreement for BCL2 and moderate agreement for Ki-67, suggesting generally consistent measurements across both methods. Bland–Altman plots confirmed that most observations fell within acceptable limits of agreement, although a mild negative bias for Ki-67 was observed. Strong Pearson correlations for both markers further supported the consistency in expression trends between the two methods.

Overall, the findings highlight the potential of computer-based methods as a reliable complement to conventional pathologist evaluations, particularly in the case of BCL2. However, they also emphasize the need to improve automated methods for markers like Ki-67 to achieve the level of detail provided by human experts. A prior study suggested that Ki-67 percentages assessed by pathologists may correlate more closely with survival outcomes than those from image analysis. This may be due to the pathologist's ability to focus on large tumor cells and exclude background lymphocytes, whereas current algorithms may lack the precision to distinguish such subtle histological features (13).

It should be noted that this study was designed to compare two integrated IHC workflows: conventional (manual staining and manual evaluation) and automated (automated staining and computer-based evaluation). Because both the staining and evaluation steps differ simultaneously, the observed differences may reflect the combined effect of these components. While this workflow-based design provides a comprehensive comparison, it limits the ability to isolate the specific impact of either staining or evaluation alone. Future studies should aim to assess these steps independently using standardized conditions to better determine their individual contributions.

Despite this limitation, automated IHC offers improved reproducibility and suitability for high-throughput applications, though it tends to be less flexible and more costly. In contrast, conventional IHC is more cost-effective and adaptable but introduces greater variability due to subjective interpretation. Notably, this study involved a single pathologist, and intra- or inter-observer variability was not assessed. Future work should incorporate multiple evaluators to determine the reproducibility of manual scoring.

From a clinical perspective, BCL2 and Ki-67 are not definitive diagnostic markers for DLBCL, but are widely used as prognostic indicators. BCL2 is associated with the regulation of apoptosis, while Ki-67 reflects cellular proliferation. Because both markers are also expressed in normal tissues, careful interpretation is essential. Accurate quantification of these proteins has important implications for risk stratification and treatment planning in patients with DLBCL.

CONCLUSIONS

In conclusion, our findings demonstrate that automated and conventional IHC workflows show good overall agreement in the assessment of BCL2 and Ki-67 expression. While minor differences exist, particularly in Ki-67 quantification, both approaches yielded broadly comparable results. Rather than positioning one method as superior, it is important to note that both methods

yielded results trending in the same direction, with each method having distinct advantages and limitations. Automated systems enhance reproducibility and standardization, while conventional methods benefit from the expert judgment of trained pathologists. These complementary strengths suggest that both methods can play important roles in modern pathology, and that their integration should be guided by clinical context, workflow capacity, and biomarker-specific considerations.

ACKNOWLEDGEMENTS

We would like to express our gratitude to Ms. Lakkana Eianleng and Ms. Lamaiporn Peerapapong for their technical assistance and Mrs. Rochana Phuackchantuck for her support with statistical analysis.

FUNDING

This work was supported by the Faculty of Medicine, Chiang Mai University, grant number ANA-2563-07765, No. 160/2564.

CONFLICTS OF INTEREST

The authors have no conflicts of interest to report.

AUTHOR CONTRIBUTIONS

P.Y.: conceptualization, data curation, formal analysis, funding acquisition, investigation, methodology, project administration, software, validation, visualization, writing – original draft, writing – review & editing; K.B.: conceptualization, data curation, formal analysis, funding acquisition, investigation, project administration, supervision, validation, writing – review & editing; A.T.: conceptualization, data curation, formal analysis, investigation, resources, validation, writing – review & editing; T.R.: conceptualization, data curation, formal analysis, investigation, resources, validation, writing – review & editing; S.A.: conceptualization, data curation, writing – review & editing; T.D. conceptualization, data curation, formal analysis, investigation, methodology, project administration, resources, software, supervision, validation, writing – review & editing.

DATA AVAILABILITY STATEMENT

The datasets generated and/or analyzed during the current study are available from the corresponding author on reasonable request.

INSTITUTIONAL REVIEW BOARD STATEMENT

The study was conducted in accordance with the Declaration of Helsinki and approved by the Ethics and Research Committee of the Faculty of Medicine, Chiang Mai University (Certificate No. 248/2021, Study Code ANA-2563-07765).

INFORMED CONSENT STATEMENT

Patient consent was waived due to the retrospective nature of the study, as approved by the Ethics and Research Committee of the Faculty of Medicine, Chiang Mai University.

REFERENCES

1. de Leval L, Hasserjian RP. Diffuse large B-cell lymphomas and burkitt lymphoma. Hematol Oncology Clin of North Am. 2009;23:791-827.
2. Leich E, Hartmann EM, Burek C, Ott G, Rosenwald A. Diagnostic and prognostic significance of gene expression profiling in lymphomas. APMIS. 2007;115: 1135-46.
3. Kim K, Jorge VM, Tiu A, Mousaa P, Gupta S, Djibo D, et al. Early Mortality after Diagnosis of Diffuse Large B-Cell Lymphoma : A Retrospective, Single Urban-Community Hospital Study. Blood. 2019;134(Supplement_1):5335.
4. Klanova M, Kazantsev D, Pokorna E, Zikmund T, Karolova J, Behounek M, et al. Anti-apoptotic MCL1 protein represents critical survival molecule for most burkitt lymphomas and BCL2-negative diffuse large B-cell lymphomas. Mol Cancer Ther. 2022;21:89-99.
5. Roh J, Cho H, Pak H-K, Lee YS, Lee S-w, Ryu J-S, et al. BCL2 super-expressor diffuse large B-cell lymphoma: a distinct subgroup associated with poor prognosis. Mod Pathol. 2022;35:480-8.
6. Punnoose E, Peale FV, Szafer-Glusman E, Lei G, Bourgon R, Do AD, et al. BCL2 Expression in first-line diffuse large B-cell lymphoma identifies a patient population with poor prognosis. Clin Lymphoma Myeloma Leuk. 2021;21:267-78:e10.
7. Harlendea NJ, Harlendo K. Ki-67 as a Marker to Differentiate Burkitt Lymphoma and Diffuse Large B-cell Lymphoma: A Literature Review. Cureus. 2022;16: e72190. PubMed PMID: 39583511
8. Scholzen T, Gerdes J. The Ki-67 protein: from the known and the unknown. J Cell Physiol. 2000;182:311-22.
9. Sadeghipour A, Taha SR, Shariat Zadeh M, Kosari F, Babaheidarian P, Fattahi F, et al. Expression and Clin-

ical Significance of Ki-67, CD10, BCL6, MUM1, c-MYC, and EBV in Diffuse Large B Cell Lymphoma Patients. Appl Immunohistochem Mol Morphol. 2024;32:309-21.
10. Broyde A, Boycov O, Strenov Y, Okon E, Shpilberg O, Bairey O. Role and prognostic significance of the Ki-67 index in non-Hodgkin's lymphoma. Am J Hematol. 2009;84:338-43.
11. Tang YL, Zhou Y, Cheng LL, Su YZ, Wang CB. BCL2/Ki-67 index predict survival in germinal center B-cell-like diffuse large B-cell lymphoma. Oncol Lett. 2017; 14:3767-73.
12. Yimpak P, Bumroongkit K, Tantiworawit A, Rattanathammethee T, Aungsuchawan S, Daroontum T. Immunohistochemistry-based investigation of MYC, BCL2, and Ki-67 protein expression and their clinical impact in diffuse large B-cell lymphoma in upper Northern Thailand. PLoS One. 2024;19:e0307253. PubMed PMID: 39038016.
13. Chabot-Richards DS, Martin DR, Myers OB, Czuchlewski DR, Hunt KE. Quantitative image analysis in the assessment of diffuse large B-cell lymphoma. Mod Pathol. 2011;24:1598-605.
14. Li LT, Jiang G, Chen Q, Zheng JN. Ki67 is a promising molecular target in the diagnosis of cancer (review). Mol Med Rep. 2015;11:1566-72.
15. González-González R, Molina-Frechero N, Carreón-Burciaga RG, López-Verdín S, Robles-Bonilla C, Pereira-Prado V, et al. Comparison between Manual and Automated Methods for Ki-67 Immunoexpression Quantification in Ameloblastomas. Anal Cell Pathol (Amst). 2016;2016:7486989. PubMed PMID: 27843757
16. Remes SM, Tuominen VJ, Helin H, Isola J, Arola J. Grading of neuroendocrine tumors with Ki-67 requires high-quality assessment practices. Am J Surg Pathol. 2012;36:1359-63.

Biomedical Sciences and Clinical Medicine 2026;65(1):51-57.
doi: 10.12982/BSCM.2026.05
https://he01.tci-thaijo.org/index.php/CMMJ-MedCMJ/index

BSCM
Biomedical Sciences and Clinical Medicine

Original Article

Open Access

Comparative Study of Guava Leaf Bioactive Extracts Using Ultrasonication Assisted Extraction

Somya Khanna, Pragati Singh and Ekta Singh Chauhan

Department of Food Science and Nutrition, Banasthali Vidyapith, Tonk, Rajasthan, India

Correspondence:
Somya Khanna, PhD,
Department of Food Science and Nutrition, Banasthali Vidyapith, Tonk, Rajasthan-304022, India.
E-mail: somyakhanna109@gmail.com

Received: October 2, 2024;
Revised: August 9, 2025;
Accepted: August 18, 2025

ABSTRACT

OBJECTIVE Guava (*Psidium guajava* L.), a member of the Myrtaceae family, is grown worldwide and is widely consumed in India because of its good nutritional value as well as its medicinal properties. various parts of the guava tree, e.g., its root, bark, leaves, and fruit, have been found to be rich in pharmacological properties. Despite the health benefits, parts of the tree other than the guava fruit are not widely used by people. Guava leaves are generally considered as a non-conventional food with high nutritive value, medicinal properties, essential oils and good amounts of bioactive compounds.

METHODS In this study, these bioactive compounds were extracted by ultrasound-assisted extraction (UAE) using three different solvents (water, ethanol and methanol) and the extracts were tested for finding the bioactive content in it.

RESULTS This study found that dilute methanol (50 : 50) extracts contain significant amounts of flavonoids, alkaloids, saponins and terpenoids. Ethanol extracts showed good quantities of tannins and aqueous extract showed good extraction of total phenolic content.

CONCLUSIONS These findings show that guava leaves are rich in bioactives compounds which can be extracted using environmentally friendly methods which can be used in food and pharmaceutical industries

KEYWORDS guava leaves, bioactives, extraction, ultrasonication assisted extraction, flavonoids

INTRODUCTION

Guava (*Psidium guajava* L.) is a well-known fruit belonging to the Myrtaceae family and is grown in tropical and subtropical regions of many countries. India holds first position worldwide in the cultivation of guava. Uttar Pradesh, Madhya Pradesh, Maharashtra and Bihar are some of the important guava growing states in the country. Allahabad District of Uttar Pradesh is famous for growing one of the best quality guava fruit in the world (1). Many pharmacological properties have been reported for the bark, roots, leaves and fruit of the plant (2, 3). Generally, guava leaves are considered as a non-conventional food as many people consume guava fruit, ignoring the nutritive as well as the medicinal properties of guava leaves. Guava leaves play an important role in treating diarrhea, gastroenteritis and other digestive problems (4, 5). They also exhibit antioxidant, anti-inflammatory and antimicrobial actions (6).

Guava leaves are rich in nutrients as they contain moisture, ash, fat, protein and carbohydrates (7). They also contain good concentrations of Ca, P, Mg, Fe, vitamin C and vitamin B-complex. They

are considered a good source of bioactive compounds such as alkaloids, flavonoids, terpenoids and phenolic compounds (8). They also contain significant amounts of essential oils (9, 10). Many functional properties, e.g., neuroprotective (11), antioxidant (12), decreasing blood pressure (13), antimicrobial (14), anti-carcinogenic, and anti-inflammatory (15) have been shown in bioactive compounds present in various parts of the plant including leaves, stems, fruits, and flowers which can be extracted using different methods.

Both conventional and non-conventional techniques are known for extracting the bioactive compounds. Methods used in conventional techniques include soxhlet extraction, maceration and hydrodistillation among others. However, extraction with these techniques generally takes long time, is costly, requires large amounts of solvent and is inefficient (16). To overcome these limitations, non-conventional extraction methods have been introduced, including ultrasound, microwave, enzyme, and pulsed electric field assisted extraction among others. These methods require less extraction time, use less solvent, have high extraction rates and reduce thermosensitive compound degradation. These methods are known as "Green Extraction" as they function in accordance with standards set by the U.S. Environmental Protection Agency (17).

The ultrasonication assisted extraction (UAE) technique is easy to use and inexpensive, reduces the quantity of solvent needed, shortens the extraction time, produces a high extraction yield, improves extract quality, allows selective extraction, uses low temperatures thus avoiding heat damage and reducing bioactive compound loss (18). It is an environmentally friendly method and hence is considered a biorefining technology. In this process, ultrasound waves at frequencies higher than 20 kHz are used to disrupt the cell wall of the plant, increasing the solvent's capacity to permeate the cells, resulting in a higher extraction yield. This process can be easily used in a laboratory using an ultrasonic bath which is easy to operate (19). In this study, the UAE approach was used for extracting bioactive compounds from guava leaves.

METHODS

Collection of plant material

Many varieties of guava are found in India. The variety "*Allahabad Safeda*" was chosen for this study. The leaves of this variety were collected from the Krishi Vigyan Kendra Farm Science Center in Banasthali Vidyapith, Newai, Rajasthan, India. The guava leaves were handpicked from the tree and were first washed under running water to remove all the dirt and soil, then were gently rinsed with distilled water. The leaves were subsequently dried in a hot air circulation oven at 80°C for 15-16 hours. The dried leaves were then crushed and ground in an electric grinder to obtain a coarse powder which was then used to extract the bioactive compounds. In this study, all results are expressed as dry weight.

Extraction of bioactive compounds

The bioactive components were extracted from the guava leaves by following and modifying methods given by Mehmood et al. (20). In this study, three extracts were prepared using distilled water, ethanol and diluted methanol: aqueous extract, ethanol extract and diluted methanol extract, respectively.

Aqueous extract (AE): 50g of dried sample was dissolved in 100ml of distilled water and the solution was heated in a water-bath at 100°C for 2 hours.

Ethanol extract (EE): 50g of dried sample was dissolved in 100ml of ethanol and was allowed to stand for 48 hours at room temperature (25-30°C).

Diluted methanol extract (DME): 50g of dried sample was dissolved in 100ml of diluted methanol (1:1 v/v) and the solution was allowed to stand for 48 hours at room temperature (25-30°C).

After the above steps, each extract was exposed to an ultrasonic water bath for 2 hours following which the solvent was evaporated using a rotary evaporator at 69 rpm with a bath temperature of 45°C until the extract was concentrated. After that, each extract was dried in a hot air circulation oven at 45-50°C to remove excess moisture. Extracts were then stored in airtight containers for further use.

Estimation of quantities of bioactive compounds

Total quantities of phenolic compounds were evaluated using the Folin-Ciocalteu method. Flavonoid content was determined using the aluminum chloride method. The quantities of alkaloids, saponins and tannins were determined following procedures described in Singh et al. (21).

To measure the terpenoid content, 100 mg of dried sample was dissolved in 9 mL of ethanol for 24 hours. The mixture was then filtered using Whatman filter paper. The resulting filtrate was extracted with 10 mL of petroleum ether using a separating funnel. The ether extract was isolated and completely dried in pre-weighed glass vials. After the ether was evaporated, the total terpenoid content (mg/g) was determined using the formula: (22).

Statistical analysis

All experiments were performed in triplicate, and the results are expressed as mean ± standard deviation (SD). The data were analyzed using Microsoft Excel. Descriptive statistics were used to calculate the mean and SD and to assess the variability among replicates.

RESULTS

Fresh guava leaves of the Allahabad Safeda variety were collected, dried and converted into a fine powder as shown in Figure 1. The powder was then used in making aqueous, ethanol and diluted

methanol extracts to determine the bioactive compounds present. Table 1 provides a comparative analysis of the bioactive compounds in AE, EE, and DME of guava leaves.

The yields obtained for aqueous, ethanol and diluted methanol extracts were 14%, 17% and 22%, respectively.

Total phenolic content. The total phenolic content of guava leaves (Figure 2) shows that the aqueous extract contains the highest quantity of phenolic compounds with 186 ± 0.4 mg GAE/g,

$$\text{Formula: Terpenoids content (mg/g)} = \frac{\text{Weight of terpenoids residue (mg)}}{\text{Weight of sample (g)}} \times 1{,}000$$

Figure 1. Fresh (left) and dry (right) guava leaves

Table 1. Bioactive compound analysis of AE, EE, and DME of guava leaves

Bioactive compound	AE	EE	DME
Total phenolic content (mg GAE/g)	186±0.4	135±0.5	164±0.7
Flavonoids (mg/g)	6.84±0.5	5.87±0.7	11.39±0.2
Alkaloids (mg/g)	11.40±0.2	10.86±0.1	11.89±0.8
Saponins (%)	0.58±0.6	0.61±0.5	1.12±0.2
Tannins (mg/L)	276±0.1	312±0.3	290±0.4
Terpenoids (mg/g)	3.81±0.3	3.88±0.6	3.96±0.7

Values are presented as means ± SD
AE, aqueous extract; EE, ethanol extract; DME, diluted methanol extract

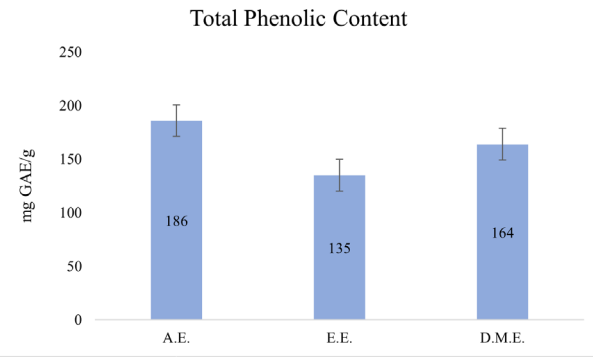

Figure 2. Total phenolic content in aqueous, ethanol and diluted methanol extract of guava leaves

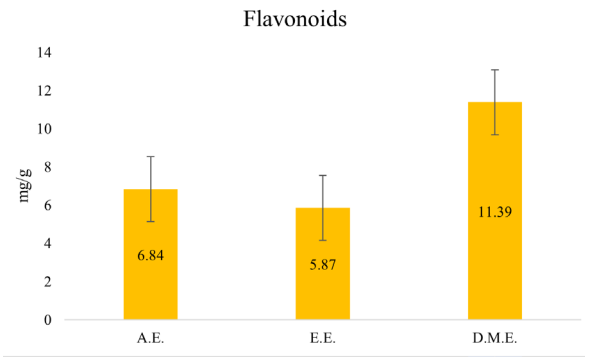

Figure 3. Flavonoid content in aqueous, ethanol and diluted methanol extract of guava leaves

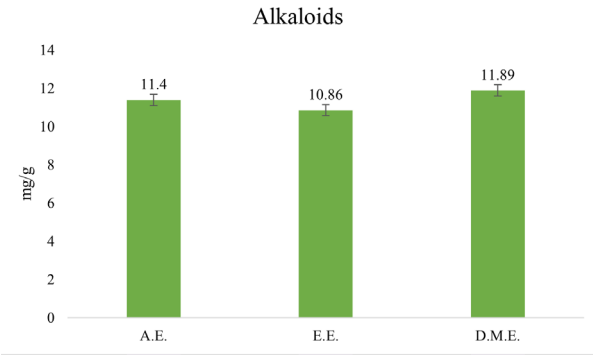

Figure 4. Alkaloid content in aqueous, ethanol and diluted methanol extract of guava leaves

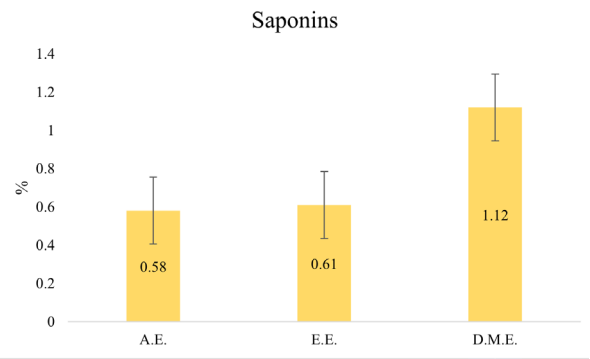

Figure 5. Saponin content in aqueous, ethanol and diluted methanol extract of guava leaves

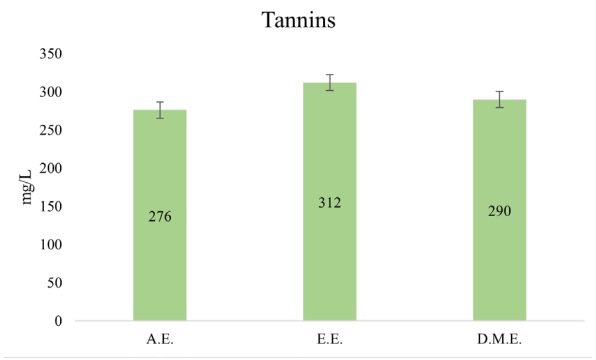

Figure 6. Tannin content in aqueous, ethanol and diluted methanol extract of guava leaves

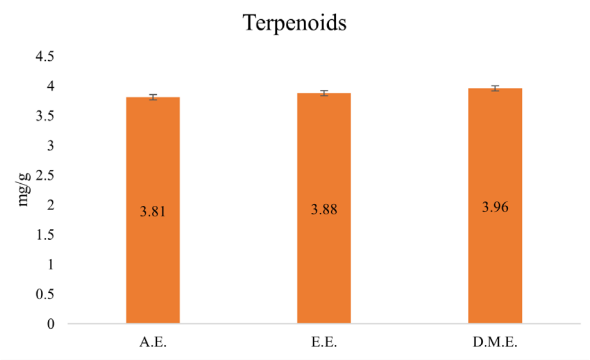

Figure 7. Terpenoid content in aqueous, ethanol and diluted methanol extract of guava leaves

followed by diluted methanol extract with 164 ± 0.7 mg GAE/g and ethanol extract with 135 ± 0.5 mg GAE/g.

Flavonoids. The flavonoid content present in guava leaves is shown in Figure 3. Diluted methanol extract had the highest content of flavonoids with 11.39 ± 0.2 mg/g followed by aqueous extract with 6.84 ± 0.5 mg/g. Ethanol extract had the lowest flavonoid content, 5.87 ± 0.7 mg/g.

Alkaloids. The alkaloid content present in guava leaves is shown in Figure 4. The highest content of alkaloids was present in diluted methanol extract with 11.89 ± 0.8 mg/g, followed by the aqueous extract with 11.4 ± 0.2 mg/g and ethanol extract which had the lowest alkaloids content, 10.86 ± 0.1 mg/g.

Saponins. The saponin content present in guava leaves is shown in Figure 5. The highest presence of saponins was in diluted methanol extract with 1.12 ± 0.2%, followed by ethanol extract with 0.61 ± 0.5%, and aqueous extract which had the lowest saponin content with 0.58 ± 0.6%.

Tannins. The tannin content of guava leaves is shown in Figure 6. The highest content of tannins

was present in ethanol extract, 312 ± 0.3 mg/L, followed by diluted methanol extract with 290 ± 0.4 mg/L and aqueous extract, 276 ± 0.1 mg/L, the lowest tannin content.

Terpenoids. The terpenoid content of guava leaves is shown in Figure 7, a maximum terpenoid content of 3.96 ± 0.7 mg/g in diluted methanol extract followed by 3.88 ± 0.6 mg/g in ethanol extract and the minimum terpenoids content, with 3.81 ± 0.3 mg/g, in aqueous extract.

DISCUSSION

The findings of total phenolic content results coincide with a similar study done using hydroethanolic extract conducted by Amaral et al. (23) where total phenolic content was found to be 185 and 150 mg GAE/g in 50% and 70% hydroethanolic extract, respectively. Another study conducted by Hartati et al. (24) reported total phenolic compound of guava leaves ethanolic extract to be 146.7 mg GAE/g. Slightly higher concentrations of total phenolic content were observed by Cerio et al., 2016 where a significantly higher concentration of total phenolic content, 304 mg GAE/g, was found in etOH/H_2O 80:20 (v/v) solvent. The findings of flavonoids in this study are in alliance with the findings by Díaz-de-Cerio et al. (25) where the flavonoids content in n-hexane leaf extract of crystal guava variety was observed to be 9.68 mg/g. Slightly higher flavonoid content, 18.66 mg/g, was observed by Pandhi et al. (26) using the UAE method. Not many studies were found related to other bioactive compounds of guava leaves.

CONCLUSIONS

The study successfully demonstrated the efficiency of UAE in isolating bioactive compounds from guava leaves using different solvents. The results indicate that diluted methanol is the most effective solvent for extracting flavonoids and alkaloids, while ethanol is superior for tannin extraction, and aqueous best depicts high total phenolic content. This finding highlights the importance of solvent selection in maximizing the yield of specific bioactive compounds. The high content of these compounds in guava leaves suggests their significant potential for use in health-promoting applications. Future research should focus on exploring the therapeutic benefits of these extracts and optimizing extraction methods for industrial applications. The findings promote the utilization of guava leaves, which are often discarded, thus adding value to guava cultivation and contributing to sustainable agricultural practices. This study had some limitations: it was carried out on a small scale under laboratory conditions which may not fully reflect real-world applications. Also, only basic methods were used to analyze the total amounts of bioactive compounds.

ACKNOWLEDGEMENTS

The authors would like to acknowledge the staff of Krishi Vigyan Kendra of Banasthali Vidyapith, Newai, Rajasthan, India, for their support in identification of the guava variety. We would also like to give special thanks to Mr. Vimal Jain for providing technological knowledge during our experiment.

FUNDING

No fundings provided.

CONFLICTS OF INTEREST

No conflicts of interest are associated with the authors for this investigation.

AUTHOR CONTRIBUTION

S.K.: collected the raw material, performed the experiment, evaluated the result and wrote the manuscript; P.S.: helped in drafting the manuscript and guided in the experiment. E.S.C.: supervised the work, guided in the experiment and revised the final manuscript.

DATA AVAILABILITY STATEMENT

All data generated or analyzed during this study are included in this published article.

INSTITUTIONAL REVIEW BOARD STATEMENT

Ethical review and approval were waived for this study, as it did not involve human participants or animals.

INFORMED CONSENT STATEMENT

Not applicable.

REFERENCES

1. Khanna S, Singh P, Chauhan ES. Nutritional analysis of Guava (Psidium guajava L.) and its incorporation in Bhakarwadi. International Journal of Food and Fermentation Technology. 2022;12:117-20.
2. Gutierrez-Montiel D, Guerrero-Barrera AL, Ramírez-Castillo FY, Galindo-Guerrero F, Ornelas-García IG, Chávez-Vela NA, et al. Guava leaf extract exhibits antimicrobial activity in extensively drug-resistant (XDR) Acinetobacter baumannii. Molecules. 2024;30: 70. PubMed PMID: 39795127.
3. Seshadri VD, Balasubramania B, Al-Dhabi NA, Esmail GA, Arasu MV. Essential oils of Cinnamomum loureirii and Evolvulus alsinoides protect guava fruits from spoilage bacteria, fungi and insect (Pseudococcus longispinus). Industrial Crops and Products. 2020; 154:1-9.
4. Khanna S, Singh P, Chauhan P, Chauhan ES. Medicinal and nutritional potential of guava leaves: a natural remedy for health and wellness. Journal of Advances in Food Science & Technology. 2025;12:13-20.
5. Laily N, Kusumaningtyas RW, Sukarti I, Rini MR. The potency of guava *Psidium guajava* (L.) leaves as a functional immunostimulatory ingredient. Procedia chemistry. 2015;14:301-7.
6. Shaheena S, Chintagunta AD, Dirisala VR, Kumar NSS. Extraction of bioactive compounds from Psidium guajava and their application in dentistry. AMB Express. 2019;9:1–9.
7. Shabbir H, Kausar T, Noreen S, Rehman HU, Hussain A, Huang Q, et al. In vivo screening and antidiabetic potential of polyphenol extracts from guava pulp, seeds and leaves. Animals (Basel). 2020;10(9):1714. PubMed PMID: 32971839
8. Morais-Braga MF, Carneiro JN, Machado AJ, Sales DL, Dos Santos AT, Boligon AA, et al. Phenolic composition and medicinal usage of Psidium guajava Linn.: Antifungal activity or inhibition of virulence? Saudi J Biol Sci. 2017;24:302-13.
9. Huynh HD, Nargotra P, Wang HM, Shieh CJ, Liu YC, Kuo CH. Bioactive compounds from guava leaves (Psidium guajava L.): characterization, biological activity, synergistic effects, and technological applications. Molecules. 2025;30:1278. PubMed PMID: 40142053
10. Naseer S, Hussain S, Naeem N, Pervaiz M, Rahman M. The phytochemistry and medicinal value of Psidium guajava (guava). Clinical Phytoscience. 2018;4:1-8.
11. Chen FY, Yu WW, Lin FX, Huang JW, Huang WM, Shuang PC, et al. Sesquiterpenoids with neuroprotective activities from the Chloranthaceae plant Chloranthushenryi. Fitoterapia. 2021;151:104871. Pub Med PMID: 33652076
12. Zhang X, Zuo Z, Yu P, Li T, Guang M, Wang L. Rice peptide nanoparticle as a bifunctional food-grade Pickering stabilizer prepared by ultrasonication: Structural characteristics, antioxidant activity, and emulsifying properties. Food Chem. 2021;343:128545. PubMed PMID: 33223302
13. Aekthammarat D, Tangsucharit P, Pannangpetch P, Sriwantana T, Sibmooh N. Moringaoleifera leaf extract enhances endothelial nitric oxide production leading to relaxation of resistance artery and lowering of arterial blood pressure. Biomed Pharmacother. 2020;130:110605. PubMed PMID: 32781358
14. Pham DQ, Pham HT, Han JW, Nguyen TH, Nguyen HT, Nguyen TD, et al. Extracts and metabolites derived from the leaves of Cassia alata L. exhibit in vitro and in vivo antimicrobial activities against fungal and bacterial plant pathogens. Industrial Crops and Products. 2021;166:1-11.
15. Hamzalıoglu A, Gökmen V. Interaction between bioactive carbonyl compounds and asparagine and impact on acrylamide. Acrylamide in Food: Analysis, Content and Potential Health Effects; Gökmen, V., Ed. 2016:355-76.
16. Agregán R, Munekata PE, Feng X, Astray G, Gullón B, Lorenzo JM. Recent advances in the extraction of polyphenols from eggplant and their application in foods. LWT. 2021;146:1-13.
17. Fu X, Wang D, Belwal T, Xie J, Xu Y, Li L, et al. Natural deep eutectic solvent enhanced pulse-ultrasonication assisted extraction as a multi-stability protective and efficient green strategy to extract anthocyanin from blueberry pomace. LWT. 2021;144:1-12.
18. Carreira-Casais A, Otero P, Garcia-Perez P, Garcia-Oliveira P, Pereira AG, Carpena M, et al. Benefits and drawbacks of ultrasound-assisted extraction for the recovery of bioactive compounds from marine algae. Int Environ Res Public Health. 2021;18:9153. PubMed PMID: 34501743
19. Hadidi M, Ibarz A, Pagan J. Optimisation and kinetic study of the ultrasonic-assisted extraction of total saponins from alfalfa (Medicago sativa) and its bioaccessibility using the response surface methodology. Food Chem. 2020;309:125786. PubMed PMID: 31704078
20. Mahmoud KF, Ali HS, Amin AA. Nanoencapsulation of bioactive compounds extracted from Egyptian prickly pears peel fruit: antioxidant and their application in guava juice. Asian J Sci Res 2018;11:574-86.
21. Singh P, Khanna S, Chauhan ES. Comparative analysis of bioactive compound extraction from beet greens: a study on the influence of solvents used in ultrasonic assisted extraction. Int J Pharm Sci & Res 2024;15: 1000-07.
22. Malik SK, Ahmad M, Khan F. Qualtitative and quantitative estimation of terpenoid contents in some important plants of Punjab, Pakistan. Pakistan Journal of Science. 2017;69:150.
23. Amaral VA, Alves TR, de Souza JF, Batain F, de Moura Crescencio KM, Soeiro VS, et al. Phenolic compounds from Psidium guajava (Linn.) leaves: effect of the extraction-assisted method upon total phenolics content and antioxidant activity. Biointerface Research in Applied Chemistry. 2021;11:9346-57.
24. Hartati R, Nadifan HI, Fidrianny I. Crystal guava (Psidium guajava L."Crystal"): evaluation of in vitro antiox-

idant capacities and phytochemical content. The Scientific World Journal. 2020;2020(1):9413727. PubMed PMID: 32952456

25. Díaz-de-Cerio E, Gómez-Caravaca AM, Verardo V, Fernández-Gutiérrez A, Segura-Carretero A. Determination of guava (Psidium guajava L.) leaf phenolic compounds using HPLC-DAD-QTOF-MS. Journal of Functional Foods. 2016;22:376-88.
26. Pandhi S, Kumar A, Rai DC. Efficacy evaluation of extraction technologies for guava (Psidium guajava L.) leaves extract. Annals of Phytomedicine. 2022;11:413-18.

Biomedical Sciences and Clinical Medicine 2026;65(1):58-67.
doi: 10.12982/BSCM.2026.06
https://he01.tci-thaijo.org/index.php/CMMJ-MedCMJ/index

BSCM
Biomedical Sciences and Clinical Medicine

Original Article

Open Access

Can the Indonesian Version of the Work-Related Quality of Life Scale-2 (WRQoLS-2) Be Used to Measure Quality of Work Life Among Hospital Personnel?

Aulia Rosinta[1], Naesinee Chaiear[1], Chatpong Ngamchokwathana[1] and Nuri Purwito Adi[2]

[1]Department of Community Medicine, Family, and Occupational Medicine, Faculty of Medicine, Khon Kaen University, Khon Kaen, Thailand; [2]Department of Community Medicine, Faculty of Medicine, Universitas Indonesia, Depok, Indonesia.

Correspondence:
Naesinee Chaiear, MD, PhD, Department of Community Medicine, Family, and Occupational Medicine, Faculty of Medicine, Khon Kaen University, Khon Kaen 40002, Thailand.
E-mail: naesinee@kku.ac.th

Received: April 3, 2025;
Revised: July 4, 2025;
Accepted: Aug 22, 2025

ABSTRACT

OBJECTIVE This study aimed to construct and validate the Work-Related Quality of Life Scale-2 (WRQoLS-2) for use in Indonesia.

METHODS A cross-cultural adaptation process, including forward and backward translations by multilingual experts, ensured linguistic and conceptual equivalence of the items. Six nursing experts assessed the content validity, and the reliability was tested using Cronbach's alpha, Intraclass Correlation Coefficients (ICCs), and Spearman rank correlation coefficients among 38 registered nurses.

RESULTS The Indonesian WRQoLS-2 showed strong content validity (S-CVI/Ave of 0.97, S-CVI/AU of 0.84) and high internal consistency (Cronbach's alpha: 0.955-0.961). The ICC analysis yielded an overall ICC of 0.921, indicating excellent reliability. Most dimensions showed positive Spearman correlations, with the exception of three items in the Stress at Work dimension, which were revised and retested. The revised items confirmed that there were no comprehension issues vis-à-vis the questionnaire.

CONCLUSIONS Overall, the Indonesian version of the WRQoLS-2 proved to be a valid and reliable tool for assessing the quality of work life among hospital personnel in Indonesia.

KEYWORDS content validity; health workers; nurses; reliability; work-related quality of life scale

INTRODUCTION

The field of workplace health has undergone significant changes over time, highlighting the importance of enhancing employee welfare across various industries. This aspect is particularly vital in healthcare settings, where the well-being and effectiveness of employees directly impact the quality of care provided to patients (1). International Labour Organization (ILO) Conventions No. 155 and No. 161 emphasize the importance of ensuring that workers achieve optimal physical, social, and mental well-being. These conventions advocate for robust measures to protect and improve health in the workplace (2), aligning with goals to enhance organizational performance, help alleviate the strain on social security and healthcare systems, and promote the long-term well-being of workers and their families (3).

Hospitals, as key institutions in the health sector, rely on productive and responsive personnel to meet patient needs effectively. Nurses, who constitute the largest segment of the health

workforce in many countries, including Indonesia, play a crucial role in patient care (4). Their welfare and productivity are intimately linked to patient satisfaction as well as to the overall efficiency and efficacy of health services (5, 6). However, nurses frequently face various occupational hazards, such as physical injuries and mental stress, which can negatively affect their well-being and their professional performance (7-9). The amalgamation of occupational risks and the intrinsically demanding nature of nursing underscores the urgency of addressing health and safety issues within this profession.

The World Health Organization (WHO) regards the health workforce as a key component of every functioning health system and as essential for improving health services globally (10). The significance of nurses in this regard has been increasingly recognized, alongside a growing awareness of the need to enhance the quality of working life (QoWL) for health workers. The concept of QoWL significantly influences the productivity and efficiency of health facilities and the quality of care provided to patients (11-13). Various models and methodologies have been developed to assess QoWL, with the Work-Related Quality of Life Scale (WRQoLS) gaining international recognition for its reliability and applicability across different cultural contexts (14). The primary challenge in translating a measurement instrument is language, as it is complex and nuanced, with words carrying different meanings and connotations across languages and cultures (15). Several studies of translated versions of the WRQoLS have been shown to have no differences in the construction of the questionnaires. In that regard, extensive evaluation of content validity is essential for achieving psychometric property equivalency to the original version.

Despite the existence of various assessment tools, there remains a noticeable lack of resources specifically designed to evaluate QoWL among nurses and health workers in Indonesia. Previous studies have attempted to adapt and translate existing QoWL assessment tools; however, the scarcity of instruments tailored to the Indonesian health context highlights an unmet need (16-18). This gap hinders the assessment of health workers' quality of work life and limits the implementation of targeted interventions to improve their well-being and job satisfaction.

Given these considerations, this study aimed to construct an Indonesian version of the WRQoLS-2 and to evaluate its content validity and reliability, recognizing the pivotal role it plays in enhancing health services and worker satisfaction. By adapting this globally recognized tool to Indonesia's specific conditions, this study aimed to provide a robust instrument for assessing the quality of nurses' work-life, thereby contributing to the development of healthier working environments and improved patient care outcomes in Indonesian hospitals.

METHODS

This was a cross-cultural adaptation study comprising three primary stages: translation of the original version, assessment of content validity, and reliability assessment of the Indonesian version of the WRQoLS-2. A flowchart summarizing the three phases of the cross-cultural adaptation process is presented in Figure 1.

Phase 1: Translation of WRQoLS-2 to Indonesian

The translation process of the WRQoLS-2 involved five stages to ensure linguistic and conceptual similarity. The process began with a forward translation conducted by two bilingual translators with a medical background to maximize the translation's accuracy and appropriateness for local health contexts. The translators worked independently, each providing their interpretation of the scale. The translations were then merged during a coordinated online meeting of health care professionals, where the goal was to address any inconsistencies and reach a unanimous agreement on the translation.

Following that initial translation, two other translators, unfamiliar with the original WRQoLS-2, performed reverse translation to convert the synthesized Indonesian version into English. This step was crucial for identifying any changes in meaning or discrepancies with respect to the original. Dr. Darren Van Laar, the developer of the scale, then reviewed the back-translated version to assess the semantic and conceptual equivalence between the original and back-translated scales.

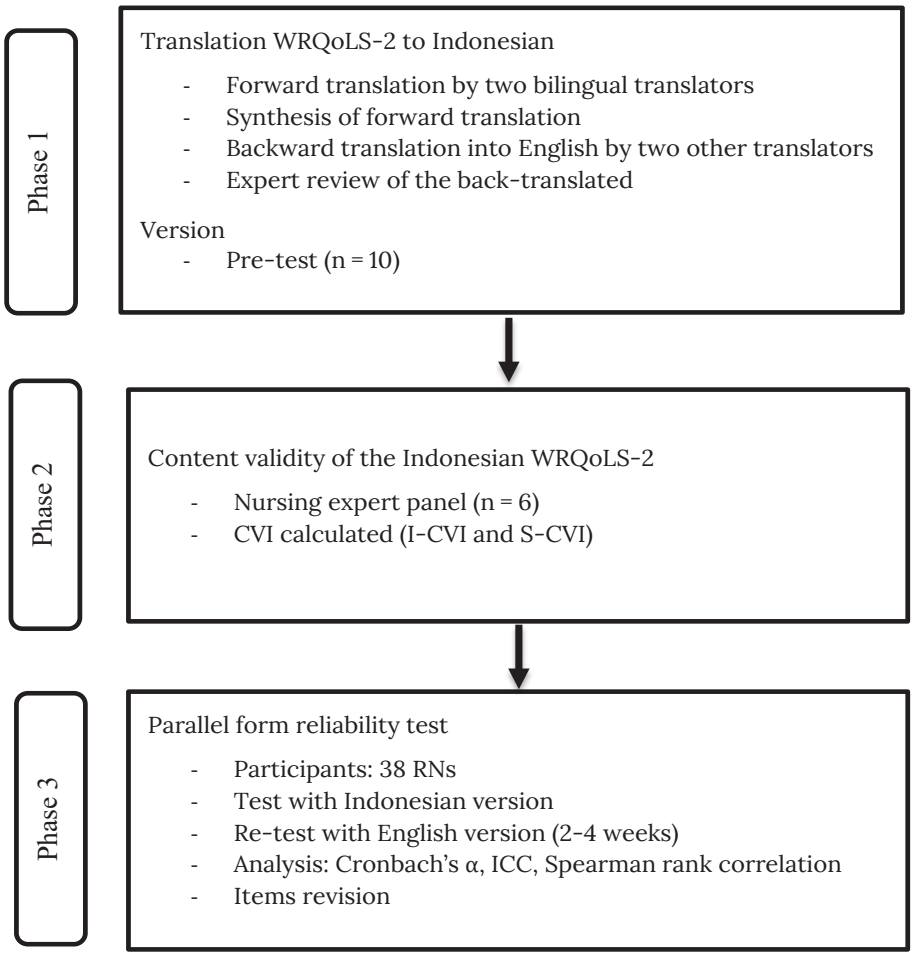

Figure 1. Overview of study design

Finally, the translated version was tested on a sample of Indonesian individuals. The number of participants (n = 10) in that pre-test phase was consistent with the recommended practices in cross-cultural adaptation studies. Previous research has demonstrated that involving 10 to 30 participants in pre-final testing is sufficient for evaluating the clarity, comprehensibility, and cultural relevance of translated items through cognitive interviews (19-21). The participants were all native speakers with professional experience in organizations or enterprises. The purpose of this testing phase was to identify any ambiguous terms, words, or sentences, thereby ensuring that the translated scale would be easily understood by the Indonesian population.

Phase 2: Content validity of the Indonesian WRQoLS-2

Content validity was assessed by six nursing professionals with expertise in academic and hospital settings. The use of six experts aligns with the widely accepted recommendations for content validity index (CVI) evaluation, suggesting that a panel of 5-10 experts is sufficient to ensure reliability and representativeness (22). Recent studies have employed panels of five to eight experts for content validation across disciplines such as medical education, health planning, and occupational safety, supporting the sufficiency of our evaluation team size (23-25). The six experts, each with a minimum of 10 years of experience in the nursing field and holding at least a postgraduate degree, were asked to evaluate the relevance of the items in the Indonesian version of the WRQoLS-2. They were briefed on the questionnaire and its dimensions and received instructions on how to conduct a content validity assessment. For this evaluation, they utilized a self-developed 4-point Likert scale to assess the suitability of the items for reflecting the dimensions and QoWL of Indonesian nurses, particularly in terms of their relevance to the Indonesian context.

Phase 3: Parallel-form reliability test

A reliability test was conducted in an Indonesian hospital and involved 38 registered nurses who met certain criteria, including being full-time employees, having 5-10 years of work experience, having employment status as civil servants, and being proficient in English. The sample size was designed for psychometric testing rather than for representativeness of the broader population. Previous studies have demonstrated that a sample size of 30 is adequate for reliability analysis (25). Our final sample of 38 nurses exceeded the recommended minimums, ensuring a reliable assessment of the scale's psychometric properties. The goal was to assess the accuracy of the WRQoLS-2 Indonesian version by comparing it to the original English version. Participants completed both the Indonesian and original English WRQoLS-2 questionnaires, with a 2-week to 1-month gap between administration of each version. This gap was consistent with the best practices in test-retest reliability research and several empirical studies which recommend a 2-4 weeks interval to reduce memory recall bias while maintaining construct stability (26-28).

The last phase of the preliminary testing included a panel of ten native speakers of Indonesian, who reviewed three items (SAW Dimension) that had shown either no or only weak correlation with the original English version in earlier evaluations. The three items were item 7 (*Saya sering merasa ditekan saat bekerja*/ I often feel under pressure at work), item 19 (*Saya sering merasa stres berlebihan saat bekerja*/ I often feel excessive levels of stress at work), and item 29 (*Saya ditekan untuk bekerja lembur*/ I am pressured to work long hours). Each participant evaluated the clarity and familiarity of these items in the Indonesian version of the questionnaire which were subsequently compared with the original English version to verify the accuracy and equivalence of the translation. Participants were also invited to suggest any improvements to the translations.

Data analysis was conducted using IBM SPSS Statistics for Windows, Version 26.0 (29). Descriptive statistics were used to present the quantitative variables. Both the item-level content validity index (I-CVI) and the scale-level content validity index (S-CVI) were calculated. I-CVI was based on the percentage of experts rating an item as relevant (scores of 3 or 4), and S-CVI was determined through two methods: S-CVI/Ave which averages the I-CVIs, and S-CVI/UA, which assesses the level of universal agreement among experts for each item. The combined CVI of 0.8 was deemed satisfactory, indicating adequate content validity (30, 31).

Reliability was confirmed with Cronbach's alpha, with values above 0.7 indicating acceptable reliability and suggesting that the items within the scale consistently measured the same underlying construct (32). The correlation between the scores from both versions was evaluated using the Spearman rank correlation coefficient, with correlations interpreted as follows: 0.90 to 1.00 (excellent), 0.80 to 0.90 (good), 0.70 to 0.80 (moderate), and below 0.70 (inadequate reliability) (33). Additionally, the Intraclass Correlation Coefficient (ICC) was used to further evaluate the reliability of the Indonesian version of the WRQOLS-2. The ICC analysis yielded a value above 0.75, which is considered excellent. ICC values of 0.60-0.74 are considered good, 0.40-0.59 are fair; and below 0.40 are poor (34). These findings underscore the internal consistency and reliability of the instrument, ensuring its suitability for the intended measurements.

This study was conducted in accordance with ethical principles and approved by the Ethics Committee of Khon Kaen University, Thailand (Ethics code: HE661377) and the Ethics Committee of Dr. Moewardi General Hospital, Indonesia (No: 1.087/VI/HREC/2023).

RESULTS

Validity of the Indonesian WRQoLS-2

The WRQoLS-2, featuring 32 items across seven dimensions, was translated into Indonesian through a detailed process outlined in the Methodology section. This process involved forward and backward back translations, enabling most items to be effectively translated into Indonesian and closely matching the original English version upon back translation. However, challenges of some specific terms and phrases necessitated careful examination and adjustments. For more details, see Supplementary 1: Forward-back translation and feedback from Dr. Darren Van Laar.

Dr. Darren Van Laar played a key role in discussions and facilitating significant changes,

leading to an enhanced translation that accurately reflects the intended meanings of certain elements. Notably, 17 items were accurately translated on the first attempt, but 15 required minor revisions to align with nuances of the original questionnaire. These revisions were intended to ensure fairness in questioning, clarify definitions of terms, and precisely capture the original creators' intended perceptions.

For example, in item 5, the term 'employer' posed some difficulty when adapting into Indonesian. The translator initially suggested using the word '*atasan*' (an Indonesian noun referring to a superior or someone in a higher position within the organizational hierarchy). '*Atasan*' is often used to denote a person's immediate supervisor or manager, as well as an employer or boss. However, Dr. Darren intended the term 'employer' to refer to the organization in general, rather than to a specific person such as a boss. After discussion, the translators agreed that 'work institution' could be used to represent an organization in general (D. Van Laar, personal communication, Nov 29, 2023).

The pre-final Indonesian version of the WRQoLS-2 was accepted following these adjustments, signifying successful adaptation that maintained the integrity of the original scale. Moreover, when ten native Indonesian speakers reviewed the Indonesian version and compared it with the original scale, their feedback indicated no difficulties in understanding the instructions and items

Content validity of the Indonesian WRQoLS-2

Content validity assessment was performed by all the experts, who deemed 27 of the 32 items as highly relevant, awarding these items a perfect item I-CVI of 1.00. Item 9 in the General Well-Being Dimension, 'Recently, I have felt unhappy and depressed,' initially received an I-CVI of 0.67 due to two values which were deemed insufficiently precise by one expert, necessitating its revision. Following expert recommendations, this item was rephrased as, 'I am currently experiencing feelings of unhappiness, depression, and pressure.' The five items finally achieved an I-CVI of 0.83, indicating adequate validity for inclusion in the translated version (35). The scale-level CVI based on universal agreement (S-CVI/UA) reached 0.84, a measure of the experts' level of consensus. An S-CVI/Ave rating of 0.97 was achieved using the averaging method. These CVI outcomes confirmed the suitability of the WRQoLS-2 for use with Indonesian registered nurses. Detailed results are presented in Table 1.

Parallel form reliability of the Indonesian WRQoLS-2

Of the 50 registered nurses (RNs) who met the specified criteria, 40 participated in the evaluation of the Indonesian version of the WRQoLS-2. Of these, 38 completed both the Indonesian and the original versions of the questionnaire. Two participants could not be reached for further data collection, resulting in 38 valid responses for the analysis. Thus, of the 50 eligible RNs, 38 completed both versions of the WRQoLS-2, yielding a response rate of 76%. This group is represent-

Table 1. Rating of item content relevance by six experts

Dimension	Number of items	Items	I-CVI average
Job and career satisfaction	6	1, 3, 8, 11, 18, 20	1.00
General well-being	6	4, 9, 10, 15, 17, 21	1.00
Home-work interface	4	5, 6, 14, 25	0.95
Stress at work	4	7, 19, 24, 29	0.83
Control at work	4	2, 12, 23, 30	1.00
Working conditions	4	13, 16, 22, 31	1.00
Employee engagement	3	26, 27, 28	1.00
Overall	1	32	1.00
Total	32		
S-CVI/Ave			0.97
S-CVI/UA			0.84

Table 2. Intraclass correlation coefficient between the translated Indonesian version WRQOLS-2 and the original WRQOLS-2

Domains	Intraclass correlation coefficient
Job and career satisfaction	0.896
General well-being	0.902
Home-work interface	0.902
Stress at work	0.964
Control at work	0.901
Working conditions	0.896
Employee engagement	0.900
Overall	0.906

ative of a skilled and committed workforce that contributes significantly to health services.

Cronbach's alpha was used to measure the internal consistency and reliability of the Indonesian adaptation of the WRQoLS-2. The findings revealed notably high Cronbach's alpha values, averaging 0.958 across dimensions and items. The employee engagement (EEN) dimension had the lowest alpha value at 0.955, while the stress at work (SAW) dimension had the highest value at 0.961. The ICC for the JCS dimension was 0.896, while the SAW dimension had an ICC of 0.964 (Table 2). The ICC analysis yielded an overall ICC of 0.921 for the seven dimensions tested.

The Spearman correlation (Table 3) provided strong evidence of the psychometric fidelity of the Indonesian WRQoLS-2 to the original version. Correlations among all dimensions of both versions were examined. The correlations ranged from 0.343 for SAW to 0.568 for WCS. All dimensions showed statistically significant correlations, in contrast to the SAW dimension. A deeper analysis of the four SAW items revealed that three items (7, 19, and 29) had poor correlations, whereas item 24 maintained a significant correlation (Table 4).

The final evaluation of the three items that had previously shown no or weak correlations led to modifications aimed at addressing potential confusion or misinterpretation. In item 7, originally translated into Indonesian as '*Saya sering merasa tertekan saat bekerja*,' the term '*tertekan*' primarily conveys internal feelings of being overwhelmed, which may not fully capture the external pressures implied by the English phrase 'I often feel pressured at work.' To more accurately reflect such external influences, the translation was amended to '*Saya sering merasa ditekan saat bekerja*,' highlighting the influence of external pressures on one's psychological state.

For item 19, 'I often feel excessive stress at work,' initially translated as '*Saya sering merasa stres berlebihan saat bekerja*,' the term '*berlebihan*' was reconsidered. Given the potential cultural differences in perception of what qualifies as 'excessive,' this translation might not accurately reflect the intensity implied in English. To clarify, '*berlebihan*' was replaced with '*melebihi batas yang wajar*,' modifying the translation to '*Saya sering merasa stres melebihi batas yang wajar saat bekerja*,' thus better communicating stress levels exceeding a reasonable threshold.

Lastly, the translation of 'I am pressured to work long hours' as '*Saya ditekan untuk bekerja lembur*' was revised to avoid the negative connotations of '*ditekan*' and the culturally specific

Table 3. Spearman correlation coefficients between the Indonesian WRQoLS-2 and the Original WRQoLS-2

Dimension		Number of items	Correlation coefficient	*p*-value
WRQoLS-2 Original	WRQoLS-2 Indonesian			
Job and career satisfaction (JCS)	JCS	6	0.554	0.000*
General well-being (GWB)	GWB	6	0.537	0.001*
Home-work interface (HWI)	HWI	4	0.457	0.004*
Stress at work (SAW)	SAW	4	0.343	0.035*
Control at work (CAW)	CAW	4	0.538	0.001*
Working conditions (WCS)	WCS	4	0.568	0.000*
Employee engagement (EEN)	EEN	3	0.405	0.012*
Overall (Ovl)	Ovl	1	0.380	0.019*

*Statistically correlation $p < 0.05$

Table 4. pearman correlation coefficients SAW dimensions between the Indonesian WRQoLS-2 and the Original WRQoLS-2

SAW dimension		Correlation coefficient	*p*-value
WRQoLS-2 Original	WRQoLS-2 Indonesian		
7	7	0.078	0.644
19	19	0.277	0.092
24	24	0.461	0.004*
29	29	0.045	0.790

*Significant correlation $p < 0.05$

implications of '*lembur*.' The phrase was altered to '*Saya dituntut untuk bekerja diluar waktu kerja*,' which more neutrally indicates a requirement to work beyond standard hours, without the suggestion of undue coercion.

DISCUSSION

The cross-cultural adaptation of the WRQOLS-2 into Indonesian involved a rigorous forward and backward translation process, similar to that described in previous studies, to ensure both linguistic and cultural relevance and to maintain conceptual equivalence across cultures (36-39). A key adaptation challenge was the term 'organization,' which in the Indonesian health context was replaced with the Indonesian phrase for 'work institution' to avoid misinterpretations and to enhance local relevance. These decisions align with the findings of studies showing that even minor terminological misalignments can significantly affect a scale's applicability and the validity of its outcomes (40,41).

The focus on content validity was instrumental, providing an established framework to guide the adaptation, thus ensuring that the scale measured the intended construct within the Indonesian cultural context (42). A panel of Indonesian health professionals was pivotal in refining the translation to convey the intended meanings, ensuring that each item was contextually appropriate (43, 44). This approach aligns with the emphasis on expert reviews in maintaining a scale's psychometric properties (45). The successful content validity assessment, indicated by a high I-CVI of 1.00 and a robust overall S-CVI, reflects a strong expert consensus on the scale's appropriateness and relevance, supporting its methodological rigor (22).

The Indonesian WRQOLS-2 demonstrated excellent internal consistency, with a Cronbach's alpha of 0.958, which is higher than that seen in previous adaptations into other languages such as the Chinese version (Cronbach's alpha of 0.93) (46). This indicates a high level of agreement among the scale items, affirming its reliability in evaluating the quality of working life among Indonesian health professionals. The scale's test-retest reliability, supported by a good ICC of 0.903, underscores its consistency across different administrations. Despite these strong indicators, some issues were noted with the 'Stress at Work' dimension (items 7, 19, and 29), leading to a targeted retest with ten native professionals to refine those item translations to better reflect cultural perceptions of workplace stress. For example, the term 'pressured' was changed to '*ditekan*' to emphasize external pressures, 'excessive stress' was modified to '*stres melebihi batas yang wajar*' to convey culturally relevant thresholds of stress, and to avoid the negative connotations of '*ditekan*' was changed to '*dituntut*' which more neutrally indicates a requirement to work beyond standard hours without suggesting undue coercion. These adjustments, informed by the iterative testing approach recommended in the cross-cultural adaptation literature, highlight the dynamic nature of translation in cross-cultural research and the necessity for continuing refinement to maintain scale integrity and relevance (47). These refinements enhance the scale's ecological validity, ensuring that it accurately reflects the realities of the Indonesian health environment, thus improving its reliability and utility for assessing workplace quality of life.

In addition, global public health priorities increasingly emphasize the importance of improving workplace conditions for health workers, as their well-being directly impacts the quality of care provided to patients (3, 5, 44). The rigorous methodology of this study could help guide similar efforts in regions that have yet to adopt such tools, supporting evidence-based policies and interventions that improve employee satisfaction and patient care outcomes globally.

This study has several limitations. First, the Indonesian version of the WRQoLS-2 was designed to assess the organizational aspects of quality of work life and is not suitable for self-employed

individuals or for assessment of individuals. Second, the instrument does not include built-in demographic or exposure measurement components; thus, organizations wishing to explore associations between quality of work and specific variables must collect contextual data independently. While this study focused exclusively on registered nurses, the WRQoLS-2 may have potential for use among other hospital personnel. However, further validation is recommended prior to applying the scale to different health professional groups.

The Indonesian WRQoLS-2 is suitable for integration into routine assessments of workforce well-being in hospitals, particularly for short-term evaluations. To enhance its utility, it is important for institutions to collect complementary data on demographics and work exposure to help contextualize the results and to support more precise interpretations. Future research should focus on validating this instrument among other health professionals (e.g., physicians, allied health staff, and midwives) and in diverse health settings (e.g., private, military, or religious-based hospitals) across various regions and employment statuses in Indonesia. Ultimately, insights from WRQoLS-2 assessments should be used to guide institutional policymaking and interventions aimed at improving the quality of work life for Indonesia's health workforce.

CONCLUSIONS

The Indonesian WRQoLS-2 is a valid and reliable tool for assessing the quality of work life among hospital nurses in Indonesia. Further studies are recommended to evaluate its applicability among other hospital personnel before broader implementation of the program.

ACKNOWLEDGMENTS

The authors would like to thank (a) the translators, nursing experts, and Professor Darren Van Laar for their contributions to the translation; (b) registered nurses at Dr. Moewardi General Hospital, Surakarta City, Indonesia, for their assistance; and (c) Mr. Bryan Roderick Hamman for assistance with the English-language presentation of the manuscript.

FUNDING

The author gratefully acknowledges the ASEAN and GMS Country Scholarship from Khon Kaen University and the Faculty of Medicine, Khon Kaen University, for funding this research [Grant Number: IN67004].

CONFLICTS OF INTEREST

The authors declare that they have no knowledge of any conflicts of interest or personal relationships that could have influenced this study.

AUTHOR CONTRIBUTIONS

A.R.: conceptualization, writing (original draft), methodology, investigation, formal analysis, software, data curation; N.C.: conceptualization, writing (review & editing), validation, methodology, formal analysis, data curation; C.N.: writing (review & editing), methodology, formal analysis; N.P.: writing (review & editing), validation, and supervision.

DATA AVAILABILITY STATEMENT

The data used are confidential.

INSTITUTIONAL REVIEW BOARD STATEMENT

The study was approved by the Ethics Committee of Khon Kaen University, Thailand (HE661377) and the Ethics Committee of Dr. Moewardi General Hospital, Indonesia (No: 1.087/VI/HREC/2023).

INFORMED CONSENT STATEMENT

Informed consent was obtained from all participants involved in the study.

SUPPLEMENTARY MATERIALS

The following supporting information can be downloaded at: Supplementary appendix

REFERENCES

1. Bakker A, Demerouti E. The job demands-resources model: state of the art. J Manag Psychol. 2007;22:309-28.
2. International Labour Organization. Convention C155 - Occupational Safety and Health Convention, 1981 (No. 155) [Internet]. 2024 [cited 2024 Dec 24]. Available from: https://www.ilo.org/resource/c155-occupational-safety-and-health-convention- 1981-no-155
3. Haddon J. The impact of employees' well-being on performance in the workplace. Strateg HR Rev. 2018; 17:72-5.

4. Suryanto S, Boyle M, Plummer V. Healthcare workforce in Indonesia. Asia Pac J Health Manag. 2017;12: 32-40.
5. Cuff P, Forstag E. The importance of well-being in the health care workforce. Appendix B. In: A design thinking, systems approach to well-being within education and practice: proceedings of a workshop [Internet]. Washington, D.C.: National Academy of Sciences; 2019 [cited 2024 Apr 12]. Available from: https://www.ncbi.nlm.nih.gov/books/NBK540859/
6. Munro C, Hope A. Improving nurse well-being: the need is urgent and the time is now. Am J Crit Care. 2022;31:4-6.
7. International Labour Organization. Nurse, general (institutional): international hazard datasheets on occupation | International Labour Organization [Internet]. 2012 [cited 2024 Dec 24]. Available from: https://www.ilo.org/publications/nurse-general-institutional-international-hazard-datasheets-occupation
8. Ribeiro R, Martins J, Marziale MHP, Robazzi MLDCC. O adoecer pelo trabalho na enfermagem: uma revisão integrativa. Rev Esc Enferm USP. 2012;46:495-504.
9. Nayak S, Mayya S, Chakravarthy K, Andrews T, Goel K, Pundir P. Work-related injuries and stress level in nursing professional. Int J Med Sci Public Health. 2016;5:1693.
10. World Health Organization AHO. Introduction and objectives of the handbook. In: Monitoring the building blocks of health systems: a handbook of indicators and their measurement strategies. WHO; 2010. p. v-xii.
11. Phan G, Vo T. A literature review on quality of working life: a case of healthcare workers. J Appl Pharm Sci. 2016;193-200.
12. Tzeng D, Chung W, Fan P, Lung F, Yang C. Psychological morbidity, quality of life and their correlations among military health care workers in Taiwan. Ind Health. 2009;47:626-34.
13. Odole A, Ogunlana M, Odunaiya N, Oyewole O, Mbada C, Onyeso O, et al. Influence of well-being and quality of work-life on quality of care among healthcare professionals in southwest, Nigeria. Sci Rep. 2023;13:7830. PubMed PMID: 37188741
14. Van Laar D, Edwards JA, Easton S. The work-related quality of life scale for healthcare workers. J Adv Nurs. 2007;60:325-33.
15. Abu Khait A, Shellman J. Transcultural adaptation in translating measurement instruments: challenges and learned lessons. Int J Nurs Knowl. 2024;35:334-44.
16. Pertiwi NI, Harding D. Adaptasi alat ukur quality of work life versi Bahasa Indonesia. Psikol Konseling. 2021;18:908.
17. Jayanegara KA. Alat ukur quality of working life Indonesia. Psikostudia J Psikol. 2020;9:18-25.
18. Fahmie A, Sujarwo A. Development of the work-related quality of life (WRQoL) scale for Indonesia. In: Gaol F, Hutagalung F, Peng C, Isa Z, Rushdan A, editor. Trends and issues in interdisciplinary behavior and social science: proceedings of the 5th International Congress on Interdisciplinary Behavior and Social Science (ICIBSoS 2016), 5-6 November 2016, Jogjakarta, Indonesia. Boca Raton: CRC Press; 2017. p. 159-64.
19. Villaça P, Carneiro J, D'Amico E, Blanchette V, Brandão L, Cassis F, et al. Process and experience of cross-cultural adaptation of a quality of life measure (CHO-KLAT) for boys with haemophilia in Brazil. Haemophilia. 2013;19:861-5.
20. Almohaya H, Bakhsh H, Bin Sheeha B, Aldhahi M, Alhasani R. Translation and cultural adaptation into Arabic of patient-reported outcome measurement information system® item banks: cognitive function abilities and physical function for samples with mobility aid users. Healthcare. 2024;12:211. PubMed PMID: 38255098
21. Tse E, Lam C, Wong C, Chin W, Etz R, Zyzanski S, et al. Cultural adaptation and content validity of a Chinese translation of the 'person-centered primary care measure': findings from cognitive debriefing. Fam Med Community Health. 2020;8:e000621. PubMed PMID: 32962989.
22. Polit D, Beck C. The content validity index: are you sure you know what's being reported? critique and recommendations. Res Nurs Health. 2006;29:489-97.
23. Guraya S, Yusoff M, Mat-Nor M, Fredericks S, Rashid-Doubell F, Harkin D, et al. Validating the medical education e-professionalism framework using the content validity index. Educ Med J. 2022;14:31-47.
24. Nicola T, Weis A. Primary health care planning workshops: construction and validation of an assessment instrument. Rev Bras Enferm. 2020;73:e20190545. PubMed PMID: 32901740
25. Yun V, Ulang N, Husain S. Enhancing content validity of the designed hierarchy of controls instrument in preventing infectious diseases on construction sites: a multidimensional approach. J Adv Res Appl Sci Eng Technol. 2023;32:508-21.
26. Cooper S, Dunsmoor J, Koval K, Pino E, Steinman S. Test-retest reliability of human threat conditioning and generalization across a 1-to-2-week interval. Psychophysiology. 2023;60:e14242. PubMed PMID: 36546410.
27. Storch E, Strawser M, Storch J. Two-week test-retest reliability of the duke religion index. Psychol Rep. 2004;94:993-4.
28. Michael K, Merrell K. Reliability of children's self-reported internalizing symptoms over short to medium-length time intervals. J Am Acad Child Adolesc Psychiatry. 1998;37:194-201.
29. IBM Corp. IBM Statistics for Windows, version 26.0. Armonk, NY: IBM Corp.; 2019.
30. Shi J, Mo X, Sun Z. Content validity index in scale development. Zhong Nan Da Xue Xue Bao Yi Xue Ban. 2012;37:152-5. PubMed PMID: 22561427.
31. Hawkins R, Swanson B, Kremer M, Fogg L. Content validity testing of questions for a patient satisfaction with general anesthesia care instrument. J Perianesth Nurs. 2014;29:28-35.
32. Tavakol M, Dennick R. Making sense of cronbach's alpha. Int J Med Educ. 2011;2:53-5.

33. Schober P, Boer C, Schwarte LA. Correlation coefficients: appropriate use and interpretation. Anesth Analg. 2018;126:1763-8.
34. Koo T, Li M. A guideline of selecting and reporting intraclass correlation coefficients for reliability research. J Chiropr Med. 2016;15:155-63.
35. Klymenko G, Liu KPY, Bissett M, Fong KNK, Welage N, Wong RSM. Development and initial validity of the in-hand manipulation assessment. Aust Occup Ther J. 2018;65:135-45.
36. Beaton D, Bombardier C, Guillemin F, Ferraz M. Guidelines for the process of cross-cultural adaptation of self-report measures. 2000;25:3186-91.
37. Mak S, Soicher J, Mayo N, Wood-Dauphinee S, Bourbeau J. Cross-cultural adaptation of the CHAMPS questionnaire in French Canadians with COPD. Can Respir J. 2016;2016:1-8.
38. Sousa V, Rojjanasrirat W. Translation, adaptation and validation of instruments or scales for use in cross-cultural health care research: a clear and user-friendly guideline. J Eval Clin Pract. 2011;17:268-74.
39. Tsai T, Luck L, Jefferies D, Wilkes L. Challenges in adapting a survey: ensuring cross-cultural equivalence. Nurse Res. 2018;26:28-32.
40. Maneesriwongul W, Dixon J. Instrument translation process: a methods review. J Adv Nurs. 2004;48:175-86.
41. Kuppelwieser V, Putinas A, Bastounis M. Toward application and testing of measurement scales and an example. Sociol Methods Res. 2019;48:326-49.
42. Hinkin T. A brief tutorial on the development of measures for use in survey questionnaires. Organ Res Methods. 1998;1:104-21.
43. Fischer-Grönlund C, Brännström M. The Swedish translation and cultural adaptation of the measure of moral distress for healthcare professionals (MMD-HP). BMC Med Ethics. 2021;22:151. PubMed PMID: 34772400.
44. Anderson DM, Mahamane E, Bauza V, Mahamadou KOB, Tantum L, Salzberg A. Effects of environmental conditions on healthcare worker wellbeing and quality of care: a qualitative study in Niger. PLOS Glob Public Health. 2023;3:e0002590. PubMed PMID: 38117837.
45. Geisinger K. Cross-cultural normative assessment: Translation and adaptation issues influencing the normative interpretation of assessment instruments. Psychol Assess. 1994;6:304-12.
46. Lin S, Chaiear N, Khiewyoo J, Wu B, Johns N. Preliminary psychometric properties of the Chinese version of the work-related quality of life scale-2 in the nursing profession. Saf Health Work. 2013;4:37-45.
47. Van De Vijver F, Hambleton RK. Translating tests. Eur Psychol. 1996;1:89-99.

Supplementary 1. The forward-backward translation and the feedback from Dr. Darren

No.	Original	Synthesis of Forward Translation	Back translation 1	Back translation 2	Comments
1.	I have a clear set of goals and aims to enable me to do my job	Saya memiliki sejumlah target dan tujuan jelas untuk bekerja	I have a number of clear targets and goals to work	I have clear targets and goals for work	Good
2.	I feel able to voice opinions and influence changes in my area of work	Saya merasa mampu menyampaikan pendapat dan membawa perubahan di lingkungan kerja	I feel like I am able to express opinions and create changes at work.	I feel like I can express my opinions and introduce changes in my work environment	Influence is weaker than introduce
3.	I have the opportunity to use my abilities at work	Saya berkesempatan mempraktikkan kemampuan saya saat bekerja	I have the opportunity to practice my capability when working.	I have the chance to practice my skills when working	Good
4.	I feel well at the moment	Saya merasa baik saat ini	I feel well at the moment.	I feel good now	OK, but feel well means both health and wellbeing
5.	My employer provides adequate facilities and	Atasan saya menyediakan cukup fasilitas dan	My employer provides sufficient facility and flexibility for me to	My boss provides enough facilities and flexibility for me so I	Employer here means the organization in general, rather

No.	Original	Synthesis of Forward Translation	Back translation 1	Back translation 2	Comments
	flexibility for me to fit work in around my family life	fleksibilitas bagi saya untuk menyesuaikan waktu kerja dan keluarga	adjust to work and family times	can adjust my time for work and family	than a specific person like a boss
6.	My current working hours / patterns suit my personal circumstances	Jam/ pola kerja saya saat ini sesuai untuk situasi pribadi saya	My work hours/pattern at the moment is suitable for my personal circumstance	My current work hours/pattern is suitable for my personal situation	Good
7.	I often feel under pressure at work	Saya sering merasa tertekan saat bekerja	I often feel pressures when working	I often feel stressed at work	Pressure can be positive, stress is always negative
8.	When I have done a good job it is acknowledged by my line manager	Jika kerja saya bagus, saya mendapatkan pujian/ imbalan dari manajer saya	If I work well, I receive compliments/rewards from my manager	If I work well, I get appreciation/reward from my manager	Acknowledged means it is recognized / seen rather than being rewarded
9.	Recently, I have been feeling unhappy and depressed	Akhir-akhir ini, saya sedang merasa tidak bahagia dan depresi	I am feeling unhappy and depressed lately	Recently, I have been feeling unhappy and depressed	Good

No.	Original	Synthesis of Forward Translation	Back translation 1	Back translation 2	Comments
10.	I am satisfied with my life	Saya puas dengan hidup saya	I am satisfied with my life.	I am satisfied with my life	Good
11.	I am encouraged to develop new skills	Saya terdorong untuk mengembangkan keterampilan baru	I am encouraged to develop new skills	I am motivated to develop new skills	Good
12.	I am involved in decisions that affect me in my own area of work	Saya terlibat dalam keputusan yang memengaruhi diri saya di lingkungan kerja	I am involved in decisions that affect me in my work environment	I am involved in decisions that affect me in the work environment	Good
13.	My employer provides me with what I need to do my job effectively	Atasan saya menyediakan apa yang saya butuhkan untuk bekerja secara efektif	My employer provides everything I need to work efficiently	My boss provides what I need to work effectively	Employer here means the overall organization rather than boss. Also effectively means doing your job well / to a good standard, not just quickly
14.	My line manager actively promotes flexible hours/patterns	Manajer saya secara aktif mempromosikan jam/pola kerja fleksibel	My manager actively promotes flexible work hours/patterns	My manager actively promotes flexible work hours/pattern	Good

No.	Original	Synthesis of Forward Translation	Back translation 1	Back translation 2	Comments
15.	In most ways my life is close to ideal	Secara garis besar, hidup saya mendekati ideal	In general, my life is almost ideal	Broadly speaking, my life is almost ideal	Good
16.	I work in a safe environment	Saya bekerja di lingkungan yang aman	I work in a safe environment	I work in a safe environment	Good
17.	Generally things work out well for me	Sebagian besar hal dalam hidup saya berjalan lancar	Most things in my life work well	Most of the things in my life go smoothly	Good
18.	I am satisfied with the career opportunities available for me here	Saya puas dengan peluang karier yang tersedia bagi saya di tempat kerja ini	I am satisfied with the career opportunities that I have in this workplace	I am satisfied with the career opportunities available for me at this workplace	Good
19.	I often feel excessive levels of stress at work	Saya sering merasa stres berlebihan saat bekerja	I often feel overwhelmingly stressed when working	I often feel extremely stressed at work	Excessive is a weaker word than extremely or overwhelmingly, more like ‘more than I would want.
20.	I am satisfied with the training I receive in order to	Saya puas dengan pelatihan yang saya terima untuk	I am satisfied with the trainings that I received to do my job at the moment	I am satisfied with the training I received for doing my current job	Good

No.	Original	Synthesis of Forward Translation	Back translation 1	Back translation 2	Comments
	perform my present job	melakukan pekerjaan saya saat ini			
21.	Recently, I have been feeling reasonably happy all things considered	Akhir-akhir ini, saya secara umum sedang merasa bahagia	Lately, I feel happy in general	Recently, generally I have been feeling happy	Reasonably happy is weaker than happy. May be better as: In general, I am feeling quite (or sufficiently?) happy at the moment
22.	The working conditions are satisfactory	Kondisi pekerjaan saya memuaskan	My working condition is satisfying	My work condition is satisfactory	Working conditions is normally taking to be the physical environment where you work
23.	I am involved in decisions that directly affect members of the public	Saya terlibat dalam pengambilan keputusan terkait langsung dengan orang banyak	I am involved in the decision makings that are directly related with many people	I am involved in the making of decisions that directly affect many people	This is always a tricky one to translate – it originally comes from a medical context where the word was 'patients' and really refers to the people the organization serves (eg students in a university), I have also seen this changed to clients or customers.
24.	I have unachievable deadlines	Saya memiliki tenggat waktu yang sulit dicapai	I have deadlines that are difficult to meet	I have unrealistic deadlines	Unachievable is a bit stronger and may be better as deadlines I could never meet

No.	Original	Synthesis of Forward Translation	Back translation 1	Back translation 2	Comments
25.	I am able to achieve a healthy balance between my work and home life	Saya bisa meraih keseimbangan yang sehat antara pekerjaan dan keluarga saya	I can have healthy work and family balance	I can achieve a healthy balance between work and family	This is OK, but in English home life would also include hobbies and leisure (eg so it works for people who don't have a family)
26.	The organisation communicates well with its employees	Tempat kerja berkomunikasi dengan baik dengan para pekerjanya	The workplace communicates well with the staff	Workplace communicates well with the employees	Organization here means the wider company or hospital you work for – so 'IBM' or 'Bangkok central hospital' rather than the specific place or dept you work in.
27.	I am proud to tell others that I am part of this organisation	Saya bangga memberitahu orang lain bahwa saya bagian dari tempat kerja ini	I am proud to inform people that I am part of this workplace	I am proud to tell others that I am part of this workplace	Organization here means the wider company or hospital you work for
28.	I would recommend this organisation as a good one to work for	Saya akan merekomendasikan tempat kerja ini sebagai tempat kerja yang baik.	I will recommend this workplace as a good workplace	I will recommend this workplace as a good workplace	Organization here means the wider company or hospital you work for

No.	Original	Synthesis of Forward Translation	Back translation 1	Back translation 2	Comments
29.	I am pressured to work long hours	Saya ditekan untuk bekerja lembur	I am pressured into working overtime	I am forced to work overtime	Not really overtime, which is more formal and people usually get paid extra for it. Long work hours could be overtime, but also could means unpaid work (eg answering emails whilst at home / on holiday)
30.	I have sufficient opportunities to question managers about change at work	Saya memiliki cukup peluang untuk mempertanyakan tentang perubahan di tempat kerja kepada manajer	I have sufficient opportunities to ask about	I have enough chances to ask about the changes in the workplace to manager	May be better as: I have enough chances to ask my manager about changes in the workplace.
31.	I am happy with the physical environment where I usually work	Saya senang dengan lingkungan fisik di tempat saya biasa bekerja	I am happy with the physical environment of where I work	I am happy with the physical environment of the place I normally work in	Good
32.	I am satisfied with the overall quality of my working life	Saya puas dengan keseluruhan kualitas kehidupan kerja saya	I am satisfied with the overall life quality of my workplace	I am satisfied with the quality of my work life in general	Good

Biomedical Sciences and Clinical Medicine 2026;65(1):68-80.
doi: 10.12982/BSCM.2026.12
https://he01.tci-thaijo.org/index.php/CMMJ-MedCMJ/index

BSCM
Biomedical Sciences and Clinical Medicine

Original Article

Open Access

Virgin Coconut Oil Inhibits Leukemic Cell Proliferation Via Apoptosis in K562 and MOLT-4 Cell Lines

Sawalee Saosathan[1], Supachai Yodkeeree[2], Arunrat Warin[3], Natthachai Duangnin[4] and Nittaya Peansub[5]

[1]Clinical Pathology Section, Regional Medical Sciences Center 1 Chiang Mai, Department of Medical Sciences, Ministry of Public Health, Chiang Mai, Thailand; [2]Department of Biochemistry, Faculty of Medicine, Chiang Mai University, Chiang Mai, Thailand; [3]Toxicology Section, Regional Medical Sciences Center 1 Chiang Mai, Department of Medical Sciences, Ministry of Public Health, Chiang Mai, Thailand; [4]Drug Section, Regional Medical Sciences Center 1 Chiang Mai, Department of Medical Sciences, Ministry of Public Health, Chiang Mai, Thailand; [5]Regional Medical Sciences Center 12/1 Trang, Department of Medical Sciences, Ministry of Public Health, Trang, Thailand

Correspondence:
Sawalee Saosathan, PhD, Clinical Pathology Section, Regional Medical Sciences Center 1 Chiang Mai, Department of Medical Sciences, Ministry of Public Health, Chiang Mai 50180, Thailand.
E-mail: benja099@gmail.com

Received: March 30, 2025;
Revised: August 17, 2025;
Accepted: August 26, 2025

ABSTRACT

OBJECTIVE Leukemia is a blood cancer which is expressed by an uncontrolled increase in abnormal white blood cells. To date, chemotherapy has been regularly used to treat leukemia. However, the major problem with chemotherapy is the side effects for leukemia patients. Nowadays, medicinal plants are of interest as an additional form of cancer treatment. Virgin coconut oil (VCO) is a source of antioxidants, anti-viral, anti-inflammatory, and anti-cancer properties. This study was designed to investigate the potential of VCO to inhibit the growth of leukemic cells by inducing cell cycle arrest and apoptosis.

METHODS The VCO was analyzed using gas chromatography coupled with mass spectrometry (GC-MS). In the experiment, two leukemic cell lines, K562 and MOLT-4, were treated with various concentrations of VCO for 48 h. Cytotoxic effects were measured using the MTT assay and compared to commercial lauric acid. Cell cycle analysis was performed using propidium iodide (PI) staining, and apoptosis was assessed using an Annexin V-FITC kit.

RESULTS The study found that VCO is primarily composed of lauric acid, caprylic acid, capric acid, myristic acid, palmitic acid, linoleic acid, oleic acid, and stearic acid. In addition, VCO showed cytotoxic effects in both K562 and MOLT-4 cells, with IC_{50} values of 618.2 µg/mL and between 654 and 760 µg/mL, respectively. Cell cycle analysis demonstrated that VCO induced accumulation of cells in the G2/M phase. Additionally, the apoptosis assay demonstrated that VCO treatment induces apoptosis, particularly in K562 cells, in a cell-dependent manner.

CONCLUSIONS VCO is a promising source of bioactive compounds which exhibit cytotoxic, cell cycle arrest and apoptotic effects on leukemic cells *in-vitro*, suggesting its potential for further investigation as an anti-leukemic agent.

KEYWORDS virgin coconut oil, lauric acid, leukemia, apoptosis, K562, MOLT-4

INTRODUCTION

Cancer is a major cause of morbidity and mortality worldwide, with nearly 20 million new cases and 9.7 million cancer-related deaths in 2022 (1). The number of new cases is anticipated to increase by 70% over the next 2 decades. Approximately one-third of cancer deaths are caused by habit-related factors such as high body mass index, lack of physical activity, low fruit and vegetable consumption, tobacco use, and alcohol use. Leukemia is among the most prevalent cancers worldwide (2, 3). In 2018, the Thai population was close to 65 million. The number of new cancer cases registered that year was 170,500 with 114,200 cancer deaths (4). In Thailand, 21 percent of the population is < 15 years of age; the number of new cancer cases in this age group is approximately 1,000/year (5). During 2007-2008 the cancer related mortality rates in Thai children aged 6-12 and 13-18 were 2.16 and 2.13 per 100,000, respectively. Leukemia is the most common cancer in Thai children (about 30.00%), followed by cancer of the brain and other areas of the nervous system (20.00%), lymphoma (18.00%), renal tumors (10.00%), and others (22.00%) (6).

Leukemia is a type of malignant neoplasm associated with organs that produce blood cells which is identified by an uncontrollable increase of blood cells (7). Development of leukemia is associated with exposure to radiation, toxic chemicals, chemotherapeutic agents, viral and other microorganisms as well as genetic disorders. It is amplified by chromosomal instability, cigarette smoking, and other environmental factors which can lead to genetic changes in leukemic cells that in turn affect the functions of other genes, including tumor suppressor genes and oncogenes. The disease can rapidly proliferate and can be classified as acute or chronic, myeloid or lymphoid (8). The forms of leukemia that impact the myeloid and lymphoid systems include acute myeloid leukemia (AML), chronic myeloid leukemia (CML), acute lymphoblastic leukemia (ALL) and chronic lymphocytic leukemia (CLL) (9).

Presently, chemotherapy is very often utilized for the treatment of leukemia. It has had a very good outcome in the early stages of treatment (10). However, the main problem of chemotherapy is the side effects on the leukemia patients, e.g., it can result in drug resistance after a long period of treatment. Active compounds from medicinal plants normally included in compilations of traditional Thai drug recipes represent a source of potential additional options for cancer treatment.

Medicinal plants represent local natural resources which long have been associated with Thai culture, e.g., as basic foods and as traditional medicines. Most medicinal plants are relatively inexpensive and are easy to find in many local areas, and most have been demonstrated to be safe and to have few side effects. Coconut oil is widely used worldwide for both food and non-food purposes. It is available in different forms, including virgin coconut oil (VCO), crude coconut oil (CCO), and refined coconut oil (RCO) (11). VCO, commonly consumed in Asia, particularly in Thailand, Malaysia, and the Philippines, is extracted from fresh coconut milk under controlled temperatures to preserve its bioactive compounds (12). These bioactive components include vitamins and polyphenols (e.g., ferulic acid, coumaric acid, gallic acid, catechin, and kaempferol or their sugar derivatives) (13, 14).

Apoptosis, or programmed cell death, is characterized by distinct morphological and biochemical changes, including cell shrinkage, cytoplasmic condensation, chromatin condensation, DNA fragmentation, and plasma membrane blebbing. It plays a crucial role in maintaining tissue homeostasis by regulating cell populations, allowing the removal of aged or damaged cells while facilitating the growth of new ones. However, carcinogens can disrupt apoptotic pathways, enabling uncontrolled cancer cell proliferation (15). Basically, cell division is regulated by cell cycle control mechanisms to ensure the production of identical cells. The cell cycle contains 4 stages: gap 1 (G1) phase, synthesis (S) phase, gap 2 (G2) phase and mitosis (M) phase during which the cell grows, replicates its DNA, and prepares for mitosis, respectively. The mitotic cell cycle can normally be divided into 2 major phases, the interphase and the M phase. During the interphase, there will be duplicates of cellular content within the cells and separated into two genetically identical daughter cells in mitosis. DNA replication occurs during the interphase during the S-phase (the synthesis phase). The interphase period, which separates the S-phase from the M-phase, is called the Gap or G1 precede the S phase and G2 phase after the

S phase. According to observational evidence, there is a gap between two main events, the duplication and dissociation of DNA. These phases are important moments for cell cycle regulation and include the decision to enter the cell cycle in the G1 and to initiate the process leading to chromosome segregation in the G2. In unicellular and multicellular eukaryotes, cell division is controlled by a complex network of control, monitoring and balancing mechanisms to ensure that no errors occur before the cells are allowed to enter and progress through the cell cycle and to divide. Checkpoints can delay cell cycle progression, or, in response to irreparable DNA damage, induce cell cycle exit or cell death (16).

VCO contains a high amount of medium-chain saturated fatty acids (MCFAs), particularly lauric acid which comprises approximately 45.00-52.00% of its total fatty acid content (17). Lauric acid has been reported to exhibit antimicrobial properties (18). For example, lauric acid and its derivative monolaurin have been shown to disrupt the cell membranes of Gram-positive bacteria and lipid-coated viruses. Additionally, they interfere with cellular responses by stimulating transduction cascades and gene transcription. Beyond its antimicrobial activity, lauric acid also plays a role in anti-inflammation by inhibition of the nuclear factor-κB (NF-κB) transcription factor activation and the phosphorylation of MAP kinases (19). Moreover, VCO has demonstrated dose-dependent cytotoxicity in various cancer cell lines, including HCT-15 (human colon cancer), HepG2 (human hepatocellular carcinoma), and RAW 264.7 (murine macrophages), by inducing apoptotic morphological changes (14). Furthermore, consuming VCO during chemotherapy has been associated with improved quality of life in breast cancer patients (20). VCO has also exhibited antiviral, anti-inflammatory (13), and antidiabetic properties (17), as well as therapeutic potential for skin disease (17). Additionally, low-dose VCO treatment has been reported to reverse hepatic structural alterations and certain biochemical changes in obese rats (21). VCO has also been shown to enhance resistance to methotrexate-induced oxidative stress and inflammation in rats (22). However, few studies have explored the anticancer properties of VCO. Calderon et al. reported that VCO inhibited the growth of SKBr-3 breast cancer cells (23), while Verma et al. demonstrated its anticancer effects in liver and oral cancer models (24). Currently, no studies have investigated the effects of VCO on cell proliferation, cell cycle arrest, and apoptosis in K562 (human erythroleukemia) and MOLT-4 (T-cell leukemia) cell lines. Therefore, the objective of this study was to evaluate the antiproliferative effects of VCO in these leukemic cell lines by assessing its ability to induce cell cycle arrest and apoptosis.

METHODS

Chemical materials

RPMI 1640 medium supplemented with 25 mM HEPES and L-glutamine, fetal bovine serum (FBS), penicillin-streptomycin, phosphate-buffered saline (PBS), and trypan blue dye solution were obtained from Cytiva HyClone™ (Logan, UT, USA). MTT dye and commercial lauric acid were purchased from Sigma-Aldrich (St. Louis, MO, USA).

Test materials

Five samples of 100% pure VCO were used in this study. Sample No. 1 was prepared traditionally using indigenous methods by a local villager. Samples No. 2-5 were commercially available and obtained from a pharmacy (Chiang Mai University Pharmacy, Chiang Mai, Thailand).

Cells and cell culture condition

The human CML cell line K562 (ATCC® CCL-243™) and the human ALL cell line MOLT-4 (ATCC® CRL-1582™) were obtained from the Cell Bank of the Division of Immunology, Department of Medical Technology, Faculty of Associated Medical Sciences, Chiang Mai University (Chiang Mai, Thailand). K562 and MOLT-4 cells were cultured in RPMI 1640 medium supplemented with 10% FBS, 25 mM HEPES, L-glutamine, 100 U/mL penicillin, and 100 µg/mL streptomycin. The cells were maintained in a humidified incubator at 37°C with 5% CO_2.

Chemical fingerprinting and fatty acid analysis using gas chromatography-mass spectrometry (GC-MS)

The VCO samples (No. 1-5) were pre-processed as follows. A 20 mg aliquot of each sample was mixed with 1 mL of methanolic NaOH and heated

at 65°C for 15 min with intermittent shaking. After incubation, the samples were cooled to room temperature for 5 min, followed by the addition of 1 mL of Milli-Q water and 1 mL of distilled hexane. The mixture was vortexed and allowed to undergo phase separation. The upper organic layer was carefully withdrawn using a micropipette without disturbing the lower aqueous phase. The hexane extract was transferred to a fresh GC vial for GC-MS analysis. Fatty acid separation was performed using a VF-5ms column on a Trace GC Ultra gas chromatograph under the following conditions. The injection port was maintained at 250°C, and the samples were introduced through a split injection mode (50 : 1 split ratio). The oven temperature was initially set at 50°C, then increased to 120°C and held for 5 min. The temperature was further ramped up to 170°C at a rate of 5°C/min and then held for 5 min, followed by an increase to 230°C at 5°C/min and then held for 5 min. Finally, the temperature was raised to 250°C at 5°C/min and held for 2 min. The separated compounds were analyzed using a TSQ Quantum XLS mass spectrometer, and the total ion chromatogram was recorded in scan mode. Mass spectra were acquired for ions ranging from m/z 50 to 500.

MTT cytotoxicity assay

The cytotoxic effects of VCO No. 1 (hand-made) and VCO No. 2-5 (commercially manufactured) were evaluated using the MTT assay. The VCO No. 1-5 were dissolved in dimethyl sulfoxide (DMSO) as a stock substance at a concentration of 25 mg/mL. Then the stock substance was diluted by 0.2% DMSO in RPMI 1640 medium to concentrations between 0-3,200 µg/mL. Briefly, K562 and MOLT-4 cells (1.0×10^4 cells/well) were seeded in 96-well plates containing 100 µL of culture medium and incubated for 24 h. Following incubation, 100 µL of fresh medium containing various concentrations of VCO (0-3,200 µg/mL) was added to each well, and the cells were incubated for an additional 48 h. After treatment, 15 µL of MTT dye solution per 100 µL of medium was added to each well, and the plates were incubated at 37°C in a humidified 5% CO_2 atmosphere for 4 h. Subsequently, 200 µL of DMSO was added to dissolve the formazan crystals. The absorbance was measured using an ELISA plate reader (Thermo Scientific, Multiskan SkyHigh, Singapore at 540 nm, with a reference wavelength of 630 nm. Higher optical density values corresponded to a greater number of viable cells capable of metabolizing MTT salts.

Cell viability was calculated using the following formula:

$$\% \text{ Cell survival} = \frac{\text{Mean absorbance in test wells}}{\text{Mean absorbance in control wells}} \times 100$$

The average cell survival rate, obtained from triplicate determinations at each concentration, was plotted as a dose-response curve. The experiment was conducted in three independent trials to ensure reproducibility. The 50.00% inhibitory concentration (IC_{50}) of VCO was determined as the lowest concentration that reduced cell viability by 50.00% compared to the untreated control or the vehicle control (0.2% DMSO in culture medium). The IC_{50} values were expressed as the mean ± standard deviation (SD) and were compared to evaluate cytotoxic activity (25). The IC_{50} values (cytotoxic doses) from the VCOs were compared to lauric acid with regard to their effects on cell cycle analysis and apoptosis assay.

Cell cycle analysis

K562 and MOLT-4 cells (5×10^5 cells/well) were seeded into 6-well plates and treated with vehicle control, VCO (No. 1 represents hand-made VCO and No. 3 represents commercial VCO with bottle identification "100% VCO, high lauric acid, premium grade, and chemical free", or lauric acid for 24 h. Following treatment, the cells were harvested, washed twice with PBS, and fixed in cold 70% ethanol at -20°C overnight. The ethanol was carefully removed by centrifugation at 1,500 x g for 3 minutes, and the cells were washed with PBS to minimize cell loss. The pelleted cells were then resuspended in 1 mL of staining solution containing 25 µg/mL RNase (United States Biological, Salem, MA, USA) and 50 µg/mL propidium iodide (PI) (Merck Millipore, Darmstadt, Germany), and incubated in the dark at room temperature for 30 minutes. Cell cycle distribution was analyzed using flow cytometry (Beckman Coulter DxFLEX, Brea, CA, USA).

Apoptosis detection via Annexin-V-FITC/PI assay

K562 and MOLT-4 cells (3×10^5 cells/well) were seeded into 6-well plates and treated with vehicle control, VCO (No. 1 and No. 3), or lauric acid at the indicated concentrations for 48 h. Following treatment, the cells were harvested by centrifugation at 1,500 × g for 3 minutes at room temperature and washed twice with ice-cold PBS. The cells were then stained with Annexin V-FITC/PI (Elabscience, Houston, TX, USA) following the manufacturer's instructions and analyzed using flow cytometry.

Statistical analysis

All data are presented as mean ± SD from the three independent experiments. The comparison between the treated and control group was performed using Student's *t*-test (for comparisons of two treatment group) (26, 27). Differences were considered statistically significant if $p < 0.05$ (*), highly significant if $p < 0.01$ (**), and extremely significant if $p < 0.001$ (***).

RESULTS

Characterization of VCO fatty acid composition

The GC-MS analysis of VCO No. 1-5 revealed an identical fatty acid composition across all samples (Figure 1A-1E), indicating consistency in their chemical profiles. The identified fatty acids included lauric acid, caprylic acid, capric acid, myristic acid, palmitic acid, linoleic acid, oleic acid, and stearic acid. These findings confirm the uniformity of the VCO samples, ensuring that any observed biological effects are attributable to the intrinsic properties of VCO rather than compositional variability.

Cytotoxic effects of VCO on K562 and MOLT-4 cell lines

As shown in Table 1, the IC_{50} value of VCO samples (No. 1-5) in K562 cells was 618.2 µg/mL, whereas lauric acid exhibited significantly higher cytotoxicity, with an IC_{50} of 42.3 µg/mL. Similarly, in MOLT-4 cells, the IC_{50} values for VCO samples ranged from 654.5 to 760.0 µg/mL (No. 1-5: 690.9, 654.5, 654.5, 690.9, and 760.0 µg/mL, respectively). In contrast, lauric acid displayed a markedly lower IC_{50} of 42.2 µg/mL, indicating its greater potency in inhibiting cell viability. The dose-dependent cytotoxic effects of VCO and lauric acid on K562 and MOLT-4 cells are illustrated in Figures 2 and 3. A progressive decline in cell viability was observed with increasing concentrations of both treatments. Notably, lauric acid induced a more pronounced reduction in cell viability at lower concentrations, further supporting its stronger cytotoxic potential compared to VCO.

VCO induces cell cycle arrest in K562 and MOLT-4 cells

The effect of VCO on cell cycle progression in K562 and MOLT-4 cells were determined. K562 cells was treated with varying concentrations (close to the IC_{50} values) of VCO No. 1 and VCO No. 3 compared to (close to the IC_{50} values) lauric acid for 24 h to evaluate their impact on cell cycle progression. As shown in Figure 4A, treatment with VCO No. 1 at 150, 300, and 500 µg/mL resulted in a dose-dependent decrease in S-phase DNA content from 29.11% to 24.91%, 25.06%, and 23.20%, respectively. Concurrently, the G2/M-phase DNA content significantly increased from 23.75% in the control to 28.06%, 32.43%, and 32.16%, respectively. Similarly, treatment with VCO No. 3 at 150, 300, and 500 µg/mL (Figure 4B) led to a decrease in S-phase DNA content from 29.11% to 25.00%, 23.30%, and 21.79%, respectively, while the G2/M-phase DNA content significantly increased from 23.75% to 28.66%, 31.13%, and 30.14%, respectively. These findings indicate that both VCO No. 1 and VCO No. 3 induce G2/M-phase cell cycle arrest in K562 cells in a dose-dependent manner. In contrast, treatment with 40 µg/mL lauric acid for 24 h reduced the G2/M-phase DNA content from 23.75% to 18.97%, while significantly increasing the G1-phase DNA content from 41.80% to 51.51% compared to the control. In MOLT-4 cells, treatment with 300 µg/mL VCO No. 1 significantly increased the G2/M-phase DNA content from 26.57% to 30.19%, while the S-phase population slightly decreased from 29.59% to 29.06% compared to the control (Figure 5A). Similarly, treatment with 300 µg/mL VCO No. 3 significantly increased the G2/M-phase DNA content from 26.57% to 30.31%, while the S-phase population decreased from 29.59% to 27.68% compared to the control (Figure 5B). Treatment with 40 µg/mL lauric acid induced a significant increase in the G1-phase population from 38.10% to 55.00%, while reducing the

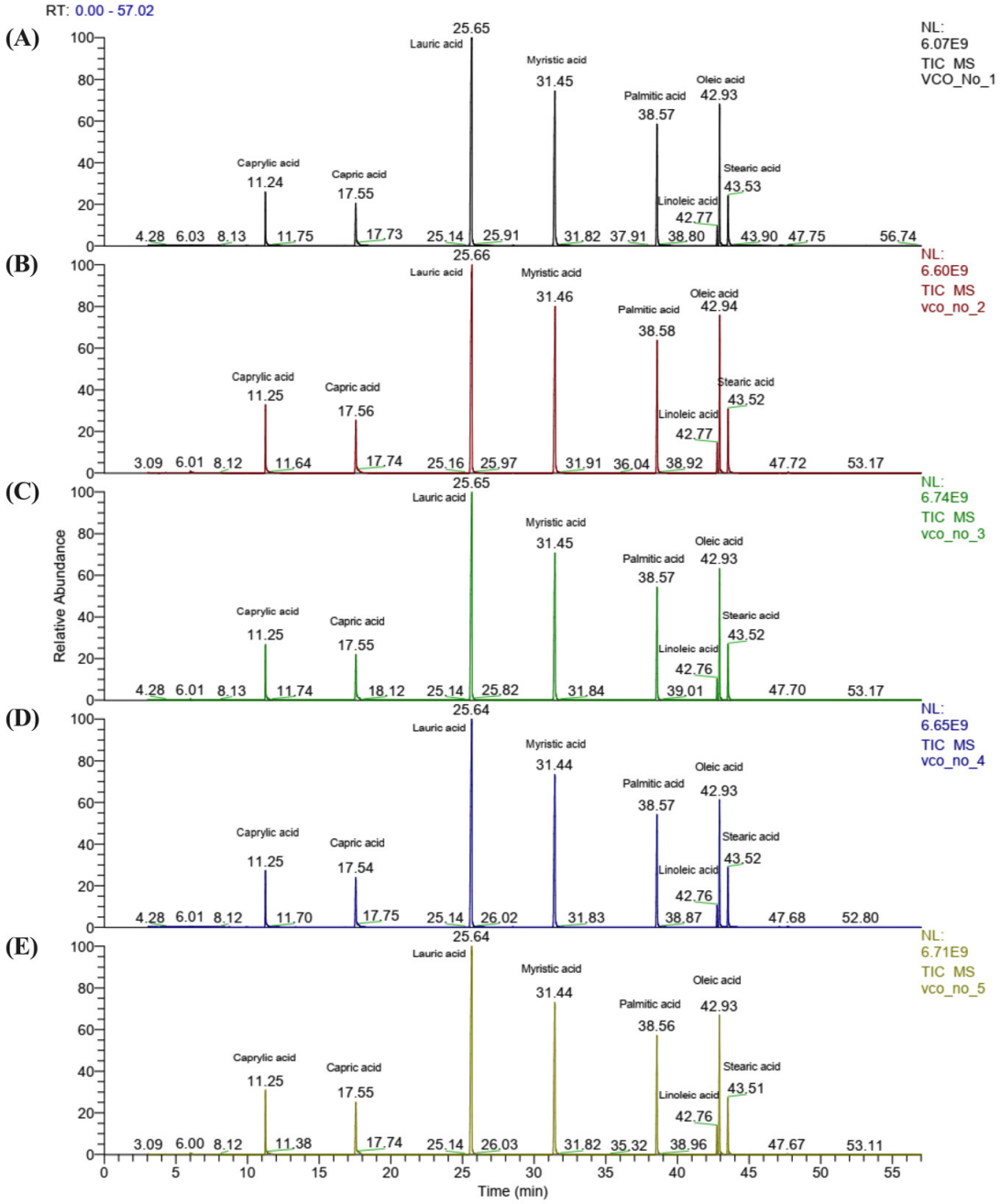

Figure 1. GC-MS characterization of the fatty acid profile in VCO No. 1-5. Total ion chromatograms of (A) VCO No. 1, (B) VCO No. 2, (C) VCO No. 3, (D) VCO No. 4, and (E) VCO No. 5, with retention times labeled at each peak.
VCO, virgin coconut oil

Table 1. IC_{50} values (mean±SD) after VCO No. 1-5 and lauric acid treatments in K562 and MOLT-4 cell lines

Compounds	IC_{50} (μg/mL)	
	K562	MOLT-4
VCO No. 1	618.2±4.94	690.9±1.28
VCO No. 2	618.2±2.94	654.5±4.20
VCO No. 3	618.2±3.15	654.5±4.02
VCO No. 4	618.2±1.37	690.9±1.29
VCO No. 5	618.2±1.98	760.0±1.85
Lauric acid	42.3±6.90	42.2±0.41

VCO, virgin coconut oil

S-phase from 29.60% to 24.30%, and the G2/M-phase from 26.57% to 14.24% in MOLT-4 cells (Figure 5A-5B).

These findings indicate that VCO No. 1 and VCO No. 3 promote G2/M-phase cell cycle arrest in a dose-dependent manner in both K562 and MOLT-4 cells. In contrast, lauric acid induces G1-phase accumulation, suggesting distinct mechanisms of action. The observed alterations in cell cycle distribution imply that VCO may exert cytostatic effects by delaying G2/M-phase

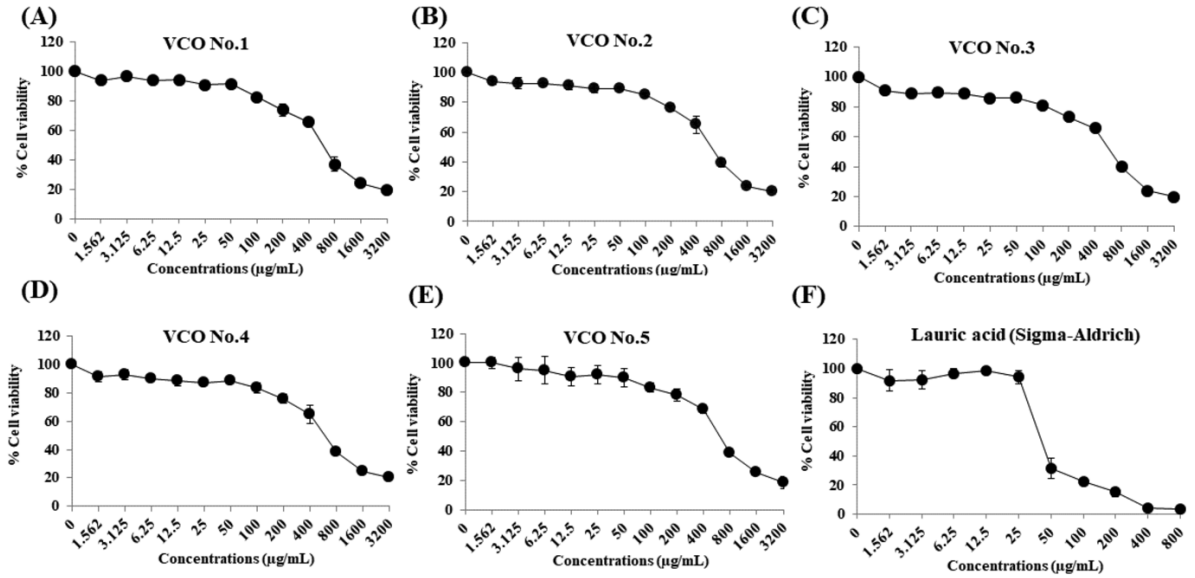

Figure 2. Cytotoxic effects of VCO No. 1-5 (A-E) and lauric acid (F) on K562 cells. Data are presented as mean ± SD from three independent experiments. VCO, virgin coconut oil.

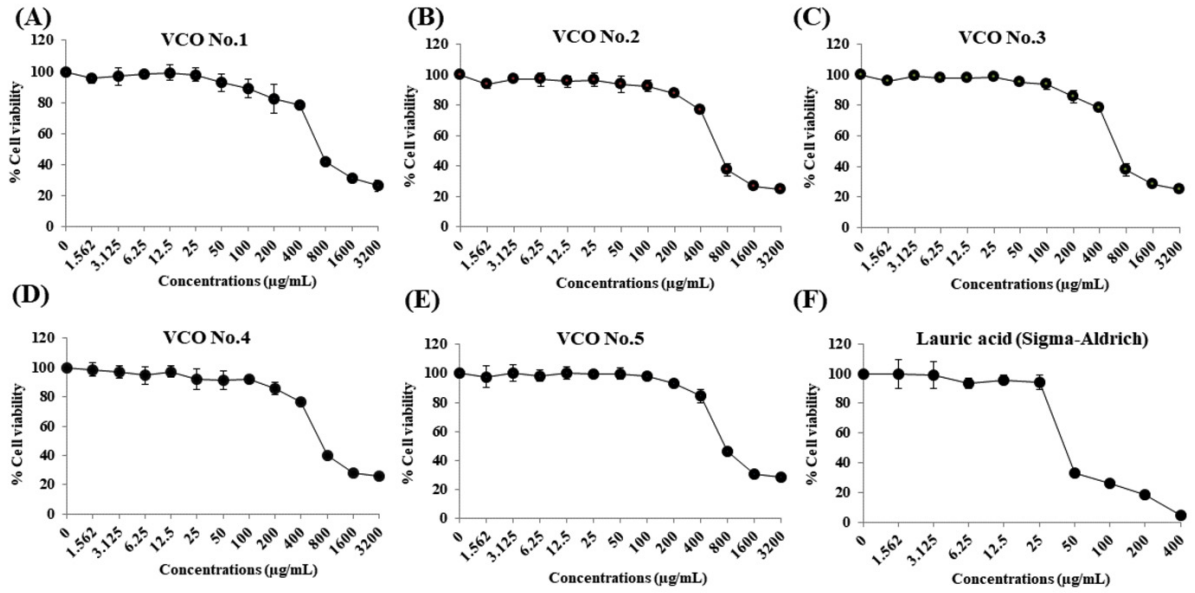

Figure 3. Cytotoxic effects of VCO No. 1-5 (A-E) and lauric acid (F) on MOLT-4 cells. Data are presented as mean ± SD from three independent experiments. VCO, virgin coconut oil

progression, whereas lauric acid facilitates G1-phase arrest. The results of chemical fingerprinting and fatty acid analysis using gas chromatography-mass spectrometry (GC-MS) showed that VCO contains a variety of fatty acids, including lauric acid, caprylic acid, capric acid, myristic acid, palmitic acid, linoleic acid, oleic acid, and stearic acid. Fatty acids other than lauric acid may cause changes in the arrest of cells in the cell cycle after treatment with VCO, which is different from treating only lauric acid in both cell lines.

Induction of apoptosis by VCO in K562 and MOLT-4 Cells

To examine VCO's role in apoptosis, we assessed the effects of VCO No. 1 and VCO No. 3 in K562 cells. Our results indicate that treatment with 300 and 500 µg/mL of VCO No. 1 for 48 h significantly increased apoptosis in a dose-dependent manner, from 4.69% in the control to 8.23% and 10.01%, respectively (Figure 6A). Likewise, treatment with 300 and 500 µg/mL VCO No. 3 resulted in significant increases in apoptosis, from 4.69% to 8.66% and 10.50%, respectively (Figure

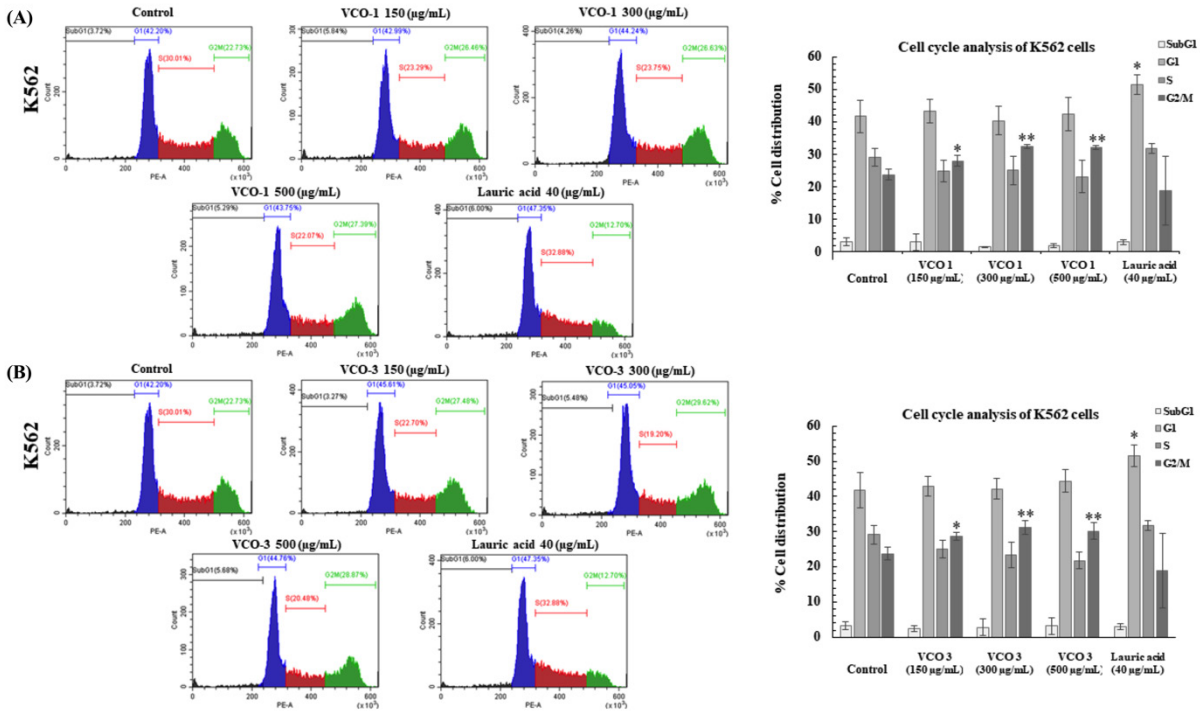

Figure 4. VCO inhibits cell cycle progression. (A) VCO No. 1 and (B) VCO No. 3. Data are presented as the mean ± SD of three independent experiments. $^{*}p < 0.05$, $^{**}p < 0.01$. VCO, virgin coconut oil.

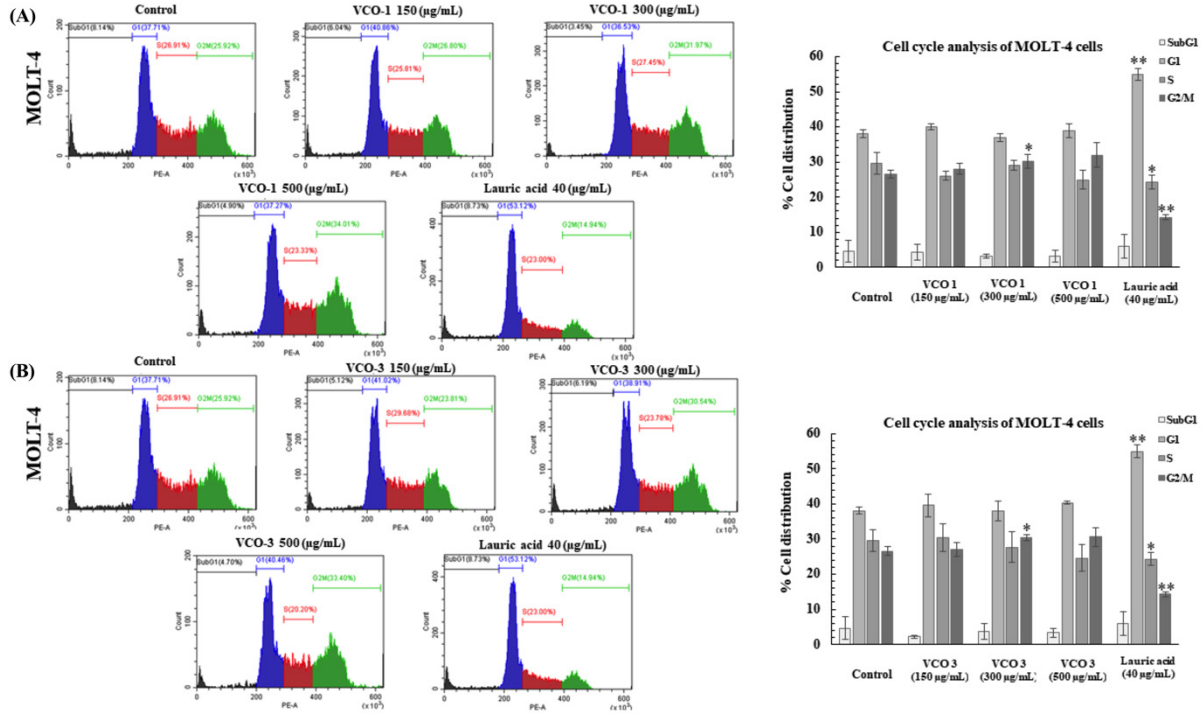

Figure 5. VCO inhibits cell cycle progression. (A) VCO No. 1 and (B) VCO No. 3. Data are presented as mean ± SD from three independent experiments. $^{*}p < 0.05$, $^{**}p < 0.01$. VCO, virgin coconut oil.

6B). Our findings further demonstrate that treatment with 40 μg/mL lauric acid markedly increased apoptotic cell death to 26.57%, while 1 μM doxorubicin induced apoptosis at a rate of 21.82%, both significantly higher than the control (Figure 6B). For the MOLT-4 cells, treatment with 300 and 500 μg/mL VCO No. 1 and VCO No. 3 for 48 h did not result in a significant increase in

apoptosis compared to the control (Figure 7A-7B). In contrast, treatment with 40 µg/mL lauric acid significantly increased apoptotic cell death from 5.53% to 9.38% (Figure 7B). Additionally, treatment with 1 µM doxorubicin induced apoptosis at a rate of 15.85%, which was significantly higher than the control (Figure 7B).

These findings indicate that VCO No. 1 and VCO No. 3 promote apoptosis in K562 cells in a dose-dependent manner, whereas lauric acid and doxorubicin significantly increased apoptotic cell death compared to control. In contrast, VCO treatment did not significantly enhance apoptosis in MOLT-4 cells, while lauric acid and doxorubicin significantly increased apoptotic cell death, suggesting a differential apoptotic response between the two cell lines.

DISCUSSION

Natural products have been widely utilized in traditional medicine because of their diverse bioactive compounds, which play a crucial role in drug discovery and development (28). Among them, VCO has garnered significant attention for its potential health benefits, including hypocholesterolemic, antidiabetic, hepatoprotective,

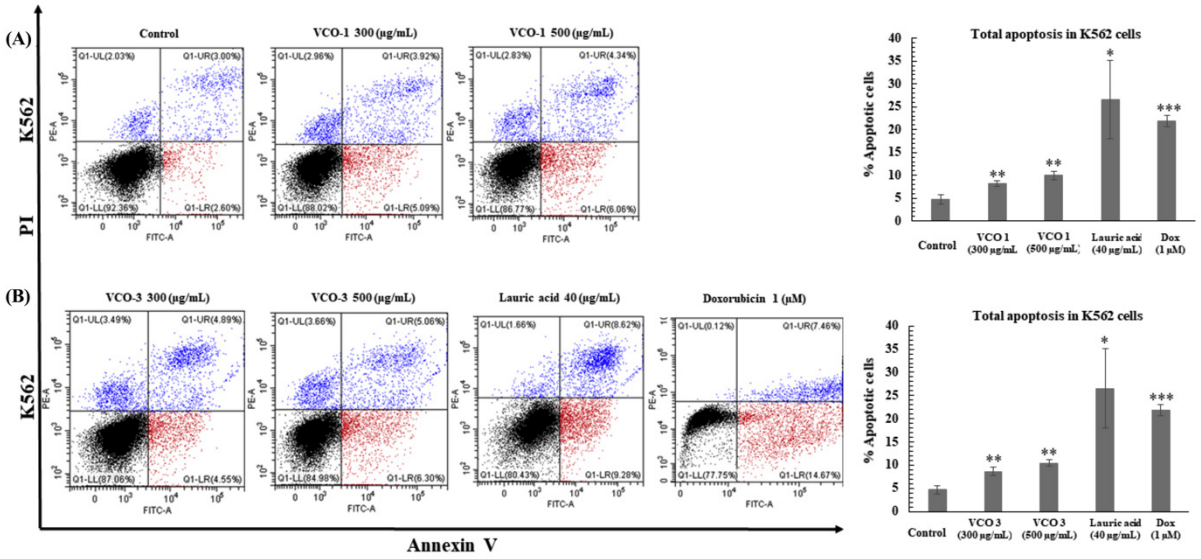

Figure 6. VCO induces apoptosis in K562 cells. (A) Effects of VCO No. 1 and (B) VCO No. 3 on apoptosis induction. Data are presented as the mean ± SD of three independent experiments. $^{*}p < 0.05$, $^{**}p < 0.01$, and $^{***}p < 0.001$.
VCO, virgin coconut oil

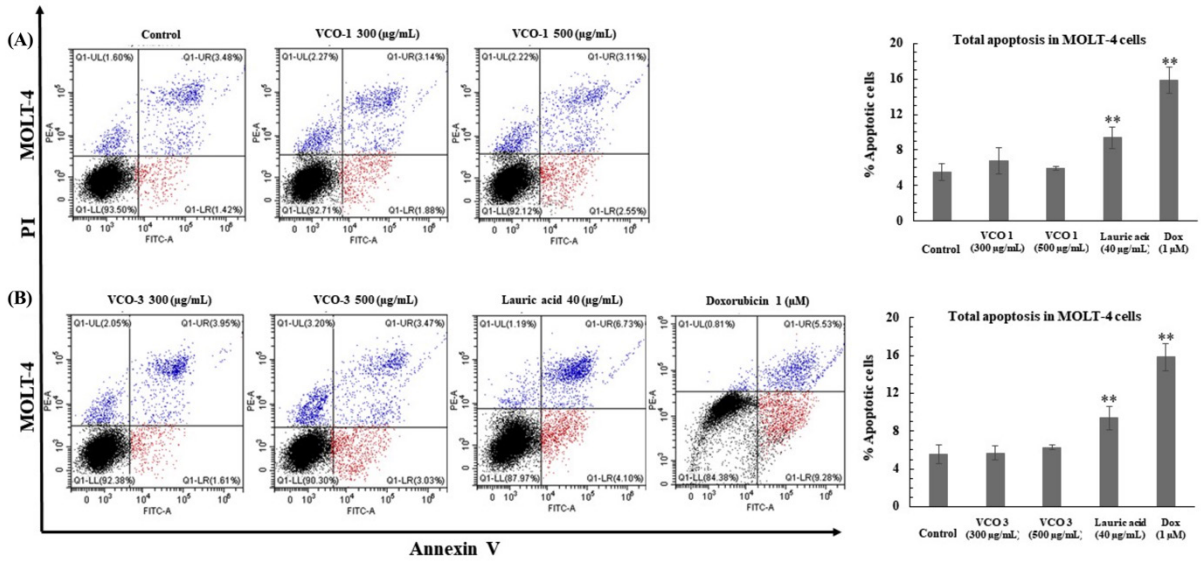

Figure 7. VCO induces apoptosis in MOLT-4 cells. (A) Effects of VCO No. 1 and (B) VCO No. 3 on apoptosis induction. Data are presented as the mean ± SD of three independent experiments. $^{*}p < 0.05$ and $^{**}p < 0.01$. VCO, virgin coconut oil.
VCO, virgin coconut oil

antioxidant, anti-inflammatory, antimicrobial, skin-moisturizing, and wound-healing properties. These effects are primarily attributed to its medium-chain fatty acids (MCFAs), particularly lauric acid (C12), which constitutes approximately 50% of VCO (17, 29-35). Despite its well-documented bioactivities, the effects of VCO on leukemia cells remain largely unexplored. To address this gap, this study investigate the effects of VCO on K562 and MOLT-4 leukemic cells, the first study to do so. Five VCO samples, including one hand-made (VCO No. 1) and four commercially manufactured (VCO No. 2-5), were analyzed. Their anti-leukemic potential was assessed by evaluating cell cycle arrest and apoptosis induction, with comparisons to lauric acid. The findings revealed that VCO exposure led to a marked decrease in leukemic cell survival, suggesting its cytotoxic potential. This effect may be attributed to the high lauric acid content in VCO, as previous studies have shown that MCFAs can disrupt cancer cell metabolism and induce apoptosis. Similarly, lauric acid exhibited strong cytotoxicity, further supporting the role of lauric acid in mediating these effects. Consistent with these findings, Tima et al. reported that *Houttuynia cordata* extract exerted cytotoxic effects on leukemic cells at comparable concentrations (36). Additionally, Sheela et al. demonstrated that lauric acid induced dose-dependent cytotoxicity in various cancer cell lines, including colorectal and liver cancer, as well as macrophages (14). These findings further highlight the potential of lauric acid as a key bioactive component contributing to the cytotoxic activity of VCO.

Based on the viability assay results, all VCO samples exhibited comparable cytotoxicity. Therefore, VCO No. 1 (hand-made) and No. 3 (manufactured) were selected to represent traditional and commercial preparations in further analyses of cell cycle arrest and apoptosis. Both induced G2/M phase arrest in K562 and MOLT-4 cells, whereas lauric acid treatment led to G1 phase accumulation. In addition, it has been reported that lauric acid induced apoptosis, reduced colon cancer cells (Caco2) and IEC-6 cells in the G0/G1 phase, resulting in S and M phase cell cycle arrest, increased reactive oxygen species (ROS), and depleted intracellular glutathione levels (37, 38). Similarly, Li et al. reported that EM23, a sesquiterpene lactone from *Elephantopus mollis*, induced apoptosis and G2/M or S phase arrest in K562 and HL-60 cells (27). Collectively, these results suggest that VCO suppresses cell proliferation and induces cell cycle arrest, leading to apoptosis in leukemic cells.

Apoptosis is crucial for tissue homeostasis, eliminating damaged cells while preserving healthy proliferation (15). Disruptions in this process can lead to mutations, malignant transformation, metastasis, and therapy resistance (39). The apoptotic effect of VCO in K562 and MOLT-4 cells was evidenced by G2/M phase arrest. Lappano et al. demonstrated that 100 μM (20 μg/mL) lauric acid induces apoptosis in breast cancer cells (40); however, the present study is the first to report the apoptotic effects of VCO on leukemic cell lines. Apoptosis assays revealed a significant increase in apoptotic K562 cells following treatment with VCO No. 1 and No. 3, whereas no significant change was observed in MOLT-4 cells. The results of cell cycle analysis showed a higher concentration of VCO in MOLT-4 cells (300 μg/mL) significantly induced greater cell accumulation in the G2/M phase than in K562 cells (150 μg/mL). Thus, K562 cells are much more sensitive to VCO than MOLT-4 cells. This differential response may be attributed to the distinct cellular origins of K562 (CML-derived lymphoblasts) and MOLT-4 (ALL-derived T-lymphoblasts), suggesting that VCO exerts its apoptotic effects in a cell type-dependent manner. Furthermore, treatment with 40 μg/mL lauric acid and 1 μM doxorubicin significantly increased apoptosis in both cell lines. These findings align with Kamalaldin et al., which reported that VCO induced apoptosis in A549 lung cancer cells but not in NCI-H1299 cells, highlighting its selective cytotoxicity based on cancer cell characteristics (41). However, its selective apoptotic activity suggests a cell type-dependent mechanism.

These findings underscore the cytotoxic effects of VCO on leukemic cells through cell cycle arrest and apoptosis, potentially mediated by its lauric acid content as the effective concentrations of VCO (e.g., 300-500 ug/mL) are quite high compared to lauric acid (40 ug/mL). Thus, in *in-vivo* and clinical studies, it is necessary to administer VCO, which mainly consists of MCTs (medium chain triglycerides; C6-C12), at a high

concentration as shown in previous studies. Regarding the potential feasibility of *in-vivo* studies, it has been reported that targeting energy metabolism with a modified diet supplemented with 25% 8- and 10-carbon MCTs may be considered as part of a multimodal treatment regimen to improve the efficacy of neuroblastoma anticancer therapy in the CD-1 Nu mouse model (42). In addition, an antiproliferative action of MCTs was evidenced in a study by Otto et al. (43). The authors of that study showed that a ketogenic diet supplemented with omega-3 fatty acids and 21.45% MCTs (6-12 carbons) inhibited tumor growth in a xenograft model of human gastric adenocarcinoma cells and increased the mean survival time of animals. The clinical application of MCTs in relation to their potent anticancer and therapeutic effects has been reported in several clinical studies. Extensive research on the ketogenic diet containing MCTs has been carried out in a pilot study conducted by Schmidt et al. in patients with advanced metastatic tumors. That study demonstrated notable improvements in patients who followed a ketogenic diet for three months (containing MCTs in a form of an oil-protein mixture: 21 g of fat with MCTs, 5 g of carbohydrate, and 14 g of proteins) in terms of physical wellbeing and observed tumor shrinkage without adverse side effects or changes in cholesterol or blood lipids (44). Nevertheless, further investigations are warranted to elucidate the underlying molecular pathways and to assess the therapeutic potential in leukemia treatment.

CONCLUSIONS

This study is preliminary to reporting the cytotoxicity of VCO in K562 and MOLT-4 leukemic cell lines. Our findings indicate that VCO inhibits leukemic cell proliferation, induces cell cycle arrest, and promotes apoptosis in both types of cells. These results suggest that VCO may inhibit the growth of leukemic cells by regulating cell cycle progression and apoptotic pathways. However, the precise molecular mechanisms underlying these effects remain unclear. Further investigations are needed to elucidate the signaling pathways involved and to determine whether the bioactive components of VCO act independently or synergistically in exerting their anticancer effects.

ACKNOWLEDGEMENTS

We are grateful to Dr. Supansa Pata, Division of Immunology, Department of Medical Technology, Faculty of Associated Medical Sciences, Chiang Mai University, for supporting us with the K562 and MOLT-4 cell lines.

FUNDING

This research received a grant from the Department of Medical Sciences, Ministry of Public Health, Thailand.

CONFLICTS OF INTEREST

There are no conflicts of interest associated with this publication and there has been no significant financial support for this work that could have influenced its outcome.

AUTHOR CONTRIBUTION

S.S.: project administration, conceptualization, methodology, formal analysis, software, original draft preparation, review, and editing; S.Y.: conceptualization, methodology, review, and editing; A.W.: formal analysis; N.D.: investigation; N.P.: funding acquisition.

DATA AVAILABILITY STATEMENT

The data that support the finding of this study are available corresponding author upon reasonable request

INSTITUTIONAL REVIEW BOARD STATEMENT

Not applicable, because of the studies not involving human

INFORMED CONSENT STATEMENT

Not applicable, because of the studies not involving human

REFERENCES

1. Bray F, Laversanne M, Sung H, Ferlay J, Siegel RL, Soerjomataram I, et al. Global cancer statistics 2022: GLOBOCAN estimates of incidence and mortality worldwide for 36 cancers in 185 countries. CA Cancer J Clin. 2024;74:229-63.
2. Miranda-Filho A, Piñeros M, Ferlay J, Soerjomataram I, Monnereau A, Bray F. Epidemiological patterns of leukaemia in 184 countries: a population-based study. Lancet Haematol. 2018;5:e14-e24. PubMed PMID: 29304322.

3. Lin K, Jia H, Cao M, Xu T, Chen Z, Song X, et al. Epidemiological characteristics of leukemia in China, 2005–2017: a log-linear regression and age-period-cohort analysis. BMC Public Health. 2023;23:1647. PubMed PMID: 37641011.
4. Sangrajrang S, Laversanne M, Bausom R, Mery L, Bray F. Cancer incidence and cancer control in Bangkok, Thailand: Results from the cancer registry 2011-15 and projections to 2035. Cancer Epidemiol. 2020;67:101765. PubMed PMID: 32585431.
5. Wiangnon S, Veerakul G, Nuchprayoon I, Seksarn P, Hongeng S, Krutvecho T, et al. Childhood cancer incidence and survival 2003-2005, Thailand: study from the Thai Pediatric Oncology Group. Asian Pac J Cancer Prev. 2011;12:2215-20.
6. Sutra S, Chirawatkul A, Bundhamcharoen K, Ekachampaka P, Wattanamano N. Cause of death Analysis by age group. Child and adolescent health situation. 2009:17-88.
7. Li J, Wang Y, Dong C, Luo L. Advancements in leukemia management: Bridging diagnosis, prognosis and nanotechnology. Int J Oncol. 2024;65:112. PubMed PMID: 39364739.
8. Arber D, Campo E, Jaffe ES. Advances in the classification of myeloid and lymphoid neoplasms. Virchows Arch. 2023;482:1-9.
9. Al-Bayati A, Al-Bayti A, Husain V. A short review about chronic myeloid leukemia. J Life Sci Res. 2023;4:15-9.
10. Forsberg M, Konopleva M. AML treatment: conventional chemotherapy and emerging novel agents. Trends Pharmacol Sci. 2024;45:430-48.
11. Chakrabarty M. Chemistry and technology of oils & fats. New Delhi: Allied Publishers; 2003.
12. Liau K, Lee Y, Chen C, Rasool A. An open-label pilot study to assess the efficacy and safety of virgin coconut oil in reducing visceral adiposity. Int Sch Res Notices. 2011;2011:949686. PubMed PMID: 22164340.
13. Zakaria Z, Somchit M, Mat Jais A, Teh L, Salleh M, Long K. In vivo antinociceptive and anti-inflammatory activities of dried and fermented processed virgin coconut oil. Med Princ Pract. 2011;20:231-6.
14. Sheela D, Narayanankutty A, Nazeem P, Raghavamenon A, Muthangaparambil S. Lauric acid induce cell death in colon cancer cells mediated by the epidermal growth factor receptor downregulation: An in silico and in vitro study. Hum Exp Toxicol. 2019;38:753-61.
15. Elmore S. Apoptosis: a review of programmed cell death. J Toxicol Pathol. 2007;35:495-516.
16. Matthews H, Bertoli C, de Bruin R. Cell cycle control in cancer. Nat. Rev. Mol. Cell Biol. 2022;23:74-88.
17. Kappally S, Shirwaikar A, Shirwaikar A. Coconut oil–a review of potential applications. Hygeia JD Med. 2015; 7:34-41.
18. Dayrit F. The properties of lauric acid and their significance in coconut oil. J Am Oil Chem Soc. 2015;92:1-15.
19. Huang W-C, Tsai T-H, Chuang L-T, Li Y-Y, Zouboulis C, Tsai P-J. Anti-bacterial and anti-inflammatory properties of capric acid against Propionibacterium acnes: a comparative study with lauric acid. J Dermatol Sci. 2014;73:232-40.
20. Law K, Azman N, Omar E, Musa M, Yusoff N, Sulaiman SA, et al. The effects of virgin coconut oil (VCO) as supplementation on quality of life (QOL) among breast cancer patients. Lipids Health Dis. 2014;13:1-7.
21. Adeyemi W, Olayaki L, Abdussalam T, Toriola A, Olowu A, Yakub A, et al. Investigation of the effects of dietary modification in experimental obesity: low dose of virgin coconut oil has a potent therapeutic value. Biomed Pharmacother. 2020;126:110110. PubMed PMID: 32244146.
22. Famurewa A, Folawiyo A, Enohnyaket E, Azubuike-Osu S, Abi I, Obaje S, et al. Beneficial role of virgin coconut oil supplementation against acute methotrexate chemotherapy-induced oxidative toxicity and inflammation in rats. Integr Med Res. 2018;7:257-63.
23. Calderon J, Burenafe M, Cabrera N, Campos IC, Capili C, Carasco M, et al. Virgin coconut oil inhibits skbr-3 breast cancer cell proliferation and synergistically enhances the growth inhibitory effects of trastuzumab (herceptin). Euro J Med Resear. 2009;14:208-14
24. Verma P, Naik S, Nanda P, Banerjee S, Naik S, Ghosh A. In vitro anticancer activity of virgin coconut oil and its fractions in liver and oral cancer cells. Anticancer Agents Med Chem. 2019;19(18):2223-30. PubMed PMID: 32244146.
25. Ampasavate C, Okonogi S, Anuchapreeda S. Cytotoxicity of extracts from fruit plants against leukemic cell lines. Afr J Pharm Pharmacol. 2010;4:13-21.
26. Agrawal S, Agrawal M, Sharma P, Gupta B, Arora S, Saxena A. Induction of apoptosis in human promyelocytic leukemia HL60 cells by an extract from Erythrina suberosa stem bark. Nutr Cancer. 2011;63:802-13.
27. Li H, Li M, Wang G, Shao F, Chen W, Xia C, et al. EM23, a natural sesquiterpene lactone from elephantopus mollis, induces apoptosis in human myeloid leukemia cells through thioredoxin-and reactive oxygen species-mediated signaling pathways. Front Pharmacol. 2016;7:77. PubMed PMID: 27064563.
28. Newman D, Cragg G. Natural products as sources of new drugs over the 30 years from 1981 to 2010. J Nat Prod. 2012;75:311-35.
29. DebMandal M, Mandal S. Coconut (Cocos nucifera L.: Arecaceae): in health promotion and disease prevention. Asian Pac J Trop Med. 2011;4:241-7.
30. Peedikayil F, Remy V, John S, Chandru T, Sreenivasan P, Bijapur GA. Comparison of antibacterial efficacy of coconut oil and chlorhexidine on Streptococcus mutans: An: in vivo: study. J Int Soc Prev Community Dent. 2016;6:447-52.
31. Sezgin Y, Ozgul B, Alptekin N. Efficacy of oil pulling therapy with coconut oil on four-day supragingival plaque growth: a randomized crossover clinical trial. Complement Ther Med. 2019;47:102193. PubMed PMID: 31780023.
32. Widianingrum DC, Noviandi CT, Salasia SIO. Antibacterial and immunomodulator activities of virgin coconut oil (VCO) against Staphylococcus aureus. Heliyon. 2019;5:e02612. PubMed PMID: 31673647.

33. Pruseth B, Banerjee S, Ghosh A. Integration of in silico and in vitro approach to reveal the anticancer efficacy of virgin coconut oil. Cord. 2020;36:1-9.
34. Deen A, Visvanathan R, Wickramarachchi D, Marikkar N, Nammi S, Jayawardana BC, et al. Chemical composition and health benefits of coconut oil: an overview. J Sci Food Agric. 2021;101:2182-93.
35. Vereau G, Méndez G, VÁSQUEZ V, GUARDIA M. Antibacterial effect of coconut oil (Cocus nucifera) on Streptococcus mutans ATCC 25175: an in vitro study. Int J Odontostomat. 2021;15:922-7.
36. Tima S, Phanphuech B, Anuchapreeda S. Cytotoxicity study of Houttuynia cordata Thunb crude extracts on HL-60 and Molt4 leukemic cell line. J Assoc Med. 2010;43:30-8.
37. Fauser J, Matthews G, Cummins A, Howarth G. Induction of apoptosis by the medium-chain length fatty acid lauric acid in colon cancer cells due to induction of oxidative stress. Chemotherapy. 2014;59:214-24.
38. Kadochi Y, Mori S, Fujiwara-Tani R, Luo Y, Nishiguchi Y, Kishi S, et al. Remodeling of energy metabolism by a ketone body and medium-chain fatty acid suppressed the proliferation of CT26 mouse colon cancer cells. Oncol Lett. 2017;14:673-80.
39. Wong R. Apoptosis in cancer: from pathogenesis to treatment. J Exp Clin Cancer Res. 2011;30:1-14.
40. Lappano R, Sebastiani A, Cirillo F, Rigiracciolo DC, Galli GR, Curcio R, et al. The lauric acid-activated signaling prompts apoptosis in cancer cells. Cell Death Discov. 2017;3:1-9.
41. Kamalaldin N, Yusop M, Sulaiman S, Yahaya B. Apoptosis in lung cancer cells induced by virgin coconut oil. Regen Res. 2015;4:30-6.
42. Aminzadeh-Gohari S, Feichtinger RG, Vidali S, Locker F, Rutherford T, O'Donnel M, et al. A ketogenic diet supplemented with medium-chain triglycerides enhances the anti-tumor and anti-angiogenic efficacy of chemotherapy on neuroblastoma xenografts in a CD1-nu mouse model. Oncotarget. 2017;8(39):64728-44.
43. Otto C, Kaemmerer U, Illert B, Muehling B, Pfetzer N, Wittig R, et al. Growth of human gastric cancer cells in nude mice is delayed by a ketogenic diet supplemented with omega-3 fatty acids and medium-chain triglycerides. BMC cancer. 2008;8(1):122. PubMed PMID: 18447912
44. Duranova H, Kuzelova L, Fialkova V, Simora V, Kovacikova E, Joanidis P, et al. Coconut-sourced MCT oil: Its potential health benefits beyond traditional coconut oil. Phytochem Rev. 2025;24:659-700.

Biomedical Sciences and Clinical Medicine 2026;65(1):81-90.
doi: 10.12982/BSCM.2026.10
https://he01.tci-thaijo.org/index.php/CMMJ-MedCMJ/index

BSCM
Biomedical Sciences and Clinical Medicine

Original Article

Open Access

Sex-specific Differences in the Association between Insulin Resistance and Metabolic Syndrome and Ferritin in Korean Adults: A Nationwide Population-based Study

Mi Young Gi[1], Ju Ae Cha[2] and Hyun Yoon[3]

[1]Department of Nursing, Christian College of Nursing, Gwangju, South Korea; [2]Department of Nursing, Chunnam Technouniversity, Gokseong-gun, Jeollanam-do, South Korea; [3]Department of Medical Laboratory Science, Wonkwang University, 460, Iksan-daero, Iksan-si, Jeollabuk-do, South Korea

Correspondence:
Hyun Yoon, PhD,
Department of Medical Laboratory Science, Wonkwang University, 460, Iksan-daero, Iksan-si, Jeollabuk-do, 54538, South Korea.
E-mail: yh9074@yahoo.co.kr

Received: May 31, 2025;
Revised: September 4, 2025;
Accepted: September 12, 2025

ABSTRACT

OBJECTIVE This study assessed the association between metabolic syndrome (MetS) and homeostasis model assessment of insulin resistance (HOMA-IR) and ferritin based on gender in Korean adults.

METHODS This study was conducted using data from 5,730 adults (aged 20 or older) and the Korea National Health and Nutrition Examination Survey.

RESULTS This study included some key findings First, HOMA-IR levels showed a positive correlation with quartiles (Q) of ferritin both in postmenopausal women ($p = 0.001$) and in men ($p < 0.001$). However, there was no statistically significant difference between the HOMA-IR levels and the Q of ferritin in premenopausal women ($p = 0.149$). Second, using the Q1 of ferritin as the reference, the ORs of MetS were positively significant in men (Q3 [OR, 1.770; 95% CI, 1.308–2.397] and Q4 [OR, 2.385; 95% CI, 1.775–3.20]) and postmenopausal women (Q4 [OR, 1.873; 95% CI, 1.351–2.596]). However, there was no significant difference between MetS and the quartiles of ferritin in premenopausal women.

CONCLUSIONS An increase in ferritin is associated with both metabolic syndrome and insulin resistance in both Korean postmenopausal women and men. However, there is no significant difference between ferritin and metabolic syndrome in premenopausal women.

KEYWORDS ferritin, metabolic syndrome, insulin resistance, gender difference, Korean adults

INTRODUCTION

Metabolic syndrome (MetS) involves metabolic abnormalities indicated by central obesity, elevated blood pressure (BP), elevated triglycerides (TGs), reduced high-density lipoprotein cholesterol (HDL-C), and elevated fasting blood glucose (FBG) and is characterized by insulin resistance (1). MetS is a strong predictor of type 2 diabetes mellitus (T2DM) and cardiovascular disease (CVD) and is closely related to increased cardiovascular mortality and morbidity (2, 3).

Iron is a component of red blood cells in the human body and plays a crucial role in the proper functioning of the immune system, the synthesis of DNA and other amino acids, and various energy metabolism processes through its role in enzymes and proteins (4). Ferritin reflects the iron store because iron is combined with apo-ferritin and

stored as serum ferritin (5). Although increased ferritin levels are sometimes used as an indicator of reduced iron deficiency anemia (IDA), excessive ferritin levels are positively correlated with insulin resistance, CVD and inflammation (6-8).

Research on ferritin and MetS is being conducted worldwide. Most of the previous studies have reported that an increase in ferritin is associated with MetS (9-11). However, the relationship between MetS and ferritin can vary by sex because of the differences in sex hormones, eating habits, and menstruation. Blood loss due to menstruation and certain dietary patterns contribute to lower ferritin levels and iron deficiency in women (12). Sex hormones, testosterone in men and estrogen in women, play a key role in regulating iron metabolism and are also linked to MetS (13). Therefore, this study aimed to conduct an analysis of the relationship between MetS and ferritin in Korean men and pre- and post- menopausal Korean women using the Korea National Health and Nutrition Examination Survey data.

METHODS

Study subjects

In the data of KNHANES V-1, the number of adults aged 20 years or older was 6,665 out of 8,958. We excluded 935 subjects for whom analytic variable data were missing, such as ferritin and various blood chemistry tests. Finally, 5,730 subjects (men, 2,469; women, 3,261 [premenopausal women, 1,620; postmenopausal women, 1,641]) were included in the statistical analysis. This study was conducted according the principles expressed in the Declaration of Helsinki (Institutional Review Board No [IRB No], 2010-02CON-21-C).

General characteristics and blood chemistry

Research participants were classified by smoking status (non-smoker or current smoker), regular exercise (no or yes), and alcohol consumption (no or yes). Anthropometric measurements included waist circumference (WC), body mass index (BMI), systolic blood pressure (SBP), and diastolic blood pressure (DBP). Clinical measurements included measurements of HDL-C, total cholesterol (TC), TGs, FBG, total iron binding capacity (TIBC), hematocrit (Hct), hemoglobin (Hb), serum iron (Fe), and ferritin levels.

Metabolic syndrome, metabolic syndrome score and HOMA-IR

MetS was defined using the diagnostic criteria of the National Cholesterol Education Program (NCEP) based on common clinical measures including WC, HDL-C, SBP, DBP, TGs, and FBG. Abdominal obesity was classified as WC ≥ 80 cm in women or WC ≥ 90 cm in men (14). Elevated BP was diagnosed by a physician as hypertension and classified as SBP ≥ 130 mmHg or DBP ≥ 85 mmHg. Elevated TGs was classified as TGs ≥ 150 mg/dL. Elevated FBG was classified as FBG ≥ 100 mg/dL. Reduced HDL-C was classified as HDL-C < 40 mg/dL in men and HDL-C < 50 mg/dL in women. If three or more of these five measures are present, it is classified as MetS (15). Participants without any of the components were classified as MSS 0, and those with 1, 2, 3, or 4 or more of the risk factors were classified as MSS 1, 2, 3, or ≥ 4, respectively. Homeostasis model assessment of insulin resistance (HOMA-IR) was calculated as [FBG (mg/dL) × fasting insulin (μU/mL)]/405 (16).

Ferritin

Levels of ferritin were measured by immunofluorescence-mat ferritin (DiaSorin Inc., Stillwater, MN, USA) using a Wallac Wizard 1470 Automatic Gamma Counter (Perkin Elmer Life Sciences, Turku, Finland). Ferritin was classified in quartiles (Q) because the cut-offs for ferritin were not yet clear. The quartiles of ferritin by gender are classified as follows: men and women together quartile 1 (Q1), 29.5 μg/L or less; quartile 2 (Q2), 29.6-59.0 μg/L; quartile 3 (Q3), 59.1-103.8 μg/L; quartile 4 (Q4), 103.9 μg/L or more. In men, Q1, 63.5 μg/L or less; Q2, 63.6-98.0 μg/L; Q3, 98.1-150.9 μg/L; Q4, 151.0 μg/L or more. In women, Q1, 19.8 μg/L or less; Q2, 19.9-38.8 μg/L; Q3, 38.9-64.1 μg/L; Q4, 64.2 μg/L or more. In premenopausal women, Q1, 11.7 μg/L or less; Q2, 11.8-24.0 μg/L; Q3, 24.1-43.2 μg/L; Q4, 43.3 μg/L or more. In postmenopausal women, Q1, 35.3 μg/L or less; Q2, 35.4-55.0 μg/L; Q3, 55.1-85.2 μg/L; Q4, 85.3 μg/L or more.

Statistical analysis

Statistical analysis was performed using SPSS (version 18.0, IBM, Chicago, IL, USA). Differences in the means and distribution of characteristics by gender were analyzed using chi-square analysis

and analysis of variance tests (Table 1). The distribution in MetS components by the quartiles of ferritin were analyzed using chi-squared (Table 2). Analysis of the covariance of ferritin concentration was done according to MSS and MetS (Table 3). The ANCOVA test for HOMA-IR was conducted according to the quartiles of ferritin (Table 4). Logistic regression analysis of the odds ratio of MetS used the following four models: 1) non-adjusted; 2) adjusted for age; 3) further adjusted for regular exercise, alcohol drinking, and smoking status; 4) further adjusted for obesity and anemia (Table 5). The statistical significance of all analyses was based on $p < 0.05$.

RESULTS

Characteristics of research subjects

Characteristics of the research subjects are presented in Table 1. Serum ferritin, Fe, and TIBC in men (n = 2,469) were 114.88 ± 71.16, 126.00 ± 49.71, and 309.14 ± 40.06 μg/dL, respectively. Serum ferritin, Fe, and TIBC in premenopausal women (n = 1,620) were 31.13 ± 26.79, 98.70 ± 47.56, and 329.05 ± 50.06 μg/dL, respectively. Serum ferritin, Fe, and TIBC in postmenopausal women (n = 1,641) were 65.10 ± 43.58, 101.45 ± 34.09, and 313.72 ± 43.88 μg/dL, respectively. The prevalence of anemia in premenopausal women (15.9%) and postmenopausal women (11.1%) was higher than in men (3.6%). The prevalence of MetS in men (24.7%) and postmenopausal women (36.6%) was higher than in premenopausal women (8.6%).

MetS components of subjects according to the quartiles of ferritin

MetS components of subjects by ferritin quartiles (Q1-Q4) in postmenopausal women, men, and premenopausal women are presented in Table 2. In men, the reduced HDL-C ($p = 0.003$), abdominal obesity ($p < 0.001$), elevated FBG ($p < 0.001$), elevated

Table 1. Clinical characteristics of research subjects

Variables	Overall (n = 5,730)	Men (n = 2,469)	Women (n = 3,261)		p-value
			Premenopausal (n = 1,620)	Postmenopausal (n = 1,641)	
Age (years), M±SE	49.12±15.71	49.58±15.66	36.56±8.32	60.84±11.42	< 0.001
Current smoker, n (%)	1,156 (20.2)	966 (39.1)	122 (7.5)	68 (4.1)	< 0.001
Alcohol drinker, n (%)	3,061 (53.4)	1,830 (74.1)	802 (49.5)	429 (26.1)	< 0.001
Regular exerciser, n (%)	618 (10.8)	262 (10.6)	156 (9.6)	200 (12.2)	0.058
Menstruation, n (%)	–	–	248 (15.3)	–	
BMI (kg/m^2), M±SE	23.60±3.34	23.99±3.15	22.51±3.41	24.08±3.29	< 0.001
Obesity, n (%)	1,814 (31.7)	917 (37.1)	329 (20.3)	595 (36.3)	< 0.001
WC (cm), M±SE	81.03±13.71	84.76±16.88	74.68±9.01	81.67±9.29	< 0.001
SBP (mmHg), M±SE	120.91±17.61	123.72±16.02	109.91±13.38	127.56±18.55	< 0.001
DBP (mmHg), M±SE	77.32±10.61	80.39±10.43	72.44±9.22	77.52±10.37	< 0.001
TC (mg/dL), M±SE	188.73±36.35	187.81±36.34	178.43±31.95	200.28±37.17	< 0.001
TGs (mg/dL), M±SE	131.18±106.72	156.54±136.03	91.72±57.44	131.99±78.57	< 0.001
HDL-C (mg/dL), M±SE	52.78±12.77	49.34±12.05	57.11±12.26	53.68±12.88	< 0.001
FBG (mg/dL), M±SE	97.23±21.65	100.33±24.62	91.11±16.47	98.61±20.11	< 0.001
Hb (mg/dL), M±SE	13.92±1.58	15.16±1.18	12.84±1.21	13.13±1.04	< 0.001
Hct (mg/dL), M±SE	41.34±4.09	44.45±3.19	38.64±2.99	39.32±2.88	< 0.001
Anemia, n (%)	526 (9.2)	88 (3.6)	257 (15.9)	181 (11.1)	< 0.001
Ferritin (μg/L), M±SE	76.95±64.67	114.88±71.16	31.13±26.79	65.10±43.58	< 0.001
Fe (μg/dL), M±SE	111.25±46.93	126.00±49.71	98.70±47.56	101.45±34.09	< 0.001
TIBC (μg/dL), M±SE	316.08±44.95	309.14±40.06	329.05±50.06	313.72±43.88	< 0.001
MetS, n (%)	1,351 (23.6)	610 (24.7)	140 (8.6)	601 (36.6)	< 0.001
HOMA-IR, M±SE	2.57±1.74	2.67±2.04	2.32±1.19	2.66±1.68	< 0.001

M, mean; BMI, body mass index; obesity, BMI ≥ 25 kg/m^2; WC, waist circumference; SBP, systolic blood pressure; DBP, diastolic blood pressure; TC, total Cholesterol; TGs, triglycerides; HDL-C, high density lipoprotein cholesterol; FBG, fasting blood glucose; Hb, hemoglobin; Hct, hematocrit; Anemia, Hb < 13 g/dL in men or Hb < 12 g/dL in women, Fe, serum iron; TIBC, total iron binding capacity; MetS, metabolic syndrome; HOMA-IR, homeostasis model assessment of insulin resistance

Table 2. MetS components and anemia according to quartile of ferritin

Gender	Variables	Serum ferritin				
		Quartile 1 (≤ 63.5 μg/L) (n = 617)	Quartile 2 (63.6–98.0 μg/L) (n = 618)	Quartile 3 (98.1–150.9 μg/L) (n = 617)	Quartile 4 (≥ 151.0 μg/L) (n = 617)	*p*-value
Men (n = 2,469)						
	Abdominal obesity	123 (19.9)	139 (22.5)	170 (27.6)	196 (31.8)	< 0.001
	Elevated BP	283 (45.9)	261 (42.2)	274 (44.4)	286 (46.4)	0.464
	Elevated TGs	158 (25.6)	178 (28.8)	232 (37.6)	273 (44.2)	< 0.001
	Reduced HDL-C	113 (18.3)	111 (18.0)	133 (21.6)	157 (25.4)	0.003
	Elevated FBG	177 (28.7)	183 (29.6)	214 (34.7)	245 (39.7)	< 0.001
	MetS	113 (18.3)	127 (20.6)	164 (26.6)	206 (33.4)	< 0.001
		Quartile 1 (≤ 11.7 μg/L) (n = 405)	**Quartile 2 (11.8–24.0 μg/L) (n = 405)**	**Quartile 3 (24.1–43.2 μg/L) (n = 405)**	**Quartile 4 (≥ 43.3 μg/L) (n = 405)**	***p*-value**
Premenopausal women (n = 1,620)						
	Abdominal obesity	91 (22.5)	91 (22.5)	100 (24.7)	123 (30.4)	0.029
	Elevated BP	55 (13.6)	40 (9.9)	47 (11.6)	51 (12.6)	0.409
	Elevated TGs	27 (6.7)	37 (9.1)	45 (11.1)	29 (7.2)	0.092
	Reduced HDL-C	112 (27.7)	104 (25.7)	115 (28.4)	119 (29.4)	0.685
	Elevated FBG	44 (10.9)	40 (9.9)	42 (10.4)	58 (14.3)	0.179
	MetS	28 (6.9)	33 (8.1)	38 (9.4)	41 (10.1)	0.382
		Quartile 1 (≤ 35.3 μg/L) (n = 410)	**Quartile 2 (35.4–55.0 μg/L) (n = 411)**	**Quartile 3 (55.1–85.2 μg/L) (n = 410)**	**Quartile 4 (≥ 85.3 μg/L) (n = 410)**	***p*-value**
Postmenopausal women (n = 1,641)						
	Abdominal obesity	212 (51.7)	219 (53.3)	245 (59.8)	255 (62.2)	0.005
	Elevated BP	190 (46.3)	185 (45.0)	199 (48.5)	219 (53.4)	0.082
	Elevated TGs	94 (22.9)	100 (24.3)	107 (26.1)	142 (34.6)	0.001
	Reduced HDL-C	140 (34.1)	171 (41.6)	171 (41.7)	200 (48.8)	< 0.001
	Elevated FBG	101 (24.6)	125 (30.4)	135 (32.9)	150 (36.6)	0.002
	MetS	115 (28.0)	145 (35.3)	147 (35.9)	194 (47.3)	< 0.001

Abdominal obesity is defined as WC ≥ 80 cm in women or WC ≥ 90 cm in men; Elevated BP is defined as SBP ≥ 130 mmHg or DBP ≥ 85 mmHg; elevated TGs is defined as TGs ≥ 150 mg/dL; reduced HDL-C is defined as HDL-C < 50 mg/dL in women or HDL-C < 40 mg/dL in men; elevated FBG is defined as FBG ≥ 100 mg/dL; MetS, metabolic syndrome

TGs ($p < 0.001$), and MetS ($p < 0.001$) showed statistically significant differences across ferritin quartiles, but elevated BP ($p = 0.464$) was not significantly different. In postmenopausal women, abdominal obesity ($p = 0.005$), reduced HDL-C ($p < 0.001$), elevated FBG ($p = 0.002$), elevated TGs ($p = 0.001$), and MetS ($p < 0.001$) showed statistically significant differences across ferritin quartiles, but elevated BP ($p = 0.082$) was not significantly different. In premenopausal women, abdominal obesity ($p = 0.029$) showed significant differences across ferritin quartiles, but the reduced HDL-C ($p = 0.685$), elevated FBG ($p = 0.179$), elevated BP ($p = 0.409$), elevated TGs ($p = 0.092$), and MetS ($p = 0.382$) were not statistically significantly different across ferritin quartiles.

Comparisons of ferritin levels according to MSS and MetS

Comparisons of ferritin concentration according to MSS and MetS in postmenopausal women, men, and premenopausal women are shown in Table 3. After adjusting for the related variables, the ferritin concentration in MetS in postmenopausal women ($p = 0.001$) and men ($p < 0.001$) were higher than in non-MetS but not in

Table 3. Comparisons of ferritin levels according to MetS and MSS in men, premenopausal women, and postmenopausal women (n = 5,730)

Gender	Category	Serum ferritin (μg/L) [M±SE (95% CI)]
Men (n = 2,469)	MSS 0	98.05±2.99 (92.19-103.91)
	MSS 1	109.66±2.71 (104.35-114.98)
	MSS 2	118.42±2.91 (112.72-124.12)
	MSS 3	131.38±3.59 (124.34-138.42)
	MSS ≥ 4	138.07±4.93 (128.40-147.73)
	p-value	< 0.001
	Non-MetS	109.12±1.64 (105.90 -122.35)
	MetS	131.53±2.99 (125.96-137.69)
	p-value	< 0.001
Premenopausal women (n = 1,620)	MSS 0	30.11±0.99 (28.16-32.05)
	MSS 1	30.10±1.17 (27.81-32.40)
	MSS 2	35.61±1.86 (31.95-39.26)
	MSS 3	35.48±2.75 (30.08-40.88)
	MSS ≥ 4	29.60±4.16 (21.45-37.76)
	p-value	0.101
	Non-MetS	30.92±0.60 (29.61-32.23)
	MetS	33.46±2.14 (28.91-38.01)
	p-value	0.299
Postmenopausal women (n = 1,641)	MSS 0	61.17±2.97 (55.36-66.99)
	MSS 1	60.74±2.29 (56.25-65.23)
	MSS 2	63.48±2.07 (59.42-67.54)
	MSS 3	68.80±2.40 (64.09-73.50)
	MSS ≥ 4	72.85±2.78 (67.40-78.30)
	p-value	0.008
	Non-MetS	62.10±1.38 (59.39-64.80)
	MetS	70.35±1.86 (66.70-74.01)
	p-value	0.001

M, mean; Adjusted for age, smoking, alcohol drinking, regular exercise, obesity, and anemia or menstruation (adjusted only premenopausal women)

premenopausal women (p = 0.299) (Table 3). In addition, ferritin levels increased with increasing MSS in postmenopausal women (p = 0.008) and men (p < 0.001) but not in premenopausal women (p = 0.101).

Comparisons of HOMA-IR by quartiles of ferritin

Comparisons of HOMA-IR by Q of ferritin in postmenopausal women, men, and premenopausal women are presented in Table 4. After adjusting for related variables, HOMA-IR levels were positively statistically significantly associated with the Q of ferritin in postmenopausal women (p = 0.001) and men (p < 0.001). However, there was no statistically significant difference between the HOMA-IR levels and the Q of ferritin in premenopausal women (p = 0.149).

Comparisons of MetS according to ferritin quartiles

Comparisons of MetS by the Q of ferritin in postmenopausal women, men, and premenopausal women are presented in Table 5. In men, after adjusting for the related variables and using the Q1 of ferritin as the reference, the ORs of MetS were positively significantly statistically correlated with Q3 (OR, 1.770; 95%CI: 1.308-2.397) and Q4 (OR, 2.385; 95%CI: 1.775-3.201) of ferritin. In postmenopausal women, using the Q1 of ferritin as the reference, the OR of MetS was significantly statistically correlated with Q4 (OR, 1.873; 95%CI: 1.351-2.596) of ferritin. However, the relationship between MetS and the ferritin quartiles in premenopausal women was not significant.

DISCUSSION

This study investigated sex-specific differences in the relationship between ferritin and MetS and MSS in Korean adults. The key finding was that serum ferritin levels showed a positive correlation with MetS and HOMA-IR in postmenopausal women and men, but not in premenopausal women.

Ferritin is found as a Fe (II)-apoferritin complex in most human organs, including the heart, liver, spleen, and kidneys, and serum ferritin levels are generally higher in men than women (17). Serum ferritin, which is an acute-phase reactant, is a marker of acute and chronic inflammation. Serum ferritin levels increase nonspecifically in chronic diseases, such as diabetes mellitus, chronic kidney disease, and coronary artery disease (18-20), and are associated with cardiovascular and all-cause mortality (21). Research on the relationship between ferritin and both MetS and HOMA-IR are being conducted all over the world. In a cohort study of Finnish adults, Hämäläinen et al. revealed that the serum ferritin level showed a positive correlation with the development of MetS (22). Chen et al. supported that serum ferritin levels were independently associated with MetS and insulin resistance in Chinese adults (23). In the present study, MetS and HOMA-IR showed a positive correlation with ferritin in the overall

Table 4. Comparisons of ferritin levels according to MetS and MSS in men, premenopausal women, and postmenopausal women (n = 5,730)

Gender	Serum ferritin	MetS, [M±SE (95% CI)]		
		Model 1	Model 2	Model 3
Men (n = 2,469)	Quartile 1	2.44±0.08 (2.38-2.60)	2.43±0.08 (2.27-2.59)	2.47±0.08 (2.31-2.63)
	Quartile 2	2.46±0.08 (2.30-2.62)	2.46±0.08 (2.30-2.62)	2.48±0.08 (2.33-2.64)
	Quartile 3	2.71±0.08 (2.55-2.87)	2.72±0.08 (2.56-2.88)	2.70±0.08 (2.55-2.86)
	Quartile 4	3.09±0.08 (2.93-3.25)	3.10±0.08 (2.94-3.26)	3.05±0.08 (2.89-3.20)
	p-value	< 0.001	< 0.001	< 0.001
Premenopausal women (n = 1,620)	Quartile 1	2.35±0.06 (2.24-2.47)	2.35±0.06 (2.23-2.47)	2.42±0.06 (2.29-2.54)
	Quartile 2	2.24±0.06 (2.12-2.35)	2.25±0.06 (2.13-2.36)	2.23±0.06 (2.12-2.34)
	Quartile 3	2.28±0.06 (2.17-2.40)	2.28±0.06 (2.17-2.40)	2.29±0.06 (2.17-2.40)
	Quartile 4	2.39±0.06 (2.28-2.51)	2.39±0.06 (2.17-2.50)	2.35±0.06 (2.23-2.46)
	p-value	0.253	0.328	0.149
Postmenopausal women (n = 1,641)	Quartile 1	2.52±0.08 (2.36-2.68)	2.45±0.08 (2.29-2.60)	2.49±0.08 (2.33-2.64)
	Quartile 2	2.53±0.08 (2.37-2.69)	2.54±0.08 (2.39-2.70)	2.51±0.08 (2.36-2.66)
	Quartile 3	2.63±0.08 (2.47-2.79)	2.60±0.08 (2.45-2.76)	2.64±0.08 (2.49-2.79)
	Quartile 4	2.96±0.08 (2.80-3.12)	2.97±0.08 (2.82-3.13)	2.93±0.08 (2.78-3.08)
	p-value	< 0.001	< 0.001	< 0.001

Mets, metabolic syndrome; M, mean
Model 1 [M ± SE (95%CI)], adjusted for age; Model 2 [M ± SE (95%CI)], Model 2 further adjusted for smoking, alcohol drinking, and regular exercise; Model 3 [M ± SE (95%CI)], Model 2 further adjusted for obesity and anemia or menstruation (adjusted only premenopausal women)

Table 5. Comparisons of Mets according to quartile of ferritin in men, premenopausal women, and postmenopausal women

Gender	Serum ferritin	MetS, [OR (95%CI)]			
		Model 1	Model 2	Model 3	Model 4
Men (n = 2,469)	Quartile 1	1	1	1	1
	Quartile 2	1.145 (0.861-1.521)	1.239 (0.928-1.653)	1.239 (0.927-1.655)	1.204 (0.883-1.641)
	Quartile 3	1.626 (1.237-2.136)**	1.875 (1.418-2.480)**	1.869 (1.411-2.476)**	1.770 (1.308-2.397)**
	Quartile 4	2.273 (1.743-2.964)***	2.646 (2.014-3.476)***	2.607 (1.981-3.432)***	2.385 (1.775-3.201)***
Premenopausal women (n = 1,620)	Quartile 1	1	1	1	1
	Quartile 2	1.194 (0.708-2.016)	1.346 (0.790-2.291)	1.325 (0.777-2.259)	1.070 (0.557-2.057)
	Quartile 3	1.406 (0.845-2.339)	1.537 (0.916-2.577)	1.536 (0.913-2.582)	1.530 (0.803-2.914)
	Quartile 4	1.517 (0.918-2.505)	1.810 (1.085-3.019)*	1.798 (1.075-3.009)*	1.521 (0.803-2.879)
Postmenopausal women (n = 1,641)	Quartile 1	1	1	1	1
	Quartile 2	1.416 (1.050-1.910)*	1.354 (0.992-1.849)	1.347 (0.986-1.840)	1.355 (0.972-1.890)
	Quartile 3	1.427 (1.058-1.925)*	1.271 (0.931-1.736)	1.273 (0.930-1.742)	1.136 (0.814-1.585)
	Quartile 4	2.363 (1.763-3.167)***	2.052 (1.512-2.784)**	2.064 (1.519-2.085)**	1.873 (1.351-2.596)**

Mets, metabolic syndrome; *$p < 0.05$, **$p < 0.01$, *** $p < 0.001$. Model 1 [OR (95%CI)], Non-adjusted; Model 2 [OR (95%CI)], adjusted for age; Model 3 [OR (95%CI)], Model 2 further adjusted for smoking, alcohol drinking, and regular exercise; Model 4 [OR (95%CI)], Model 3 further adjusted for obesity and anemia or menstruation (adjusted only for premenopausal women)

Korean population (Supplementary Tables 1, 2 and 3). The mechanism for the relationship between MetS and ferritin may contribute to impaired insulin extraction and insulin secretion. MetS is characterized by insulin resistance (1), and iron overload can contribute to insulin resistance. Hepatic iron overload can be caused by impaired insulin extraction (24), and iron overload in pancreatic beta cells can result from impaired insulin secretion (25). Another mechanism in the relationship involves hepcidin, which is produced by the liver and serves as a key regulator of iron homeostasis. In insulin resistant diseases such as T2DM and MetS, an increase in hepcidin increases the ferritin levels (26).

In the present study, we analyzed men, premenopausal women, and postmenopausal women separately. Our results found that MetS and

HOMA-IR showed a statistically positive correlation with the quartiles of ferritin in both men and postmenopausal women, but in premenopausal women (Tables 4 and 5). The relationship between MetS and ferritin can differ by country, race, gender, and subjects with or without an underlying disease. Ghamarchehreh et al. showed that in Iranian patients with non-alcoholic fatty liver disease, the serum ferritin and MetS levels were not statistically significantly different in men (p = 0.952), but serum ferritin levels in MetS were lower than those in non-MetS in women (p = 0.004) (27). In a study based on the Third National Health and Nutrition Examination Survey (NHANES III) data in the US, Jehn et al. reported that serum ferritin levels were independently associated with MetS in non-diabetic premenopausal (p trend = 0.03) and postmenopausal women (p trend < 0.001), but not in men (p trend = 0.11) (28). In our results in men and postmenopausal women, four components of MetS, but not elevated BP, were positively associated with ferritin (Table 2). However, only abdominal obesity among the MetS components showed a positive correlation with ferritin in premenopausal women. This suggests that a positive correlation with ferritin exists between MetS and MSS in postmenopausal women and men, but not in premenopausal women. In addition, HOMA-IR showed a positive correlation with ferritin in postmenopausal women and men, but not in premenopausal women (Table 4). The findings of these studies are similar to our results. Han et al. investigated gender differences in the relationship between MetS and ferritin in the population-based China Health and Nutrition Survey (29). In men, four components of MetS (with the exception of high BP) were positively associated with ferritin, and MetS showed a positive correlation with the quartiles of ferritin (p < 0.001). In women, only high TG among the MetS components showed a positive correlation with ferritin, and the incidence of MetS was not statistically significant (p = 0.192). In another study, Ma et al. revealed that HOMA-IR showed a positive correlation with the tertiles of ferritin in men (p trend < 0.001) and postmenopausal women (p trend < 0.001), but not in premenopausal women (p trend = 0.929) after adjusting for related variables (30).

Although we cannot definitively specify the mechanisms for the sex-specific difference in the relationship between ferritin and MetS found in our study, we think that menopause and sex hormones may be a contributing factor. Menopause causes many physiological changes because of the decrease in estrogens. Premenopausal women have a lower risk of developing MetS than men, but the incidence of MetS can increase in postmenopausal women because the protective function of female hormones is greatly reduced due to a rapid decline in estrogen levels (31). In our results, the incidence of MetS in premenopausal women was lower than in men, but the incidence of MetS in postmenopausal women higher than in men. In terms of iron homeostasis, elevated levels of stored iron result in upregulation of hepcidin production to prevent iron overload, inhibiting further uptake of exogenous iron (32). Estrogens markedly decrease circulating hepcidin levels in humans (33). When estrogen decreases in premenopausal women, iron and stored iron levels in the body decrease due to upregulation of hepcidin levels, but this may be different in postmenopausal women. Sze et al. reported that an aberrant ferritin upregulation in the ovaries of aging female rats resulted in iron accumulation and inflamm-aging via NF-κB-induced nitric oxide synthase (34). They argued that acute ferritin upregulation exerts beneficial effects, but chronic upregulation may cause toxicity to cells due to iron accumulation and accelerate the decrease in endogenous estradiol biosynthesis. In addition, Matta et al. revealed that ferritin in postmenopausal women showed a positive correlation with hepcidin regardless of the level of estradiol, and that estradiol, hepcidin, and ferritin were higher in the metabolic syndrome than in the non-metabolic syndrome (35).

Estrogens prevent pancreatic β cell apoptosis and help protect functions, adapt to insulin resistance and maintain insulin content (36). Among the estrogens, 17β-estradiol improves insulin sensitivity and suppresses hepatic gluconeogenesis through inhibition of Foxo-1 via activation of estrogen receptor α-PI3K-Akt signaling (37). Male Zucker diabetic fat rats treated with 17β-estradiol had reduced levels of TGs and free fatty acids in the pancreatic islets, indicating reduced lipotoxicity and beta cell dysfunction (38). In our results,

MetS and HOMA-IR showed a positive correlation with the quartiles of ferritin in postmenopausal women and men, but were not significant in premenopausal women. These results suggest that insulin resistance could be expected to increase as ferritin increases, but it is thought that insulin resistance and glucose homeostasis in premenopausal women are maintained due to female hormones. Gender differences (the presence or absence of menopause in women) are evidenced in lifestyles (eating habits, physical activity, drinking, and smoking) and acute and chronic diseases (39, 40). For this reason, several researchers have argued that the model of medical hypotheses should consider these effects in women and men (especially, menopause in women) (41, 42).

Our research has several limitations. First, although we analyzed data of a representative sample of Korean adults from the KNHANES V-1, our findings have limitations in terms of generalizing to all ethnicities and the global population due to the study population and sample size. Second, C-reactive protein, estrogens, and hepcidin are important determinants of ferritin levels in men and women. However, these variables were not included in the KNHANES V-1 study, and so they should be included as variables for MetS and ferritin in future studies. Third, Although the sample is representative of the Korean population, the findings may not apply to other ethnicities or global populations due to genetic, dietary, and lifestyle differences. Fourth, this study was cross-sectional, which may limit its ability to establish a causal gender-specific relationship between ferritin and MetS. Therefore, to obtain more accurate and generalizable results, studies on hormonal regulation and gene-environment interaction or cohort studies on these relationships are needed.

CONCLUSIONS

This study investigated the sex-specific differences in the association between ferritin and MetS in Korean adults. Ferritin showed a statistically significant positive correlation with MetS in Korean postmenopausal women and men, but not in premenopausal women.

ACKNOWLEDGEMENTS

None

FUNDING

This paper was financially supported by Christian College of Nursing.

CONFLICTS OF INTEREST

We declare no conflicts of interests.

AUTHOR CONTRIBUTIONS

M.Y.G.: performed formal analysis and wrote the manuscript, integrated the data, contributed to the study design and revised the manuscript; H.Y.: performed formal analysis and wrote the manuscript, integrated the data, contributed to the study design and revised the manuscript; J.A.C.: integrated the data.

All authors read and approved the final version of this manuscript for publication.

DATA AVAILABILITY STATEMENT

Approval of the KNHANES data is available through https://knhanes.kdca.go.kr/knhanes/. Korea Disease Control and Prevention Agency (KDCA) permits access to all of these data via download for any researcher who promises to follow the research ethics.

INSTITUTIONAL REVIEW BOARD STATEMENT

This study has been conducted according the principles expressed in the Declaration of Helsinki (Institutional Review Board No, 2010-02CON-21-C).

INFORMED CONSENT STATEMENT

All participants in the survey signed an informed written consent.

SUPPLEMENTARY MATERIALS

The following supporting information can be downloaded at: Supplementary file

REFERENCES

1. Reaven, GM. Role of insulin resistance in human disease. Diabetes. 1988;37:1598-607.
2. Markopoulou P, Papanikolaou E, Analytis A, Zoumakis E, Siahanidou T. Preterm Birth as a risk factor for metabolic syndrome and cardiovascular disease in adult life: a systematic review and meta-analysis. J Pediatr. 2019;21:69-80.
3. Obunai K, Jan,i S, Dangas GD. Cardiovascular morbidity and mortality of the metabolic syndrome. Med Clin North Am. 2007;91:1169-184.

4. Padwal MK, Murshid M, Nirmale P, Melinkeri RR. Association of serum ferritin levels with metabolic syndrome and insulin resistance. J Clin Diagn Res. 2015;9:11-3.
5. Cook JD, Flowers CH, Skikne BS. The quantitative assessment of body iron. Blood. 2003;101:3359-64.
6. Conrad ME, Umbreit JN, Moore EG. Iron absorption and transport. Am J Med Sci. 1999;318:213-29.
7. Williams MJ, Poulton R, Williams S. Relationship of serum ferritin with cardiovascular risk factors and inflammation in young men and women. Atherosclerosis. 2002;165:179-84.
8. Başar Gökcen B, Akdevelioğlu Y, Canan S, Bozkurt N. Evaluation of the relationship between serum ferritin and insulin resistance and visceral adiposity index (VAI) in women with polycystic ovary syndrome. Eat Weight Disord. 2021;26:1581-93.
9. Yi KH, Hwang JS, Lim SW, Lee JA, Kim DH, Lim JS. Ferritin level is associated with metabolic syndrome and elevated alanine aminotransferase in children and adolescents. J Pediatr Endocrinol Metab. 2016;29:1337-44.
10. Suárez-Ortegón MF, Blanco E, McLachlan S, Fernandez-Real JM, Burrows R, Wild SH, et al. Ferritin levels throughout childhood and metabolic syndrome in adolescent stage. Nutr Metab Cardiovasc Dis. 2019;29:268-78.
11. Cho MR, Park JK, Choi WJ, Cho AR, Lee YJ. Serum ferritin level is positively associated with insulin resistance and metabolic syndrome in postmenopausal women: A nationwide population-based study. Maturitas. 2017;103:3-7.
12. Nolte S, Maier C, Klügel S, Weyh C, Hacker S, Badenhorst C, et al. Menstrual blood loss as an initial trigger for adaptation of iron metabolism in eumenorrheic female athletes-An exploratory study. Physiol Rep. 2025;13:e70522. PubMed PMID: 40856157
13. Qiu F, Wu L, Yang G, Zhang C, Liu X, Sun X, et al. The role of iron metabolism in chronic diseases related to obesity. Mol Med. 2022;28(1):130. PubMed PMID: 36335331
14. WHO. Western Pacific Region. 2000. International association for the study of obesity task force, the Asia-Pacific Perspective: redefining obesity and its treatment, Health Communications Australia, Sydney, Australia. 2000, 15-21.
15. Yoon H, Jeong DK, Lee KS, Kim HS, Moon AE, Park J. Relationship between metabolic syndrome and metabolic syndrome score and beta cell function by gender in Korean populations with obesity. Endocr J. 2016;63:785-93.
16. Cho HE, Yang SB, Gi MY, Cha JA, Park SY, Yoon H. The Relationship between the Lipid Accumulation Product and Beta-cell Function in Korean Adults with or without Type 2 Diabetes Mellitus: The 2015 Korea National Health and Nutrition Examination Survey. Endocr Res. 2022;47:80-8.
17. Andrews NC. Disorders of iron metabolism. N Engl J Med. 1999;341:1986-95.
18. Li J, Cao Y. Serum ferritin as a biomarker for diabetes and insulin resistance: a further study. Acta Diabetol. 2015;52:417-9.
19. Kang HT, Linton JA, Kwon SK, Park BJ, Lee JH. Ferritin level is positively associated with chronic kidney disease in Korean men, based on the 2010-2012 Korean National Health and Nutrition Examination Survey. Int J Environ Res Public Health. 2016;13:1058. PubMed PMID: 27801876
20. Pourmoghaddas A, Sanei H, Garakyaraghi M, Esteki-Ghashghaei F, Gharaati M. The relation between body iron store and ferritin, and coronary artery disease. ARYA Atheroscler. 2014;10:32-6.
21. Kadoglou NPE, Biddulph JP, Rafnsson SB, Trivella M, Nihoyannopoulos P, Demakakos P. The association of ferritin with cardiovascular and all-cause mortality in community-dwellers: The English longitudinal study of ageing. PLoS One. 2017;12:e0178994. PubMed PMID: 28591160
22. Hämäläinen P, Saltevo J, Kautiainen H, Mäntyselkä P, Vanhala M. Serum ferritin levels and the development of metabolic syndrome and its components: a 6.5-year follow-up study. Diabetol Metab Syndr. 2014;6:114. PubMed PMID: 25371712
23. Chen L, Li Y, Zhang F, Zhang S, Zhou X, Ji L. Association of serum ferritin levels with metabolic syndrome and insulin resistance in a Chinese population. J Diabetes Complications. 2017;31:364-8.
24. Niederau C, Berger M, Stremmel W, Starke A, Strohmeyer G, Ebert R, et al. Hyperinsulinaemia in non-cirrhotic haemochromatosis: impaired hepatic insulin degradation? Diabetologia. 1984;26:441-4.
25. Wilson JG, Lindquist JH, Grambow SC, Crook ED, Maher JF. Potential role of increased iron stores in diabetes. Am J Med Sci. 2003;325:332-9.
26. Vela D, Leshoski J, Gjorgievska ES, Hadzi-Petrushev N, Jakupaj M, Sopi RB, et al. The role of insulin therapy in correcting hepcidin levels in patients with type 2 diabetes mellitus. Oman Med J. 2017;32:195-200.
27. Ghamarchehreh ME, Jonaidi-Jafari N, Bigdeli M, Khedmat H, Saburi A. Iron status and metabolic syndrome in patients with non-alcoholic fatty liver disease. Middle East J Dig Dis. 2016;8:31-8.
28. J Jehn M, Clark JM, Guallar E. Serum Serum ferritin and risk of the metabolic syndrome in U.S. adults. Diabetes Care. 2004:27:2422-8.
29. Han LL, Wang YX, Li J, Zhang XL, Bian C, Wang H, et al. Gender differences in associations of serum ferritin and diabetes, metabolic syndrome, and obesity in the China Health and Nutrition Survey. Mol Nutr Food Res. 2014;58:2189-95.
30. Ma H, Lin H, Hu Y, Li X, He W, Jin X, et al. Serum ferritin levels are associated with insulin resistance in Chinese men and post-menopausal women: the Shanghai Changfeng study. Br J Nutr. 2018;120:863-71.
31. J Janssen I, Powell LH, Crawford S, Lasley B, Sutton-Tyrrell K. Menopause and the metabolic syndrome: the Study of Women's Health Across the Nation. Arch Intern Med. 2008;168:1568-75.

32. Wallace DF. The regulation of iron absorption and homeostasis. Clin Biochem Rev. 2016;37:51-62.
33. Lehtihet M, Bonde Y, Beckman L, Berinder K, Hoybye C, Rudling M, et al. Circulating hepcidin-25 is reduced by endogenous estrogen in humans. PLoS One. 2016;11:e0148802. PubMed PMID: 26866603
34. Sze SCW, Zhang L, Zhang S, Lin K, Ng TB, Ng ML, et al. Aberrant transferrin and ferritin upregulation elicits iron accumulation and oxidative inflammaging causing ferroptosis and undermines estradiol biosynthesis in aging rat ovaries by upregulating NF-Kb-activated inducible nitric oxide synthase: first demonstration of an intricate mechanism. Int J Mol Sci. 2022;23:12689. PubMed PMID: 36293552
35. Matta R, AbdElftah M, Essawy M, Saedii A. Interplay of serum hepcidin with female sex hormones, metabolic syndrome, and abdominal fat distribution among premenopausal and postmenopausal women. Egypt J Intern Med. 2022;34:8.
36. Alemany M. Estrogens and the regulation of glucose metabolism. World J Diabetes. 2021;12:1622-54.
37. Yan H, Yang W, Zhou F, Li X, Pan Q, Shen Z, et al. Estrogen improves insulin sensitivity and suppresses gluconeogenesis via the transcription factor foxo1. Diabetes. 2019;68:291-304.
38. Tiano JP, Delghingaro-Augusto V, Le May C, Liu S, Kaw MK, Khuder SS, et al. Estrogen receptor activation reduces lipid synthesis in pancreatic islets and prevents β cell failure in rodent models of type 2 diabetes. J Clin Invest. 2011;121:3331-42.
39. Martin LA, Critelli JW, Doster JA, Powers C, Purdum M, Doster MR, et al. Cardiovascular risk: gender differences in lifestyle behaviors and coping strategies. Int J Behav Med. 2013;20:97-105.
40. Ngo ST, Steyn FJ, Mccombe PA. Gender differences in autoimmune disease. Front Neuroendocrin. 2014;35:347-69.
41. Regitz-Zagrosek V. Sex and gender differences in health. Science & Society Series on Sex and Science. EMBO Rep. 2012;13:596-603.
42. Morrow EH. The evolution of sex differences in disease. Biol Sex Differ. 2015;6:5. PubMed PMID: 25774286

Supplementary table 1. Comparisons of Mets according to quartile of ferritin in overall population

(*n* = 5,730)

Gender	Serum ferritin (μg/L)	MetS			
		Model 1	Model 2	Model 3	Model 4
Overall population (*n* = 5,730)	Quartile 1 (*n* = 1,434)	1	1	1	1
	Quartile 2 (*n* = 1,431)	1.768 (1.451–2.153)**	1.414 (1.150–1.737)**	1.415 (1.151–1.739)**	1.306 (1.041–1.638)*
	Quartile 3 (*n* = 1,433)	2.166 (1.786–2.627)***	1.708 (1.386–2.406)**	1.713 (1.390–2.113)**	1.456 (1.157–1.832)**
	Quartile 4 (*n* = 1,432)	3.143 (2.606–3.791)***	3.044 (2.448–3.787)***	3.055 (2.455–3.802)***	2.504 (1.972–3.180)***

*$p < 0.05$, **$p < 0.01$, and ***$p < 0.001$. Model 1 [OR (95% CI)], Non-adjusted; Model 2 [OR (95% CI)], adjusted for age and gender; Model 3 [OR (95% CI)], Model 2 further adjusted for smoking, alcohol drinking, and regular exercise; Model 4 [OR (95% CI)], Model 3 further adjusted for obesity and anemia

Supplementary table 2. Comparisons of HOMA-IR according to quartile of ferritin in overall population

(*n* = 5,730)

Gender	Serum ferritin (μg/L)	HOMA-IR		
		Model 1	Model 2	Model 3
Overall population (*n* = 5,730)	Quartile 1 (*n* = 1,434)	2.38 ± 0.05 (2.29–2.48)	2.37 ± 0.05 (2.28–2.47)	2.44 ± 0.05 (2.35–2.54)
	Quartile 2 (*n* = 1,431)	2.47 ± 0.05 (2.38–2.56)	2.45 ± 0.05 (2.36–2.54)	2.48 ± 0.05 (2.39–2.57)
	Quartile 3 (*n* = 1,433)	2.50 ± 0.05 (2.42–2.59)	2.51 ± 0.05 (2.42–2.60)	2.49 ± 0.05 (2.40–2.58)
	Quartile 4 (*n* = 1,432)	2.92 ± 0.05 (2.82–3.10)	2.92 ± 0.05 (2.83–3.02)	2.84 ± 0.05 (2.75–2.93)
	p-value	< 0.001	< 0.001	< 0.001

Model 1 [M ± SE (95% CI)], adjusted for age and gender; Model 2 [M ± SE (95% CI)], Model 2 further adjusted for smoking, alcohol drinking, and regular exercise; Model 3 [M ± SE (95% CI)], Model 2 further adjusted for obesity and anemia.

Supplementary table 3. Comparisons of ferritin levels according to MetS and MSS in overall population (*n* = 5,730)

Gender	Category	Serum ferritin (μg/L) [M ± SE (95% CI)]
Overall population	MSS 0	65.62 ± 1.56 (62.56–68.68)
(*n* = 5,730)	MSS 1	71.98 ± 1.47 (69.10–74.86)
	MSS 2	81.32 ± 1.66 (78.06–84.57)
	MSS 3	91.08 ± 2.07 (87.02–95.15)
	MSS ≥ 4	96.13 ± 2.66 (90.92–101.35)
	p-value	< 0.001
	Non-MetS	72.85 ± 0.89 (71.12–74.59)
	MetS	90.76 ± 1.70 (87.43–94.08)
	p-value	< 0.001

Adjusted for age, gender, smoking, alcohol drinking, regular exercise, obesity, and anemia.

Biomedical Sciences and Clinical Medicine 2026;65(1):91-99.
doi: 10.12982/BSCM.2026.08
https://he01.tci-thaijo.org/index.php/CMMJ-MedCMJ/index

BSCM
Biomedical Sciences and Clinical Medicine

Original Article

Open Access

Validity and Reliability of the Thai Version of the Barthel Index Self-Report (BI-SR-TH) for People with Spinal Cord Injury

Siam Tongprasert[1], Sirinna Mekkij[1,2], Pratchayapon Kammuang-lue[1] and Tinakon Wongpakaran[3]

[1]Department of Rehabilitation Medicine, Faculty of Medicine, Chiang Mai University, Chiang Mai, Thailand; [2]Department of Rehabilitation Medicine, Phrae Hospital, Phrae, Thailand; [3]Department of Psychiatry, Faculty of Medicine, Chiang Mai University, Chiang Mai, Thailand

Correspondence:
Pratchayapon Kammuang-lue, MD, Department of Rehabilitation Medicine, Faculty of Medicine, Chiang Mai University, 110 Inthawaroros Road, Sri Phum, Muang, Chiang Mai 50200, Thailand .
E-mail: pratchayapon.k@cmu.ac.th

Received: January 31, 2025;
Revised: September 4, 2025;
Accepted: September 4, 2025

ABSTRACT

OBJECTIVE This study aimed to cross-culturally translate and evaluate the psychometric properties of the Thai version of the Barthel Index Self-Report (BI-SR-TH) for Thai people with spinal cord injury (SCI).

METHODS A descriptive cross-sectional validation and reliability study was conducted at the Maharaj Nakorn Chiang Mai Hospital, involving 109 Thai people aged 18 or older with either traumatic or non-traumatic SCI. The English postal version of the Barthel Index was translated into Thai following standard cross-cultural procedures, including forward and backward translation. Participants completed both the BI-SR-TH and the Thai EuroQoL (EQ-5D-5L) questionnaires via self-report and clinician assessment using the Barthel Index. The BI-SR-TH was re-administered to the participants one week later. Psychometric evaluation included assessments of internal consistency (Cronbach's alpha), concurrent validity (Spearman's correlation with clinician-rated BI), construct validity (convergent and discriminant validity assessed by correlations with relevant and distinct EQ-5D-5L domains), and test-retest reliability (intraclass correlation coefficient, ICC). The agreement between the BI-SR-TH and BI scores was assessed using ICC and the Bland-Altmand Altman analysis. Item-level agreement was assessed using the Kappa statistic.

RESULTS The BI-SR-TH demonstrated good internal consistency (Cronbach's alpha = 0.836) and excellent concurrent validity with a clinician-rated BI (r = 0.884). In terms of construct validity, the BI-SR-TH showed strong negative correlations with relevant EQ-5D-5L domains, e.g., mobility, self-care, and usual activities (r = −0.67 to −0.81, $p < 0.01$), demonstrating convergent validity. In contrast, correlations with unrelated domains such as anxiety and pain were weak or nonsignificant, indicating discriminant validity. The total score agreement between BI-SR-TH and the clinician BI was high (ICC = 0.916), and Bland-Altman analysis indicated a small mean difference. Most BI-SR-TH items showed good agreement with clinician ratings (Kappa 0.61–0.72) with the exception of the bowels and bladder items which showed only fair agreement (Kappa = 0.34 and 0.35, respectively). Test-retest reliability was also high (ICC = 0.924).

CONCLUSIONS The BI-SR-TH is a valid and reliable tool for assessing functional independence in Thai people with SCI. However, the bowels and bladder items require further refinement for this population

KEYWORDS Barthel Index, self report, functional status, spinal cord injury, reliability and validity

INTRODUCTION

Spinal cord injury (SCI) is a leading cause of major disability worldwide. Individuals with SCI usually lose the ability to perform some daily activities. As a result, tools to measure functional independence are essential for the rehabilitation process. There are several instruments for measuring this aspect, including the Barthel Index (BI) (1). The BI was initially developed for patients with stroke and neuromuscular diseases (1, 2). The assessment consists of a set of topics related to the ability to perform self-care activities, mobility, and bowel and bladder management across 10 domains, with scores ranging from 0 to 20. Healthcare providers conduct in-person interviews with patients or caregivers and evaluate patients by observing their functional abilities. The BI has been found to have good validity and reliability, and is widely used in clinical practice (2, 3). Psychometric properties of the BI have also been tested in persons with spinal cord injury (PwSCI). The BI has previously been translated and utilized to evaluate PwSCI in the Republic of Türkiye where it demonstrated good reliability and validity (4). In Thailand's intermediate care system, the BI is used in the evaluation of patients' level of independence during rehabilitation, including those with SCI, stroke, traumatic brain injury, and fractured hip (5). The simplicity and ease of use of the BI enables quick and efficient assessments, and its standardized scoring system allows for consistent comparisons of functional status across diverse patient populations. While the BI is less specific for SCI than instruments such as the Spinal Cord Independence Measure (SCIM) or the Spinal Cord Ability Ruler (SCAR), it offers a broad overview of functional independence. This makes the BI especially valuable when detailed assessment tools are unavailable or when a general measure of disability across various diagnoses is needed. In addition, the BI's widespread familiarity and acceptance in clinical practice supports its ongoing use for monitoring patient progress and guiding rehabilitation planning, particularly in resource-limited settings.

Gompertz and colleagues developed a postal version of the BI. It is a self-administered BI assessment consisting of a set of 10 questions, as in the original version, but with multiple-choice answer formats that patients can complete by themselves. That version has been tested for psychometric properties in stroke patients and has demonstrated good reliability (6). Subsequent studies in Parkinson's disease and stroke patients have also demonstrated its good validity (7, 8). Self-reported assessment can be used to collect data from many patients simultaneously, particularly in circumstances where telemedicine is growing. It is convenient for long-term patient data collection, allowing continuous monitoring of changes and reducing the workload of health care providers. Previous studies have shown the development and psychometric properties testing of the self-reported BI, but it has not yet been translated into Thai. Furthermore, studies have focused only on stroke and Parkinson's disease patients, but no research has been published on PwSCI. The objectives of this study are to translate and cross-culturally adapt the postal version of the BI by Gompertz et al. (6) into a Thai version and to evaluate its psychometric properties in SCI individuals.

METHODS

This study protocol was approved by the Research Ethics Committee of the Faculty of Medicine, Chiang Mai University, study code: REH-2564-08232. The study was conducted in two phases. The first phase involved translating the self-reported BI from English to Thai. The second phase evaluated the validity and reliability of the Thai version of the Barthel Index Self-Report (BI-SR-TH) in PwSCI.

Participants

Individuals with traumatic or non-traumatic SCI who visited the Department of Rehabilitation Medicine at Maharaj Nakorn Chiang Mai Hospital between August 2021 and March 2022 were recruited. The inclusion criteria comprised individuals aged 18 or older who were proficient in spoken Thai and could read Thai independently. Individuals with severe cognitive impairment or severe mental disorders who were unable to complete the assessment independently were excluded.

Research instruments

Thai version of the BI-SR-TH

Permission for translation of the BI-SR-TH was granted by Dr. Pandora Pound, a colleague of Dr. Patrick Gompertz, via electronic mail. The process of translation and cross-cultural adaptation into Thai was carried out for the self-reported BI. Initially, a forward translation was completed, resulting in two separate draft versions of the BI-SR-TH. These translations were independently conducted by two individuals, a physiatrist specializing in spinal cord medicine from the Department of Rehabilitation Medicine at Chiang Mai University, and a linguistic expert from the Humanities Academic Service Center at the same university. The researchers analyzed the items from the two draft versions and synthesized them into a single draft of the BI-SR-TH. Subsequently, back translation of that single draft was performed independently by two native English speakers who were proficient in Thai. Neither of the two translators was a health professional, and both were unaware of the original version of the self-reported BI. Once the translations were completed, they were submitted to Dr. Pandora Pound for review and feedback. Following her suggestions, the initial draft of the BI-SR-TH was revised into a pre-final version. Twenty-five Thai individuals with SCI tested the pre-final version of the BI-SR-TH to identify any areas of possible confusion or misunderstanding (9). Internal consistency was assessed using Cronbach's alpha, which yielded a value of 0.646, indicating questionable reliability. The Kappa statistic, used to evaluate the agreement between the pre-final version of the BI-SR-TH and the original BI, showed moderate to substantial agreement for most items; however, the bladder item exhibited poor agreement (K = 0.02). In response to this feedback, the bladder item was modified in the final version. It was changed from "need urinary catheterization" (0 point) to "need assistance with urinary catheterization" (0 point). The final version of the BI-SR-TH is included in the supplementary appendix.

The Barthel Index

The BI is a clinician-rated ordinal scale developed by Collin et al. (2) to assess a person's ability to perform ten common self-care and basic mobility activities. These activities include feeding, bathing, grooming, dressing, bowel and bladder management, toileting, transfers (from bed to chair and back), mobility on level surfaces, and stair negotiation. Administered through observation and/or structured interview by healthcare professionals, the total score range is from 0 to 20, with higher scores indicating greater functional independence. The BI has been widely used to evaluate functional independence in patients with various conditions, including SCI (4, 5).

The Thai Version of the EQ-5D-5L Health Questionnaire

The EQ-5D-5L questionnaire is used to evaluate health-related quality of life. This questionnaire has been translated into more than 160 languages globally, including Thai (10). It is used to assess health-related quality of life, particularly for monitoring treatment results in hospitals, clinical research, health technology assessment, and monitoring the quality of life of the general population and of patients, including PwSCI (11). The EQ-5D-5L consists of two parts. The first part includes five dimensions: mobility, self-care, usual activities, pain/discomfort, and anxiety/depression. Each question has five possible answers based on severity, ranging from no problems to unable/extreme problems. The second part evaluates health status via a Visual Analog Scale (VAS).

Data collection

After obtaining informed consent, demographic information and lesion characteristics of the participants were collected through interviews and reviews of medical records using the International SCI Core Data Set (version 3.0) (12). Participants then independently completed two self-administered questionnaires: the BI-SR-TH and the Thai version of the EQ-5D-5L (10). For participants unable to write due to hand or arm limitations, caregivers were permitted to assist with writing, but were not allowed to help interpret or explain any items. On the same day, a clinician-administered BI assessment was performed by one of five rehabilitation medicine residents, all of whom had received standardized training including a one-hour clinical demonstration and a review of the modified BI, as recommended by Shah et al., to ensure competency. The evaluators demonstrated high interrater reliability ($r > 0.9$) (13). To prevent bias, raters were blinded to the

BI-SR-TH responses, and both physicians and participants remained unaware of each other's scores. For inpatients, all assessments were conducted the day before discharge. To evaluate test-retest reliability, participants were provided with a copy of the BI-SR-TH in a sealed envelope and instructed to complete it again one week later, returning the questionnaire either by mail or electronically. The flow of the study is presented in the CONSORT flow diagram (Figure 1).

Statistical analysis

Sample size calculations

The sample size was calculated by the Bland-Altman method (14) using Medcalc version 19.7. Based on the research by Sutton et al. (8), the expected mean of difference was set at -1.0, and the expected standard deviation of differences at 0.9, with a maximum allowed difference between methods of 3.2. This resulted in a calculated sample size of at least 106 participants. For assessing test-retest reliability using the formula from Green et al. (15), the expected mean of difference was set at 0.4, and the expected standard deviation of differences at 1.0, which yielded an estimated sample size of 51 individuals. Ultimately, the final sample size consisted of a minimum of 106 participants.

$$n = \frac{(t_{n-1,\,\alpha/2} + t_{n-1,\,\beta})^2}{d^2}$$

All statistical data analyses were conducted using IBM SPSS version 22. The demographic data are presented using descriptive statistics, including frequency, percentage, mean, and standard deviation. Additionally, the total scores of the BI and the Thai version of the BI-SR-TH are shown. The floor and ceiling effects were considered significant if they exceeded 15% (16).

Reliability and validity analysis

- Reliability: Internal consistency was assessed using Cronbach's alpha, with a threshold of 0.7 or above considered acceptable (15). Test-retest reliability was evaluated with the intraclass correlation coefficient (ICC), where a value of at least 0.7 was deemed adequate (16).

- Concurrent validity: Criterion validity between BI and BI-SR-TH was determined using Spearman's ICC (r), which ranges from -1.00 to 1.00. Negative values indicate an inverse relationship. The levels of correlation were categorized as follows: $r \geq 0.75$ was very strong; $0.50 < r < 0.75$ was

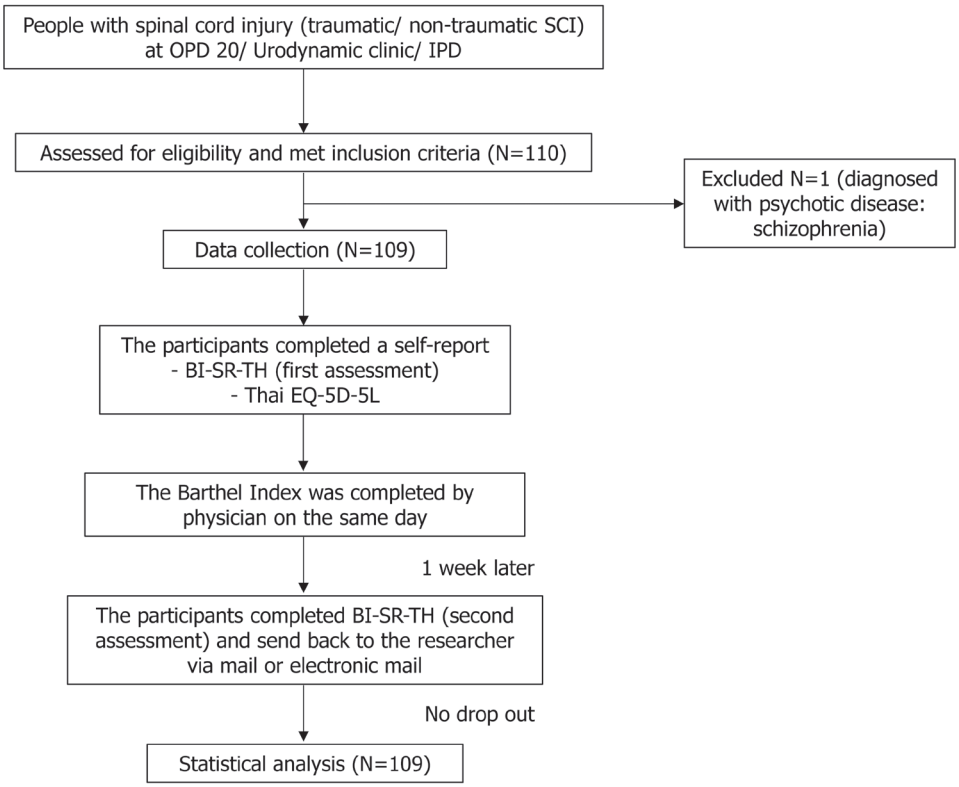

Figure 1. CONSORT flow diagram

strong; 0.25 < r < 0.50 was moderate; r < 0.25 was weak (16).

- Construct validity was examined through convergent and discriminant validity using the Thai EQ-5D-5L. The Spearman's ICC (r) was used to evaluate this correlation.

- Agreement: Agreement between the totals of BI and BI-SR-TH were analyzed using the Bland-Altman plot, with the limit of agreement (LOA) set at a mean difference ± 1.96 SD (16). An Intraclass ICC greater than 0.7 was considered acceptable (16). Kappa values were used to assess agreement for each item, with interpretations as follows: K < 0.2 was considered poor, 0.21-0.40 was considered fair, 0.41-0.60 was considered moderate, 0.61-0.80 was considered good, and 0.81-1.00 was considered very good/fairly complete (17).

RESULTS

Characteristics of the study population

A total of 109 individuals with either traumatic or non-traumatic spinal cord injuries participated in the study. Most participants were male (79 out of 109, or 72.5%), and the average age was 49 years. Most had T1-S3 paraplegia with ASIA (American Spinal Injury Association) Impairment Scale categories A, B, or C (60 out of 109, or 55.0%). Most participants had completed a secondary education. The characteristics of the study population are detailed in Table 1.

Psychometric properties of the BI-SR-TH

Each of the 109 participants answered all 10 BI questions and completed the BI-SR-TH questionnaire, a response rate of 100%. The average total scores for BI and BI-SR-TH are displayed in Table 2, which indicate comparable total scores and a floor and ceiling effect of 0.0-5.5%.

Internal consistency: Cronbach's alpha was 0.836, and the Cronbach's alpha of each item deleted from the BI-SR-TH are shown in Table 3.

Table 1. Demographic and clinical characteristics of the study population

	N (%) or mean ± SD
Age (year)	48.9±16.0
20-29 years	16 (14.7)
30-59 years	62 (56.9)
≥ 60 years	31 (28.4)
Gender	
Male	79 (72.5)
Female	30 (27.5)
Education	
No education	1 (0.9)
Primary school education	37 (33.9)
Secondary school	48 (44.0)
Bachelor's degree	23 (21.1)
Etiology of SCI	
Traumatic	86 (78.9)
Non-traumatic	23 (21.1)
Time since injury (year)	
< 1 year	26 (23.9)
1-4 years	16 (14.7)
5-9 years	22 (20.2)
10-14 years	20 (18.3)
> 15 years	25 (22.9)
Severity of SCI	
C1-4 AIS A, B, C	10 (9.2)
C5-8 AIS A, B, C	16 (14.7)
T1-S3 AIS A, B, C	60 (55.0)
AIS D at any level	23 (21.1)

N, number; SD, standard deviation; SCI, spinal cord injury; AIS, ASIA impairment scale

Table 2. Total scores of the Barthel Index and the Thai version of the Barthel Index Self-Report

	Barthel Index Total scores (score 0-20)	BI-SR-TH Total scores	
		First assessment (score 0-20)	Second assessment (score 0-20)
Mean±SD	11.88±5.78	12.42±4.80	12.64±4.99
Median (IQR)	14 (8)	14 (6)	14 (6)
Min	0	1	0
Max	20	20	20
Floor effect, n (%)	4 (3.7)	0 (0.0)	1 (0.9)
Ceiling effect, n (%)	6 (5.5)	6 (5.5)	5 (4.6)

BI-SR-TH, Thai version of the Barthel Index Self-Report; SD, standard deviation; IQR, interquartile range

Table 3. Internal consistency (Cronbach's alpha and Cronbach's alpha if item deleted) within BI-SR-TH

	Cronbach's alpha
Total	0.836
Cronbach's alpha if item deleted	
BI-SR-TH-bowel	0.842
BI-SR-TH-bladder	0.858
BI-SR-TH-grooming	0.816
BI-SR-TH-toilet	0.789
BI-SR-TH-feeding	0.810
BI-SR-TH-transfer	0.782
BI-SR-TH-mobility	0.823
BI-SR-TH-dressing	0.793
BI-SR-TH-stair	0.833
BI-SR-TH-bathing	0.811

BI-SR-TH, Thai version of the Barthel Index Self-Report

Test and retest reliability: The test-retest reliability was excellent, with an ICC of 0.924 (95%CI: 0.890-0.947).

Concurrent validity: There was a very strong correlation between the total scores of BI and BI-SR-TH, with a Spearman's ICC of 0.884.

Construct validity:

- Convergent validity: The relationship between the BI-SR-TH and the Thai EQ-5D-5L was assessed by correlating similar measures. The Spearman's ICC for the BI-SR-TH mobility item and the Thai EQ-5D-5L mobility item was -0.665 ($p < 0.05$). For the BI-SR-TH dressing item and the Thai EQ-5D-5L self-care item, the coefficient was -0.810 ($p < 0.05$). These results indicate significant inverse correlations at strong and very strong levels.
- Discriminant or divergent validity: Correlations were examined between dissimilar measures, e.g., the BI-SR-TH mobility item and the Thai EQ-5D-5L pain item, both of which yielded a Spearman's ICC of -0.011 ($p = 0.912$). The correlation between the BI-SR-TH dressing item and the Thai EQ-5D-5L anxiety item was -0.125 ($p = 0.196$), indicating weak or no correlation (Table 4).

Agreement:

- The agreement of total scores between the BI and BI-SR-TH was within an acceptable range, with an ICC of 0.916. The Bland-Altman analysis showed a mean score difference of -0.541 between the two measurements, with limits of agreement ranging from -4.797 to 3.714 (Table 5). Most data points from both assessments fell within this acceptable range, as shown in Figure 2.
- Agreement between each item of the BI and BI-SR-TH was good (Kappa values between 0.61 and 0.72) for all items except the bowels and bladder items, which had fair agreement with Kappa coefficients of 0.34 and 0.35, respectively (Table 6).

Table 4. Spearman's Correlation Coefficient between the Thai EQ-5D-5L and the Thai version of the Barthel Index Self-Report

Spearman's Correlation Coefficient	BI-SR-TH									
Thai EQ-5D-5L	**Bowel**	**Bladder**	**Grooming**	**Toileting**	**Feeding**	**Transfer**	**Mobility**	**Dressing**	**Stair**	**Bathing**
Mobility	-0.064	-0.085	-0.212*	-0.264**	-0.218*	-0.303**	-0.665**	-0.173	-0.532**	-0.208*
Self-care	-0.136	-0.124	-0.573**	-0.769**	-0.612**	-0.786**	-0.372**	-0.810**	-0.198*	-0.659**
Activities	-0.113	-0.002	-0.359**	-0.689**	-0.366**	-0.640**	-0.270**	-0.544**	-0.216*	-0.628**
Pain	-0.082	-0.082	-0.110	-0.289**	-0.033	-0.251**	-0.011	-0.218*	-0.019	-0.238*
Anxiety	-0.123	-0.069	-0.167	-0.269**	-0.148	-0.275**	-0.114	-0.125	-0.036	-0.154

*Correlation is significant at the 0.05 level (2-tailed); **Correlation is significant at the 0.01 level (2-tailed).
BI-SR-TH, Thai version of the Barthel Index Self-Report; Thai EQ-5D-5L, Thai version of EuroQoL Group 5 dimensions 5 levels

Table 5. Intraclass correlation coefficients, differences in the mean, and concurrent validity analysis between the total scores of the Barthel Index and the Thai version of the Barthel Index Self-Report

	Intraclass correlation (95%CI)	Mean difference		Concurrent validity	
		Mean diff (95%CI)	95% limit of agreement	Spearman's correlation coefficient	95%CI
Total scores	0.916 (0.880 to 0.942)	-0.541 (-0.954 to -0.129)	-4.797 to 3.714	0.884	0.835 to 0.920

CI, confidence interval

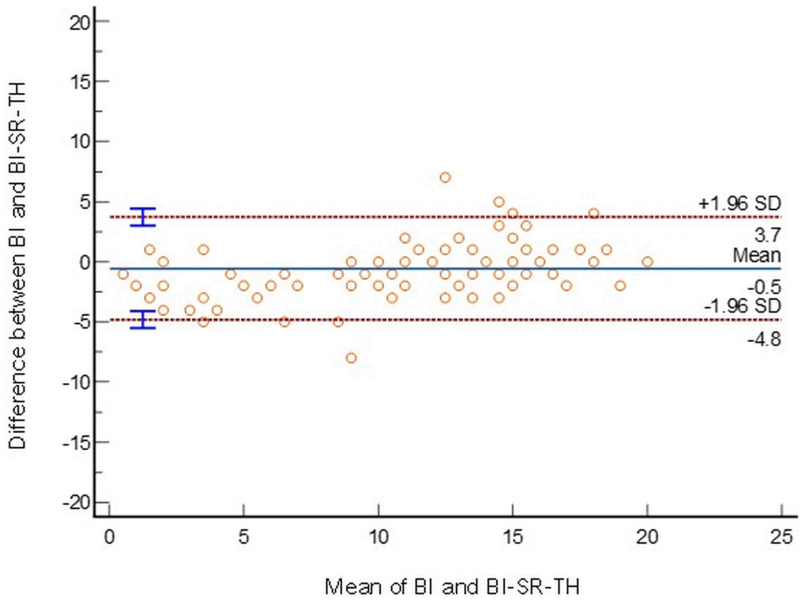

Figure 2. The Bland-Altman plot illustrates the mean differences between BI and BI-SR-TH measurements, showing a few outliers in the total scores. The error bars indicate variability at lower mean values.

Table 6. K value for each item of the Barthel Index and the BI-SR-TH

Item	K (SE)
Bowels	0.34 (0.07)
Bladder	0.35 (0.07)
Grooming	0.72 (0.09)
Toilet	0.68 (0.06)
Feeding	0.72 (0.09)
Transfer	0.61 (0.06)
Mobility	0.70 (0.06)
Dressing	0.71 (0.06)
Stairs	0.64 (0.11)
Bathing	0.71 (0.07)

K, Kappa coefficients; SE, standard error; BI-SR-TH, Thai version of the Barthel Index Self-Report

DISCUSSION

This study developed and validated a Thai version of the BI-SR-TH which demonstrated good validity and reliability for use with individuals having SCI. The BI-SR-TH showed acceptable internal consistency (Cronbach's alpha = 0.836) and very good concurrent validity, with a clinician-rated BI (r = 0.884). These results are higher than those reported by Morley and colleagues, who found a Cronbach's alpha of 0.69 and a correlation of r = 0.64 in Parkinson's disease patients using the postal version of the BI (7). Construct validity was supported through correlations with the Thai EQ-5D-5L. Strong negative correlations between BI-SR-TH and EQ-5D-5L domains such as mobility, self-care, and usual activities confirmed convergent validity, as these domains conceptually overlap with the BI. In contrast, weak or nonsignificant correlations between BI-SR-TH and EQ-5D-5L domains such as anxiety and pain supported discriminant validity, indicating that the instrument does not strongly associate with unrelated constructs. The validated Thai EQ-5D-5L was chosen for these assessments based on its reliability in chronic and neurological conditions (18) and its inclusion of both overlapping and distinct domains. While SCIM is a valuable tool for assessing the functional abilities of individuals with SCI, we chose not to focus on it for this study because SCIM does not include items for assessing discriminant validity. Test-retest reliability of the questionnaire was also high and was in line with previous studies, e.g., Gompertz and colleagues (6). The floor and ceiling effects were within acceptable limits (< 15.0%) (16).

Agreement between BI and BI-SR-TH total scores were strong (ICC = 0.916), comparable to results by Sutton et al. in stroke patients (ICC = 0.90) (8). Mean differences between BI-SR-TH and clinician-rated BI were negligible, with most Bland-Altman plot points within acceptable limits, supporting equivalence between the two formats. Consistent with previous research (8), the BI-SR-TH tended to yield slightly higher scores. However, the agreement between the BI and BI-SR-TH was lower for bowel and bladder items, as

was observed by Sutton et al. (K = 0.24). Sutton et al. speculated that this might be due to patients feeling uncomfortable answering questions about incontinence (8).

The most inconsistent response in the bladder item was that the physician assessed the BI as "incontinence or catheterized and unable to manage alone (0)," while some participants' responses to the BI-SR-TH were "never incontinent" (2 points). Two points (continent) in the BI was intended to include participants who could manage their urinary catheters themselves; however, if a participant required assistance even without leakage, they would be assessed as "(0)." In the BI-SR-TH version, based on discussions with participants, it was found that there was an issue in cases where participants could not manage their urinary catheters themselves but did not have urine leakage sometimes misunderstanding the question and electing "never incontinent" (2 points) instead of "need assistance with urinary catheterization" (0 points)" This likely resulted in only a fair agreement when the BI and the BI-SR-TH were compared.

A similar issue was observed for the bowels items. Participants who could not manage bowel care themselves but did not experience incontinence chose to respond with "never experienced incontinence" (2 points) instead of answering "incontinence all the time or need someone to give an enema" (0 points). Another point of difference was that the physician assessed "continence (2 points)" but the participants responded with 1 "occasional accident" (1 point). This might be due to the BI specifying a time frame for the bladder and bowel evaluations (over the past week). Those who did not experience incontinence during that week would be evaluated as "continence (2)." However, in the postal version by Gompertz et al. (6), there was no specified time frame in the description, allowing patients who experienced incontinence more than a week ago to choose "occasional accident" (1 point).

Due to the aforementioned issues, the authors believe that additional changes in the bowels and bladder items in the BI-SR-TH would enhance understanding and validity. This could potentially be achieved by adding phrases such as "completely managed alone" in the response option "never incontinent/never an accident" (2 points) and including the phrase "in the past week" in the descriptions of both the bladder and bowels items (the BI-SR-TH with additional suggestions is provided in the supplementary appendix). Since items other than the bowel and bladder aspects in BI-SR-TH were consistent with BI, we did not find it necessary to conduct further investigations or make changes in those items. Considering the inconsistencies observed between the BI and the BI-SR-TH, it is also possible that the BI-SR-TH, by being self-administered and sensitive to SCI-related issues, may ultimately provide a more accurate reflection of patients' true functional abilities. Future research should compare these formats against real-world outcomes and quality of life.

There were several limitations to this study. While the overall score agreement was strong, the agreement for bowel and bladder items was only fair. Factor analysis was not performed, and the study did not collect data on questionnaire completion time. The sample included only individuals with SCI; therefore, validation in other populations, such as stroke or other neurological conditions, is warranted. Further research should also explore how cultural differences affect self-reporting behaviors to ensure broader applicability and cross-cultural validity.

CONCLUSIONS

The BI-SR-TH demonstrated good internal consistency, good validity, excellent test-retest reliability, as well as good overall agreement with the clinician-rated version. However, agreement for the bowels and bladder items was only fair. Given the importance of these functions for people with SCI, further refinement of these items is recommended to enhance the tool's suitability for this population before widespread implementation.

ACKNOWLEDGMENTS

The authors would like to acknowledge Ms. Chanya Sachdev, Mr. John William Macmillan, and Mr. Clayton James Shuttleworth for their assistance in translating the self-reported BI and Mrs. Rochana Phuackchantuck for guidance on research statistics. The authors also wish to thank Nut Khunchompoo, MD., Tassaya Buranapakorn, MD., Nattha Boonthanakorn, MD., Patsaporn Jarupathirun, MD., and Niracha Luengutaisilp, MD. as well as residents of the Department of Rehabilitation Medicine, Faculty of Medicine, Chiang Mai University, for the data collection.

FUNDING

This study was funded by a grant from the Faculty of Medicine, Chiang Mai University (grant no 19-2565)

CONFLICTS OF INTEREST

The authors have no conflict of interest to report.

AUTHOR CONTRIBUTIONS

S.T.: designed the research questions and methodology, analyzed the data, and wrote the preliminary version of the manuscript; S.M.: designed the research questions and methodology, collected the data, analyzed the data, and wrote the preliminary version of the manuscript; P.K.: designed the research questions and methodology, analyzed the data, wrote the preliminary version, and revised the final version of the manuscript; T.W.: designed the research questions and methodology, analyzed the data, and wrote the preliminary version of the manuscript.

DATA AVAILABILITY

The data that support the findings of this study are available from the corresponding author upon reasonable request.

INSTITUTIONAL REVIEW BOARD STATEMENT

The study was conducted in accordance with the Declaration of Helsinki and approved by the Research Ethics Committee of the Faculty of Medicine, Chiang Mai University (study code: REH-2564-08232, approved on 12 July 2021).

INFORMED CONSENT STATEMENT

Informed consent was obtained from all participants involved in the study.

SUPPLEMENTARY MATERIALS

The following supporting information can be downloaded at: Supplementary appendix

REFERENCES

1. Mahoney FI, Barthel DW. Functional evaluation: the Barthel Index. Md State Med J. 1965;14:61-5.
2. Collin C, Wade DT, Davies S, Horne V. The Barthel ADL Index: a reliability study. Int Disabil Stud. 1988;10:61-3.
3. Wade DT, Collin C. The Barthel ADL Index: a standard measure of physical disability? Int Disabil Stud. 1988;10:64-7.
4. Küçükdeveci AA, Yavuzer G, Tennant A, Süldür N, Sonel B, Arasil T. Adaptation of the modified Barthel Index for use in physical medicine and rehabilitation in Turkey. Scand J Rehabil Med. 2000;32:87-92.
5. Sirindhorn National Medical Rehabilitation Institute [Internet]. Nonthaburi: Sirindhorn National Medical Rehabilitation Institute; c2024 [cited 2024 Nov 24]. Available from: https://www.snmri.go.th/wp-content/uploads/2021/11/IMCkpi-template2565_250664-SNMRI-1.pdf
6. Gompertz P, Pound P, Ebrahim S. A postal version of the Barthel Index. Clin Rehabil. 1994;8:233-9.
7. Morley D, Selai C, Thompson A. The self-report Barthel Index: preliminary validation in people with Parkinson's disease. Eur J Neurol. 2012;19:927-9.
8. Sutton CJ, Watkins CL, Cook N, Leathley MJ, McAdam J, Dey P. Postal and face-to-face administration of stroke outcome measures: can mixed modes be used? Stroke. 2013;44:217-9
9. Connelly LM. Pilot studies. Medsurg Nurs. 2008;17:411-2.
10. Pattanaphesaj J. Health-related quality of life measure (EQ-5D-5L): measurement property testing and its preference-based score in Thai population [dissertation]: Salaya (Thailand): Mahidol University; 2014.
11. Whitehurst DG, Suryaprakash N, Engel L, Mittmann N, Noonan VK, Dvorak MF, et al. Perceptions of individuals living with spinal cord injury toward preference-based quality of life instruments: a qualitative exploration. Health Qual Life Outcomes. 2014;12:50.
12. Biering-Sorensen F, Charlifue S, Chen Y, New PW, Noonan V, Post MWM, et al. International Spinal Cord Injury Core Data Set (version 3.0)-including standardization of reporting. Spinal Cord. 2023;61:65-8.
13. Shah S, Vanclay F, Cooper B. Improving the sensitivity of the Barthel Index for stroke rehabilitation. J Clin Epidemiol. 1989;42:703-9.
14. Lu M-J, Zhong W-H, Liu Y-X, Miao H-Z, Li Y-C, Ji M-H. Sample size for assessing agreement between two methods of measurement by Bland-Altman method. Int J Biostat. 2016;12.
15. Green J, Forster A, Young J. A test-retest reliability study of the Barthel Index, the Rivermead Mobility Index, the Nottingham Extended Activities of Daily Living Scale and the Frenchay Activities Index in stroke patients. Disabil Rehabil. 2001;23:670-6.
16. Terwee CB, Bot SD, de Boer MR, van der Windt DA, Knol DL, Dekker J, et al. Quality criteria were proposed for measurement properties of health status questionnaires. J Clin Epidemiol. 2007;60:34-42.
17. Brennan P, Silman A. Statistical methods for assessing observer variability in clinical measures. BMJ. 1992;304:1491-4.
18. Sonsa-ardjit N, Sakthong P. Reliability and validity of the Thai version of EQ-5D-5L questionnaire on patients with chronic disease. Chula Med J. 2015;59:489-501.

Supplementary Appendix

Barthel Questionnaire (English Version)

These are some questions about your ability to look after yourself.
They may not seem to apply to you. Please answer them all.
Tick one box in each section like this: ☑

Bathing In the bath or shower, do you: ……. *Remember - tick one box only*	manage on your own?		1
	need help getting in and out?		0
	need other help?		
	never have a bath or shower?		
	need to be washed in bed?		
Stairs Do you climb stairs at home: ……. *Remember - tick one box only*	without any help?		2
	with someone carrying your frame?		1
	with someone encouraging you?		
	with physical help?		
	not at all?		0
	don't have stairs?		
Dressing Do you get dressed: ……. *Remember - tick one box only*	without any help?		2
	just with help with buttons?		1
	with someone helping you most of the time?		0
Mobility Do you walk indoors: ……. *Remember - tick one box only*	without any help apart from a frame?		3
	with one person watching over you?		2
	with one person helping you?		
	with more than one person helping?		0
	not at all?		
	or do you use a wheelchair independently (e.g. to go around corners)?		1
Transfer Do you move from bed to chair: ……. *Remember - tick one box only*	on your own?		3
	with a little help from one person?		2
	with a lot of help from one or more people?		1
	not at all?		0
Feeding Do you eat food: ……. *Remember - tick one box only*	without any help?		2
	with help cutting food or spreading butter		1
	with more help?		0

Toilet use Do you use the toilet or commode: …… *Remember - tick one box only*	without any help?		2
	with some help but can do some thing?		1
	with quite a lot of help?		0
Grooming Do you brush your hair and teeth, wash your face and shave: ……. *Remember - tick one box only*	without help?		1
	with help?		0
Bladder (during the past week) Are you incontinent of urine? *Remember - tick one box only*	never (manage on your own)		2
	less than once a week		
	less than once a day		1
	more often		0
	have a catheter managed for you?		
Bowels (during the past week) Do you soil yourself? *Remember - tick one box only*	never (manage on your own		2
	Occasional accident		1
	all the time		0
	need someone to give you an enema?		

Note: The recommendations made by the researcher for further improvements have been underlined

Barthel Questionnaire (Thai Version; BI-SR-TH)

แบบสอบถามบาร์เธล

แบบประเมินชุดนี้มีไว้เพื่อให้ท่านประเมินความสามารถในการประกอบกิจวัตรประจำวัน
กรุณาตอบคำถามทั้งหมด แม้บางข้ออาจดูเหมือนไม่เกี่ยวข้องกับคุณ
ทำเครื่องหมาย ☑เพียง 1 ช่องในแต่ละหัวข้อ

การอาบน้ำ คุณอาบน้ำได้โดย..... *หมายเหตุ – เลือกเพียง 1 ตัวเลือกเท่านั้น*	อาบน้ำได้ด้วยตนเอง		1
	ต้องช่วยเหลือในการเข้าและออกบริเวณอาบน้ำ		0
	ต้องการความช่วยเหลือด้านอื่นๆ		
	ไม่เคยอาบน้ำเลย		
	ต้องเช็ดตัว/อาบน้ำบนเตียง		
การขึ้นลงบันได คุณขึ้นลงบันไดที่บ้านได้โดย..... *หมายเหตุ – เลือกเพียง 1 ตัวเลือกเท่านั้น*	ไม่ต้องการความช่วยเหลือใด ๆ		2
	โดยต้องมีคนช่วยถืออุปกรณ์ช่วยเดิน		1
	โดยต้องมีคนช่วยให้กำลังใจ		
	โดยต้องช่วยเหลือทางกาย		
	ไม่ได้ขึ้นลงบันไดเลย		0
	ไม่มีบันได		
การแต่งตัว คุณแต่งตัวได้โดย..... *หมายเหตุ – เลือกเพียง 1 ตัวเลือกเท่านั้น*	แต่งตัวได้ด้วยตนเอง		2
	โดยต้องมีคนช่วยติดกระดุม		1
	โดยต้องมีคนช่วยเหลือเกือบตลอดเวลา		0
การเคลื่อนที่ คุณเดินในบ้านโดย..... *หมายเหตุ – เลือกเพียง 1 ตัวเลือกเท่านั้น*	เดินได้เอง หรือใช้เพียงอุปกรณ์ช่วยเดิน		3
	โดยต้องมีคนเฝ้าระวัง 1 คน		2
	โดยต้องมีคนช่วยเหลือ 1 คน		
	โดยต้องมีคนช่วยเหลือ 2 คนขึ้นไป		0
	ไม่สามารถเดินหรือใช้วีลแชร์ด้วยตนเองได้		
	หรือคุณใช้วีลแชร์ได้ด้วยตนเอง (เข้าออกมุมต่างๆได้)		1
การเคลื่อนย้ายตัว คุณย้ายตัวเองจากเตียงไปที่เก้าอี้ได้โดย..... *หมายเหตุ – เลือกเพียง 1 ตัวเลือกเท่านั้น*	ย้ายได้ด้วยตนเอง		3
	โดยต้องการคน 1 คนช่วยเหลือเล็กน้อย		2
	โดยต้องการคน 1 คนขึ้นไป ช่วยเหลืออย่างมาก		1
	ไม่สามารถย้ายตัวได้เลย		0

การรับประทานอาหาร คุณรับประทานอาหารได้โดย..... *หมายเหตุ – เลือกเพียง 1 ตัวเลือกเท่านั้น*	ทานอาหารได้ด้วยตนเอง		2
	โดยต้องช่วยเหลือในการตัดอาหารหรือทาเนย		1
	โดยต้องช่วยเหลือมากกว่าข้อด้านบน		0
การใช้ห้องน้ำ คุณสามารถใช้ห้องน้ำ หรือเก้าอี้นั่งถ่ายเพื่อขับถ่ายได้โดย..... *หมายเหตุ – เลือกเพียง 1 ตัวเลือกเท่านั้น*	ไม่ต้องการความช่วยเหลือใด ๆ		2
	โดยทำบางอย่างได้เอง แต่ต้องช่วยเหลืออยู่บ้าง		1
	ทำได้โดยต้องการความช่วยเหลืออย่างมาก		0
การดูแลความสะอาดใบหน้า คุณหวีผม แปรงฟัน ล้างหน้า และโกนหนวดได้โดย..... *หมายเหตุ – เลือกเพียง 1 ตัวเลือกเท่านั้น*	ดูแลได้โดยไม่ต้องการความช่วยเหลือ		1
	โดยต้องการความช่วยเหลือ		0
การถ่ายปัสสาวะ <u>(ช่วง 1 สัปดาห์ที่ผ่านมา)</u> คุณปัสสาวะเล็ดราดหรือไม่ *หมายเหตุ – เลือกเพียง 1 ตัวเลือกเท่านั้น*	ไม่เคยปัสสาวะเล็ดราด<u>และจัดการได้ด้วยตนเอง</u>		2
	เล็ดราดบ้าง 1 ครั้งใน 2-3 สัปดาห์		
	เล็ดราดบ้าง 1 ครั้งใน 2-3 วัน		1
	ปัสสาวะเล็ดราดบ่อยๆ		0
	คุณต้องมีผู้ช่วยในการใช้สายสวนหรือคาสายสวนปัสสาวะ		
การถ่ายอุจจาระ <u>(ช่วง 1 สัปดาห์ที่ผ่านมา)</u> คุณอุจจาระเล็ดราดหรือไม่ *หมายเหตุ – เลือกเพียง 1 ตัวเลือกเท่านั้น*	ไม่เคยอุจจาระเล็ดราด<u>และจัดการได้ด้วยตนเอง</u>		2
	เล็ดราดเป็นบางครั้ง		1
	เล็ดราดตลอดเวลา		0
	หรือคุณต้องมีผู้ช่วยในการสวนถ่ายอุจจาระ		

หมายเหตุ: ข้อเสนอที่ผู้วิจัยแนะนำให้มีการปรับปรุงเพิ่มเติม ได้ทำการขีดเส้นใต้ไว้

Biomedical Sciences and Clinical Medicine 2026;65(1):100-110.
doi: 10.12982/BSCM.2026.09
https://he01.tci-thaijo.org/index.php/CMMJ-MedCMJ/index

BSCM
Biomedical Sciences and Clinical Medicine

Original Article

Open Access

Uncovering the Molecular Landscape of Secreted Phosphoprotein 1 and Its Expression Network in Kidney Renal Papillary Cell Carcinoma

Danang Prasetyaning Amukti[1], Ria Indah Pratami[2], Moch Saiful Bachri[2] and Daru Estiningsih[1]

[1]Department of Pharmacy, Faculty of Health Sciences, Alma Ata University, Yogyakarta, Indonesia; [2]Faculty of Pharmacy, Ahmad Dahlan University, Yogyakarta, Indonesia

Correspondence:
Danang Prasetyaning Amukti, PhD
Department of Pharmacy, Faculty of Health Sciences, Alma Ata University, Yogyakarta, Indonesia.
E-mail: amuktidanang@gmail.com

Received: May 22, 2025;
Revised: August 27, 2025;
Accepted: September 12, 2025

ABSTRACT

OBJECTIVE This study aims to investigate the expression pattern of Secreted Phosphoprotein 1 (*SPP1*), its prognostic relevance, and the associated co-expression gene network in kidney renal papillary cell carcinoma (KIRP).

METHODS Publicly available transcriptomic and clinical datasets were analyzed using GEPIA, UALCAN, and the GTEx Portal. *SPP1* expression levels in KIRP versus normal kidney tissues were evaluated, followed by Kaplan–Meier survival analysis stratified by ethnicity, gender, and body weight. Co-expression analysis was performed to identify genes significantly correlated with *SPP1* and to explore their potential biological functions.

RESULTS *SPP1* expression was significantly upregulated in KIRP tissues compared with normal kidney tissues, consistent with GTEx data showing naturally high expression in kidney cortex and medulla. High *SPP1* expression was associated with poorer overall survival, particularly among Caucasian patients, while no significant survival differences were observed by gender or body weight. Ten genes strongly co-expressed with *SPP1*, *MLLT3*, *AKIRIN2*, *YIPF1*, *SESTD1*, *LAMC1*, *FAS*, *ABCC3*, *MTHFD1L*, *ANXA2P2*, and *ARHGAP29* were identified, many of which are implicated in cell adhesion, migration, extracellular matrix remodeling, and apoptosis resistance.

CONCLUSIONS *SPP1* is markedly overexpressed in KIRP and correlates with unfavorable prognosis, highlighting its potential as a diagnostic and prognostic biomarker. The identified *SPP1*-associated co-expression gene network may offer novel insights and therapeutic targets for improving molecular-based interventions in KIRP.

KEYWORDS kidney renal papillary cell carcinoma, Secreted Phosphoprotein 1, UALCAN, GEPIA

INTRODUCTION

Kidney cancer is one of the leading causes of urological cancer deaths worldwide, with kidney renal papillary cell carcinoma (KIRP) being the second major subtype after clear cell renal cell carcinoma (ccRCC) (1). Although KIRP exhibits a relatively less aggressive biological behavior compared to ccRCC, its response to therapy remains variable and incompletely understood. Although KIRP is generally considered less aggressive than ccRCC, there remains a strong need for reliable biomarkers and more tailored therapeutic strategies. Epidemiological data indicate that KIRP accounts for approximately 10–15% of all renal cell

carcinoma (RCC) cases worldwide, representing the second most common subtype after ccRCC. Importantly, advanced-stage KIRP is associated with poor outcomes, with reported 5-year survival rates as low as 40–50%. Moreover, unlike ccRCC, KIRP often shows variable responses to standard systemic therapies, including tyrosine kinase inhibitors and immunotherapy, underscoring the heterogeneity of its biology. This clinical variability highlights the necessity of identifying molecular biomarkers that could improve risk stratification, guide therapeutic decision-making, and potentially enable the development of targeted treatments specifically for KIRP (2). Advances in omics approaches, especially transcriptomics, have opened up new opportunities to identify specific biomarkers that can be used for early diagnosis, risk stratification, and more targeted therapy. In this context, identifying genes that play a key role in the pathogenesis of KIRP is an urgent need to personalize therapy and improve patient prognosis (3). One candidate gene that has attracted attention in cancer research is Secreted Phosphoprotein 1 (*SPP1*), also known as osteopontin. *SPP1* is a multifunctional glycoprotein involved in various biological processes such as cell adhesion, migration, angiogenesis, and regulation of immune responses (4, 5). Overexpression of *SPP1* has been reported in various cancer types, including breast, lung, prostate, and liver cancers, and is often associated with poor prognosis and increased metastatic potential. However, the specific role of *SPP1* in KIRP has not been comprehensively explored (6). Given the potential multifunctionality of *SPP1* in the tumor microenvironment, further investigation of its expression in the context of KIRP may open new avenues for the development of molecular biomarkers (7).

Gene expression-based analytical approaches from bioinformatics databases allow for systematic analysis of *SPP1* expression levels between tumor tissues and paired normal tissues (8, 9). In addition, gene expression correlation analysis provides information on other genes co-expressed with *SPP1*, which may reflect interrelated molecular pathways or transcriptional regulation (10). The identification of these genes may enhance our understanding of the molecular mechanisms underlying KIRP and may facilitate the development of more accurate and sensitive biomarker panels. In this study, we evaluated *SPP1* expression in KIRP tissues compared with normal kidney tissues and identified genes with the most similar expression patterns (co-expression) to *SPP1* (11). The main objectives of this study were to explore the biological role of *SPP1* in KIRP and to construct a gene expression network that may be clinically relevant (12). We hypothesize that increased expression of *SPP1* and its co-expressed genes may reflect the activation of specific molecular pathways that support tumor growth and progression. It is anticipated that the results of this study will provide important contributions to the molecular understanding of KIRP and will support the development of new biomarkers and therapeutic targets in the future.

METHODS

This study used a public data-based bioinformatics approach to evaluate gene expression of SPP1 in KIRP papillary renal cancer (13, 14). All analyses were performed in silico utilizing gene expression databases from the GEPIA (Gene Expression Profiling Interactive Analysis) platform (GEPIA2 v2021), UALCAN (update 2022), and Genotype-Tissue Expression (GTEx) Portal v8, which provide access to large-scale transcriptomic data from The Cancer Genome Atlas (TCGA) and GTE) projects, respectively.

Analysis of *SPP1* expression and survival using GEPIA

Gene expression analysis and prognostics *SPP1* on KIRP is carried out using GEPIA (*Gene Expression Profiling Interactive Analysis*, http://gepia.cancer-pku.cn), an R-based platform that uses RNA-seq data from The Cancer Genome Atlas (TCGA) and GTEx (15). To evaluate the differential expression of the *SPP1* gene between KIRP tumor tissues and normal kidney tissues, the feature used was "Box Plot" on GEPIA. The analysis parameters were set as follows: log2 fold change (log2FC) cutoff of 1 and p <0.01. The type of analysis selected was Differential Expression Analysis, with the data type selected as "KIRP vs Normal". The resulting graph is a box-and-whisker plot that visually shows the distribution of *SPP1* expression in the normal and tumor groups, as well as the statistical value of the t-test. Furthermore,

survival analysis was performed to determine the relationship between *SPP1* expression levels and the prognosis of KIRP patients. The feature "Survival Analysis" in GEPIA is used to generate Kaplan-Meier curves, which compare the probability of survival between patient groups by high expression and low expression from the *SPP1* gene. Group separation was performed automatically based on median gene expression. The survival types analyzed were overall survival (OS), with the median group cutoff data separation method and the log-rank test statistical method. The results are visualized in the form of a Kaplan-Meier plot, equipped with hazard ratio (HR), *p*-value, and number of patients in each group. A $p < 0.05$ was considered to indicate statistical significance. This analysis aims to assess the potential of *SPP1* as a prognostic biomarker in KIRP based on its transcriptomic expression and its effect on patient clinical outcomes (16).

Survival analysis based on SPP1 gene expression using UALCAN

To evaluate the effect of gene expression *SPP1* on the prognosis of patients with KIRP, survival analysis was performed using the platform UALCAN (https://ualcan.path.uab.edu). UALCAN is a web-based bioinformatics portal that provides access to clinical and transcriptomic data from TCGA, enabling analysis of gene expression and the relationship between gene expression and clinical outcomes, including patient survival (17). In this analysis, *SPP1* expression data in KIRP patients were grouped into two categories based on median expression: group high expression (high expression) and group low expression (low expression). Survival analysis was performed using the method Kaplan-Meier survival plot, provided by UALCAN, to compare the cumulative survival probabilities between the two groups over time. Differences between survival curves were tested using the $\chi 2$ test log-rank test, which is automatically calculated by the platform. The value $p < 0.05$ was considered statistically significant. The resulting data were visualized in the form of Kaplan-Meier curves with information on the number of patients in each group, *p*-value, and median survival time when available (18).

SPP1 Normal Expression Analysis Using GTEx Portal

To obtain an overview of gene expression *SPP1* in normal kidney tissue, data from GTEx Portal (https://gtexportal.org), a repository of RNA-seq gene expression data derived from healthy tissues of various human donors was used. The platform provides TPM (transcripts per million) based genetic expression information, enabling high-quality comparison of expression across normal tissues (19, 20). Using the feature gene expression browser on the GTEx portal, a search was carried out on the *SPP1* gene and its expression data was extracted from kidney tissue, specifically in two anatomical subtypes, namely kidney cortex and kidney medulla, if available. Expression data are visualized in the form of a boxplot, which shows the distribution of *SPP1* expression values from a number of normal kidney tissue samples. These results were used as physiological control references to compare with *SPP1* gene expression in KIRP tumor tissues from the TCGA database (21, 22).

Correlation analysis of gene expression against SPP1

To identify the genes that are most similar in expression to *SPP1* on KIRP, correlation analysis was carried out using the platform GEPIA (http://gepia.cancer-pku.cn). GEPIA offers features "Similar Gene Detection", which allows searching for genes with the most similar expression patterns based on the entire RNA-seq dataset from TCGA and GTEx (23). In this analysis, *SPP1* was used as the query gene. GEPIA calculated the value of the Pearson Correlation Coefficient (PCC) between *SPP1* expression and each of the other genes in the KIRP dataset. Genes with the highest PCC values were selected for further analysis, focusing on strong positive correlations (PCC > 0.5). The results of the analysis are visualized in Table 1, which includes information on gene symbols, gene IDs, and correlation values.

RESULTS

SPP1 expression in various types of cancer based on GEPIA analysis

To evaluate gene expression *SPP1* in various cancer types, expression analysis was performed using RNA-seq data available through GEPIA, which combines TCGA and GTEx datasets. This graph shows the comparison of median *SPP1* expression levels between tumor tissues (represented by pink bars) and normal tissues (represented by dark gray bars) across various cancer types. The results of the analysis show that *SPP1*

expression is consistently higher in tumor tissues than in normal tissues, especially in KIRP, Kidney Chromophobia (KICH), and Kidney Renal Clear Cell Carcinoma (KIRC). This marked increase in KIRP expression supports the hypothesis that *SPP1* plays a role in the pathogenesis of papillary renal cancer. In addition, the pattern of increased *SPP1* expression is also observed in several other cancer types, such as breast cancer (BRCA) and glioblastoma (GBM), although not as strong as that seen in renal cancer. These results can also be seen in Figure 1.

SPP1 expression in KIRP based on UALCAN analysis

UALCAN analysis revealed that *SPP1* expression was significantly elevated in KIRP tumor tissues compared with normal kidney tissues. These results are visualized in the form of a boxplot, where *SPP1* expression in tumor samples (red) appears much higher compared to normal samples (blue). This difference in expression is statistically significant, with a $p < 0.01$, indicating the involvement of *SPP1* in the pathogenesis of KIRP. The consistently higher *SPP1* expression in KIRP tissue supports the hypothesis that *SPP1* may play a role in the process of proliferation, migration, and remodeling of the tumor microenvironment. These findings strengthen the potential of *SPP1* as a molecular biomarker for diagnosis, prognosis, and as a therapeutic target in papillary kidney cancer. The detailed statistical results are presented in Figure 2.

SPP1 expression analysis in KIRP based on GEPIA and UALCAN platforms

To further evaluate *SPP1* expression in KIRP cancer, gene expression analysis was performed using two major bioinformatics platforms, namely GEPIA and UALCAN. In GEPIA analysis (Figure 3A), *SPP1* expression in KIRP tumor tissue appeared significantly higher than in normal tissue. Visualization in the form of a scatter plot showed the distribution of transcripts per million (TPM) values, with the KIRP tumor group standing out significantly above normal tissue. This confirmed the strong upregulation of *SPP1* in KIRP tumor tissue. Meanwhile, analysis using UALCAN (Figure 3B) showed similar results through boxplot visualization. The level of *SPP1* expression in primary tumor tissue (n = 290) was significantly higher than in normal kidney tissue (n = 32), with a median expression more than twice that of normal tissue. Statistical analysis showed a significant difference ($p < 0.01$), strengthening the evidence that *SPP1* overexpression is an important molecular characteristic of KIRP. The consistency of findings from these two platforms suggests that *SPP1* may play a key role in KIRP pathogenesis and has potential as a diagnostic biomarker or molecular therapeutic target.

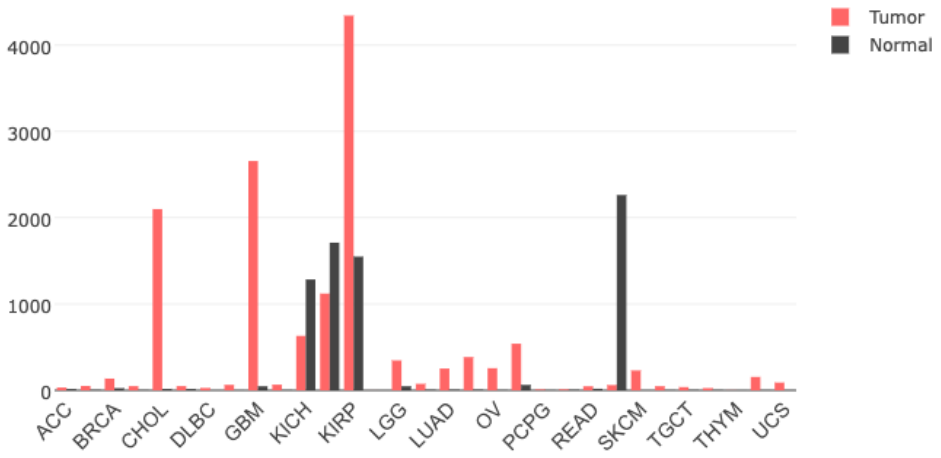

Figure 1. *SPP1* Gene expression in various types of cancer and normal tissues
ACC, adenocortical carcinoma; BRCA, breast invasive carcinoma; CHOL, cholangiocarcinoma; DLBC, diffuse large B-cell lymphoma; GMB, glioblastoma; KICH, kidney chromophobe; KIRP, kidney renal papillary cell carcinoma; LGG, low-grade glioma; LUAD, lung adenocarcinoma; OV, ovarian cancer; PCPG, pheochromocytoma and paraganglioma; READ, rectum adenocarcinoma; SKCM, skin cutaneous melanoma; TGCT, testicular germ cell tumors; THYM, thymoma, UCS, uterine carcinosarcoma

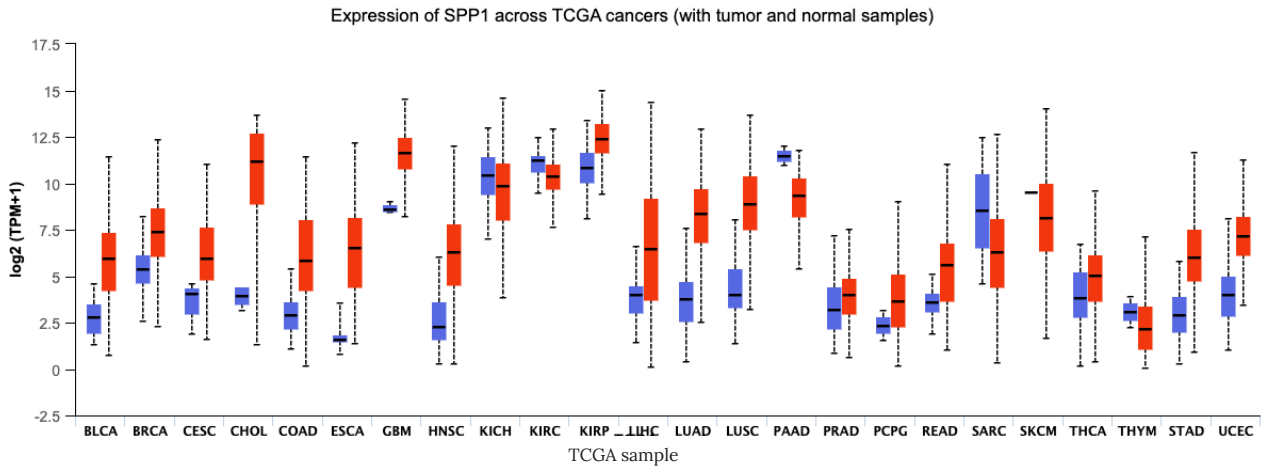

Figure 2. *SPP1* gene expression in KIRP tissue and normal kidney tissue based on UALCAN analysis, normal tissue (blue); tumor tissue (red)
BLCA, bladder urothelial carcinoma; BRCA, breast invasive carcinoma; CESC, cervical squamous cell carcinoma; CHOL, cholangiocarcinoma; COAD, colon adenocarcinoma; ESCA, esophageal cancer; GMB, glioblastoma; HNSC, head and neck squamous cell carcinoma; KICH, kidney chromophobe; KIRC, kidney renal clear cell carcinoma; KIRP, kidney renal papillary cell carcinoma; LIHC, liver hepatocellular carcinoma; LUAD, lung adenocarcinoma; LUSC, lung squamous cell carcinoma; PAAD, pancreatic ductal adenocarcinoma; PRAD, prostate adenocarcinoma, PCPG, pheochromocytoma and paraganglioma; READ, rectum adenocarcinoma; SARC, sarcoma, SKCM, skin cutaneous melanoma; THCA, thyroid carcinoma; THYM, thymoma, STAD, stomach adenocarcinoma UCEC, uterine corpus endometrial carcinoma

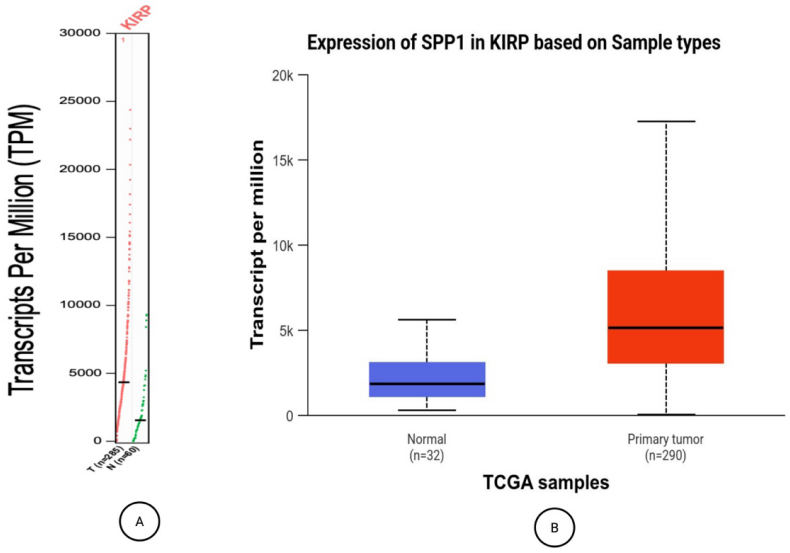

Figure 3. *SPP1* expression analysis in KIRP across two platforms. (A) Scatter plot from GEPIA showing significantly higher *SPP1* expression in KIRP tumor tissues compared with normal kidney tissues ($p < 0.01$). TPM values are displayed with median and interquartile ranges. (B) Boxplot from UALCAN showing *SPP1* expression levels in KIRP tumor samples (n = 290) versus normal kidney tissues (n = 32). Median tumor expression is more than twice that of normal tissues ($p < 0.01$).

Identification of highest co-expression genes against *SPP1* in KIRP

As part of the gene expression network exploration, expression correlation analysis was performed using datasets from GEPIA. The results of the analysis showed that several genes had the most similar expression patterns to *SPP1* in KIRP. The gene with the highest correlation was *SESTD1* (PCC = 0.65), followed by *AKIRIN2* (PCC = 0.59), *YIPF1* (PCC = 0.57), *SESTD1* (PCC = 0.55), and *LAMC1* (PCC = 0.54). Other genes such as *FAS*, *SESTD1*, *MTHFD1L*, *ANXA2P2*, and *ARHGAP29* also showed strong correlations with PCC values above 0.53. This co-expression suggests that these genes are likely involved in molecular pathways that are interconnected with *SPP1* function,

Table 1. List of genes with the highest co-expression with *SPP1* in KIRP based on expression correlation analysis in GEPIA

Gene symbol	Gene ID	PCC
MLLT3	ENSG00000171843	0.65
ENDING2	ENSG00000135334	0.59
YIPF1	ENSG00000058799	0.57
SESTD1	ENSG00000187231	0.55
LAMC1	ENSG00000135862	0.54
FAS	ENSG00000026103	0.54
ABCC3	ENSG00000108846	0.54
MTHFD1L	ENSG00000120254	0.54
ANXA2P2	ENSG00000231991	0.54
ARHGAP29	ENSG00000137962	0.53

PCC, Pearson Correlationship Coefficient

especially in processes such as cell migration, adhesion, tissue remodeling, and resistance to apoptosis. This finding opens up opportunities for further studies of these genes, both as part of a predictive biomarker network and as molecular therapeutic targets for KIRP as summarized in Table 1.

Relationship between SPP1 expression and prognosis of KIRP patients

Survival analysis using the GEPIA platform showed that *SPP1* expression levels were associated with the prognosis of KIRP patients. The Kaplan-Meier survival plot (Figure 4) showed that patients with high *SPP1* expression (high expression) had a lower overall probability of survival compared to patients with low expression (low expression). Statistically, this difference was significant with a $p < 0.05$, indicating that *SPP1* overexpression may be associated with worse clinical outcomes in KIRP patients. These findings strengthen the potential role of *SPP1* as a negative prognostic biomarker, where increased expression of this gene may reflect greater tumor aggressiveness and a worse prognosis.

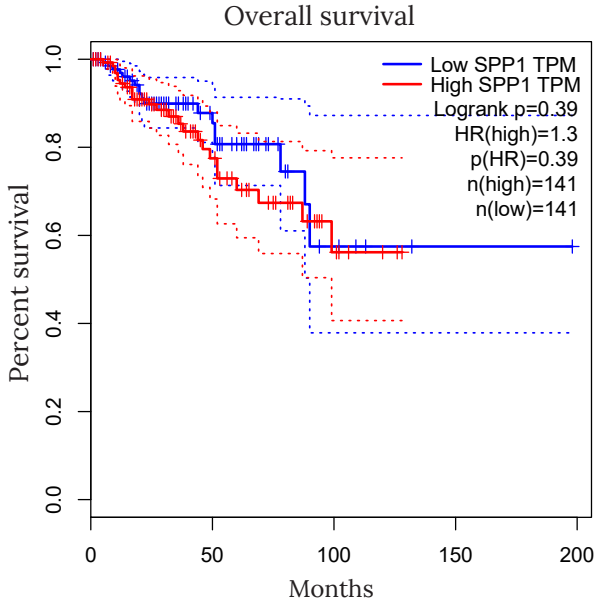

Figure 4. Kaplan-Meier analysis of the relationship between *SPP1* expression and overall survival of KIRP patients using GEPIA

Relationship between SPP1 Expression and Prognosis of KIRP Patients Based on Survival Analysis

Survival analysis of KIRP patients based on *SPP1* expression was performed using data from the UALCAN platform. The results of the survival analysis (Figure 5A) Kaplan-Meier survival plot showed patients with high *SPP1* expression tended to have a lower probability of survival than patients with low or moderate expression. However, this difference did not reach statistical significance ($p = 0.36$). This finding suggests that although there was a trend of decreased survival in the high expression group, *SPP1* expression alone may not be strong enough to independently predict the prognosis of KIRP patients. When stratification was performed based on patient race (Figure 5B), it was found that the combination of *SPP1* expression and race factors gave significant results ($p = 0.045$). In particular, Caucasian patients with high *SPP1* expression showed lower survival rates than other groups. These results indicate that the effect of *SPP1* expression on prognosis may also depend on the genetic or racial background of the patient. Further analysis based on patient gender (Figure 5C) showed that there was no significant difference in survival rate based on *SPP1* expression between male and female patients ($p = 0.42$). This suggests that gender does not modify the relationship between *SPP1* expression and clinical outcome in KIRP. Survival analysis based on weight category (Figure 5D) similarly showed no significant difference ($p = 0.69$) in the prognosis of KIRP patients based on *SPP1* expression. Thus, weight status does not appear to influence the impact of *SPP1* expression on patient survival.

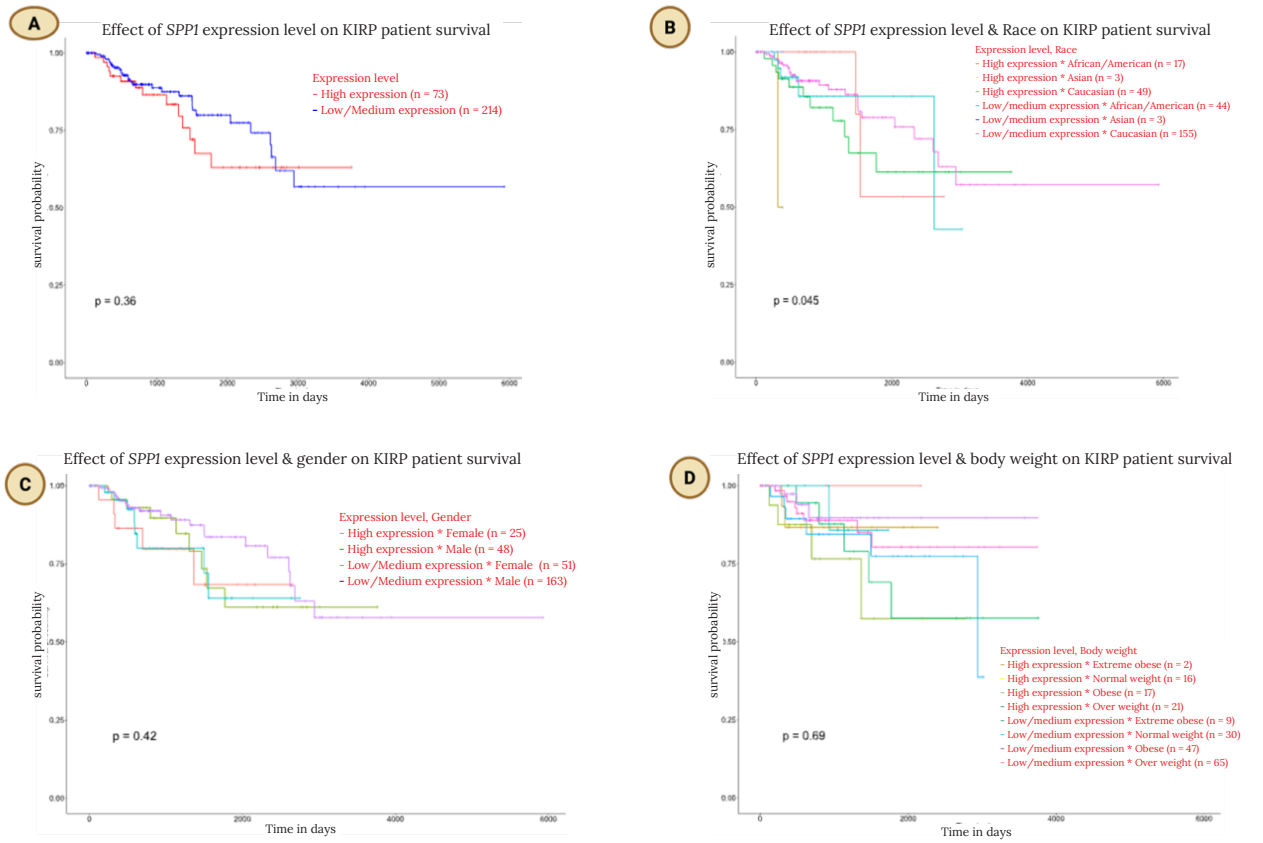

Figure 5. Kaplan-Meier survival plot of KIRP patients based on *SPP1* expression. (A) Overall survival stratified by high versus low *SPP1* expression (p = 0.36, not significant). (B) Survival stratified by race, showing significantly worse prognosis in Caucasian patients with high *SPP1* expression (p = 0.045). (C) Survival stratified by gender, showing no significant difference between male and female patients (p = 0.42). (D) Survival stratified by patient weight category, showing no significant difference (p = 0.69).

Normal expression of *SPP1* gene based on GTEx data

Physiological expression analysis of the *SPP1* gene in various normal human tissues was performed using data from GTEx Portal. The visualization resulted in the form of violin plots showed that *SPP1* expression varied among various tissues. The highest expression was detected in kidney cortex and kidney medulla tissues. These data strengthen the finding that increased *SPP1* expression was observed in KIRP tissues. Thus, *SPP1* has potential as an important molecular indicator in detecting abnormal biological changes in KIRP as can be seen in Figure 6.

DISCUSSION

In this study, *SPP1* gene expression was found to be significantly increased in KIRP tissues compared with normal kidney tissues. Data from the GEPIA and UALCAN platforms showed consistent results, with *SPP1* expression in KIRP tumors more than double that in normal tissues, a statistically significant difference (p < 0.01) (18, 23). Additional analysis from the GTEx Portal showed that *SPP1* had relatively high expression levels in both kidney cortex and kidney medulla tissues (24). This confirms that the increase in *SPP1* in KIRP is not simply a result of physiological variability but rather reflects specific molecular deregulation in tumor tissues. *SPP1*, as a multifunctional glycoprotein, is known to be involved in a number of important biological processes, including cell adhesion, migration, extracellular matrix remodeling, and modulation of the immune response in the tumor microenvironment (25). Overexpression of *SPP1* in KIRP can be assumed to enhance tumor aggressiveness through activation of pro-inflammatory and pro-metastatic pathways, accelerate local tissue invasion, and support the formation of distant metastases (26). This is in line with data on various other cancers, such as breast, lung, and liver cancer, where *SPP1* functions as a major

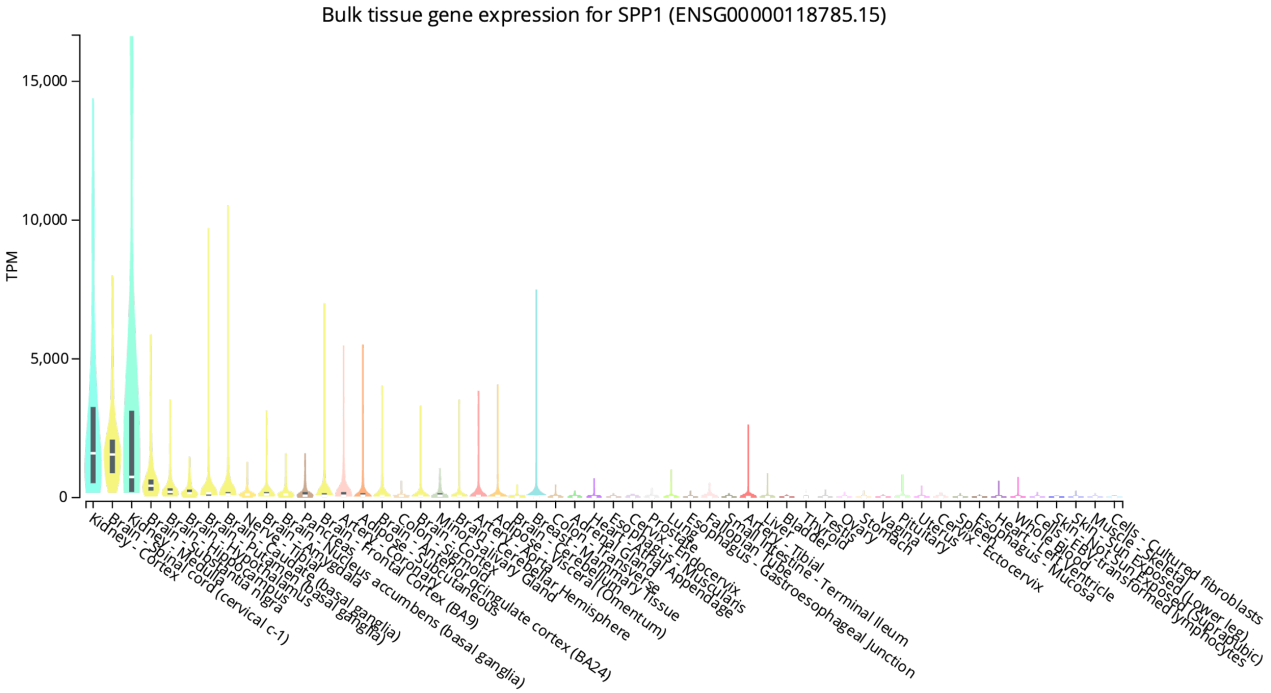

Figure 6. Distribution of *SPP1* gene expression in various normal human tissues based on data from the GTEx portal

mediator of tumor phenotype changes towards a more invasive direction. Clinically, KIRP demonstrates variable outcomes. While early-stage KIRP is often associated with favorable prognosis, advanced-stage disease suggests a markedly worse outcome, with reported 5-year survival rates as low as 40–50%. Population-based data also indicate that KIRP contributes significantly to renal cancer-related mortality, particularly in patients with metastatic or treatment-resistant disease. Moreover, the relatively poor response of KIRP to conventional targeted therapy and immunotherapy further underscores its clinical aggressiveness in advanced settings. In this context, the identification of prognostic biomarkers such as *SPP1* may be particularly valuable, as they could help refine risk stratification, better predict therapeutic response, and ultimately improve clinical decision-making in patients with KIRP (27).

Interestingly, we observed a discrepancy between the results obtained from GEPIA and UALCAN. While GEPIA analysis indicated that high *SPP1* expression was significantly associated with worse OS, the UALCAN platform showed a similar trend but without statistical significance in the overall cohort. Several factors may underlie this inconsistency. First, cohort composition and sample size differ between the two platforms: GEPIA integrates TCGA and GTEx datasets, resulting in a broader and more heterogeneous cohort, whereas UALCAN relies solely on TCGA-KIRP data, which may reduce statistical power. Second, differences in statistical methods are likely contributors: GEPIA applies log-rank tests with median cutoffs for survival group stratification, while UALCAN employs χ^2-based log-rank statistics with automatic subgrouping, which can influence outcome significance. Third, data normalization and processing pipelines vary between platforms. GEPIA uses an integrated normalization strategy across TCGA and GTEx, while UALCAN utilizes level 3 TCGA RNA-seq data processed by its own pipeline. These differences may lead to subtle variations in expression quantification and survival estimates. Acknowledging these platform-specific discrepancies is important, as it emphasizes the need for multi-cohort validation and highlights that survival associations should be interpreted with caution unless replicated across independent datasets. Next, the relationship between *SPP1* expression levels and clinical prognosis of KIRP patients was explored through GEPIA and UALCAN-based Kaplan-Meier analysis. The results of GEPIA showed that patients with high *SPP1* expression had worse OS than those with low expression, with a $p < 0.05$. This indicates that *SPP1* may serve as a negative prognostic biomarker. However, the results of UALCAN, although showing a similar trend, did not reach statistical significance overall ($p = 0.36$). Interestingly, when strati-

fied by race, high *SPP1* expression in Caucasian patients showed a significant association with worse outcomes (p = 0.045). Collectively, these observations indicate that our race-specific findings from UALCAN align with known epidemiologic and outcome disparities in RCC, reinforcing the need for race-aware validation of *SPP1* as a prognostic biomarker in KIRP. Population heterogeneity in KIRP outcomes may partly reflect genetic differences. For example, MET alterations and FH mutations, which drive papillary RCC subtypes, occur with variable frequency across populations, while APOL1 risk variants—common in individuals of African ancestry—have been associated with poorer renal outcomes. These findings highlight the importance of validating prognostic biomarkers such as *SPP1* in multi-ethnic cohorts. Further analysis based on patient gender (Figure 5C) found no significant difference in survival. Taken together, these findings suggest that high *SPP1* expression may serve as a negative prognostic marker in KIRP. The GEPIA results demonstrated statistical significance for overall survival, likely reflecting the larger integrated cohort and higher statistical power achieved by combining TCGA and GTEx data. By contrast, UALCAN did not show significance in the overall analysis, but its subgroup stratification (e.g., by race) revealed clinically meaningful differences, particularly in Caucasian patients. This indicates that while GEPIA may provide stronger statistical evidence of association, UALCAN highlights population-specific heterogeneity that could be clinically relevant. Therefore, both platforms are complementary: GEPIA supports the general prognostic role of *SPP1* in KIRP, whereas UALCAN underscores the importance of considering patient demographics and molecular diversity when interpreting prognostic biomarkers. These insights strengthen the significance of *SPP1* expression, not only as a potential universal biomarker but also as a candidate for personalized prognostic evaluation in specific subgroups of KIRP patients.

These results underscore the importance of considering genetic or ethnic background variables in the interpretation of molecular biomarkers. Genetic factors underlying population heterogeneity may modulate tumor responses to *SPP1* expression or affect its downstream signaling pathways. Meanwhile, analysis based on patient gender and weight showed no significant association, indicating that the influence of *SPP1* on prognosis seems to be more intrinsic to the tumor rather than modified by external factors such as hormonal or metabolic (28). Overall, these findings place *SPP1* as a potential prognostic biomarker candidate in KIRP, although further validation with a larger cohort and multivariate analysis is needed to strengthen its application in clinical practice (29).

Furthermore, gene co-expression analysis showed that *SPP1* forms a close molecular expression network with several other genes that have relevant biological functions in cancer progression. *SESTD1* , AKIRIN2, *LAMC1*, FAS, and *SESTD1* genes showed high PCC with *SPP1*, indicating involvement in similar biological pathways. *SESTD1* is associated with transcriptional regulation and hematopoiesis, which may contribute to the dynamics of tumor cell proliferation. *LAMC1*, as part of the laminin gamma chain, plays a role in cell interaction with the extracellular matrix and has been associated with increased migration and cancer invasion in various tumor types. Co-expression of *SPP1* with FAS, a master regulator of apoptosis, suggests potential involvement in evasion of programmed cell death, a critical mechanism in the development of therapy-resistant tumors (30). Furthermore, co-expression with *AKIRIN2* and *SESTD1* extends the indication that *SPP1* may be involved in the regulation of inflammatory signals and remodeling of the cell cytoskeleton. The integration of these data makes it clear that *SPP1* does not act alone, but rather is part of a complex molecular network that regulates the aggressive phenotype of KIRP. These findings open up opportunities to develop combination-based therapeutic strategies, targeting not only *SPP1*, but also critical co-expression pathways that may enhance the efficacy of molecular interventions against papillary renal cancer.

CONCLUSIONS

This study showed that *SPP1* was significantly more highly expressed in KIRP tissues compared to normal kidney tissues, based on GEPIA and UALCAN analysis, and supported by GTEx data showing low *SPP1* expression in healthy kidneys.

SPP1 overexpression was associated with worse clinical prognosis, especially in Caucasian patients, while there was no significant difference based on gender or body weight. Gene expression correlation analysis identified ten genes with the highest co-expression with *SPP1*, namely, *SESTD1* , AKIRIN2, *YIPF1*, *SESTD1*, *LAMC1*, FAS, *SESTD1*, *MTHFD1L*, ANXA2P2, and *ARHGAP29*, which may possibly play a role in cell adhesion, migration, extracellular matrix remodeling, and resistance to apoptosis pathways. Overall, these findings confirm that *SPP1* has strong potential as a diagnostic biomarker, prognostic biomarker, and molecular therapeutic target in the management of KIRP.

ACKNOWLEDGMENTS

The authors gratefully acknowledge the support from Alma Ata University, Yogyakarta, Indonesia.

FUNDING

The authors have no funding to report.

CONFLICTS OF INTEREST

The authors declare no conflicts of interest regarding the publication of this paper.

AUTHOR CONTRIBUTIONS

D.P.A.: conceptualization, methodology, writing – review & editing; R.I.P.: data curation, writing – original draft preparation; M.S.B.: formal analysis, software, validation, resources; D.E.: formal analysis; R.I.P.: visualization, investigation; D.E.: Visualization, Investigation; D.P.A.: supervision, project administration, funding acquisition;

All authors have read and agreed to the published version of the manuscript.

DATA AVAILABILITY STATEMENT

All datasets analyzed in this study are publicly available from GEPIA (http://gepia.cancer-pku.cn), UALCAN (https://ualcan.path.uab.edu), and the GTEx Portal (https://gtexportal.org).

INSTITUTIONAL REVIEW BOARD STATEMENT

This study used publicly available datasets containing de-identified patient information. Therefore, ethical approval was not required. The study complies with the Declaration of Helsinki principles for ethical research.

INFORMED CONSENT STATEMENT

Patient consent was waived because the study used publicly available de-identified datasets.

REFERENCES

1. Colavita JPM, Todaro JS, de Sousa M, May M, Gómez N, Yaneff A, et al. Multidrug resistance protein 4 (MRP4/ABCC4) is overexpressed in clear cell renal cell carcinoma (ccRCC) and is essential to regulate cell proliferation. Int J Biol Macromol. 2020;161:836-47.
2. Xie W, Zhang Y, Zhang Z, Li Q, Tao L, Zhang R. ISG15 promotes tumor progression via IL6/JAK2/STAT3 signaling pathway in ccRCC. Clin Exp Med. 2024; 24:140. PubMed PMID: 38951255
3. Wang B, Li M, Li R. Identification and verification of prognostic cancer subtype based on multi-omics analysis for kidney renal papillary cell carcinoma. Front Oncol. 2023;13:1169395. PubMed PMID: 37091151
4. Liu K, Hu H, Jiang H, Liu C, Zhang H, Gong S, et al. Upregulation of secreted phosphoprotein 1 affects malignant progression, prognosis, and resistance to cetuximab via the KRAS/MEK pathway in head and neck cancer. Mol Carcinog. 2020;59:1147-158.
5. Hsu LC, Li CJ, Lin LT, Pan LF, Wen ZH, Sheu JJ, et al. Multi-omics reveals the role of osteopontin/secreted phosphoprotein 1 in regulating ovarian aging. J Pers Med. 2024;14:78. PubMed PMID: 38248779
6. Zhang Z, Liu B, Lin Z, Mei L, Chen R, Li Z. *SPP1* could be an immunological and prognostic biomarker: From pan-cancer comprehensive analysis to osteosarcoma validation. FASEB J. 2024;38(14):e23783. PubMed PMID: 39037571
7. Zhao G, Wang Y, Zhou J, Ma P, Wang S, Li N. Pan-cancer analysis of polo-like kinase family genes reveals polo-like kinase 1 as a novel oncogene in kidney renal papillary cell carcinoma. Heliyon. 2024 Apr 9;10(8):e29373. PubMed PMID: 38644836
8. Guo Z, Huang J, Wang Y, Liu XP, Li W, Yao J, et al. Analysis of expression and its clinical significance of the secreted phosphoprotein 1 in lung adenocarcinoma. Front Genet. 2020;11:547. PubMed PMID: 32595698
9. Zheng Y, Hao S, Xiang C, Han Y, Shang Y, Zhen Q, et al. The correlation between *SPP1* and immune escape of EGFR mutant lung adenocarcinoma was explored by bioinformatics analysis. Front Oncol. 2021;11:592854. PubMed PMID: 34178613
10. Wang J, Hao F, Fei X, Chen Y. *SPP1* functions as an enhancer of cell growth in hepatocellular carcinoma targeted by miR-181c. Am J Transl Res. 2019;11:6924-37.
11. Nedjadi T, Ahmed ME, Ansari HR, Aouabdi S, Al-Maghrabi J. Identification of *SPP1* as a prognostic biomarker and immune cells modulator in urothelial bladder cancer: a bioinformatics analysis. Cancers (Basel). 2023 Dec 4;15(23):5704. PubMed PMID: 38067407
12. Li S, Yang R, Sun X, Miao S, Lu T, Wang Y, et al. Identification of *SPP1* as a promising biomarker to predict clinical outcome of lung adenocarcinoma individuals.

Gene. 2018;679:398-404. PubMed PMID: 30240883
13. Amukti DP, Wazni AR, Irham LM, Sulistyani N, Ma'ruf M, Adikusuma W, et al. Identifying pathogenic variants associated with Alzeimer by integrating genomic databases and bioinformatics approaches. InE3S Web of Conferences 2024 (Vol. 501, p. 01021). EDP Sciences.
14. Irham LM, Adikusuma W, La'ah AS, Chong R, Septama AW, Angelina M. Leveraging Genomic and Bioinformatic Analysis to Enhance Drug Repositioning for Dermatomyositis. Bioengineering (Basel).2023;10(8):890. PubMed PMID: 37627776
15. Li C, Tang Z, Zhang W, Ye Z, Liu F. GEPIA2021: integrating multiple deconvolution-based analysis into GEPIA. Nucleic Acids Res. 2021;49(W1):W242-W246. PubMed PMID: 34050758
16. Tang Z, Li C, Kang B, Gao G, Li C, Zhang Z. GEPIA: a web server for cancer and normal gene expression profiling and interactive analyses. Nucleic Acids Res. 2017;45(W1):W98-W102. PubMed PMID: 28407145
17. Chandrashekar DS, Karthikeyan SK, Korla PK, Patel H, Shovon AR, Athar M, et al. UALCAN: An update to the integrated cancer data analysis platform. Neoplasia. 2022;25:18-27.
18. Chandrashekar DS, Bashel B, Balasubramanya SAH, Creighton CJ, Ponce-Rodriguez I, Chakravarthi BVSK, et al. UALCAN: A portal for facilitating tumor subgroup gene expression and survival analyses. Neoplasia. 2017;19:649-58.
19. Humolungo DT, Anjani R, Irham LM, Sulistyani N, Ma'ruf M, Amukti DP, et al. Identification of pathogenic gene variants in carpal tunnel syndrome using bioinformatics approaches. InE3S Web of Conferences 2024 (Vol. 501, p. 01022). EDP Sciences.
20. Gumelar G, Ulfa MM, Amukti DP, Irham LM, Yuliani S, Adikusuma W, et al. Harnessing genomic and bioinformatic data to broaden understanding of leukaemia across continents. Scripta Medica (Banja Luka). 2024;55:717–25.
21. Irham LM, Amukti DP, Adikusuma W, Singh D, Chong R, Basyuni M, et al. Applied of bioinformatics in drug discovery and drug development: bioinformatic analysis 1996-2024. In: BIO Web of Conferences. EDP Sciences; 2025.
22. Irham LM, Amukti DP, Adikusuma W, Singh D, Chong R, Basyuni M, et al. Applied of bioinformatics in drug discovery and drug development: bioinformatic analysis 1996-2024. In: BIO Web of Conferences. EDP Sciences; 2025.
23. Tang Z, Kang B, Li C, Chen T, Zhang Z. GEPIA2: an enhanced web server for large-scale expression profiling and interactive analysis. Nucleic Acids Res. 2019 Jul 2;47(W1):W556-W560. PubMed PMID: 31114875
24. Irham LM, Amukti DP, Adikusuma W, Singh D, Chong R, Pranata S, et al. Trends in drug repurposing for chronic hepatitis-B infection:bibliometric-basedapproach1990-2024. In: BIO Web of Conferences. EDP Sciences; 2025.
25. Liu Y, Cheng X, Xi P, Zhang Z, Sun T, Gong B. Bioinformatic analysis highlights SNHG6 as a putative prognostic biomarker for kidney renal papillary cell carcinoma. BMC Urol. 2023;23(1):54. PubMed PMID: 37004005
26. Sun G, Shang Z, Liu W. *SPP1* regulates radiotherapy sensitivity of gastric adenocarcinoma via the Wnt/Beta-Catenin pathway. J Oncol. 2021;2021:1642852. PubMed PMID: 34367279
27. Chen K, Li Y, Ni J, Yang X, Zhou Y, Pang Y, et al. Identification of a novel subtype of *SPP1*+ macrophages expressing SIRPα: implications for tumor immune evasion and treatment response prediction. Exp Hematol Oncol. 2024;13(1):119. PubMed PMID: 39696410
28. Zhao K, Ma Z, Zhang W. Comprehensive analysis to identify *SPP1* as a prognostic biomarker in cervical cancer. Front Genet. 2022;12:732822. PubMed PMID
29. Xu X, Lin J, Wang J, Wang Y, Zhu Y, Wang J, et al. *SPP1* expression indicates outcome of immunotherapy plus tyrosine kinase inhibition in advanced renal cell carcinoma. Hum Vaccin Immunother. 2024 Dec 31;20(1):2350101. PubMed PMID: 38738709
30. Zhang Y, Du W, Chen Z, Xiang C. Upregulation of PD-L1 by *SPP1* mediates macrophage polarization and facilitates immune escape in lung adenocarcinoma. Exp Cell Res. 2017;359:449-57. PubMed PMID: 28830685.

Biomedical Sciences and Clinical Medicine 2026;65(1):111-118.
doi: 10.12982/BSCM.2026.14
https://he01.tci-thaijo.org/index.php/CMMJ-MedCMJ/index

BSCM
Biomedical Sciences and Clinical Medicine

Original Article

Open Access

Next-Generation Dental Bone Implants – Sustainable 3D Nanostructures Derived from Animal By-Products: A Preliminary Study

Vajpayee Kritika and Rethinam Senthil

Department of Pharmacology, Saveetha Dental College and Hospitals, Saveetha Institute of Medical and Technical Sciences (SIMATS), Saveetha University, Chennai, Tamilnadu, India

Correspondence:
Rethinam Senthil, PhD,
Department of Pharmacology,
Saveetha Dental College and Hospitals, Saveetha Institute of Medical and Technical Sciences (SIMATS), Saveetha University,
Chennai-600 077, Tamilnadu,
India.
E-mail: senthilbiop@gmail.com

Received: December 20, 2024;
Revised: September 11, 2025;
Accepted: September 15, 2025

ABSTRACT

OBJECTIVE The development of next-generation dental bone implants focuses on sustainable, bioactive materials derived from animal by products, offering a cost-effective and eco-friendly alternative for bone regeneration. This study explores the fabrication of a 3D nano-structured dental implant (3D-DI) using fish bone collagen (FBC) and fibrin nanoparticles (FN), chosen for their excellent biocompatibility, bioactivity, and availability.

METHODS FBC and FN scaffolds were synthesized and incorporated into an implant framework. Fourier-transform infrared spectroscopy (FTIR) analysis confirmed the presence of bioactive functional groups. High-resolution scanning electron microscopy (HRSEM) characterized the porous microstructure (100–500 nm) as conducive to cell adhesion and proliferation. *In-vitro* cytotoxicity (MTT assay) and cell viability (live cell staining) were evaluated using MG63 osteoblast-like cells.

RESULTS The 3D-DI demonstrated significant bioactivity after 14 days in simulated body fluid (SBF), with a mineralization rate of 68% ($p < 0.01$). MG63 cell viability increased to 85% after 72 hours ($p < 0.05$) (ANOVA using Microsoft Excel Office 2013), indicating excellent biocompatibility. Mechanical testing showed compressive strength of 83.41 ± 0.56 MPa and tensile strength of 76.83 ± 0.81 MPa suitable for load-bearing dental and orthopedic applications ($p < 0.05$).

CONCLUSIONS This study presents a novel approach for transforming animal waste into sustainable, bioactive dental bone implants, offering an eco-friendly alternative to conventional graft materials. Unlike previous reports that primarily focus on single-component or synthetic scaffolds, 3D-DI exhibits superior mechanical strength, enhanced mineralization, and excellent biocompatibility. These unique properties highlight its potential for load-bearing dental and orthopedic applications, addressing the current gap in development of cost-effective, high-performance biomaterials from bio-waste sources.

KEYWORDS dental implant, 3D structure, bioactive, biocompatibility, animal by-Producs

INTRODUCTION

When a person with good general oral health loses one or more teeth due to periodontal disease, trauma, or other causes, dental implants are a good solution. Surgically placed in the jaw bone (also known as surgically traumatized bone) beneath the gums, dental implants—sometimes referred to as artificial tooth roots—can support an artificial crown in the absence of natural teeth (1).

Used to support an artificial crown in the absence of natural teeth, dental implants—also referred to as artificial tooth roots—are biocompatible metal anchors that are surgically placed in the jaw bone or surgically damaged bone behind the gums. Failures of implant integration continue to occur and are challenging to predict even with their widespread clinical use. Because of the fierce and intense competition between dental surgeons and implant manufacturers, it is challenging to estimate dental implant success rates with any degree of accuracy (2).

The mechanical environment is changed when one or more implants are surgically inserted into the mandible. In reaction to implant implantation and loading, bone remodels internally, rearranging its structure as described by Wolff's law (3). Most current biomechanical research assumes 100% bone–implant contact, which overlooks the possibility of full contact between the implant and the bone. Implant surface topography and bone quality which are routinely observed in clinical settings are just two of the variables that affect the relationship between the implant and the surrounding bone (4-6).

The marine food product industry uses its waste to create higher-value biomaterials. Numerous products derived from processed fish waste have been used in diverse applications, including animal feed, collagen, chitosan, natural colors, biodiesel/biogas, and bone implants. Collagen makes up the majority of the protein in bones, while hydroxyapatite bone minerals are also abundant. Plate-like tiny crystals of hydroxyapatite (HA) are implanted in collagen, which serves as a structural framework, strengthening the bone (7, 8). Muntean et al. (9) present a comprehensive review of the production and characteristics of mollusk shell–derived hydroxyapatite, highlighting its bioactivity, osteoconductivity, sustainability, and potential for dental implant coatings and bone graft substitutes.

The aim of this investigation was to synthesize a 3D nano-structured dental implant (3D-DI) from biowaste. Using fourier-transform infrared spectroscopy (FTIR), thermogravimetric analysis (TGA), and high resolution scanning electron microscopy (HRSEM), the BI produced was evaluated for its physicochemical properties. An *in-vitro* study of 3D-DI was conducted using MG63 osteoblast-like cell lines.

METHODS

Preparation of fish bone collagen (FBC)

Fish bone waste was obtained from a local fish market (Vanagaram, Chennai, Tamil Nadu 600095) for use in the present study. The bone portion was then removed and cleaned. Later, the fishbone was defatted by treating it with acetone and ethanol. The bones were cut into small-sized pieces and then demineralized using 2N HCI followed by H_2O_2 treatment. The samples were washed thoroughly with cold distilled water and ground to form a paste. The resultant fine paste was subjected to centrifugation (8,000-10,000 rpm). The supernatant was collected and its pH was adjusted to the required level. The supernatant was then further centrifuged at 12,000 rpm.

Preparation of fibrin nanoparticles (FN)

Bovine blood collected from a municipal slaughterhouse was stirred well using a glass rod to obtain fibrin which was then washed with distilled water and incubated in 0.5M sodium acetate and 30% hydrogen peroxide. The fibrin was then washed with distilled water, ground using a mortar and pestle (mechanical homogenizer), and stored at −20 °C. The fibrin was then treated with NaOH, to make a clear, yellow-colored solution which was treated with HCL under vigorous stirring at the required pH and the resultant formation of fibrin nanoparticles.

Preparation of 3D dental implant (3D-DI)

3D-DI was prepared by mixing FBC, FN, calcium carbonate and biopolymer gelatin in a ratio of 5:1:8:0.5 by weight. The resultant mixture was packed into a glass tube and extruded with a suitable glass rod. The cylindrical implant formed was cut into the required length and cured at 30°C for 12 h then at 100°C for 4-5 h. Computer-aided

design (CAD) software was used with the dried material to model the 3D structure of the implant.

RESULTS

Physicochemical properties

UV-Vis spectroscopy is a valuable method for determining the existence and optical characteristics of FN (Figure 1A). FN typically shows a characteristic absorption peak in the UV area, indicating its proteinaceous nature. This peak often appears between 270 nm and 290 nm, demonstrating the absorption of aromatic amino acids such as tyrosine, tryptophan, and phenylalanine, which are important components of fibrin proteins. The strength and position of the peak can confirm the effective creation of fibrin nanoparticles while also providing information on their concentration, purity, and potential for aggregation. Furthermore, any shifts in the peak position could suggest changes in the structural conformation or interactions with other components in a composite system. The FTIR spectrum was used to examine and identify the functional groups in the samples, as illustrated in Figure 1B and C. The FN exhibited a peak of around 2,600 cm^{-1}, showing the presence of particular linkages associated to protein structures, likely linked to N-H stretching vibrations. This indicates the fibrin's contribution to the total bioactivity of the composite material. These peaks reflect each component's own chemical signatures, providing information on their composition and functional properties, which are critical for their roles in bioactive bone implants. Furthermore, collagen sample FTIR spectra showed a peak of about 1,300 cm^{-1}, which corresponds to the bending vibrations of C-H bonds and amide III bands, confirming the existence of collagen-specific functional groups.

Figure 2A shows the FTIR analysis of 3D-DI. The 3D-DI exhibited a strong absorption band at 2,200 cm^{-1}, indicating stretching vibrations

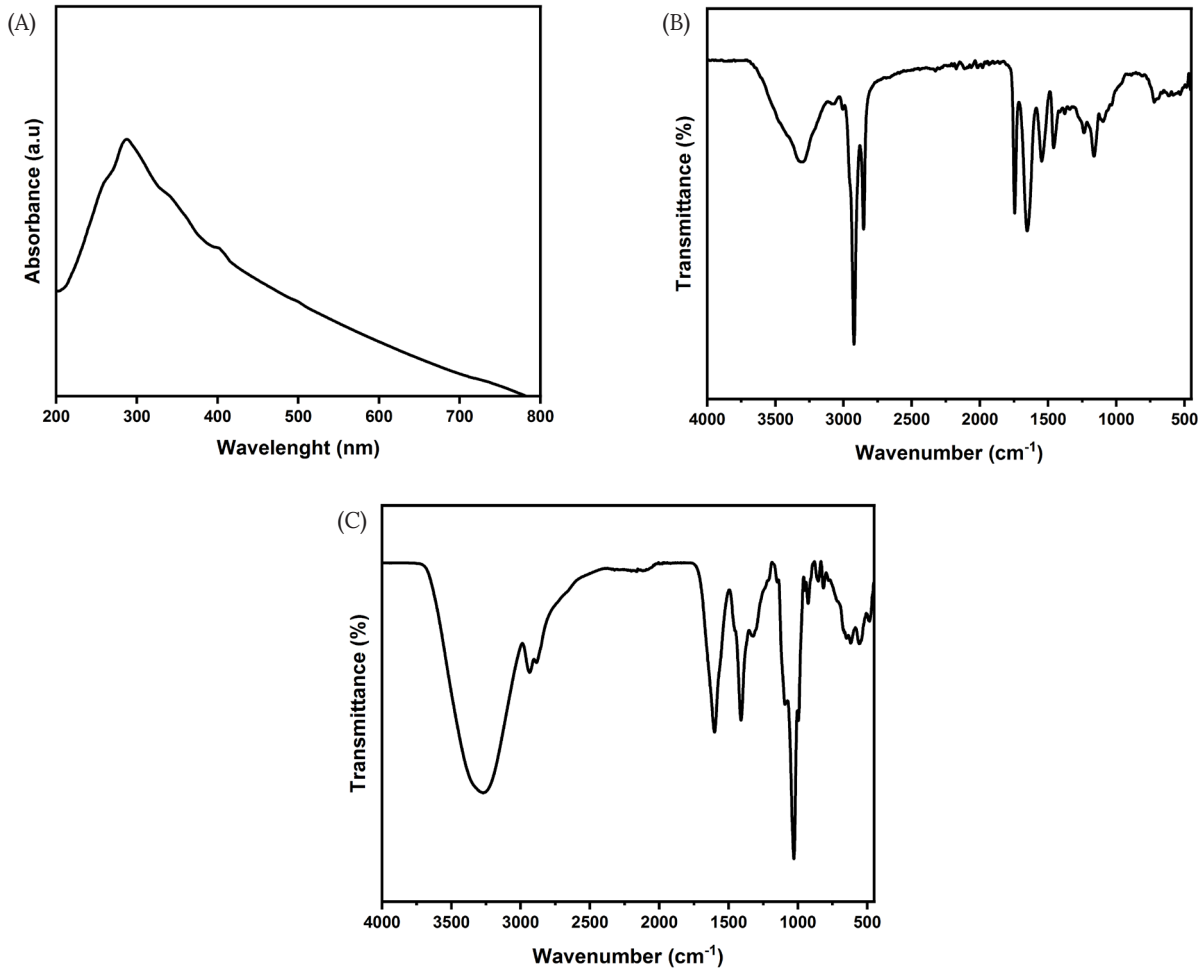

Figure 1. (A) UV-Vis spectroscopy analysis of fibrin nanoparticles, (B) Fourier transform infrared spectroscopy of fibrin nanoparticles, (C) Fourier transform infrared spectroscopy analysis of fish bone collagen

of carbonyl (C = O) or other organic functional groups. These vibrations are critical for the implant's structural stability. Figure 2B shows the thermal stability of a 3D-DI made of collagen, fibrin nanoparticles, and calcium carbonate. TGA was utilized to determine the material's stability. Moisture evaporation causes initial weight loss at lower temperatures, whereas collagen and fibrin degradation causes significant weight loss between 250°C and 350°C. The final degradation happens above 500°C, which corresponds to the breakdown of calcium carbonate. The 3D-DI has exceptional temperature stability, making it appropriate for biomedical applications. Figure 2C depicts the surface morphology of a 3D-DI made of collagen, fibrin nano-particles, and calcium carbonate. This material was thoroughly examined using HRSEM to gain a better understanding of its microstructure. The HRSEM images show a highly porous architecture with linked nano-sized pores that promote cell adhesion and nutrient exchange, both of which are important for bone tissue regeneration. The collagen component adds flexibility, and the fibrin nanoparticles improve bioactivity and cell interactions. The addition of calcium carbonate increases the scaffold's osteoconductivity, which promotes bone mineralization. The homogeneous distribution of these components inside the 3D matrix maintains structural integrity, allowing the implant to replicate natural bone tissue, encouraging faster integration and healing in the dental setting.

The mechanical properties of a 3D-DI made of FBC, FC, and calcium carbonate were assessed in terms of tensile strength, compressive strength, and water permeability. The collagen-based implant's tensile strength was 76.83 ± 0.81 MPa, demonstrating that it can sustain stretching pressures. The 3D-DI compressive strength (83.41 ± 0.56 MPa) indicates its resistance to compres-

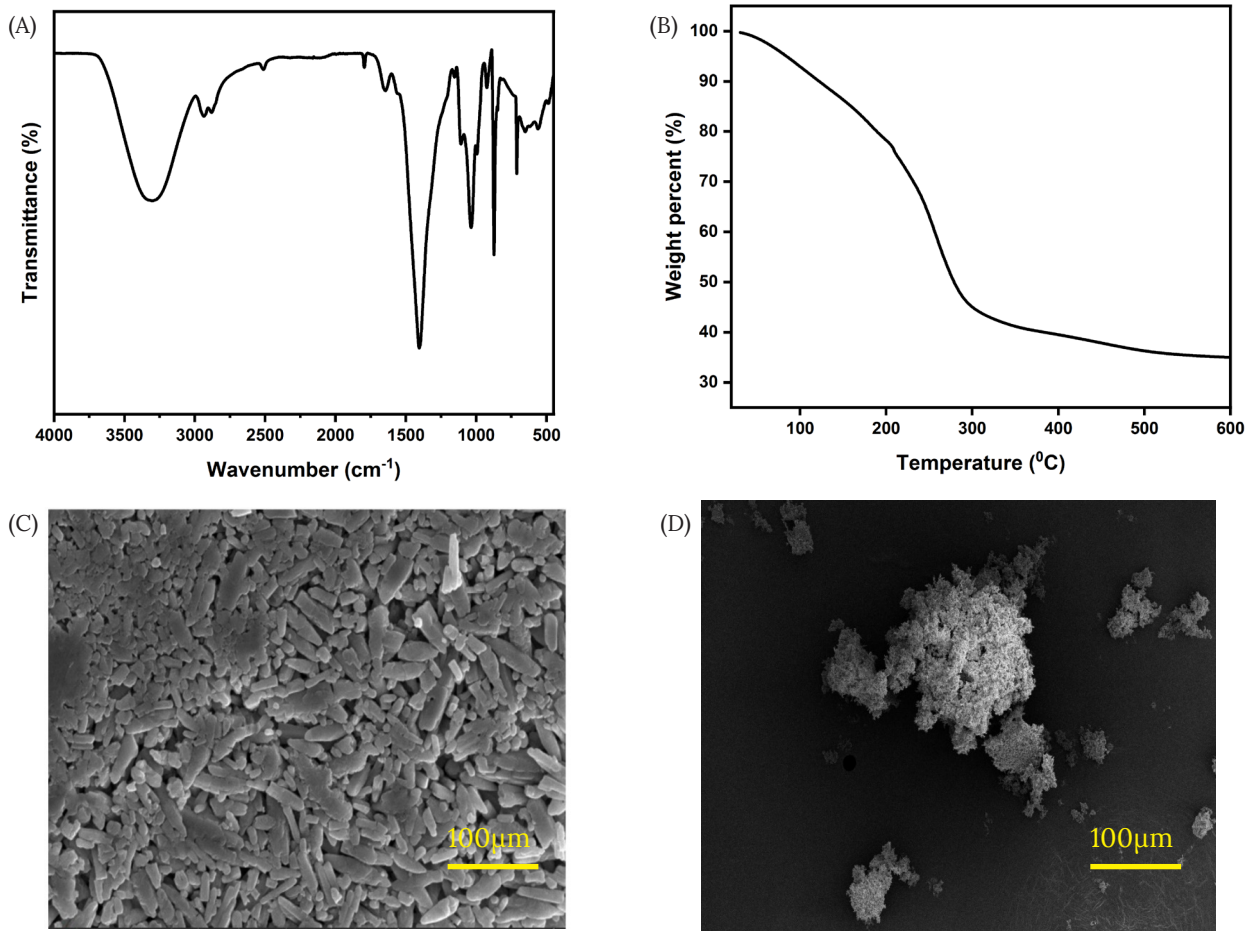

Figure 2. (A) Fourier transform infrared spectrum of 3D-DI, (B) thermogravimetric analysis curve of 3D-DI, (C) high resolution scanning electron microscope image of 3D-DI, (D) high resolution scanning electron microscope picture of 3D-DI after simulated bodily fluid treatment

sion, which is important for bone growth. The water absorption capacity (27.34 ± 1.65%) shows its ability to retain moisture, which is crucial for hydration and biocompatibility.

Bioactivity test

The bioactivity of the 3D-DI, composed of FBC, FN, and calcium carbonate as demonstrated in HRSEM is shown in Figure 2D. The implant was tested in phosphate buffer solution (PBS) to evaluate its ability to support mineral deposition, which is crucial for bone regeneration. During the test, the material was immersed in PBS to simulate physiological conditions, and its interaction with the solution was monitored over time. The formation of hydroxyapatite-like layers on the surface of the implant, indicated by mineral deposits, confirms its bioactivity. This suggests that the collagen and fibrin nanoparticles promote cell interaction, while the calcium carbonate enhances osteoconductivity, encouraging bone-like mineral formation. The bioactivity test highlights the material's potential for effective bone regeneration in dental applications.

***In-vitro* analysis**

Figure 3A shows the *in-vitro* evaluation of the control and 3D-DI sample. The 3D-DI was evaluated on the MG63 osteoblast-like cell line to determine its biocompatibility and ability to promote cell growth. The cells were cultivated on both the control and 3D-DI surfaces to determine how they affected cell attachment, growth, and viability at 48 and 78 h. The results show that the 3D-DI improved cell adhesion and proliferation, indicating that it has bioactive qualities and is suitable for bone tissue engineering. The combination of collagen and fibrin created a favorable environment for cell contact, whereas calcium carbonate increased osteoconductivity, which is required for bone repair. This *in-vitro* investigation verifies the implant's suitability for dental bone restoration. The fluorescence surface morphology images show in 3D-DI and control interacts with cells (Figure 3B). Fluorescence microscopy was utilized to investigate the adhesion and dispersion of MG63 cells on the 3D-DI surface. The fluorescently marked cells enabled easy identification of cell shape, spreading, and density across the implant. The image shows evenly distributed cells adhering to the porous

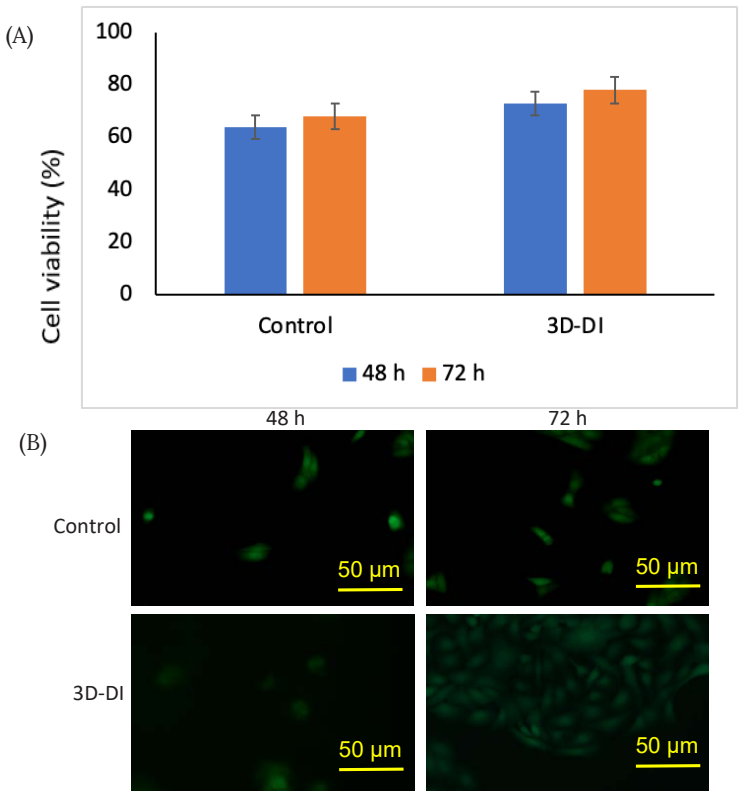

Figure 3. (A) MTT assay showing the viability of MG-63 cells for the control and 3D-DI groups. (BS) Fluorescence micrographs (20X) of MG-63 cells cultured for 48 and 72 hours.

structure, demonstrating efficient cell infiltration and interaction with the FBC, FN, and calcium carbonate components. The fluorescent signal shows cytoskeletal structure, implying that the implant facilitates cell adhesion and proliferation. These findings confirm the 3D-DI potential for bone tissue regeneration by demonstrating its biocompatibility and ability to enable cellular integration.

DISCUSSION

The complete assessment of the 3D-DI demonstrates its remarkable potential for bone regeneration. The UV-Vis spectroscopy study of FN proved its proteinaceous composition by revealing typical absorption peaks, indicating effective nanoparticle production (10). FTIR spectra revealed information about the chemical structures of collagen, fibrin, and calcium carbonate, indicating the presence of functional groups required for bioactivity and stability. The characteristic peaks of each material component, particularly the amide III bands in collagen and the N-H stretching in fibrin, contribute to the composite implant's overall structural integrity and biofunctionality (11, 12). HRSEM and fluorescent microscopy revealed the implant's highly porous design, which promotes effective cell attachment and interaction. This porosity is vital for cell infiltration and nutrition exchange, both of which are necessary for bone tissue repair. The equally distributed cells seen in fluorescence pictures indicate that the implant's material composition, notably the fibrin nanoparticles and collagen, supports cellular proliferation and integration (13, 14).

The bioactivity and thermal stability tests confirmed the implant's ability to enable bone-like mineral formation and to endure physiological circumstances. The creation of hydroxyapatite-like layers on the implant's surface following immersion in PBS proved its osteoconductivity, which was caused by calcium carbonate's contribution to mineralization (15). TGA revealed that the implant can maintain structural integrity at a variety of temperatures, assuring its suitability for biological purposes. *In-vitro* testing employing the MG63 cell line confirmed the implant's biocompatibility, with results indicating increased cell growth and adherence compared to control samples. These findings indicate that the combination of collagen, fibrin nanoparticles, and calcium carbonate provides an optimal environment for osteoblast function, making this 3D-DI a promising candidate for clinical usage in bone tissue engineering and dental repair.

The remarkable performance of the 3D-DI composite aligns well with prior research showing that fibrin-based scaffolds—especially when combined with osteoconductive bioceramics—enhance osteoblast adhesion, proliferation, and differentiation, acting as both a provisional matrix and a delivery platform for bioactive molecules (16). Likewise, nanostructured collagen scaffolds with high porosity and inorganic components have been shown to mimic native bone architecture, facilitating cell migration, mineral deposition, and mechanical integration *in-vivo* (17). These outcomes—demonstrating hydroxyapatite-like mineral formation, robust structural stability, and favorable MG63 osteoblast responses—further substantiate the applicability of the 3D-DI as a biomimetic and efficient scaffold for bone regeneration.

This discussion highlights the promising potential of the 3D-DI synthesized using FBC, FN, and calcium carbonate. The physicochemical characterization confirmed the retention of critical functional groups, thermal stability, and a highly porous architecture that enhances cell adhesion, nutrient exchange, and osteoconductivity. The excellent mechanical properties, including tensile and compressive strength, make the implant suitable for load-bearing dental applications, mimicking the natural strength and flexibility of bone tissue. Bioactivity analysis demonstrated the formation of hydroxyapatite-like deposits, indicating the implant's capability to support mineralization, which is essential for bone regeneration. *In-vitro* studies using the MG63 osteoblast-like cell line confirmed enhanced cell adhesion, proliferation, and biocompatibility, underscoring the scaffold's suitability for bone tissue engineering. The combination of FBC and FN created a bioactive environment conducive to cellular interactions, while calcium carbonate promoted osteogenic responses. These results confirm 3D-DI as an eco-friendly, cost-effective, and biocompatible alternative to conventional implants, addressing critical clinical needs in bone repair and paving the way for sustainable regenerative dentistry solutions.

CONCLUSIONS

The 3D-DI, made of FBC, FN, and calcium carbonate, shows great promise for bone tissue regeneration. The material's bioactivity was demonstrated by mineral deposition in simulated bodily fluid, and its biocompatibility and ability to induce cell proliferation were established using MG63 cell cultures. Structural study with FTIR, HRSEM, and fluorescence microscopy revealed a highly porous, stable implant that promotes cell adhesion and proliferation. The implant's heat stability enhances its usefulness for biomedical applications. Overall, the study demonstrates the implant's potential for dental bone regeneration and regenerative medicine.

ACKNOWLEDGMENTS

None

FUNDING

This research received no specific grant from any funding agency in the public, commercial, or not-for-profit sectors.

CONFLICT OF INTEREST

The authors have no conflicts of interest to report.

AUTHOR CONTRIBUTION

V.K.: methodology, software; R.S.: conceptualization, methodology, software, supervision , writing – review & editing.

All authors have read and agreed to the published version of the manuscript."

DATA AVAILABILITY STATEMENT

All data generated or analyzed during this study are included in this published article

INSTITUTIONAL REVIEW BOARD STATEMENT

This study did not involve any experiments on human participants or animals, and therefore, Institutional Review Board approval was not required. All experimental procedures were performed using in vitro and material-based methods.

INFORMED CONSENT STATEMENT

Not under consideration for publication elsewhere

REFERENCES

1. Kochar SP, Reche A, Paul P. The Etiology and Management of Dental Implant Failure: A Review. Cureus. 2022;14:e30455. PubMed PMID: 36415394.
2. Dutta SR, Passi D, Singh P, Atri M, Mohan S, Sharma A. Risks and complications associated with dental implant failure: Critical update. Natl J Maxillofac Surg. 2020;11:14-9.
3. Chavarri-Prado D, Brizuela-Velasco A, Álvarez-Arenal Á, Dieguez-Pereira M, Pérez-Pevida E, Viteri-Agustín I, et al. The bone buttress theory: the effect of mechanical loading of bone on osseointegration of dental implants. Biology (Basel). 2020;10:12. PubMed PMID: 33379218
4. Lian Z, Guan H, Ivanovski S, Loo Y, Johnson N, Zhang H. Effect of bone to implant contact percentage on bone remodelling surrounding a dental implant. Int J Oral Maxillofac Surg. 2010;39:690-8.
5. Shayeb M, Elfadil S, Abutayyem H, Shqaidef A, Marrapodi M, Cicciù M, Minervini G. Bioactive surface modifications on dental implants: a systematic review and meta-analysis of osseointegration and longevity. Clin Oral Investig. 2024;28:592. PubMed PMID: 39392473
6. Alshadidi A, Dommeti V, Aldosari L, Hassan S, Okshah A, Merdji A, et al. Influence of surface texturing and coatings on mechanical properties and integration with bone tissue: an in silico study. Front Bioeng Biotechnol. 2024;12:1439262. PubMed PMID: 39286343
7. Sultan FA, Routroy S, Thakur M. Understanding fish waste management using bibliometric analysis: A supply chain perspective. Waste Manag Res. 2023;41:531-53.
8. Taneja A, Sharma R, Khetrapal S, Sharma A, Nagraik R, Venkidasamy B, et al. Value addition employing waste bio-materials in environmental remedies and food sector. Metabolites. 2023;13:624. PubMed PMID: 37233665
9. Muntean FL, Olariu I, Marian D, Olariu T, Petrescu EL, Olariu T, et al. Hydroxyapatite from Mollusk Shells: Characteristics, Production, and Potential Applications in Dentistry. Dent J (Basel). 2024;12:409. PubMed PMID: 39727466
10. Raghul M, Mukesh G, Haridevamuthu B, Snega P, Raman P, et al. Plausible antioxidant and anticonvulsant potential of brain-targeted naringenin-conjugated graphene oxide nanoparticles. Biomass conversion and biorefinery. 2024;18:22125-36.
11. Wu J, Wang S, Zheng Z, Li J. Biologically inspired electrospun collagen/silk fibroin/bioactive glass composited nanofibrous scaffold to accelerate the treatment efficiency of bone repair. Regen Ther. 2022;21:122-38.

12. Baskar V, Ramkumar S, Ramasamy P, Santhosh Kumar MP, Muthu T, Marks K, et al. Unveiling novel applications of fruit pomace for sustainable production of value-added products and health benefits: a review. Food Biosci. 2024;61:104533
13. Senthil R, Çakır S. Nano apatite growth on demineralized bone matrix capped with curcumin and silver nanoparticles: dental implant mechanical stability and optimal cell growth analysis. J Oral Biosci. 2024;66:232-40.
14. Senthil R. Epoxy resin bioactive dental implant capped with hydroxyapatite and curcumin nanoparticles: a novel approach. Oral Maxillofac Surg. 2024;28:1303-12.
15. Senthil R, Roy A, Lakshmi T. Mineralized collagen fiber-based dental implant: novel perspectives. J Adv Oral Res. 2024; 15:62-9
16. Songjie L, Xin D, Han C, Tong L, Bo L, Yikun J, et al. Developing fibrin-based biomaterials/scaffolds in tissue engineering. Bioact Mater. 2024;40:597-623.
17. Li Y, Liu Y, Li R, Bai H, Zhu Z, Zhu L, et al. Collagen-based biomaterials for bone tissue engineering. Mater Des. 2021;210:110049.

Biomedical Sciences and Clinical Medicine 2026;65(1):119-128.
doi: 10.12982/BSCM.2026.04
https://he01.tci-thaijo.org/index.php/CMMJ-MedCMJ/index

BSCM
Biomedical Sciences and Clinical Medicine

Review Article

Open Access

ANGPT2 as a Therapeutic Target in Endometriosis: Evolving Perspectives in Angiogenesis - *ANGPT2*, an Emerging Target in Endometriosis Therapy

Sheeja MJ[1], Sumanth Kumar B[2], N Muninathan[3], K Ramesh Kumar[4], Joby P Jose[5], Jeena Jose[5], Sreekutty M[5], Jisha A M[5], Parvathy S[5], Jineesh V C[5], Sindhu K[5], Sreeja Sreenivasan[5] and Dinesh Roy D[6]

[1]Meenakshi Academy of Higher Education and Research (MAHER- Deemed to be University), West K.K Nagar, India; [2]Department of Biochemistry, Meenakshi Academy of Higher Education and Research, Chennai, India; [3]Scientist, Central Research Lab, Meenakshi Medical College and Research Institute, Kanchipuram, Enathur, Tamil Nadu, India; [4]Laboratoy Director, Biochemistry, Metropolis Health Care Limited, India; [5]Research Scholar, Meenakshi Academy of Higher Education and Research (MAHER- Deemed to be University), West K.K Nagar, India; [6]Genetika, Centre for Advanced Genetic Studies, Thiruvananthapuram, Kerala, India

Correspondence:
Sumanth Kumar B, PhD,
Department of Biochemistry,
Meenakshi Academy of Higher Education and Research,
Chennai, Tamil Nadu, India
E-mail: bsumanthkumar108@gmail.com

Dinesh Roy D, PhD,
CEO & Senior Cytogeneticist,
Genetika, Centre for Advanced Genetic Studies, Thiruvananthapuram, Kerala, India
E-mail: drdineshroyd@gmail.com

Received: May 13, 2025;
Revised: July 31, 2025;
Accepted: August 7, 2025

ABSTRACT

Endometriosis is a chronic, estrogen-dependent inflammatory condition marked by the ectopic implantation of endometrial-like tissue, most commonly involving the ovaries, peritoneum, and pelvic structures. This ectopic tissue responds to hormonal cycles, leading to symptoms such as pelvic pain, dysmenorrhea, dyspareunia, and infertility. A critical process in the pathophysiology of endometriosis is angiogenesis, which sustains lesion growth and survival. Angiopoietin-2 (Ang-2), encoded by the *ANGPT2* gene, is a key regulator of abnormal vascular remodeling in endometriosis, acting as a vascular destabilizer and enhancing angiogenic responses, particularly in conjunction with vascular endothelial growth factor (VEGF).

This review synthesizes current evidence on the pathological role of Ang-2 in endometriosis-associated angiogenesis and evaluates its potential as a molecular target for therapy. A comprehensive literature search was performed using PubMed, Scopus, Google Scholar, and Web of Science, covering articles published from 1997 to 2025. Relevant studies were selected based on Ang-2's involvement in angiogenesis, its expression patterns in endometriotic tissue, and the outcomes of therapeutic interventions.

The findings reveal that *ANGPT2* expression is upregulated in endometriotic lesions and is modulated by hypoxia, estrogen, and inflammatory factors. Elevated levels of Ang-2 are associated with increased disease severity and vascular immaturity in lesions. Preclinical studies targeting Ang-2, either alone or in combination with VEGF inhibitors, have demonstrated reductions in lesion vascularization and growth, highlighting its therapeutic promise.

In conclusion, Ang-2 serves as a critical mediator of pathological angiogenesis in endometriosis and presents a promising target for novel anti-angiogenic therapies. Further translational research and clinical trials are warranted to explore its full therapeutic potential.

KEYWORDS angiogenesis, ectopic endometrial tissue, endometriosis, therapeutic targets, vascular endothelial growth factor, vascular remodeling

INTRODUCTION

Endometriosis is a chronic and debilitating disease characterized by the presence of endometrial tissue, including glandular epithelium and stroma, outside the uterine cavity (1-3). The World Health Organization (WHO) highlights its profound impact on quality of life, causing pelvic pain, fatigue, depression, infertility, dysmenorrhea, and even malignant transformations. It affects approximately 6.0% of women, with another 5.4% suspected of having the condition (4–6).

In endometriosis, retrograde menstruation introduces menstrual blood into the peritoneal cavity, leading to oxidative stress and immune responses. These changes promote the release of inflammatory cytokines and pro-angiogenic factors that disrupt the peritoneal microenvironment (7, 8). Angiogenesis, essential for endometrial growth and repair during the menstrual cycle, is similarly central to the pathophysiology of endometriosis (9, 10). It also plays a pivotal role in other gynecological disorders such as abnormal uterine bleeding and endometrial cancer (11–13).

Throughout the menstrual cycle, angiogenesis and vascular remodeling establish new vasculature in the endometrium, facilitating cell proliferation and differentiation (14). This process is tightly regulated by several angiogenic factors including vascular endothelial growth factor (VEGF), angiopoietin-1 (Ang-1), angiopoietin-2 (Ang-2), C-X-C motif chemokine ligand 12 (CXCL12), and IL-6, whose expression is modulated by hypoxia and sex hormones (15). VEGF, a potent signaling protein, promotes endothelial proliferation and neovascularization. In endometriosis, VEGF is upregulated in ectopic lesions, peritoneal fluid, and serum, supporting lesion establishment and progression via hypoxia, inflammation, and estrogen signaling.

Among the angiogenic mediators, Ang-2 has recently emerged as a key player in the angiogenesis pathway (16). Ang-2 interacts with VEGF in a regulatory network that governs endometrial angiogenesis (17, 18). While Ang-1 stabilizes blood vessels by enhancing endothelial junctions, Ang-2 competes for the same receptor to promote vascular remodeling and destabilization (19–23). Selectively expressed in the ovary, uterus, and placenta, Ang-2 facilitates VEGF-driven angiogenesis by weakening cell–cell and cell–matrix adhesion (24–26).

Elevated *ANGPT2* expression and enhanced angiogenic activity have been observed more frequently in women with endometriosis compared to unaffected individuals (10, 27). *ANGPT2* is thus considered a promising therapeutic target, with both *in-vitro* and *in-vivo* studies exploring its modulation via mRNA regulation and other strategies (28, 29). In this manuscript, *ANGPT1*, *ANGPT2*, *ANGPT3*, and *ANGPT4* are denoted as gene symbols, while Ang-1 and Ang-2 refer to their protein forms to reflect functional roles in angiogenesis. Despite emerging insights, the precise molecular mechanisms of *ANGPT2* remain to be fully elucidated. This study investigates factors influencing *ANGPT2* expression, its therapeutic potential in endometriosis, and the clinical value of targeting Ang-2 in anti-angiogenic therapy.

METHOD

A comprehensive literature review was conducted to explore the role of *ANGPT2* in the pathogenesis and therapeutic potential in endometriosis. Biomedical databases, including PubMed, Scopus, Web of Science, and Google Scholar, were searched using relevant keywords such as angiogenesis, ectopic endometrial tissue, endometriosis, therapeutic targets, VEGF, and vascular remodeling. Boolean operators were applied to refine search results, and filters such as clinical trials, systematic reviews, publication within the last five years, and free full-text availability, were used to enhance relevance. From an initial yield of nearly 20,000 articles, screening based on titles, abstracts, and full-text review narrowed the selection to 74 key publications that offered substantial insights into *ANGPT2*'s involvement in vascular remodeling, inflammation, hormonal regulation, and angiogenic imbalance in endometriosis. Both preclinical and clinical studies were included to provide a comprehensive understanding of the molecular and translational aspects of *ANGPT2* in disease progression and its potential as a therapeutic target.

Physiological angiogenesis in the endometrium

The human endometrium undergoes cyclic growth and regeneration in response to hypoxia and sex steroid interactions throughout the menstrual cycle (12, 30). These dynamic changes are closely associated with angiogenesis, a tightly regulated process by which new blood vessels

form through sprouting, elongation, and intussusception by endothelial cells (11, 12). Angiogenesis plays a fundamental role in endometrial remodeling necessary for reproduction, including follicular maturation, corpus luteum function, and uterine preparation for implantation.

Endometrial vascular development is finely controlled by the interaction of pro-angiogenic and anti-angiogenic factors, ensuring appropriate vessel formation and remodeling. Hypoxia and female sex hormones independently influence the expression of these factors, thereby maintaining vascular homeostasis under both physiological and pathological conditions, including the progression of endometriosis (15, 31). Pro-angiogenic signals stimulate endothelial activation and vessel sprouting, while anti-angiogenic molecules constrain excessive neovascularization, maintaining vascular stability (15, 32).

Key pro-angiogenic mediators involved in this regulatory network include VEGF, angiopoietins, chemokine CXCL12, fibroblast growth factor-2 (FGF-2), platelet-derived growth factor (PDGF), and matrix metalloproteinases (MMPs). These promote vascular growth and endothelial cell activity. Conversely, anti-angiogenic molecules such as soluble VEGF receptor-1 (sVEGFR-1), endostatin, maspin, and thrombospondin-1 (TSP-1) act as inhibitory controls. This intricate balance governs not only cyclic endometrial regeneration but also broader physiological processes like wound healing, and plays a role in pathological conditions such as cancer and endometriosis. Understanding the modulation of these pathways offers potential for targeted angiogenic therapies.

This coordinated regulation of angiogenic balance is illustrated in Figure 1, where pro-angiogenic molecules (e.g., VEGF, *ANGPT*, epidermal growth factor (EGF), PDGF), denoted by upward arrows, enhance endothelial activation and vessel formation, while anti-angiogenic factors (e.g., sVEGFR-1, endostatin, maspin, TSP-1), indicated by downward arrows, serve to inhibit the process. The figure underscores the dynamic interplay of these opposing factors in governing angiogenesis.

Role of *ANGPT1 and ANGPT2* in endometrial vascular remodeling

Angiopoietins play a crucial role in regulating blood vessel growth, maturation, and regression, working in close coordination with VEGF to modulate angiogenesis (23, 33, 17). The angiopoietin family includes *ANGPT1*, *ANGPT2*, *ANGPT3*, and *ANGPT4*, of which *ANGPT1* and *ANGPT2* are the most extensively studied (34, 35). While *ANGPT1* is widely expressed across various tissues, *ANGPT2* expression is predominantly localized to the ovary, uterus, and placenta. In the human endometrium, their expression patterns vary with the menstrual cycle. During the secretory phase, Ang-1 is primarily localized around blood vessels in the stromal region, whereas Ang-2 is expressed in the glandular epithelium and endothelium (24, 36).

Functionally, Ang-1 binds to the Tie-2 receptor to promote blood vessel stability, integrity, and quiescence. It also supports physiological angiogenesis during ovulation by maintaining endothelial cell survival and vessel maturation. In contrast, Ang-2 acts as a natural antagonist of Ang-1 by competitively binding to Tie-2 without activating it, thereby inhibiting Tie-2 signaling (37, 38). This results in vessel destabilization and extracellular matrix loosening—key preparatory steps for angiogenesis.

The action of Ang-2 is highly context-dependent. In the presence of VEGF, Ang-2 facilitates endothelial proliferation and sprouting, promoting

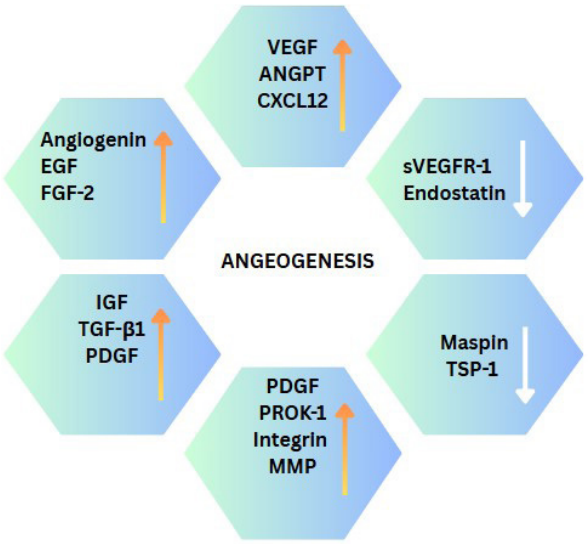

Figure 1. An illustration of the complex network of pro-angiogenic and anti-angiogenic factors involved in angiogenesis, highlighting key molecular mediators such as VEGF, *ANGPT*, CXCL12, and TSP-1, and their regulatory roles in vascular development and remodeling. Orange upward arrows indicate pro-angiogenic factors, while white downward arrows represent anti-angiogenic factors.

neovascularization. However, in the absence of VEGF, Ang-2-induced destabilization leads instead to vessel regression due to impaired pericyte recruitment and endothelial disassembly (23, 25, 26). This dual functionality makes Ang-2 a pivotal modulator of vascular plasticity, capable of either promoting or inhibiting angiogenesis depending on the angiogenic milieu.

The dynamic balance between Ang-1 and Ang-2 is essential for endometrial vascular remodeling, especially during cyclic regeneration and implantation. An increased Ang-2/Ang-1 ratio is indicative of vascular destabilization—a prerequisite for new vessel formation—and may serve as a marker of endothelial activation and remodeling capacity (39). This tightly regulated angiopoietin-Tie2 signaling axis ensures proper vascular adaptation throughout the menstrual cycle and reproductive processes.

Molecular regulation of *ANGPT2* expression

Hypoxia serves as a central regulator of endometrial angiogenesis during the premenstrual period. As oxygen levels decline during menstruation, hypoxia-inducible factor-1α (*HIF-1α*) stabilizes and activates key proangiogenic genes such as *VEGF*, *ANGPT1*, *ANGPT2*, Tie-2, PDGF, basic fibroblast growth factor (*bFGF*), and monocyte chemoattractant protein-1 (*MCP-1*), thereby initiating vascular remodeling processes (40–42). Under hypoxic conditions, *ANGPT1* expression markedly decreases, while *ANGPT2* levels remain relatively stable, leading to an elevated *ANGPT2/ANGPT1* ratio. This imbalance, especially in the presence of VEGF, promotes endothelial destabilization and subsequent neovascularization (43). Additionally, hypoxia induces the expression of other angiogenic mediators like CYR61 and leptin, and upregulates osteopontin and cysteine-rich protein 61 via the COX-2/prostaglandin pathway. Estrogen and prostaglandins also enhance *HIF-1α* stabilization, establishing a positive feedback loop that intensifies the hypoxia-driven angiogenic cascade. This loop modulates both angiogenic and anti-angiogenic factors, thereby fine-tuning *ANGPT2* activity and vascular dynamics in the endometrium (44).

Importantly, the influence of hypoxia on angiopoietin expression extends to extra-endometrial sites. In the hypoxic peritoneal microenvironment characteristic of endometriosis *HIF-1α* suppresses the transcription factor chicken ovalbumin upstream promoter-transcription factor II, resulting in increased angiopoietin levels and enhanced vascularization of ectopic lesions (45).

Female steroid hormones, notably estrogen and progesterone, also exert critical control over *ANGPT2* expression. Estrogen upregulates VEGF and downregulates *ANGPT1*, thereby increasing the *ANGPT2/ANGPT1* ratio and fostering a pro-angiogenic environment favorable for endometrial vessel development (46). In contrast, progesterone displays a nuanced role. During the secretory phase, it supports vascular maturation. Progestins reduce *ANGPT2* while maintaining *ANGPT1*, effectively lowering the *ANGPT2/ANGPT1* ratio and exerting anti-angiogenic effects (43). In early pregnancy, *ANGPT2* expression in the uterine endometrium is modulated by progesterone, likely contributing to vascular remodeling via the Tie-2 pathway. Supporting this, progesterone has been shown to upregulate *ANGPT2* in human uterine microvascular endothelial cells (HUtMECs), underlining its role in gestational angiogenesis (47).

In hypoxic, inflammatory conditions like endometriosis, elevated *ANGPT2* levels activate the Ang-2/Tie2 signaling axis, which antagonizes *ANGPT1*-mediated vessel stabilization. This shift facilitates VEGF-A-driven endothelial proliferation and migration, promoting pathological angiogenesis (48). Pichiule et al. demonstrated that hypoxia enhances *ANGPT2* expression in endothelial cells through both transcriptional mechanisms and mRNA stabilization, resulting in increased intracellular and secreted Ang-2 protein levels.

Estrogen further promotes endometrial angiogenesis by stimulating endothelial cell proliferation, migration, and vessel stabilization (49). However, in endometriosis, heightened estrogenic activity intensifies inflammation, pain, and infertility by upregulating VEGF and suppressing *ANGPT1*, thus raising the *ANGPT2/ANGPT1* ratio and driving aberrant vascular growth (46, 50). Although progesterone ordinarily regulates inflammation and decidualization, impaired signaling in endometriosis contributes to ectopic tissue implantation and disease progression (51). Typically, post-ovulatory progesterone surge limits endometrial proliferation (52), but in endometriosis, progesterone resistance exacerbates the

ANGPT2/ANGPT1 imbalance, further promoting pathological angiogenesis (43, 53).

ANGPT2 in endometriosis pathogenesis

In endometriosis, retrograde menstruation allows menstrual blood to enter the peritoneal cavity, triggering oxidative stress and immune responses. This disrupts peritoneal homeostasis and promotes the release of pro-angiogenic factors that drive neovascularization and the formation of microvascular networks (7, 8). Pathological angiogenesis, characterized by unregulated blood vessel growth, results from dysregulation in key signaling pathways Fsuch as VEGF, Notch, Angiopoietin-Tie, and FGF (15). The eutopic endometrium of affected individuals exhibits elevated angiogenic potential, with increased expression of Ang-1 and Ang-2 compared to non-endometriotic tissue. As angiogenesis is essential for the establishment and maintenance of endometriotic lesions, targeting Ang-2 has emerged as a promising therapeutic approach (27, 54, 29).

Neovascularization is central to endometriosis progression, with Ang-2 functioning as a critical modulator (55, 26). Overexpression of *ANGPT2* in both ectopic and eutopic endometrial tissues contributes to lesion development and is being explored as a potential biomarker for disease severity. In synergy with VEGF, Ang-2 enhances the production of MMPs, particularly MMP-1 and MMP-9, which facilitate tissue invasion and remodeling. Moreover, Ang-2 promotes vessel sprouting by antagonizing the stabilizing effect of Ang-1 on the Tie2 receptor (55, 27), a mechanism further supported by studies demonstrating functional interplay between Ang-2 and VEGF (29). The Ang-2/Ang-1 ratio increases during early angiogenic phases and fluctuates with disease progression, reflecting dynamic vascular demands (56). Dysregulated ANGPT signaling has also been associated with reproductive complications, including miscarriage (57).

Clinical studies have shown significantly elevated levels of VEGF, Ang-1, Ang-2, MMP-1, and MMP-9 in the eutopic endometrium of endometriosis patients compared to controls, reinforcing their role in disease pathophysiology (58). Sampson's seminal theory of retrograde menstruation, proposed in 1925, remains the most widely accepted explanation for endometriosis development (59–61). An endometrial environment enriched with angiogenic and proteolytic factors is more likely to give rise to ectopic implants upon migration into the peritoneal cavity (58). Notably, Hur et al. reported that during the secretory phase, the *ANGPT2/ANGPT1* mRNA expression ratio was significantly elevated in eutopic endometrium from women with endometriosis relative to healthy controls. The predominance of Ang-2 over Ang-1 at the Tie2 receptor, in the presence of VEGF, may lead to persistent immature neovascularization—a hallmark of endometriotic lesions (27).

Therapeutic targeting of *ANGPT2* in endometriosis

Zhou et al. identified miR-205-5p as a pivotal regulatory molecule in endometriosis, demonstrating its role in controlling ectopic endometrial stromal cell migration, invasion, and apoptosis by directly targeting *ANGPT2* and modulating the Ang-2–AKT/ERK signaling pathway. Their findings revealed an inverse relationship between miR-205-5p and *ANGPT2* expression, with reduced miR-205-5p and elevated *ANGPT2* levels correlating with greater disease severity, thereby positioning the miR-205-5p–*ANGPT2* axis as a promising and highly specific therapeutic target. Unlike broad-spectrum anti-angiogenic therapies that may compromise normal vascular integrity and lead to systemic adverse effects, *ANGPT2*-targeted interventions selectively disrupt pathological neovascularization within endometriotic lesions, preserving healthy vasculature. Additionally, miRNA-based or *ANGPT2*-specific approaches allow for localized delivery, reducing systemic exposure and enhancing treatment safety (28).

Similarly, Chen et al. demonstrated that administration of the traditional Chinese medicine Hua Yu Xiao Zheng (HYXZ) decoction in a rat model of endometriosis significantly reduced lesion size and downregulated VEGF and *ANGPT2* expression. While VEGF inhibition remains a conventional anti-angiogenic strategy, *ANGPT2* targeting offers a more refined approach by destabilizing vasculature specific to ectopic endometrial tissue. This focused inhibition may improve disease control while minimizing vascular-related side effects, reinforcing *ANGPT2*'s dual role as a biomarker and therapeutic target (29).

Endometriosis-associated angiogenesis provides a strong rationale for anti-angiogenic therapy as a targeted, non-hormonal treatment option. To this end, various angiogenic blockers have been evaluated, offering alternatives to hormone-based therapies (32). Table 1 summarizes various pharmacological agents with anti-angiogenic effects on endometriosis.

Angiogenesis is central to ectopic lesion establishment and progression. Its dysregulation, particularly the overexpression of *ANGPT1* and *ANGPT2* in eutopic endometrial tissues, contributes significantly to the disease pathophysiology (27, 68). In the presence of *VEGF*, *ANGPT2* promotes MMP activation, facilitating tissue invasion (69). Its dominance over *ANGPT1* via the Tie-2 receptor further promotes immature and persistent neovascularization (70, 71). Thus, inhibiting *ANGPT2* may effectively curb aberrant angiogenesis, suppress lesion growth, and improve overall disease outcomes (28).

Unlike conventional anti-angiogenic treatments that broadly suppress vascular proliferation, *ANGPT2*-specific therapies offer greater precision by selectively targeting abnormal and immature vessels within endometriotic lesions. This mechanism helps to minimize off-target effects and preserve normal vascular function. Moreover, these therapies are amenable to localized delivery methods, such as intra-peritoneal administration or direct lesion injection, further reducing systemic toxicity.

In contrast to hormone-based treatments often associated with undesirable effects including androgenic symptoms (e.g., increased facial hair, deepened voice), weight gain, fluid retention, acne, mood instability, and heightened risk of thromboembolism, *ANGPT2*-targeted therapies offer a more favorable safety profile (72).

Clinically, *ANGPT2* inhibition has demonstrated multiple benefits: more precise lesion suppression, reduced pelvic pain, fewer ectopic implants, lower microvascular density, enhanced apoptosis, decreased VEGF levels in peritoneal fluid, fibrosis of endometriotic lesions, resolution of refractory dysmenorrhea, and upregulation of hormone receptor expression in affected tissues (32, 63, 73, 74). These outcomes underscore the potential of *ANGPT2* as both a therapeutic target and as a prognostic indicator in the effective management of endometriosis.

Safety considerations and limitation of *ANGPT2*-targeted therapies

Anti-angiogenic therapy may adversely impact normal physiological processes such as ovulation and wound healing. As a result, it may have adverse impacts on reproductive function and pose teratogenic risks when used to treat endometriosis in women of reproductive age (32). The therapeutic approach towards regulating Ang-2 for endometriosis requires further investigation to fully understand its benefits and potential consequences. More studies are needed to comprehensively

Table 1. Summary of various pharmacological agents with anti-angiogenic effects on endometriosis, detailing their mechanisms of action such as VEGF inhibition, *HIF-1α* suppression, and MMP regulation, which contribute to the reduction of lesion size and vascularization

Drug	Anti-angiogenic effects on endometriosis	Mode of action	Reference
Angiostatin	Restricts the number of endometriotic lesions	Inhibits VEGF and bFGF signaling	(62)
Anti-*VEGF* antibody	Reduces *VEGF* levels in peritoneal fluid and micro vessel density	Neutralizes active *VEGF* and blocks its receptor	(63)
2-Methoxyestradiol	Suppresses *HIF-1α* and *VEGF* expression	Inhibits *HIF-1α* expression and its transcriptional activity	(64)
Simvastatin	Reduces micro vessel density	Downregulates *VEGF* synthesis and suppresses MMP secretion	(65)
Celecoxib	Reduces micro vessel density	Inhibits COX-2	(66)
Retinoic acid	Reduces the volume of endometriotic implants	Directly downregulates *VEGF* production	(67)

VEGF, vascular endothelial growth factor; bFGF, basic fibroblast growth factor, HIF-α, hypoxia-inducible factor alpha

evaluate the effectiveness and safety of targeting Ang-2 in the management of endometriosis.

CONCLUSIONS

This study underscores the pivotal role of *ANGPT2* in endometriosis, with a particular focus on the regulatory mechanisms governing its expression and its therapeutic potential. The findings suggest that targeting Ang-2 may help alleviate endometriosis symptoms and enhance clinical outcomes by modulating key angiogenic signaling pathways.

However, several limitations must be considered. Much of the current evidence is derived from *in-vitro* or animal studies, which may not accurately reflect human physiological conditions. Moreover, the precise molecular mechanisms by which Ang-2 contributes to angiogenesis remain incompletely understood. Its regulation by hormones such as progesterone appears inconsistent, particularly in the context of progesterone resistance, a common feature in endometriosis.

While anti-angiogenic therapies targeting Ang-2 show therapeutic promise, they may also disrupt normal reproductive functions, including ovulation and wound healing, raising important safety concerns for women of reproductive age. Additionally, the lack of clinical trials validating Ang-2 as a therapeutic target highlights a critical gap, and it is likely that targeting Ang-2 alone may be insufficient due to the complex and redundant nature of angiogenic signaling networks in endometriosis.

Despite these challenges, this study offers a novel perspective by integrating the upstream regulatory influences of hypoxia, estrogen, and inflammatory mediators on *ANGPT2* expression within the endometriotic microenvironment. Unlike earlier studies that mainly reported elevated Ang-2 levels, our review emphasizes the dynamic regulation of Ang-2 and positions it not only as a biomarker of disease severity, but also as a dual-action therapeutic target capable of disrupting both pathological neovascularization and chronic inflammation.

This dual role enhances the rationale for developing Ang-2–focused therapeutic interventions as part of clinical management strategies for endometriosis. To fully realize this potential, further research is essential to validate these findings, clarify Ang-2's molecular functions, and rigorously assess the efficacy and safety of targeted anti-angiogenic therapies. Continued investigation will not only support therapeutic development for endometriosis but may also inform strategies for other gynecological disorders marked by aberrant angiogenesis.

ACKNOWLEDGMENTS

We sincerely appreciate the support provided by Meenakshi Academy of Higher Education and Research, Chennai, Tamil Nadu, India, and Genetika, Centre for Advanced Genetic Studies, Thiruvananthapuram, Kerala, India.

FUNDING

This research received no specific grant from funding agencies in the public, commercial, or not-for-profit sectors.

CONFLICT OF INTEREST

There was no conflict of interest in this manuscript.

AUTHOR CONTRIBUTION

S.M.J.: conceptualization of the study, methodology design, sample collection, laboratory work (biochemical and molecular analyses), data acquisition, statistical analysis, and manuscript drafting, support in genetic data analysis and visualization, referencing, and manuscript formatting; S.K.B.: supervision, critical review of study design, interpretation of molecular data, guidance in laboratory methodologies, and manuscript revision for important intellectual content; N.M.: validation of biochemical assay procedures, clinical correlation of metabolic findings, and critical inputs in manuscript development; K.R.K.: clinical insight into endocrine aspects, interpretation of hormonal and metabolic data, and contribution to discussion and conclusions; J.P.J., J.J., S.M., J.A.M.: assistance in sample processing, ELISA/RT-PCR experimentation, data entry, and preliminary statistical valuation; P.S., J.V.C., S.K.,: Support in genetic data analysis and visualization, referencing, and manuscript formatting; D.R.D.: conceptual supervision, molecular diagnostics consultation (MC4R expression), manuscript review, critical editing, and final approval of the version to be published.

DATA AVAILABILITY STATEMENT

This review is based on previously published studies. All data supporting the findings are available in the cited literature. Additional information can be provided by the authors upon reasonable request.

INSTITUTIONAL REVIEW BOARD STATEMENT

This review article does not report on new experimental research involving humans or animals; therefore, ethics approval was not required.

INFORMED CONSENT STATEMENT

This review article does not include research involving human participants; therefore, informed consent was not required.

REFERENCES

1. Giudice LC. Clinical practice. Endometriosis. N Engl J Med. 2010;362:2389-98.
2. Macer ML, Taylor HS. Endometriosis and infertility: a review of the pathogenesis and treatment of endometriosis-associated infertility. Obstet Gynecol Clin North Am. 2012;39:535-49.
3. Kennedy S, Bergqvist A, Chapron C, D'Hooghe T, Dunselman G, Greb R, et al. ESHRE guideline for the diagnosis and treatment of endometriosis. Hum Reprod. 2005;20:2698-704.
4. Harder C, Velho RV, Brandes I, Sehouli J, Mechsner S. Assessing the true prevalence of endometriosis: a narrative review of literature data. Int J Gynaecol Obstet. 2024;167:883-900.
5. Dunselman G, Vermeulen N, Becker C, Calhaz-Jorge C, D'Hooghe T, De Bie B, et al. ESHRE guideline: management of women with endometriosis. Hum Reprod. 2014;29:400-12.
6. Nnoaham K, Hummelshoj L, Webster P, D'Hooghe T, De Cicco Nardone F, De Cicco Nardone C, et al.; World Endometriosis Research Foundation Global Study of Women's Health Investigators. Impact of endometriosis on quality of life and work productivity: a multicenter study across ten countries. Fertil Steril. 2011;96:366-73.
7. Samimi M, Pourhanifeh M, Mehdizadehkashi A, Eftekhar T, Asemi Z. The role of inflammation, oxidative stress, angiogenesis, and apoptosis in the pathophysiology of endometriosis: basic science and new insights based on gene expression. J Cell Physiol. 2019; 234:19384-92.
8. Tarokh M, Ghaffari Novin M, Poordast T, Tavana Z, Nazarian H, Norouzian M, et al. Serum and peritoneal fluid cytokine profiles in infertile women with endometriosis. Iran J Immunol. 2019;16:151-62.
9. Kiss E, Saharinen P. Anti-angiogenic targets: angiopoietin and angiopoietin receptors. In: Tumor angiogenesis: a key target for cancer therapy. 2019:227–50.
10. Krikun G, Huang S, Schatz F, Salafia C, Stocco C, Lockwood C. Thrombin activation of endometrial endothelial cells: a possible role in intrauterine growth restriction. Thromb Haemost. 2007;97:245-53.
11. Lockwood C. Mechanisms of normal and abnormal endometrial bleeding. Menopause. 2011;18:408-11.
12. Harmsen M, Wong C, Mijatovic V, Griffioen A, Groenman F, Hehenkamp W, et al. Role of angiogenesis in adenomyosis-associated abnormal uterine bleeding and subfertility: a systematic review. Hum. Reprod. Update. 2019;25:647-71.
13. Don E, Middelkoop M, Hehenkamp W, Mijatovic V, Griffioen A, Huirne JA. Endometrial angiogenesis of abnormal uterine bleeding and infertility in patients with uterine fibroids—a systematic review. Int J Mol Sci. 2023;24:7011. PubMed PMID: 37108180
14. Virdis A, Dell'Agnello U, Taddei S. Impact of inflammation on vascular disease in hypertension. Maturitas. 2014;78:179-83.
15. Okada H, Tsuzuki T, Murata H, Kasamatsu A, Yoshimura T, Kanzaki H. Regulation of angiogenesis in the human endometrium. In: Harada T, editor. Uterine Endometrial Function. Tokyo: Springer Japan; 2016. p. 83–103.
16. Scholz A, Plate K, Reiss Y. Angiopoietin-2: a multifaceted cytokine that functions in both angiogenesis and inflammation. Ann NY Acad Sci. 2015;1347:45-51.
17. Girling J, Rogers P. Regulation of endometrial vascular remodelling: role of the vascular endothelial growth factor family and the angiopoietin-TIE signaling system. Reprod Camb Engl. 2009;138:883-93.
18. Lash G, Innes B, Drury J, Robson S, Quenby S, Bulmer J. Localization of angiogenic growth factors and their receptors in the human endometrium throughout the menstrual cycle and in recurrent miscarriage. Hum Reprod. 2012;27:183-95.
19. Zhong X, Fei Y, Zhao H, Chen J, Gao M, Huang Y, et al. Mechanistic studies and therapeutic potential of angiopoietin in head and neck tumor angiogenesis. Front. Oncol. 2025;15:1529225. PubMed PMID: 40260291
20. Wang R, Yang M, Jiang L, Huang M. Role of Angiopoietin-Tie axis in vascular and lymphatic systems and therapeutic interventions. Pharmacol. Res. 2022;182: 106331. PubMed PMID: 35772646
21. Sack K, Kellum J, Parikh S. The angiopoietin-Tie2 pathway in critical illness. Crit Care Clin. 2020;36:201-16.
22. Akwii R, Sajib M, Zahra F, Mikelis C. Role of angiopoietin-2 in vascular physiology and pathophysiology. Cells. 2019;8:471. PubMed PMID: 3110888
23. Ahmad A, Nawaz MI. Molecular mechanism of VEGF and its role in pathological angiogenesis. J Cell Biochem. 2022;123:1938-65.
24. Gale N, Yancopoulos G. Growth factors acting via endothelial cell-specific receptor tyrosine kinases: VEGFs, angiopoietins, and ephrins in vascular development. Genes Dev. 1999;13:1055-66.

25. Hanahan D. Signaling vascular morphogenesis and maintenance. Science. 1997;277:48-50.
26. Amalinei C, Căruntu ID, Giuşcă SE, Balan RA. Complex mechanisms of matrix metalloproteinases involvement in endometrial physiology and pathology—an update. In: Chakraborti S, Dhalla NS, editors. Proteases in Human Diseases. Singapore: Springer; 2017. p. 41–67.
27. Hur S, Lee J, Moon H, Chung H. Angiopoietin-1, angiopoietin-2 and Tie-2 expression in eutopic endometrium in advanced endometriosis. MHR Basic Sci Reprod Med. 2006;12:421-6.
28. Zhou C, Liu M, Wang W, Wu S, Huang Y, Chen G, et al. miR-205-5p inhibits human endometriosis progression by targeting *ANGPT2* in endometrial stromal cells. Stem Cell Res Ther. 2019;10:1-3.
29. Chen Z, Gong X. Effect of Hua Yu Xiao Zheng decoction on the expression levels of vascular endothelial growth factor and angiopoietin-2 in rats with endometriosis. Exp Ther Med. 2017;14:5743-50.
30. Jabbour H, Kelly R, Fraser H, Critchley H. Endocrine regulation of menstruation. Endocr Rev. 2006;27:17-46.
31. Taylor R, Lebovic D, Mueller M. Angiogenic factors in endometriosis. Ann NY Acad Sci. 2002;955:89-100.
32. Chung M, Han S. Endometriosis-associated angiogenesis and anti-angiogenic therapy for endometriosis. Front Glob Womens Health. 2022;3:856316. PubMed PMID: 35449709
33. Wen L, Yan W, Zhu L, Tang C, Wang G. The role of blood flow in vessel remodeling and its regulatory mechanism during developmental angiogenesis. Cell. Mol. Life Sci. 2023;80:162. PubMed PMID: 37221410
34. Thurston G. Role of Angiopoietins and Tie receptor tyrosine kinases in angiogenesis and lymphangiogenesis. Cell Tissue Res. 2003;314:61-8.
35. Thomas M, Augustin H. The role of the Angiopoietins in vascular morphogenesis. Angiogenesis. 2009;12: 125-37.
36. Hewett P, Nijjar S, Shams M, Morgan S, Gupta J, Ahmed A. Down-regulation of angiopoietin-1 expression in menorrhagia. Am J Pathol. 2002;160:773-80.
37. Joussen A, Ricci F, Paris LP, Korn C, Quezada-Ruiz C, Zarbin M. Angiopoietin/Tie2 signaling and its role in retinal and choroidal vascular diseases: a review of preclinical data. Eye. 2021;35:1305-16.
38. Chi Y, Yu S, Yin J, Liu D, Zhuo M, Li X. Role of Angiopoietin/Tie2 system in sepsis: A potential therapeutic target. Clin. Appl. Thromb. Hemost. 2024;30: 10760296241238010. PubMed PMID: 38449088
39. Diamond J, Wu B, Agarwal N, Bowles D, Lam E, Werner T, et al. Pharmacokinetic drug-drug interaction study of the angiopoietin-1/angiopoietin-2-inhibiting peptibody trebananib (AMG 386) and paclitaxel in patients with advanced solid tumors. Invest New Drugs. 2015;33:691-9.
40. Aberdeen G, Wiegand S, Bonagura Jr T, Pepe G, Albrecht E. Vascular endothelial growth factor mediates the estrogen-induced breakdown of tight junctions between and increase in proliferation of microvessel endothelial cells in the baboon endometrium. Endocrinology. 2008;149:6076-83.
41. Salamonsen L. Tissue injury and repair in the female human reproductive tract. Reproduction. 2003;125: 301-11.
42. Kumar K, Dasgupta C, Das D. Cell growth kinetics of Chlorella sorokiniana and nutritional values of its biomass. Bioresour Technol. 2014;167:358-66.
43. Tsuzuki T, Okada H, Cho H, Shimoi K, Miyashiro H, Yasuda K, et al. Divergent regulation of angiopoietin-1, angiopoietin-2, and vascular endothelial growth factor by hypoxia and female sex steroids in human endometrial stromal cells. Eur J Obstet Gynecol Reprod Biol. 2013;168:95-101.
44. Hsiao K, Lin S, Wu M, Tsai S. Pathological functions of hypoxia in endometriosis. Front Biosci (Elite Ed). 2015;7:309-21.
45. Fu J, Hsiao K, Lee H, Li W, Chang N, Wu M, et al. Suppression of COUP-TFII upregulates angiogenin and promotes angiogenesis in endometriosis. Hum Reprod. 2018;33:1517-27.
46. Harfouche R, Echavarria R, Rabbani S, Arakelian A, Hussein M, Hussain S. Estradiol-dependent regulation of angiopoietin expression in breast cancer cells. J Steroid Biochem Mol Biol. 2011;123:17-24.
47. Park Y, Choi J, Seol J. Angiopoietin-2 regulated by progesterone induces uterine vascular remodeling during pregnancy. Mol Med Rep. 2020;22:1235-42.
48. Hata A. Functions of microRNAs in cardiovascular biology and disease. Annu Rev Physiol. 2013;75:69-93.
49. Miller VM, Duckles SP. Vascular actions of estrogens: functional implications. Pharmacol Rev. 2008;60:210-41.
50. Chen H, Malentacchi F, Fambrini M, Harrath A, Huang H, Petraglia F. Epigenetics of estrogen and progesterone receptors in endometriosis. Reprod Sci. 2020;27: 1967-74.
51. Patel B, Rudnicki M, Yu J, Shu Y, Taylor R. Progesterone resistance in endometriosis: origins, consequences and interventions. Acta Obstet Gynecol Scand. 2017;96:623-32.
52. Burney R, Talbi S, Hamilton A, Vo K, Nyegaard M, Nezhat C, et al. Gene expression analysis of endometrium reveals progesterone resistance and candidate susceptibility genes in women with endometriosis. Endocrinology. 2007;148:3814-26.
53. Torry D, Leavenworth J, Chang M, Maheshwari V, Groesch K, Ball E, et al. Angiogenesis in implantation. J Assist Reprod Genet. 2007;24:303-15.
54. Groothuis P, Nap A, Winterhager E, Grümmer R. Vascular development in endometriosis. Angiogenesis. 2005;8:147-56.
55. Lin J, Lin H, Xu Z, Yang Z, Hong C, Wang Y, et al. Angiogenesis in atrial fibrillation: A literature review. Biomedicines. 2025;13:1399. PubMed PMID: 40564118
56. Weigel M, Krämer J, Schem C, Wenners A, Alkatout I, Jonat W, et al. Differential expression of MMP-2, MMP-9 and PCNA in endometriosis and endometrial carcinoma. Eur J Obstet Gynecol Reprod Biol. 2012;

160:74-8.
57. Morooka N, Gui N, Ando K, Sako K, Fukumoto M, Hasegawa U, et al. Angpt1 binding to Tie1 regulates the signaling required for lymphatic vessel development in zebrafish. Development. 2024;151:dev202269. PubMed PMID: 38742432
58. Di Carlo C, Bonifacio M, Tommaselli G, Bifulco G, Guerra G, Nappi C. Metalloproteinases, vascular endothelial growth factor, and angiopoietin 1 and 2 in eutopic and ectopic endometrium. Fertil Steril. 2009; 91:2315-23.
59. Gordts S, Koninckx P, Brosens I. Pathogenesis of deep endometriosis. Fertil Steril. 2017;108:872-85.
60. Sampson JA. Heterotopic or misplaced endometrial tissue. Am J Obstet Gynecol. 1925;10:649-64.
61. Wang Y, Nicholes K, Shih I. The origin and pathogenesis of endometriosis. Annu Rev Pathol Mech Dis. 2020;15:71-95.
62. Zahra F, Sajib M, Mikelis C. Role of bFGF in acquired resistance upon anti-VEGF therapy in cancer. Cancers (Basel). 2021 Mar 20;13(6):1422. PubMed PMID: 33804681
63. Ricci A, Olivares C, Bilotas M, Meresman G, Barañao R. Effect of 21vascular endothelial growth factor inhibition on endometrial implant development in a murine model of endometriosis. Reprod Sci. 2011;18:614-22.
64. Hu CJ, Iyer S, Sataur A, Covello K, Chodosh L, Simon M. Differential regulation of the transcriptional activities of hypoxia-inducible factor 1 alpha (*HIF-1α*) and HIF-2α in stem cells. Mol. Cell. Biol. 2006;26:3514–26.
65. Dulak J, Józkowicz A. Anti-angiogenic and anti-inflammatory effects of statins: relevance to anti-cancer therapy. Curr Cancer Drug Targets. 2005;5:579-94.
66. Dogan E, Saygili U, Posaci C, Tuna B, Caliskan S, Altunyurt S, et al. Regression of endometrial explants in rats treated with the cyclooxygenase-2 inhibitor rofecoxib. Fertil Steril. 2004;82:1115-20.
67. Ozer H, Boztosun A, Açmaz G, Atılgan R, Akkar OB, Kosar MI. The efficacy of bevacizumab, sorafenib, and retinoic acid on rat endometriosis model. Reprod Sci. 2013;20:26-32.
68. Bouquet de Joliniere J, Fruscalzo A, Khomsi F, Stochino Loi E, Cherbanyk F, Ayoubi JM, et al. Antiangiogenic therapy as a new strategy in the treatment of endometriosis? The first case report. Front Surg. 2021 Dec 6;8:791686
69. Etoh T, Inoue H, Tanaka S, Barnard GF, Kitano S, Mori M. Angiopoietin-2 is related to tumor angiogenesis in gastric carcinoma: possible *in vivo* regulation via induction of proteases. Cancer Res. 2001;61:2145-53.
70. Chung H, Lee J, Moon H, Hur S, Park M, Wen Y, et al. Matrix metalloproteinase-2, membranous type 1 matrix metalloproteinase, and tissue inhibitor of metalloproteinase-2 expression in ectopic and eutopic endometrium. Fertil. Steril. 2002;78:787-95.
71. Mitsuhashi N, Shimizu H, Ohtsuka M, Wakabayashi Y, Ito H, Kimura F, et al. Angiopoietins and Tie-2 expression in angiogenesis and proliferation of human hepatocellular carcinoma. Hepatology. 2003;37:1105-13.
72. Health Match staff & Health Match Pty Ltd. A quick guide to hormonal therapies and endometriosis. Health Match. 2022 Jun 2.
73. Laschke M, Menger M. Anti-angiogenic treatment strategies for the therapy of endometriosis. Hum. Reprod. Update. 2012;18:682-702.
74. Li Y, Adur M, Kannan A, Davila J, Zhao Y, Nowak R, et al. Progesterone alleviates endometriosis via inhibition of uterine cell proliferation, inflammation and angiogenesis in an immunocompetent mouse model. PLoS One. 2016;11:e0165347. PubMed PMID: 27776183

Biomedical Sciences and Clinical Medicine 2026;65(1):129-139.
doi: 10.12982/BSCM.2026.11
https://he01.tci-thaijo.org/index.php/CMMJ-MedCMJ/index

BSCM
Biomedical Sciences and Clinical Medicine

Review Article

Open Access

MC4R: A Genetic Key to Metabolic and Cardiovascular Disorders

Joby P Jose [1], Sumanth Kumar B[2], N Muninathan[3], K Ramesh Kumar[4], Vishnu M G[1], Sebastian J Pengiparambil[1], Sinha Mathew[1], Harisree P H[1], Roshma Retnakaran[1], Pinchulatha K[1], Thahira A[1], Swathi T[1] and Dinesh Roy D[5]

[1]Meenakshi Academy of Higher Education and Research (MAHER- Deemed to be University), West K.K Nagar, Chennai, Tamil Nadu, India; [2]Department of Biochemistry, Meenakshi Academy of Higher Education and Research, Chennai, Tamil Nadu, India; [3]Central Research Lab, Meenakshi Medical College and Research Institute, Kanchipuram, Enathur, Tamil Nadu, India; [4]Biochemistry, Metropolis Health care limited, Kerala, India; [5]Genetika Centre for Advanced Genetic Studies, Thiruvananthapuram, India

Correspondence:
Sumanth Kumar B, MBBS, MD, Department of Biochemistry, Meenakshi Academy of Higher Education and Research, Chennai, Tamil Nadu, India.
E-mail: bsumanthkumar108@gmail.com

Dinesh Roy D, PhD, Cytogeneticist, Genetika Centre for Advanced Genetic Studies, Thiruvananthapuram, Kerala, India.
E-mail: drdineshroyd@gmail.com

Received: May 3, 2025;
Revised: August 22, 2025;
Accepted: September 18, 2025

ABSTRACT

The melanocortin-4 receptor (MC4R) is a critical regulator of energy homeostasis, lipid metabolism, and cardiovascular risk factors. First cloned in 1993, MC4R's role in appetite regulation was confirmed through animal studies, and its genetic mutations were later identified as major contributors to monogenic obesity. This review synthesizes current research on MC4R's genetic variations and their implications for obesity, metabolic disorders, and cardiovascular health. A systematic literature review was conducted, adhering to PRISMA guidelines, with data extracted from PubMed, Scopus, Web of Science, and Google Scholar. Studies from 1992 to 2025 focusing on MC4R mutations, their effects on obesity, type 2 diabetes, dyslipidemia, and hypertension, as well as their contribution to cardiovascular risk were included. Recent insights highlight rare MC4R variants, such as p.Ser36Thr and p.Ala175Thr which are associated with severe obesity, and novel structural variants, e.g., p.Ser85Gly, which destabilize signaling pathways. Loss-of-function MC4R variants cause hyperphagia and early-onset obesity, whereas gain-of-function variants enhance satiety, providing protection against obesity. MC4R dysfunction also impacts glucose homeostasis and lipid metabolism, thereby increasing the risk of type 2 diabetes, dyslipidemia, and hypertension. Additionally, alterations in MC4R increase cardiovascular risk via pathways involving energy imbalance, sympathetic activation, and endothelial dysfunction. This review highlights the genetic underpinnings of MC4R in metabolic and cardiovascular diseases and underscores the need for developing targeted therapeutic strategies.

KEYWORDS melanocortin-4 receptor, metabolic disorders, cardiovascular disorders, obesity, MC4R mutations

INTRODUCTION

The melanocortin 4 receptor (MC4R) is a protein encoded by the MC4R gene in humans. It is a type of G-protein-coupled receptor (GPCR) that binds to α-melanocyte stimulating hormone (α-MSH). This receptor plays a crucial role in regulating energy homeostasis, feeding behavior, metabolism, and body weight (1). The MC4R was first cloned in 1993 using degenerate PCR, although its function was initially unclear. Subsequent research suggested its potential role in regulating energy homeostasis, a hypothesis that was con-

firmed in 1997 by seminal studies in mice which demonstrated the receptor's influence on appetite and energy balance. By 1998, human genetic studies identified mutations in the MC4R gene as a cause of monogenic obesity (2).

The MC4R gene, located on chromosome 18q21.3, encodes a 332-amino acid protein that serves as a key regulator of energy homeostasis, appetite, food intake, and body weight at the hypothalamic level. As a prototypical GPCR and one of the five members of the melanocortin receptor family, MC4R plays a pivotal role in maintaining energy balance (3, 4). It is activated by melanocortin's peptide hormones derived from the proteolytic cleavage of the proopiomelanocortin (POMC) protein (5). The receptor is widely expressed in the brain, including regions such as the cortex, thalamus, hypothalamus, brainstem, and spinal cord. In addition to its critical role in energy metabolism, MC4R influences blood pressure, heart rate, and erectile function (6). Dysregulation of MC4R signaling contributes to dyslipidemia, characterized by elevated triglycerides and low-density lipoprotein (LDL) cholesterol (7). It also exacerbates insulin resistance and promotes the release of adipokines, such as resistin, which are implicated in inflammation and endothelial dysfunction, thereby increasing cardiovascular risk (8). These diverse functions underscore MC4R's importance as a target for treating metabolic and cardiovascular disorders.

This review will delve into the critical role of MC4R in metabolic and cardiovascular disorders, highlighting its genetic influence on energy balance, obesity, and related comorbidities. It will also explore the potential effect of targeting MC4R pathways for therapeutic interventions to mitigate these risks. By identifying populations with genetic variations in MC4R and developing precision-based treatment strategies, healthcare professionals and researchers can advance the development of improved metabolic and cardiovascular health outcomes globally.

METHODS

The stepwise approach depicted in Figure 1 illustrates the rigorous assessment of full-text articles, ensuring the inclusion of studies directly addressing the MC4R-metabolic and cardiovascular link.

MC4R: STRUCTURE AND FUNCTION

MC4R is a rhodopsin-like class A peptide GPCR and belongs to the melanocortin receptor family, which comprises five receptor subtypes (MC1R to MC5R) (9). MC4R encodes a protein called

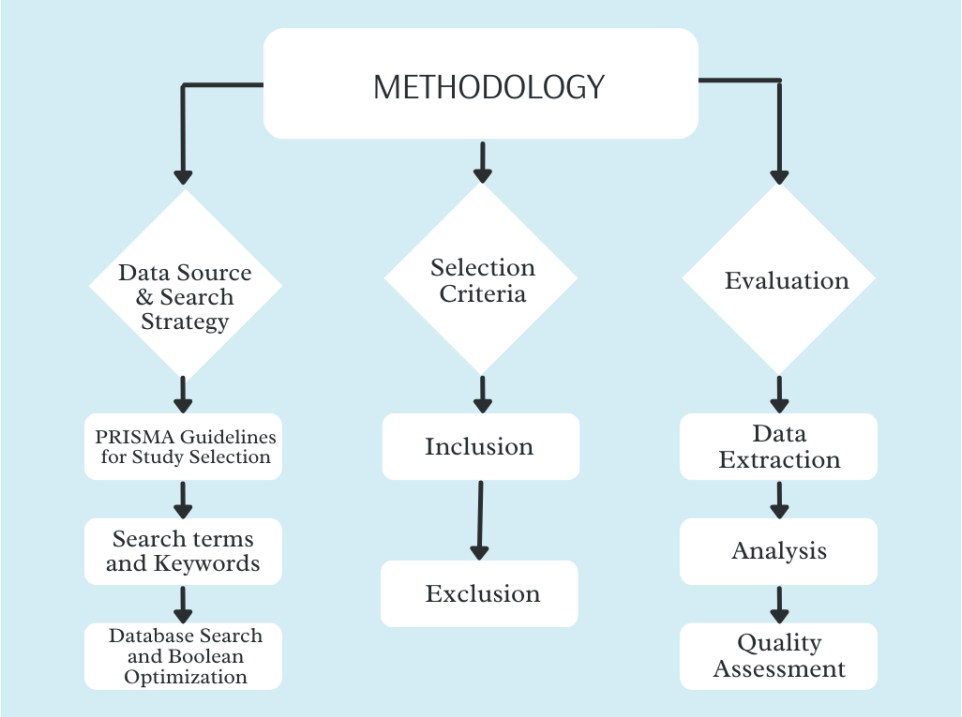

Figure 1. Methodology

melanocortin 4 receptor, primarily expressed in the hypothalamus, where it regulates appetite and satiety. It functions as a GPCR that binds to α-MSH (10). Activation of MC4R by its natural agonists, α-MSH or β-MSH, induces appetite-suppressing effects (11).

MC4R primarily couples with the stimulatory G-protein transducer (Gs) to activate adenylyl cyclase (AC), resulting in the production of intracellular cyclic adenosine monophosphate (cAMP) and subsequent activation of protein kinase A (PKA). In addition to Gs-mediated signaling, MC4R can engage other G-protein-dependent cytosolic transducers, including Gi and Gq/11 (12). Furthermore, MC4R also interacts with G-protein-independent transducers such as β-arrestin and the Kir7.1 ion channel (13).

The MC4R is a crucial component of the leptin-melanocortin molecular axis, which governs hunger, satiety, and energy balance. Brain-derived hormones, such as α-MSH and agouti-related peptide (AgRP), regulate this axis. When α-MSH, an agonist, binds to MC4R, it activates signaling pathways in the brain that promote satiety and reduce food intake. In contrast, AgRP, an inverse agonist, blocks this effect, thereby stimulating appetite (14). MC4R is essential for regulating food intake, energy homeostasis, and body weight (15). Mutations in the MC4R gene can significantly affect metabolic outcomes. Loss-of-function mutations in MC4R or deficiencies in POMC, the precursor of melanocortin receptor agonists, are linked to hyperphagia and severe early-onset obesity (16). Conversely, gain-of-function mutations enhance satiety, decrease food intake, and contribute to lower body weight (17).

MC4R SIGNALING PATHWAYS AND DOWNSTREAM EFFECTS.

MC4R, a GPCR, primarily signals through the stimulatory G-protein (Gs), leading to the activation of AC and the subsequent intracellular production of cAMP. The elevated cAMP levels activate PKA, which phosphorylates various target proteins to elicit diverse cellular responses (14). Functionally, MC4R is crucial for maintaining energy balance by regulating both food intake and energy expenditure, as its activation suppresses appetite and promotes energy utilization (2). Beyond its metabolic roles, MC4R activation also affects cardiovascular function by contributing to the regulation of blood pressure and heart rate (18).

Guo et al., highlighted that MC4R plays a critical role in maintaining physiological balance across multiple systems. In energy homeostasis, MC4R regulates both food intake and energy expenditure, with its activation reducing appetite and promoting energy utilization, making it essential for body weight management (19). In the cardiovascular system, MC4R activation contributes to the regulation of blood pressure and heart rate, supporting cardiovascular stability (18). Its influence also extends to glucose and lipid metabolism, where MC4R signaling optimizes glucose utilization and lipid storage, thereby reducing the risk of metabolic disorders (20). Zhao et al. emphasized MC4R's role in the nervous system, including regulation of pain perception, anxiety, stress responses, and sensory processing (21). This wide-ranging functionality underscores MC4R's significance in maintaining systemic health and overall homeostasis.

ROLE OF MC4R IN THE CENTRAL NERVOUS SYSTEM AND PERIPHERAL TISSUES

MC4R is predominantly expressed in the hypothalamus, particularly in the paraventricular nucleus (PVN), the dorsal motor nucleus of the vagus (DMV), and the intermediolateral nucleus of the spinal cord (IML), where it plays a central role in regulating energy balance and feeding behavior. Additionally, MC4R participates in central nervous system (CNS) functions, including stress modulation, neuropathic pain regulation, and cardiovascular homeostasis (22). Beyond the CNS, MC4R expression extends to adipose tissue, influencing lipid metabolism and energy expenditure (23). It is also present in intestinal L cells, where it contributes to the secretion of incretin hormones that regulate glucose homeostasis (24). Furthermore, MC4R is expressed in peripheral nerves and muscles, supporting organ homeostasis and tissue regeneration (22).

RECENT FINDINGS ON MC4R VARIANTS

MC4R (melanocortin-4 receptor) variants are known to play a significant role in obesity and metabolic disorders. The identification and functional characterization of rare and pathogenic MC4R variants across diverse populations provide

valuable insights into the genetic basis of severe obesity. In a Brazilian cohort, several rare missense mutations, including p.Ser36Thr, p.Val103Ile, p.Ala175Thr, and p.Ile251Leu2, were significantly associated with elevated body weight and BMI, highlighting the impact of these genetic alterations on obesity susceptibility (25). Further investigations in Qatar uncovered two novel variants, c.253A>G (p.Ser85Gly) and c.802T>C (p.Tyr268His), in individuals with morbid obesity. Functional analyses revealed that these variants destabilized MC4R protein structure, impairing its signaling pathways and underscoring its critical role in energy regulation and weight control (26). In Singapore, studies on Asian children with severe early-onset obesity identified the variants c.127C>A (p.Gln43Lys) and c.272T>G (p.Met91Arg), both of which exhibited defective cAMP signaling, a key pathway in energy homeostasis. These mutations disrupt MC4R function, leading to disturbances in metabolism (27). Collectively, these studies highlight the global prevalence and functional importance of MC4R variants in the etiology of severe obesity, providing a foundation for targeted therapeutic strategies and precision medicine approaches.

Table 1 presents recent studies conducted in different populations, identifying specific MC4R variants and their functional implications in obesity, emphasizing structural, signaling, and phenotypic associations.

MC4R AND METABOLIC DISORDERS

Obesity and weight regulation

Obesity affects over 30% of adults and children worldwide, representing a critical public health challenge. It results from an imbalance in energy homeostasis and is associated with various comorbidities, including type 2 diabetes, cardiovascular diseases, certain cancers, infertility, and psychological conditions such as depression (28). While an obesogenic environment and sedentary lifestyle are major contributors, genetic factors also play a significant role in regulating body weight (29).

Although most cases of obesity have a polygenic basis, a subset of individuals develop monogenic obesity, often caused by pathogenic variants in genes that influence the leptin-melanocortin pathway, an essential hypothalamic system for appetite regulation (30). Among these, mutations in the MC4R gene, a G-protein-coupled receptor, are the most common cause of monogenic obesity, significantly impairing energy balance and appetite control (2). This highlights the interplay between genetic predisposition and environmental factors in obesity and underscores the need for precision-targeted therapeutic strategies.

Genetic insights into MC4R mutations

Mutations in the MC4R gene, typically inherited in an autosomal dominant manner, are the most frequent monogenic cause of obesity, with over 200 variants identified (25). These mutations occur in 2-3% of tested populations and account for approximately 6% of obesity cases, establishing them as the leading cause of non-syndromic monogenic obesity (29).

Heterozygous loss-of-function mutations are the most prevalent, whereas homozygous or compound heterozygous mutations are less common (31, 32). Individuals with inactivating

Table 1. Recent studies on MC4R variants and their findings

Study	Location/ population	MC4R Variants Identified	Findings
Identification of a rare and potential Pathogenic MC4R variant in a Brazilian Patient with adulthood-onset severe obesity	Brazil	p.Ser36Thr, p.Val103Ile, p.Ala175Thr, p.Ile251Leu	Variants associated with higher body weight and BMI (25)
Functional characterization of novel MC4R variants	Qatar	c.253A>G p.Ser85Gly, c.802T>C p.Tyr268His	Variants destabilize MC4R structure and affect signalling pathways (26)
MC4R variants in Asian children with severe obesity	Singapore	c.127C>A p.Gln43Lys, c.272T>G p.Met91Arg	Variants show defective cAMP signalling activity (27)

mutations-of-function mutations often exhibit early-onset obesity, hyperphagia, hyperinsulinemia, increased linear growth, and elevated bone mineral density (33). Prevalence rates vary among ethnic groups, with lower frequencies (less than 1%) observed in Asian populations and estimates of less than 2% in large Caucasian European and American cohorts (34).

Conversely, gain-of-function mutations in MC4R exert protective effects. These variants are associated with lower body mass index (BMI) and reduced risks of obesity, type 2 diabetes, and coronary artery disease. Their protective effects are attributed to variants favoring β-arrestin-biased signaling, which enhances mitogen-activated protein kinase pathway activation. This unique signaling mechanism represents a promising therapeutic target for weight management and treatment of obesity-related cardiometabolic conditions (17).

While monogenic obesity arises from single-gene mutations such as those in MC4R, polygenic obesity results from the combined influence of multiple common genetic variants and is considerably more prevalent (35). Understanding these distinct genetic contributions provides potential avenues for precision medicine approaches in obesity management.

Table 2 summarizes the types of MC4R genetic mutations, their prevalence, and associated phenotypic consequences, distinguishing between loss-of-function, gain-of-function, and compound heterozygous variants with relevance to obesity and metabolic health.

Associated gene mutations

Mutations in the MC4R gene are the primary genetic cause of monogenic obesity, encompassing various mutation types, including missense, nonsense, and frameshift mutations, which result in partial or complete loss of MC4R function (25). These alterations impair the receptor's capacity to regulate energy balance, thereby contributing to severe obesity. Common variants near the MC4R gene, such as rs17782313 and rs17700633, have been extensively studied and are linked to increased susceptibility to obesity and insulin resistance, further highlighting the gene's role in metabolic regulation (36). In addition to these common variants, rare MC4R mutations, including p.Ser36Thr, p.Val103Ile, p.Ala175Thr, and p.Ile251Leu, have been identified in individuals with severe obesity, underscoring the significant contribution of rare genetic alterations to extreme phenotypes (25). Collectively, these findings emphasize the critical role of MC4R in energy homeostasis and its importance as a target for understanding and managing obesity.

Type 2 diabetes and insulin resistance

The MC4R plays a crucial role in regulating energy balance and insulin secretion. It is essential for controlling appetite and maintaining metabolic homeostasis, and its dysfunction can result in various metabolic abnormalities (20). According to Morgan and colleagues, MC4R signaling in the hypothalamus influences glucose homeostasis and insulin sensitivity (37). Research has demonstrated a link between MC4R dysfunction and an increased risk of type 2 diabetes.

Table 2. Genetic variants in MC4R and their implications for obesity

Mutation type	Prevalence	Phenotypic effects	References
Loss-of-function (LoF)	2–3% in tested populations; ~6% of obesity cases	Early-onset obesity - Hyperphagia - Hyperinsulinemia - Increased linear growth - Elevated bone mineral density	(29, 31, 32, 33)
Homozygous/compound heterozygous LoF	Rare	More severe phenotypes than heterozygous mutations	(31)
Gain-of-function (GoF)	Rare, protective	- Lower body mass index - Reduced risk of obesity - Reduced risk of type 2 diabetes - Reduced risk of coronary artery disease	(17)

Insulin resistance, hyperglycemia, and other metabolic disturbances are frequently observed in individuals with MC4R alterations (38). A 2015 study by Morgan et al. highlighted that MC4R signaling in the lateral hypothalamus is critical for regulating glucose tolerance and sympathetic activity, both of which are essential for maintaining metabolic health (37).

Dyslipidemia and hypertension

Dyslipidemia and hypertension are key cardiovascular risk factors that often coexist. Dyslipidemia is characterized by abnormal blood lipid levels, including elevated total cholesterol, triglycerides, and LDL cholesterol, along with reduced high-density lipoprotein (HDL) cholesterol levels (39). Hypertension, commonly known as high blood pressure, damages blood capillaries and promotes atherosclerosis, significantly increasing the risk of heart disease and stroke (40). Recent studies have highlighted that MC4R signaling in the CNS plays a critical role in regulating energy balance, food intake, and fat storage. The MC4R exerts significant influence on lipid metabolism by coordinating both central and peripheral mechanisms. Through various signaling pathways, MC4R modulates lipid metabolism in white adipose tissue (WAT) and brown adipose tissue. This dual regulatory function underscores its importance in maintaining energy homeostasis and preventing metabolic dysregulation (41).

MC4R and lipid metabolism

The MC4R plays an essential role in lipid metabolism by coordinating energy balance and fat distribution through both central and peripheral mechanisms (42). Within the CNS, MC4R is a key component of the hypothalamic leptin-melanocortin signaling pathway, which regulates appetite and energy expenditure (43). By modulating sympathetic nervous system (SNS) activity, MC4R affects adipose tissue metabolism. Specifically, it promotes lipolysis in WAT via β-adrenergic receptor activation, facilitating fat breakdown. Concurrently, MC4R activation enhances thermogenesis in brown adipose tissue, increasing energy expenditure by converting stored lipids into heat (41). Emerging studies also suggest that MC4R may directly interact with lipid-metabolizing enzymes, further emphasizing its role in maintaining lipid homeostasis. These functions highlight MC4R's potential as a therapeutic target for obesity and related metabolic disorders (44).

Hypertensive effects of MC4R dysfunction in obesity

Dysfunction of the MC4R in obesity can exacerbate the development of hypertension. Obesity is a major risk factor for hypertension, and disruptions in MC4R can further exacerbate this risk by affecting energy balance and metabolic regulation (45). According to Metzger et al., impaired MC4R signaling is associated with elevated blood pressure and a higher likelihood of cardiovascular complications (42).

Potential mechanisms linking MC4R to cardiovascular risk factors

MC4R is involved in several physiological processes that contribute to cardiovascular risk factors. According to Kleinau and co-authors, MC4R plays a pivotal role in regulating energy homeostasis, influencing both food intake and energy expenditure, which are essential for maintaining metabolic balance. Disruption of MC4R function, often through gene mutations, can lead to obesity, a condition that substantially increases the risk of cardiovascular diseases (46). Koochakpoor and colleagues highlighted that obesity associated with MC4R dysfunction is also closely linked to alterations in lipid metabolism, including dyslipidemia, a well-established risk factor for cardiovascular conditions (44). Furthermore, MC4R dysfunction exacerbates the inflammatory response and endothelial dysfunction, both key contributors to the progression of cardiovascular diseases (47). According to da Silva et al., activation of the SNS due to MC4R disruption further amplifies these risks by increasing blood pressure and heart rate, thereby placing additional strain on the cardiovascular system (48). Collectively, these processes highlight the integral role of MC4R not only in metabolic regulation but also in the pathophysiology of obesity-related cardiovascular diseases.

MC4R AND CARDIOVASCULAR DISEASE

Genetic alterations in MC4R are strongly linked to obesity and metabolic syndrome, both of which are major contributors to cardiovascular disease (CVD) (2). Investigating the connection

between MC4R and CVD may facilitate the development of targeted therapeutic strategies. MC4R is located in the hypothalamus, where it plays a pivotal role in controlling appetite and satiety. As a component of the melanocortin system, it helps monitor and respond to over-nutrition, thereby regulating metabolism to prevent obesity. When MC4R malfunctions, it can result in hyperphagia (excessive eating) and early-onset obesity, both of which elevate the risk of cardiovascular diseases (49). Recent research has identified MC4R variants, such as rs17782313, as contributors to an increased risk of obesity and metabolic dysfunction. Carriers of these variants often exhibit higher BMI, increased waist circumference, and elevated blood glucose levels, all recognized risk factors for cardiovascular diseases (50). Cardiometabolic syndrome comprises a group of conditions that increase the risk of heart disease, stroke, and diabetes. MC4R deficiency disrupts glucose homeostasis, thereby raising the likelihood of insulin resistance and type 2 diabetes, primarily because MC4R is essential for maintaining energy balance and metabolic regulation (51).

Impact on insulin sensitivity

A 2024 study by Guo and co-authors explored the impact of hypothalamic MC4R knockout specifically in POMC neurons on insulin sensitivity. The findings revealed that MC4R deficiency impairs insulin sensitivity by modulating Kir2.1 activity. Deletion of MC4R in POMC neurons resulted in increased food intake, reduced energy expenditure, and disrupted systemic glucose regulation (19). Mechanistically, the study by Cui et al. identified a direct interaction between MC4R and Kir2.1, and that silencing Kir2.1 reversed the negative effects of MC4R ablation on energy expenditure and glucose homeostasis (52). Another study by Ni et al. examined the role of MC4R in pancreatic islets and its regulation of insulin secretion via the cAMP and β-arrestin-1 pathways (20). That research demonstrated that MC4R activation by the agonist NDP-α-MSH significantly increased the expression of prohormone convertase 1/3 (PC1/3), a key factor in insulin secretion. Conversely, MC4R inhibition with the antagonist AgRP reduced PC1/3 expression. These results indicate that MC4R regulates PC1/3 expression through the cAMP and β-arrestin-1 pathways, thereby modulating insulin secretion (20).

MC4R in hypertension

Da Silva and fellow authors in 2019 highlighted the role of the brain MC4R in modulating SNS activity. Dysregulated MC4R signaling increases SNS activity, promoting hypertension, a major contributor to CVD. The study emphasized that MC4R activation is critical not only for obesity-induced hypertension but also for other forms of hypertension associated with heightened SNS activity (48). Sull and co-authors investigated the association of MC4R variants with diabetes and CVD in Korean men and women. The study found that individuals with the TC/CC genotype of the MC4R rs17782313 SNP exhibited a higher risk of diabetes and cardiovascular disease, independent of obesity, suggesting a direct role of MC4R in cardiovascular regulation (7). Collectively, these studies underscore the importance of MC4R in blood pressure regulation and highlight its potential as a therapeutic target for hypertension and cardiovascular disease.

MC4R and atherosclerosis

Mutations in the MC4R gene, known to cause monogenic obesity, can trigger systemic inflammation, a major contributor to endothelial dysfunction and the development of atherosclerosis (2). The MC4R pathway plays an essential role in managing energy balance, glucose levels, and lipid metabolism. Impaired MC4R signaling disrupts these metabolic processes, leading to increased inflammation and a heightened risk of atherosclerosis (53). Altered lipid metabolism caused by MC4R variants can significantly accelerate plaque formation. Research by Adamska-Patruno and co-authors indicates that these mutations are associated with reduced visceral fat accumulation but cause a relatively greater increase in postprandial carbohydrate utilization. This metabolic shift can elevate circulating lipid concentrations, promoting the development of atherosclerotic plaques and increasing the risk of coronary artery disease (54).

THERAPEUTIC IMPLICATIONS OF MC4R

Recent advancements have focused on developing both agonists and antagonists targeting MC4R to address metabolic disorders. Among

these, setmelanotide, an MC4R agonist, has demonstrated significant therapeutic potential for severe obesity associated with genetic defects in the leptin-melanocortin pathway. Clinical studies have shown its effectiveness, with a phase 3 trial reporting substantial weight loss and reduced hunger levels in individuals with POMC- or LEPR deficiency-related obesity. The treatment was generally well tolerated, with no new safety concerns identified (55).

In addition to obesity management, MC4R modulation may confer cardiovascular benefits. Research indicates that MC4R agonists can improve metabolic profiles, potentially aiding in the prevention and management of cardiovascular diseases (1). However, translating these promising preclinical findings into clinical practice remains challenging.

Emerging technologies, such as CRISPR-Cas9, offer potential for correcting alterations in MC4R, paving the way for precision medicine (56). Furthermore, combining MC4R agonists with other agents, such as GLP-1 receptor agonists, has shown synergistic effects, enhancing weight loss and improving metabolic outcomes (57). These developments underscore the therapeutic potential of MC4R-targeted interventions in addressing obesity and its related comorbidities.

CONCLUSIONS

In conclusion, the MC4R gene is a central regulator in the pathogenesis of metabolic and cardiovascular disorders, particularly through its role in obesity. Mutations in the MC4R gene, which include missense, nonsense, and frameshift alterations, often impair receptor function, leading to severe obesity. Common variants, such as rs17782313 and rs17700633, are associated with a higher risk of obesity and insulin resistance, while rare mutations, including p.Ser36Thr, p.Val103Ile, and p.Ala175Thr, contribute to more extreme obesity phenotypes. These genetic alterations disrupt the receptor's normal regulation of energy balance, emphasizing the critical role of MC4R in both weight management and metabolic health.

Moreover, alterations in MC4R influence cardiovascular function in addition to contributing to obesity. As obesity is a well-established risk factor for CVDs, MC4R dysfunction can exacerbate conditions such as hypertension, dyslipidemia, and atherosclerosis, thereby increasing overall cardiovascular risk. The intersection of obesity and cardiovascular health associated with MC4R variants highlights the need to better understand its genetic and physiological mechanisms.

Future research on MC4R may facilitate the development of innovative therapeutic strategies, including targeted interventions to restore MC4R function or modulate its signaling pathways. Such approaches would be particularly beneficial for individuals with genetic predispositions to obesity and cardiovascular diseases, paving the way for more personalized treatments. Overall, MC4R remains a key genetic factor at the forefront of understanding the complex relationship between metabolic and cardiovascular disorders, highlighting its potential as a therapeutic target to address these interconnected health challenges.

Future perspectives

Therapeutic strategies targeting MC4R hold significant promise for addressing obesity-related cardiovascular risks. The development of selective MC4R agonists, gene therapy approaches to correct pathogenic variants, and combination therapies with other metabolic regulators, such as GLP-1 receptor agonists, may enhance efficacy in weight reduction and cardiometabolic risk management. Moreover, advances in precision medicine and CRISPR-Cas9 technologies could enable personalized interventions tailored to specific MC4R genotypes, allowing clinicians to optimize treatment for individuals at highest risk of metabolic and cardiovascular complications. Collectively, these emerging approaches highlight a new era in translating genetic insights into effective therapies for obesity-associated cardiovascular disease.

ACKNOWLEDGMENTS

We sincerely appreciate the support provided by Meenakshi Academy of Higher Education and Research, Chennai, Tamil Nadu, India, and Genetika, Centre for Advanced Genetic Studies, Thiruvananthapuram, Kerala, India.

FUNDING

There are no funding sources to report.

CONFLICT OF INTEREST

The authors report no potential conflict of interest.

AUTHOR CONTRIBUTION

J.P.J.: conceptualization, methodology design, sample collection, laboratory work (biochemical and molecular analyses), data acquisition, statistical analysis, and manuscript drafting; S.K.B.: supervision, critical review of study design, interpretation of molecular data, guidance in laboratory methodologies, and manuscript revision for important intellectual content; N.M.: validation of biochemical assay procedures, clinical correlation of metabolic findings, and critical inputs in manuscript development; K.R.K.: administrative support, regulatory approvals, and institutional coordination for ethical clearance and research execution; N.M.: clinical insight into endocrine aspects, interpretation of hormonal and metabolic data, and contribution to discussion and conclusions; VMG, SJP, SM, ST: assistance in sample processing, ELISA/RT-PCR experimentation, data entry, and preliminary statistical evaluation; HPH, RR, PK, TA: support in genetic data analysis and visualization, referencing, and manuscript formatting; DRD: conceptual supervision, molecular diagnostics consultation (MC4R expression), manuscript review, critical editing, and final approval of the version to be published.

DATA AVAILABILITY STATEMENT

This review synthesizes and critically analyzes data from previously published studies; all data are publicly available through the cited literature, ensuring transparency and reproducibility of the findings discussed.

INSTITUTIONAL REVIEW BOARD STATEMENT

This review article does not report on new experimental research involving humans or animals; therefore, ethics approval was not required.

INFORMED CONSENT STATEMENT

This review article does not include research involving human participants; therefore, informed consent was not required.

REFERENCES

1. Sharma S, Garfield AS, Shah B, Kleyn P, Ichetovkin I, Moeller IH, et al. Current mechanistic and pharmacodynamic understanding of melanocortin-4 receptor activation. Molecules. 2019 24:1892. PubMed PMID: 31100979
2. Tao YX. The melanocortin-4 receptor: physiology, pharmacology, and pathophysiology. Endocr Rev. 2010; 31:506-43.
3. Oswal A, Yeo GS. The leptin melanocortin pathway and the control of body weight: lessons from human and murine genetics. Obes Rev. 2007;8:293-306.
4. Breit A, Büch TR, Boekhoff I, Solinski HJ, Damm E, Gudermann T. Alternative G protein coupling and biased agonism: new insights into melanocortin-4 receptor signalling. Mol Cell Endocrinol. 2011;331:232-40.
5. Cooray SN, Clark AJ. Melanocortin receptors and their accessory proteins. Mol Cell Endocrinol. 2011;331:215-21.
6. Siljee-Wong JE. Melanocortin MC4 receptor expression sites and local function. Eur J Pharmacol. 2011; 660:234-40.
7. Sull JW, Kim G, Jee SH. Association of MC4R (rs17782313) with diabetes and cardiovascular disease in Korean men and women. BMC Med Genet. 2020; 21:160. PubMed PMID: 32807123.
8. Carrasco-Luna J, Navarro-Solera M, Gombert M, Martín-Carbonell V, Carrasco-García Á, Del Castillo-Villaescusa C, et al. Association of the rs17782313, rs17773430 and rs34114122 polymorphisms of/near MC4R gene with obesity-related biomarkers in a Spanish pediatric cohort. Children. 2023;10:1221. PubMed PMID: 37508717.
9. Mountjoy KG, Robbins LS, Mortrud MT, Cone RD. The cloning of a family of genes that encode the melanocortin receptors. Science. 1992;257:1248-51.
10. Dubern B, Clément K, Pelloux V, Froguel P, Girardet JP, Guy-Grand B, et al. Mutational analysis of melanocortin-4 receptor, agouti-related protein, and α-melanocyte-stimulating hormone genes in severely obese children. J Pediatr. 2001;139:204-9.
11. Biebermann H, Kühnen P, Kleinau G, Krude H. The neuroendocrine circuitry controlled by POMC, MSH, and AGRP. Appetite. 2012;(209):47-75.
12. Kühnen P, Krude H, Biebermann H. Melanocortin-4 receptor signalling: importance for weight regulation and obesity treatment. Trends Mol Med. 2019;25:136-48.
13. Ghamari-Langroudi M, Digby GJ, Sebag JA, Millhauser GL, Palomino R, Matthews R, et al. G-protein-independent coupling of MC4R to Kir7.1 in hypothalamic neurons. Nature. 2015;520:94-8.
14. Fontaine T, Busch A, Laeremans T, De Cesco S, Liang YL, Jaakola VP, et al. Structure elucidation of a human melanocortin-4 receptor specific orthosteric nanobody agonist. Nat Commun. 2024;15:7029. PubMed PMID: 39353917.

15. Aykut A, Özen S, Gökşen D, Ata A, Onay H, Atik T, et al. Melanocortin 4 receptor (MC4R) gene variants in children and adolescents having familial early-onset obesity: genetic and clinical characteristics. Eur J Pediatr. 2020;179:1445-52.
16. Kühnen P, Clément K, Wiegand S, Blankenstein O, Gottesdiener K, Martini LL, et al. Proopiomelanocortin deficiency treated with a melanocortin-4 receptor agonist. N Engl J Med. 2016;375:240-6.
17. Lotta LA, Mokrosiński J, de Oliveira EM, Li C, Sharp SJ, Luan JA, et al. Human gain-of-function MC4R variants show signaling bias and protect against obesity. Cell. 2019;177:597-607.
18. Liu Z, Hruby VJ. MC4R biased signalling and the conformational basis of biological function selections. J Cell Mol Med. 2022;26:4125-36.
19. Guo H, Xin Y, Wang S, Zhang X, Ren Y, Qiao B, et al. Hypothalamic POMC neuron-specific knockout of MC4R affects insulin sensitivity by regulating Kir2.1. Mol Med. 2024;30:34. PubMed PMID: 38448811.
20. Ni Z, Wang Y, Shi C, Zhang X, Gong H, Dong Y. Islet MC4R regulates PC1/3 to improve insulin secretion in T2DM mice via the cAMP and ¤-arrestin-1 pathways. Appl Biochem Biotechnol. 2022;194:6164-78.
21. Zhao Y, Xin Y, Chu H. MC4R is involved in neuropathic pain by regulating JNK signaling pathway after chronic constriction injury. Front Neurosci. 2019;13:919. PubMed PMID: 31551683
22. Xu H, Zhang H, Fang Y, Yang H, Chen Y, Zhang C, et al. Activation of the melanocortin-4 receptor signaling by ¤-MSH stimulates nerve-dependent mouse digit regeneration. Cell Regen. 2021;10:1. PubMed PMID: 33937937.
23. You P, Hu H, Chen Y, Zhao Y, Yang Y, Wang T, et al. Effects of melanocortin 3 and 4 receptor deficiency on energy homeostasis in rats. Sci Rep. 2016;6:34938. PubMed PMID: 27713523
24. Zhan C. POMC neurons: feeding, energy metabolism, and beyond. Neural Regul Metab. 2018; 1090:17-29.
25. Salum KC, de Souza GO, Abreu GD, Campos Junior M, Kohlrausch FB, Carneiro JR, et al. Identification of a rare and potential pathogenic MC4R variant in a Brazilian patient with adulthood-onset severe obesity. Front Genet. 2020;11:608840. PubMed PMID: 33362866
26. Mohammed I, Selvaraj S, Ahmed WS, Al-Barazenji T, Hammad AS, Dauleh H, et al. Functional characterization of novel MC4R variants identified in two unrelated patients with morbid obesity in Qatar. Int J Mol Sci. 2023 Nov 15;24(22):16361. PubMed PMID: 38003551
27. Ong SG, Dehghan R, Dorajoo R, Liu JJ, Sng AA, Lee YS, et al. Novel melanocortin-3 and -4 receptor functional variants in Asian children with severe obesity. J Clin Endocrinol Metab. 2024;109:e1249-59.
28. Bray GA, Kim KK, Wilding JP; World Obesity Federation. Obesity: a chronic relapsing progressive disease process. A position statement of the World Obesity Federation. Obes Rev. 2017;18:715-23.
29. Farooqi IS, Keogh JM, Yeo GS, Lank EJ, Cheetham T, O'Rahilly S. Clinical spectrum of obesity and mutations in the melanocortin 4 receptor gene. N Engl J Med. 2003;348:1085-95.
30. Ignatieva EV, Afonnikov DA, Saik OV, Rogaev EI, Kolchanov NA. A compendium of human genes regulating feeding behavior and body weight, its functional characterization and identification of GWAS genes involved in brain-specific PPI network. BMC Genet. 2016;17:89-116.
31. O'Rahilly S, Farooqi IS, Yeo GS, Challis BG. Minireview: human obesity—lessons from monogenic disorders. Endocrinology. 2003;144:3757-64.
32. Drabkin M, Birk OS, Birk R. Heterozygous versus homozygous phenotype caused by the same MC4R mutation: novel mutation affecting a large consanguineous kindred. BMC Med Genet. 2018;19:135. PubMed PMID: 30068297
33. Delhanty PJ, Bouw E, Huisman M, Vervenne RM, Themmen AP, van der Lely AJ, et al. Functional characterization of a new human melanocortin-4 receptor homozygous mutation (N72K) that is associated with early-onset obesity. Mol Biol Rep. 2014;41:7967-72.
34. Hinney A, Hohmann S, Geller F, Vogel C, Hess C, Wermter AK, et al. Melanocortin-4 receptor gene: case-control study and transmission disequilibrium test confirm that functionally relevant mutations are compatible with a major gene effect for extreme obesity. J Clin Endocrinol Metab. 2003;88:4258-67.
35. Farooqi IS, O'Rahilly S. Genetics of obesity in humans. Endocr Rev. 2006;27:710-8.
36. Qi L, Kraft P, Hunter DJ, Hu FB. The common obesity variant near MC4R gene is associated with higher intakes of total energy and dietary fat, weight change and diabetes risk in women. Hum Mol Genet. 2008;17:3502-8.
37. Morgan DA, McDaniel LN, Yin T, Khan M, Jiang J, Acevedo MR, et al. Regulation of glucose tolerance and sympathetic activity by MC4R signaling in the lateral hypothalamus. Diabetes. 2015;64:1976-87.
38. Khodarahmi M, Kahroba H, Jafarabadi MA, Mesgari-Abbasi M, Farhangi MA. Dietary quality indices modifies the effects of melanocortin-4 receptor (MC4R) rs17782313 polymorphism on cardio-metabolic risk factors and hypothalamic hormones in obese adults. BMC Cardiovasc Disord. 2020;20:57. PubMed PMID: 32019489
39. Huang L, Liu Z, Zhang H, Li D, Li Z, Huang J, et al. The association between serum lipid profile levels and hypertension grades: A cross-sectional study at a health examination center. High Blood Press Cardiovasc Prev. 2025;32:87-98.
40. Poznyak AV, Sadykhov NK, Kartuesov AG, Borisov EE, Melnichenko AA, Grechko AV, et al. Hypertension as a risk factor for atherosclerosis: Cardiovascular risk assessment. Front Cardiovasc Med. 2022;9:959285. PubMed PMID: 36072873
41. Nogueiras R, Wiedmer P, Perez-Tilve D, Veyrat-Du-

rebex C, Keogh JM, Sutton GM, et al. The central melanocortin system directly controls peripheral lipid metabolism. J Clin Invest. 2007;117:3475-88.
42. Metzger PJ, Zhang A, Carlson BA, Sun H, Cui Z, Li Y, et al. A human obesity-associated MC4R mutation with defective Gq/11α signaling leads to hyperphagia in mice. J Clin Invest. 2024;134: e165418. PubMed PMID: 38175730
43. Anthofer L, Gmach P, Uretmen Kagiali ZC, Kleinau G, Rotter J, Opitz R, et al. Melanocortin-4 receptor PLC activation is modulated by an interaction with the monocarboxylate transporter 8. Int J Mol Sci. 2024;25:7565. PubMed PMID: 39062808
44. Koochakpoor G, Daneshpour MS, Mirmiran P, Hosseini SA, Hosseini-Esfahani F, Sedaghatikhayat B, et al. The effect of interaction between melanocortin-4 receptor polymorphism and dietary factors on the risk of metabolic syndrome. Nutr Metab (Lond). 2016;13:35. PubMed PMID: 27186233
45. Rahati S, Qorbani M, Naghavi A, Pishva H. Association and interaction of the MC4R rs17782313 polymorphism with plasma ghrelin, GLP-1, cortisol, food intake and eating behaviors in overweight/obese Iranian adults. BMC Endocr Disord. 2022;22:234. PubMed PMID: 36123585
46. Kleinau G, Heyder NA, Tao YX, Scheerer P. Structural complexity and plasticity of signaling regulation at the melanocortin-4 receptor. Int J Mol Sci. 2020;21:5728. PubMed PMID: 32785054
47. Litwin M, Kułaga Z. Obesity, metabolic syndrome, and primary hypertension. Pediatr Nephrol. 2021;36:825-37.
48. da Silva AA, do Carmo JM, Wang Z, Hall JE. Melanocortin-4 receptors and sympathetic nervous system activation in hypertension. Curr Hypertens Rep. 2019;21:46. PubMed PMID: 31028563
49. Yang Y, Xu Y. The central melanocortin system and human obesity. J Mol Cell Biol. 2020;12:785-97.
50. Zhang Y, Li S, Nie H, Wang X, Li X, Wen J, et al. The rs17782313 polymorphism near MC4R gene confers a high risk of obesity and hyperglycemia, while PGC1α rs8192678 polymorphism is weakly correlated with glucometabolic disorder: a systematic review and meta-analysis. Front Endocrinol (Lausanne). 2023;14:1210455. PubMed PMID: 37621650
51. Roumi Z, Mirzababaei A, Abaj F, Davaneghi S, Aali Y, Mirzaei K. The interaction between polyphenol intake and genes (MC4R, Cav-1, and Cry1) related to body homeostasis and cardiometabolic risk factors in overweight and obese women: a cross-sectional study. Front Nutr. 2024;11:1410811. PubMed PMID: 39104759
52. Cui M, Cantwell L, Zorn A, Logothetis DE. Kir Channel Molecular Physiology, Pharmacology, and Therapeutic Implications. Handb Exp Pharmacol. 2021;267:277-356.
53. Chen S, Zhao L, Sherchan P, Ding Y, Yu J, Nowrangi D, et al. Activation of melanocortin receptor 4 with RO27-3225 attenuates neuroinflammation through AMPK/JNK/p38 MAPK pathway after intracerebral hemorrhage in mice. J Neuroinflammation. 2018;15:106. PubMed PMID: 29642894
54. Adamska-Patruno E, Goscik J, Czajkowski P, Maliszewska K, Ciborowski M, Golonko A, et al. The MC4R genetic variants are associated with lower visceral fat accumulation and higher postprandial relative increase in carbohydrate utilization in humans. Eur J Nutr. 2019;58:2929-41.
55. Clément K, van den Akker E, Argente J, Bahm A, Chung WK, Connors H, et al. Efficacy and safety of setmelanotide, an MC4R agonist, in individuals with severe obesity due to LEPR or POMC deficiency: single-arm, open-label, multicentre, phase 3 trials. Lancet Diabetes Endocrinol. 2020;8:960-70.
56. Musunuru K. CRISPR and cardiovascular diseases. Cardiovasc Res. 2023;119:79-93.
57. Dahir NS, Gui Y, Wu Y, Sweeney PR, Rouault AA, Williams SY, et al. Subthreshold activation of the melanocortin system causes generalized sensitization to anorectic agents in mice. J Clin Invest. 2024;134:e178250. PubMed PMID: 39007271

Biomedical Sciences and Clinical Medicine 2026;65(1):140-144.
doi: 10.12982/BSCM.2026.13
https://he01.tci-thaijo.org/index.php/CMMJ-MedCMJ/index

BSCM
Biomedical Sciences and Clinical Medicine

Short Communication

Open Access

Phenethylamine Does Not Accelerate Healing in *Staphylococcus aureus*-infected Wounds in Mice

Hana Dian Mufida, Dewi Hidayati, Enny Zulaika and Arif Luqman

Biology Department, Institut Teknologi Sepuluh Nopember, Surabaya, Indonesia

Correspondence:
Arif Luqman, PhD,
Biotechnology Study Program,
Biology Department, Institut
Teknologi Sepuluh Nopember
Surabaya, Indonesia .
E-mail: arif.luqman@its.ac.id

Received: March 11, 2025;
Revised: August 27, 2025;
Accepted: Sep 12, 2025

ABSTRACT

OBJECTIVE Bacterial infections can lead to a delay in the wound healing process. Recent studies have reported that trace amines accelerate wound healing by enhancing keratinocyte migration thus promoting a faster wound re-epithelization process. This study aimed to investigate the effects of phenethylamine on *Staphylococcus aureus*-infected wounds by using a mouse model.

METHODS This study used mice as a model for in vivo skin wound experiments. *S. aureus* was applied on skin wounds on the backs of the mice. Phenethylamine in different concentrations was also applied either once daily or every two days. The wound diameter, abscess formation, and swollen area were observed every two days for 14 days.

RESULTS Different concentrations and frequencies of phenethylamine applications on the wound exhibited no significant wound healing acceleration. Phenethylamine applications also did not show significant effects on abscess formation or swelling.

CONCLUSIONS *S. aureus* infection may overwhelm the wound healing acceleration effects of phenethylamine resulting in no significant improvement in healing.

KEYWORDS phenethylamine, wound healing, *Staphylococcus aureus*, infection

INTRODUCTION

Bacterial infection in wounds complicates the treatment and significantly hinders the healing process. Infected wounds are often characterized by prolonged inflammation, tissue damage, and an impedimented re-epithelization process. These events can lead to the chronic wound formation (1). *Staphylococcus aureus* (*S. aureus*) is one of the major pathogens causing wound infections (2). *S. aureus* can colonize and invade the injured tissues, trigger the intense inflammation responses, and recruit excessive neutrophils to the wound area (3). The persistence of inflammation and tissues degradation caused by *S. aureus* infection can substantially impede the healing process and increase the risk of abscess formation (3, 4).

Previous publications have reported that trace amines accelerate wound healing in mouse models (5). These compounds, produced by human skin commensals (6), act as partial antagonist of the β-adrenergic receptors, promoting keratinocytes migrations, fibroblasts proliferation, and ultimately accelerate wound closing (7). One of the trace amines, phenethylamine, has shown a potential to boost wound healing in uninfected wounds in a mouse model. This study aimed to investigate the effects of phenethylamine application on *S. aureus*-infected wounds. Using a mouse model, wee valuated

the effects of phenethylamine at various concentrations and frequencies of applications on wound closing, abscess formation, and swelling of the wound area to determine its therapeutic potential in infected wounds.

METHODS

Bacterial preparation for inoculum in wounds

S. aureus USA300 LAC was inoculated into tryptic soy broth medium (TSB) and incubated at 37°C with 200 rpm agitation overnight. The next day, the bacterial cells were pelleted, washed, and resuspended in sterile 0.9% NaCl solution.

Wound experiments in mice

The wound experiments were performed according to a previous publication (5). DDY mice (male, 6-8 weeks, 25-35 gram) were used in this study with 4 mice in each of 10 experimental groups, a total of 40 mice. Prior to the wounding, the mice were anesthetized with ketamine/xylazine (10 : 1) with a dose of 0.04 mg/g mouse weight. The backs of the mice were shaved, and four circular full-thickness wounds (4 mm in diameter) were made on the back skin of each mouse using a skin biopsy punch. The *S. aureus* USA300 suspension was then applied (10 µL) on the wound at 3 x 10^8 CFU. Phenethylamine dissolved at sterile 0.9% NaCl at various concentrations (6.25, 12.5, 25, and 50 µg/mL) was applied topically (10 µL) on the wounds 2 hour after the bacterial infection. The control used in this experiment is the application of sterile 0.9% NaCl. Phenethylamine was applied to the wounds of all the mice either daily or every two days. The wound diameter, abscess formation, and swollen area diameter were observed every 2 days for 14 days.

Statistical analysis

The significance of the wound diameter data was analyzed using the Friedman test with Dunn's multiple comparison test. The data on abscess formation and diameter of the swollen area were analyzed using repeated measures (RM) one-way ANOVA with Tukey's multiple comparisons test. Statistical significance was defined as $p < 0.05$.

RESULTS

The effects of phenethylamine topical application on *S. aureus*-infected wounds were recorded as the wound diameter, the presence of abscess formation and the diameter of the swollen area. The concentrations of phenethylamine were selected based on previous findings that daily application of 25 µg/mL significantly accelerated wound healing in a non-infected model (5). To explore the therapeutic window under infectious conditions, we included both lower and higher concentrations (6.25, 12.5, 25, and 50 µg/mL). In addition, two dosing schedules (daily application and once every two days) were employed to evaluate whether treatment frequency modulates efficacy in *S. aureus* USA300-infected wounds. However, we observed no significant acceleration of wound closing in the experimental animals compared to controls. The application of a high concentration of phenethylamine (50 µg/mL) both every day and every two days decelerated the wound closing significantly (Figure 1A-1B). Abscess formation was observed 2 days post wounding and *S. aureus* infection was observed on the wounds in both the experimental and the control groups, but with varied prevalence. In most cases, the abscess formation was no longer observed after the sixth day with the exception of some mice treated with phenethylamine at concentrations of 12.5, 25, and 50 µg/mL. Statistical analysis showed that treatment with phenethylamine at various concentrations with different application frequencies had no significant effect on abscess formation (Figure 1C). Swelling surrounding the wounds was only observed in the group with phenethylamine application every two days, and no statistically significant difference was observed between the different concentrations of phenethylamine applied (Figure 1D).

DISCUSSION

We observations in this study differ from those in a previous publication (5), e.g., we did not observe a wound closing acceleration effect from the application of phenethylamine on the *S. aureus*-infected wound. This difference could be due to the fact that antagonistic activities of phenethylamine on β-adrenergic receptors in fibroblasts inhibit their proliferation and migration

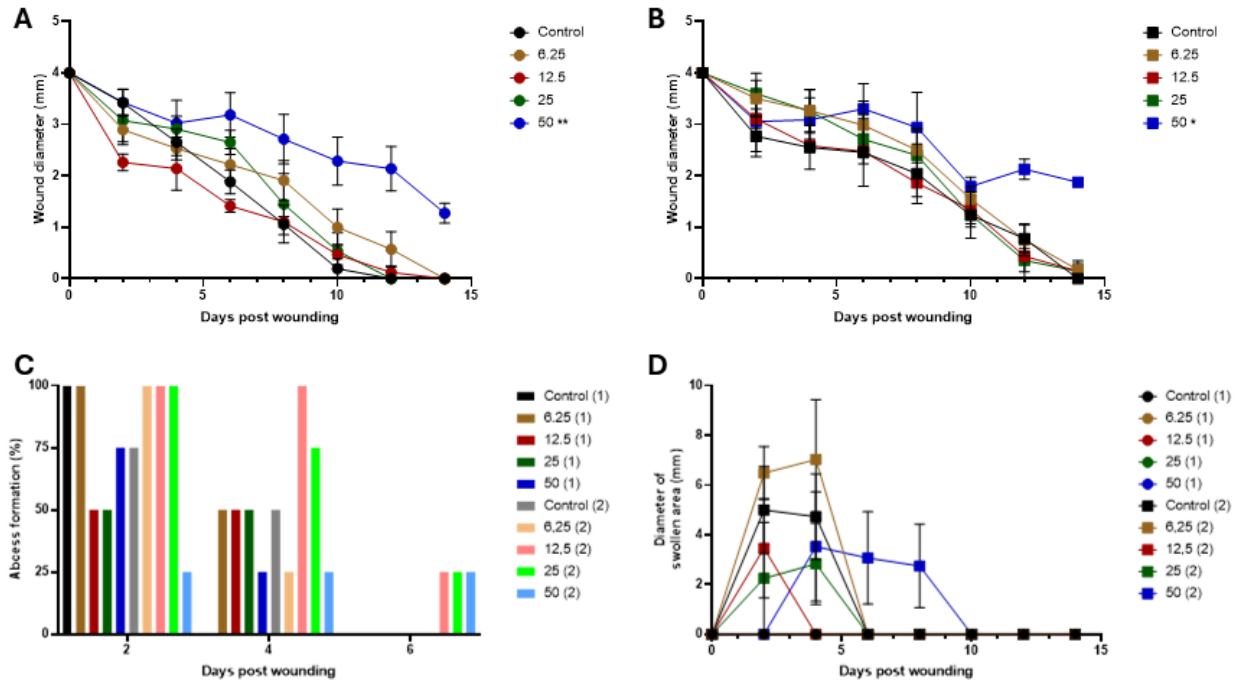

Figure 1. Phenethylamine topical application on *S. aureus*-infected wounds did not show significant affects. Phenethylamine was applied topically at various concentrations on wounds inoculated with *S. aureus* USA300 LAC. The application of phenethylamine did not show any significant enhancement in wound closing between daily application (A) and every two days application (B). Phenethylamine application also showed no significant effect on abscess formation on infected wounds (C) or on the swollen area surrounding the wound (D). The wound diameter data were analysed using the Friedman test, while the abscess formation and swollen area were analysed using repeated measures one-way ANOVA with Tukey's multiple comparisons test. Figure legends represent the concentration of phenethylamine used in the experiments and the number inside the brackets indicates the frequency of phenethylamine application: 1 means daily application and 2 means application every two days. $^{*}p < 0.05$; $^{**}p < 0.01$.

causing a delay in wound healing (7). Moreover, the bacterial infection in wounds can delay healing by triggering a continuous influx of neutrophils to the wound (3, 7, 8). The excessive neutrophils in a wound can lead to further necrosis and extracellular matrix degradation due to the proteases and free oxygen radicals released by neutrophils (9). The presence of excessive neutrophils in the wound leads to the formation of abscess (4), which were observed in all of the treatment groups in this study. The severity of infection induced by *S. aureus* USA300, a highly virulent and invasive strain, may have further masked any potential positive effects of phenethylamine. In a severe infection context, bacterial load and prolonged inflammation are likely the dominant factors determining wound outcome (1, 10-12), overshadowing subtle host-modulatory effects of trace amines.

Swelling, however was observed only in the groups of mice in which the phenethylamine application was done every two days, even in rather than daily, including the control group where only 0.9% NaCl was applied. This suggests that more frequent wound irrigation may help reduce swelling by mechanically removing excess proinflammatory cytokines and cellular debris from the wound area. The irrigation process limits the accumulation of proinflammatory mediators, thereby dampening the inflammatory response and accelerating the transition to the proliferative phase of wound healing. Thus, reducing local cytokine concentrations through more frequent irrigation may help prevent prolonged inflammation and accompanying swelling (13). The virulence factors of *S. aureus* USA300 could possibly override the potential wound healing enhancement effects of phenethylamine. Additionally, infection-associated inflammation may reduce the host responsiveness to trace amines.

This study has some limitations. Only one bacterial strain and one infection model were tested, and the duration of treatment was relatively short. It is possible that different dosing regimens, longer treatment courses and/or co-administration with

antibiotics could yield different outcomes. Moreover, while phenethylamine concentrations were selected based on previous studies in non-infected wounds, their efficacy may vary under infectious conditions where pharmacodynamics and host–pathogen interactions are altered.

Future studies should investigate whether phenethylamine might exert synergistic effects when combined with standard antimicrobial therapy, whether its activity differs with other *S. aureus* strains or less virulent pathogens, and whether modified dosing strategies can improve therapeutic efficacy. These investigations will be important to clarifying the translational potential of phenethylamine in infected wound healing.

CONCLUSIONS

This study demonstrates that topical application of phenethylamine at various concentrations does not significantly affect wound closure, abscess formation, or swelling in *S. aureus*-infected wounds. The severity of infection and associated inflammatory response likely outweighed potential wound-healing effects, possibly compounded by antagonistic actions of phenethylamine on fibroblast β-adrenergic receptors. While limited to a single strain and treatment regimen, these findings highlight the importance of evaluating candidate therapies under clinically relevant infectious conditions, and future work should test phenethylamine in combination with antimicrobial therapy under varied infection severities and with extended dosing strategies.

ACKNOWLEDGMENTS

We would like to thank Prof. Friedrich Götz for kindly providing the strain used in this study. This work was supported by Return Fellowship from Alexander von Humboldt Foundation.

FUNDING

This research was supported by the Alexander von Humboldt Foundation through Return Fellowship awarded to Arif Luqman and by the Kementerian Pendidikan Tinggi, Sains dan Teknologi (Ministry of Higher Education, Science and Technology, Indonesia) under the Penelitian Fundamental Reguler scheme, with main contract number: 017/C3/DT.05.00/PL/2025 and sub-contract number: 1234/PKS/ITS/2025. The authors gratefully acknowledge these institutions for their generous support.

CONFLICTS OF INTEREST

The authors have no conflicts of interest to report.

AUTHOR CONTRIBUTION

H.D.M.: investigation, methodology, data curation, writing – original draft; E.Z.: supervision, validation, writing – original draft; D.H.: supervision, validation, writing – original draft; A.L.: conceptualization, methodology, funding acquisition, resources, supervision, validation, formal analysis, visualization, writing – original draft, writing – review & editing. All authors have read and agreed to the published version of the manuscript.

DATA AVAILABILITY STATEMENT

All data generated or analyzed during this study are included in this published article.

INSTITUTIONAL REVIEW BOARD STATEMENT

The wound healing experiment using mice were approved by the Ethic Commission of Faculty of Veterinary Medicine, Universitas Airlangga, Surabaya, Indonesia (No. 3.KE.091.10.2020).

INFORMED CONSENT STATEMENT

Not applicable

REFERENCES

1. Rahim K, Saleha S, Zhu X, Huo L, Basit A, Franco OL. Bacterial Contribution in Chronicity of Wounds. Microb Ecol. 2017;73:710-21.
2. Serra R, Grande R, Butrico L, Rossi A, Settimio UF, Caroleo B, et al. Chronic wound infections: the role of Pseudomonas aeruginosa and Staphylococcus aureus. Expert Rev Anti Infect Ther. 2015;13:605-13.
3. Peschel A, Otto M. Phenol-soluble modulins and staphylococcal infection. Nat Rev Microbiol. 2013;11:667-73.
4. Pigozzo AB, Missiakas D, Alonso S, Dos Santos RW, Lobosco M. Development of a Computational Model of Abscess Formation. Front Microbiol. 2018;9:1355. PubMed PMID: 29997587.
5. Luqman A, Muttaqin MZ, Yulaipi S, Ebner P, Matsuo M, Zabel S, et al. Trace amines produced by skin bacteria accelerate wound healing in mice. Commun Biol. 2020;3(1):277. PubMed PMID: 32483173

6. Luqman A, Ohlsen K. Adrenergic system: A gateway of reciprocal signaling between host and bacteria. Current Opinion in Endocrine and Metabolic Research. 2024;35:100523.
7. Luqman A, Gotz F. The Ambivalent Role of Skin Microbiota and Adrenaline in Wound Healing and the Interplay between Them. Int J Mol Sci. 2021;22:4996. PubMed PMID: 34066786.
8. Edwards R, Harding KG. Bacteria and wound healing. Curr Opin Infect Dis. 2004;17:91-6.
9. Wilgus TA, Roy S, McDaniel JC. Neutrophils and Wound Repair: Positive Actions and Negative Reactions. Adv Wound Care (New Rochelle). 2013;2:379-88.
10. Uberoi A, McCready-Vangi A, Grice EA. The wound microbiota: microbial mechanisms of impaired wound healing and infection. Nat Rev Microbiol. 2024;22:507-21.
11. Zhao R, Liang H, Clarke E, Jackson C, Xue M. Inflammation in Chronic Wounds. Int J Mol Sci. 2016;17:2085. PubMed PMID: 27973441.
12. Jones SG, Edwards R, Thomas DW. Inflammation and wound healing: the role of bacteria in the immuno-regulation of wound healing. Int J Low Extrem Wounds. 2004;3:201-8.
13. Tao Q, Ren J, Ji Z, Wang B, Zheng Y, Li J. Continuous topical irrigation for severely infected wound healing. J Surg Res. 2015;198:535-40.